ARKANSAS REFLECTION CRACKING ANALYSIS AND OVERLAY DESIGN PROCEDURE

REPORT No. UA-3/1

February 1982

S. B. Seeds, B. F. McCullough
and R. F. Carmichael
ARE Inc.-ENGINEERING CONSULTANTS
2600 Dellana Lane - Austin, Texas - 78746

Arkansas

Prepared for
UNIVERSITY OF ARKANSAS
FAYETTEVILLE, ARKANSAS

TECHNICAL REPORT STANDARD TITLE PAGE

1. Report No.	2. Government Accession No.	3. Recipient's Catalog No.

Title and Subtitle

Arkansas Reflection Cracking Analysis and Overlay Design Procedure

5. Report Date: April 83

6. Performing Organization Code:

7. Author(s)

S. B. Seeds, B. F. McCullough and R. F. Carmichael

8. Performing Organization Report No.: UA - 3/1

9. Performing Organization Name and Address

Austin Research Engineers, Inc.
2600 Dellana Lane
Austin, Texas 78746

10. Work Unit No.:

11. Contract or Grant No.: TRC - 61

12. Sponsoring Agency Name and Address

University of Arkansas, Fayetteville, AR 72701
and
Arkansas State Highway & Transportation Department
P.O. Box 2261, Little Rock, AR 72203

13. Type of Report and Period Covered: Final

14. Sponsoring Agency Code: TRC - 61

15. Supplementary Notes

16. Abstract

This report presents the results of a study to develop a reflection cracking analysis and overlay design procedure for the State of Arkansas. The study was conducted in cooperation with the University of Arkansas and the Arkansas State Highway and Transportation Department (AHTD). In developing the analysis and design procedure for minimizing reflection cracking in asphalt concrete (flexible) overlays of rigid pavements, an earlier computer model developed for the FHWA, RFLCR, was improved, modified and calibrated to the field performance of experimental overlay projects in both Arkansas and Texas. Consideration was also given to the results obtained by the University of Arkansas on 3 instrumented overlay sites on I-30 near Benton, Arkansas. The resulting design method was also adapted to a nomograph procedure for use by AHTD.

17. Key Words	18. Distribution Statement
reflection cracking, flexible overlays, rigid pavement, thermal movement, differential vertical movement, fatigue, rehabilitation design	No restrictions. This document is available to the public through the National Technical Information Service, Springfield, Virginia 22161.

19. Security Classif. (of this report)	20. Security Classif. (of this page)	21. No. of Pages	22. Price
Unclassified	Unclassified	273	

Form DOT F 1700.7 (8-69)

ACKNOWLEDGEMENT

The authors of this paper gratefully acknowledge the valuable assistance and direction provided by Dr. Robert C. Welch (University of Arkansas) in collecting, processing and summarizing the scientific data from the instrumented overlay sites near Benton, Arkansas. Thanks are also extended to Earl Kirkpatrick, Jerry Westerman and Mike Limbird (Arkansas State Highway and Transportation Department) for their cooperation in conducting the highway condition surveys and obtaining the field pavement samples for use in laboratory testing.

EXECUTIVE SUMMARY

The primary objective of this study was to develop a reflection cracking analysis and overlay design procedure for use in selecting appropriate asphalt concrete hot-mix (ACHM) overlay design alternatives for portland cement concrete (PCC) pavements in Arkansas. Accordingly, a summary of the significant aspects and accomplishments of this study is provided here.

A review of the literature on the current practices for controlling reflection cracking indicated that several measures have been tried. Categorically, these include the use of 1) treatments to the existing PCC pavement (e.g., crack filling and sealing, breaking and seating and subsealing or undersealing), 2) stress or strain relieving interlayers (e.g., bond breakers, fabrics and tack or seal coats), 3) cushion courses, 4) overlay treatments (e.g., reinforcement, asphalt specifications and additives), and 5) increased overlay thickness. Many states and other agencies have conducted experiments with these different control measures and have met with varying degrees of success. Because of the presence of at least two types of distress mechanisms which can lead to reflection cracking and the fact that most of the studies did not include any field measurements prior to overlay placement as part of their experiment, it was often impossible to attribute success or failure to the effectiveness of the control methods or the potential (or lack of potential) in the original pavement for the development of reflection cracking. Thus, based on the literature review, it was concluded that in order to establish a design procedure for use in Arkansas, it would be necessary to 1) consider the effects and significance of the different distress mechanisms which lead to reflection cracking, 2) consider the effectiveness of the different control methods used in Arkansas with respect to the two known distress mechanisms, and 3) include field measurements of slab movement for the two distress criteria. The two main distress mechanisms identified were differential vertical movements between adjacent slabs and the combined effect of temperature drops and thermal related contraction of the underlying slab.

The field measurements, data collection and laboratory testing described in Chapters 3 and 4 were obtained for use in both calibrating the new procedure and for providing criteria for the selection of appropriate input data to use afterwards. Field measurements consisted of:

1. data obtained by the University of Arkansas from a specially instrumented experimental overlay project near Benton, and

2. data collected by AHTD using the Dynaflect and a special strain gauge apparatus to establish the potential for both differential vertical and horizontal slab movements in different types of PCC pavements in Arkansas.

The supplementary data included:

1. information and survey data obtained by AHTD and the Center for Transportation Research (at the University of Texas) on the performance of various overlay projects in Arkansas and Texas, and

2. data obtained from the National Climatic Center on the distribution of temperature within Arkansas.

Lastly, laboratory testing of various Arkansas pavement materials included:

1. thermal coefficient tests on AC and PCC specimens,

2. indirect tensile tests for dynamic and creep moduli of AC specimens, and

3. compression tests for static elastic moduli of PCC specimens.

The development of the design procedure, presented in Chapter 5, basically consisted of the extensive improvement, modification, and calibration of a design procedure originally developed by ARE Inc for the Federal Highway Administration (Ref. 1). The most significant improvement in the new procedure is its consideration of fatigue in the two models based on differential vertical slab movements (shear strain model) and horizontal slab movements (tensile strain model). The calibration of the two models relied heavily on the analysis of all the data discussed in Chapters 3 and 4. The result was a computer program called ARKRC-2 which is capable of considering many different types of methods for controlling reflection cracking, but is calibrated only for the methods currently used in Arkansas, i.e., strain-absorbing open-graded base courses, varying overlay thickness and to some extent, the placement of a bond breaker prior to overlay placement. The tensile strain model component predicts the life of a given overlay alternative (in years) corresponding to a 50 percent level of reflection cracking. This value can then be translated into an overlay age at a different level of reflection cracking specified by the user. The shear strain model component, on the other hand, provides criteria for the selection of joints (or cracks) which may require undersealing or increased overlay thickness to minimize the potential for differential vertical movements after overlay. The latter uses 18-kip single axle load applications as its fatigue consideration.

After the completion of the computerized ARKRC-2 procedure, statistical experiments were conducted (Chapter 7) on the tensile strain component model of the program in order to arrive at direct-solution equations for predicting overlay life for both jointed and continuous pavements in two composite climatic regions in Arkansas. These equations along with those derived for the shear strain component model were then translated into design nomographs suitable for use in the AHTD Highway Design Manual (Appendix D).

Then, in order to demonstrate the new design procedure and to provide some basis for its implementation, an example overlay design problem was prepared using field data from a jointed pavement on I-30. These results are presented in Chapter 8.

Finally, conclusions and recommendations about the results of the study were made and are presented in Chapter 9. The most significant of the recommendations was that it may be beneficial to combine two or more reflection cracking control methods in cases where a great potential for slab movement is exhibited.

TABLE OF CONTENTS

LIST OF FIGURES

LIST OF TABLES

CHAPTER 1
INTRODUCTION

BACKGROUND

Reflection cracking is a form of pavement distress in which a crack in the original pavement propagates to the surface of an overlay or other form of rehabilitation. Small amounts of cracking are not considered to be a severe distress manifestation as by itself a crack may not diminish the pavement structural capacity considerably. However, a crack may permit water to penetrate and undermine the support provided by the underlying layers and the long terms effects of this are considered to be severe. One of the main benefits of placing an overlay is the seal it provides against the intrusion of water. It is of great importance then, to insure that premature or excessive reflection cracking does not totally destroy this seal.

Past experience has shown that it is not possible to design an overlay so that reflection cracking will be completely eliminated. It is possible however, to design one so that reflection cracking will be minimized. Some of the techniques available for minimizing reflection cracking include (in no specific order):

1. increased overlay thickness,
2. placement of an intermediate or cushion layer prior to overlay,
3. placement of a bond breaker,
4. placement of high tensile strength fabric as a stress relieving layer,
5. placement of wire or other type reinforcement along with the overlay,
6. pavement undersealing at joints (or cracks),
7. use of softer asphalt or rubber-asphalt in the paving mix, and
8. pavement breaking prior to overlay placement.

Several studies of these different preventive techniques have been conducted in order to determine which are most cost effective. Unfortunately, because of a lack of planning or the lack of sufficient funds to conduct large enough experiments with adequate field measurements both before and after overlay, the results of these studies have been largely inconclusive about the effectiveness of the different techniques.

Recognizing this and the need for an adequate engineering design procedure for minimizing reflection cracking in the state, the Arkansas State Highway and Transportation Department (AHTD) sponsored a joint project with the University of Arkansas and Austin Research Engineers, Inc (ARE) to conduct field and laboratory experiments on overlay projects in the state and use the data (along with any other pertinent information) to develop an analysis and design procedure for evaluating the trade-offs between different alternatives for minimizing reflection cracking in asphalt concrete overlays. The University of Arkansas was selected for the project because of its experience in in-site electronic testing, while ARE, Inc was selected because of its prior experience in developing an overlay design and reflection cracking analysis procedure for the Federal Highway Administration (Ref. 1).

OBJECTIVE

The overall objective of this study is to develop a design procedure and design criteria for use in the design of Asphalt Concrete Hot Mix (ACHM) overlays on Portland Cement Concrete (PCC) pavements in Arkansas. The intermediate objectives are:

1. Develop a mathematical model that simulates the mechanism(s) producing reflection cracking,
2. Calibrate the model to predict the performances observed on in-service pavements, and
3. Produce a simplified procedure that may be included in a design manual.

SCOPE OF STUDY

The final design procedure was planned to be a hand solution method for inclusion in a design manual and an alternative computer based method for more sophisticated analyses. The hand solution method is a simplification of the latter developed by considering the effects of certain significant factors while holding the less significant ones constant for Arkansas conditions.

The accomplishments of these new design procedures will enable the engineer to develop specifications and techniques that are desirable and economical in the rehabilitation of PCC pavements. Special emphasis is given to field data from instrumented overlay sites in Arkansas to determine the effects of horizontal and vertical movements of joints and cracks in PCC pavements on the performance of an ACHM overlay.

SCOPE OF REPORT

The end product of this study will be a design manual, which will consist of tables, nomographs, equations and computer programs that will consider both environmental and wheel loadings in the design of ACHM overlays for PCC pavements. Primary development work in this study will be directed towards establishing a better and more complete method for preventing the occurrence of reflection cracks in asphalt concrete overlays of PCC pavements. In order to accomplish the project objective to the fullest extent possible, the following tasks were defined and the accomplishment of each documented in the different chapters of this report:

1. Conduct literature survey (Chapter 2)
2. Collect data on horizontal and vertical movements of joints and cracks in PCC pavements, including temperature and wheel load effects (Chapter 3)
3. Obtain field pavement samples and conduct laboratory testing to determine material properties (Chapter 4)

4. Analyze data and develop design procedure which considers the effects of wheel loads and environment (Chapter 5)
5. Document use and application of programs (Chapter 6)
6. Develop equations, tables and nomographs for use in design of ACHM overlays on PCC pavements (Chapter 7)
7. Provide implementation examples of design procedure (Chapter 8)
8. Provide conclusions and recommendations about the results of the study (Chapter 9)

CHAPTER 2
REVIEW OF CURRENT PRACTICES FOR CONTROL OF REFLECTION CRACKING

In this chapter, an overview of the current practices is presented, followed by a definition of the distress mechanisms. Next, the literature reviewed in this study is summarized.

OVERVIEW

Reflection cracking was recognized as one of the principle forms of distress in resurfaced pavements at the 1932 Annual Meeting of the Highway Research Board. This led to a great deal of experimentation of various techniques for the control of reflection cracking in the 1930's, 40's, and early 50's. With the advent of the Interstate Highway Program, the emphasis was on new construction. The obvious rehabilitation needs in the late 1960's and 1970's included reflection cracking. Thus, at a Workshop on Pavement Rehabilitation in 1974, reflection cracking was again recognized as still being a major problem (Ref. 2). Apparently, the problem of minimizing reflection cracking had not been resolved.

In 1970, the U.S. Department of Transportation, Federal Highway Administration, initiated the National Experimental and Evaluation Program (NEEP), Project No. 10, "Reducing Reflection Cracking in Bituminous Overlay." Until this study in which thirteen states participated (Ref. 3), there had been no large scale concentrated nor coordinated research effort to determine ways of reducing or ideally preventing reflection cracking from occurring. A recent report by the U.S. Army Engineer Waterways Experiment Station concerning a review of the results of the NEEP Project No. 10 concluded that "no known treatment will completely prevent the formation of reflection cracks. Some treatments do delay the formation of cracks, while others do not appear to help at all" (Ref. 3). Clearly, what works well in Virginia may not necessarily work well in Arkansas, nor Arizona, Florida, or Idaho. Similarly, the solution which

is applicable for the control of differential vertical deflection levels is not the same solution that will work well to restrain horizontal movements created by temperature changes.

The present state of the art for preventing reflection cracking in hot-mix asphalt concrete overlays of PCC pavements is, therefore, empirical in nature or based to a large degree on experience gained from trial and error methods used on in-service highways. A definition of reflection cracking is contained in Highway Research Board's Special Report 113 (Ref. 4) which states that "it is the cracking of an overlay above underlying cracks or joints." A more detailed description is that reflection cracks are fractures in an overlay or surface course that are a "reflection" of the crack or joint pattern in the underlying layer, and may be either environmentally or traffic induced. Such cracking must be prevented to retain the structural integrity of the overlay, preclude water intrusion to the lower layers, and maintain a smooth riding surface.

DEFINING THE DISTRESS MECHANISMS

The two basic mechanisms leading to the development of reflection cracking are 1) horizontal movements of the underlying slab, and 2) differential vertical movements across a pavement discontinuity in the original surface, i.e. joint or crack (Ref. 5, 6, 7, 8). As stated by Finn (Ref. 8), "a well-developed and generally accepted description of the mechanisms and response variables associated with reflection cracking has not been established." There has been a considerable amount of field observations and theoretical analyses concerning reflection cracking, but there have not been many controlled projects where sufficient data were obtained to accurately determine the effects of factors associated with this type of cracking (Ref. 10). In the following sections, a brief explanation of the two basic mechanisms leading to reflection cracking is presented.

Horizontal Movements

It has been generally accepted that the major cause of reflection cracking is due to horizontal movements as a result of expansion and contractions of the existing PCC slab from temperature and moisture changes. These cracks usually start to occur within the first year of service and then accelerate with traffic and the initiation of the first crack (Ref. 2, 10, 11). Because of the bond between the overlay and concrete pavement, the tensile forces developed from joint movements are transferred to the asphalt concrete, thus the asphalt tensile stresses become critical in the area above the joints (of cracks). This development of reflection cracking due to environmental loading is dependent upon the magnitude and rate of temperature drop, slab length, overlay thickness, gauge length across the joint, and properties of the resurfacing material. Hence, these factors must be included in any model used to evaluate the environmental effects. Data available concerning asphalt concrete overlays over existing asphalt concrete also indicate this to be a problem (Ref. 12, 13, 14, 15). Some attempts have been made to measure the magnitudes of these including the work of Dantin in Arkansas (Ref. 16, 17).

Differential Vertical Movements

Not only can volume changes in the underlying materials contribute to the development of reflection cracking, but repeated traffic loadings induce, in a flexural way, shear stresses which can cause reflection cracking (Ref. 9). Traffic loadings produce differential movements at discontinuities (i.e. joints and cracks) resulting in shear stress concentrations in the overlay material at the joints (Ref. 43, 44). Therefore, reflection cracking caused by differential vertical deflections is a shear-fatigue phenomenon and is dependent on the magnitude of the differential deflection which exists across the joint or crack. The factors which are important in differential deflections are magnitude of load, amount of load transfer across the joint or crack, the differential subgrade support underneath the slab, and/or the existence of voids.

Hence, as was the case previously, any model for evaluation should consider these factors.

SUMMARY OF LITERATURE REVIEWED

A large number of references have been collected and reviewed to evaluate the current state of the art, for the prevention of reflection cracking. A great deal of this information comes from a previous study performed by ARE Inc for the Federal Highway Administration (Ref. 1), a review prepared by the U.S. Army Engineers Waterways Experimentation Station (Ref. 3), and the list of references compiled by Dantin (Ref. 16). The extensive reference list in this report can be reviewed in more detail; however, for the reader's benefit, the information is summarized herein. First, the advantages, disadvantages, and concepts are summarized relative to the different types of preventative methods used. Even though field experience and some laboratory work has been conducted, solutions to the problem are only in the early stage of development. This is because much of the detailed information from field studies are inconclusive due to the limited age and/or the amount of data collected. Next, a summary of experience nationwide is presented in a format that the user may apply to his problem. The third section is a summary of the Arkansas experience.

Preventive Methods Used

The primary objective of any overlay design is to provide a highway with adequate performance over a maximum useful life with minimum required maintenance. Asphalt concrete overlays represent the most widely used and accepted form of roadway resurfacing due to low initial cost, ease of application and surface characteristics. Therefore, most information given on preventive methods is concerned with asphaltic concrete overlays, for which reflection cracking is more severe than for PCC overlays.

Existing methods of analysis and design of overlays do not consider the problem of reflection cracking directly. However, several techniques have been used experimentally for the control of reflection cracking. These have varied from placing a material over the crack to prevent bonding of the overlay at the point, to breaking the pavement itself into smaller pieces prior to overlaying. These treatments, none of which have become universally accepted, generally fall into one of the five classifications:

1) Treatments to existing PCC pavements,
   - Crack filling and sealing
   - Breaking and seating pavement
   - Subsealing joints and cracks
2) Stress or strain relieving interlayers,
   - Bond breakers
   - Fabrics
   - Tack or seal coats
3) Cushion courses,
4) Special overlay treatments,
   - Fabric or steel reinforcement
   - Asphalt specifications and additives
5) Increased overlay thickness.

Based on the factors influencing the development of reflection cracks, it was possible to evaluate the various techniques by considering how they should perform with respect to the mechanism causing failure.

Tables 2.1 through 2.5 list the advantages, disadvantages, pertinent comments, and some reference sources for each preventative method reviewed. In preventing these cracks, the treatment, to be of practical application, not only should eliminate reflection cracks, but should not: 1) reduce the strength, stability, or service life of the overlay of existing pavement, 2) add excessive costs, 3) delay construction progress, nor 4) require special skills, techniques or equipment (Ref. 6, 7).

Table 2.1. Treatments to Existing PCC Pavements.

Preventative Method	Advantages	Disadvantages	Comments	References
Crack Sealing and Filling	* Stops moisture from entering base	* Does not prevent horizontal or differential vertical movements	* Normally used only for AC pavements	2, 23, 24
		* Can result in blowups in PCC	* Has not produced significant reduction in reflection cracking	
		* Labor intensive		
Breaking and Seating PCC Pavement	* Reduces horizontal movement potential (smaller pieces)	* Not effective on existing PCC pavements on strong subgrades	* Does reduce reflection cracks in overlays of PCC pavement on weak subgrades	2, 6, 13, 25, 26, 27, 28, 29, 30, 31, 32, 33
	* Reduces differential deflection caused by voids	* Loss of structural integrity in existing PCC thereby requiring extra AC overlay		
	* Stops slab rocking	* Added construction costs		
Subsealing of Joints and Cracks	* Reestablishes lost support	* Expense	* Works well where differential deflection conditoins cause reflection cracking to vertical movements	9, 13, 34, 35, 36, 37, 38, 39
	* Increases the strength of foundation materials	* Not effective against the mechanism of horizontal movements		
	* Reduces differential vertical movements			

Table 2.2. Stress or Strain Relieving Interlayers

Preventative Method	Advantages	Disadvantages	Comments	References
Bond Breakers (sand, wax paper, aluminum foil, building paper, stone dust, metal strips, etc.)	* Increases gauge length for strain development * May waterproof lower layers * Does not effect drainage or vertical clearance requirements	* Adds no structural capacity to the pavement * Does not improve existing problems of voids or differential vertical deflections * Shoving or rippling may occur in areas of accleration or braking	* No major benefits are gained for the cost unless overlay is PCC over PCC	2, 13, 15, 40, 41, 42, 43, 44
Fabrics	* Increases gauge length for strain development * Waterproofs lower layers * Can be used only at joints * Doesn't effect drainage or vertical clearance requirements	* No ability to distribute shear stress * Expensive	* Has shown good results where vertical differential deflections are not a problem	3, 15, 40, 41, 42, 43
Tack or Seal Coats	* Quick and easy * May increase guage length * Waterproofing * Addition of ground tread rubber in emulsion form has shown potential to reduce reflection cracking	* Costly * No real demonstrated success at preventing reflection cracking * May bond AC to PCC thereby causing increased strain due to PCC slab horizontal movement * Shoving or rippling may occur in the AC overlays	* There are mixed results in the performance documented to date	40, 41, 42, 43

Table 2.3. Cushion Courses

Preventative Method	Advantages	Disadvantages	Comments	References
Granular or Asphalt Treated Cushion Courses	* Helps insulate existing slab thereby decreasing localized horizontal movements	* Introduction of water conduit or reservoir between layers	* A costly solution which must nonetheless be carefully designed	2, 6, 16, 22, 25, 33, 45, 46, 47
	* Decrease the transfer of existing horizontal movements to the new overlay	* Critical stresses in overlay can be increased, depending on modulus and thickness of cushion course, causing failure of overlay by fatigue		
	* Absorbs some of differential deflections at joints and cracks	* Cost and availability of high quality of granular materials		
		* Increased elevation of roadway		
		* Structural capacity of existing roads not fully utilized		

Table 2.4. Special Overlay Treatments

Preventative Method	Advantages	Disadvantages	Comments	References
Steel or Fabric Reinforcement	* Increases strength of overlay layer * Fabrics can reduce temperature related cracks but cannot distribute shear stresses * Steel can distribute both vertical and horizontal stresses * Fabrics add waterproofing barrier	* Corrosion problems have been documented for steel reinforcement * Both reinforcements are costly	* Can be an effective measure to to increase the strength of overlay, however, results to date are still experimental * There exists a wide variability in documented results	3, 7, 19, 20, 30, 34, 42, 48, 49, 50, 51, 52
Special Asphalt Mix Specifications	* Some cracks may heal in warmer weather * Overlay could absorb more vertical and horizontal movement prior to cracking * No problems associated with grade change	* Permanent deformation may become a problem * Availability of admixture (granulated rubber) or specific grade of asphalt may cause excess expense	* Strains indicated in severe climates are greater than even softest mixture can endure * Fillers and additives alone have not been shown to increase performance for a long time	2, 6, 7, 12, 13, 53, 54, 55, 56, 57, 58, 59, 60, 61

Table 2.5. Increased Overlay Thickness

Preventative Method	Advantages	Disadvantages	Comments	References
Increased Overlay Thickness	* Retards initiation and growth of cracks	* Cost	* Regardless of thickness some degree of reflection cracking can be expected	6, 7, 16, 23, 30, 32, 48, 62, 63
	* Insulates existing pavement from excessive temperature change	* Problems with drainage and structure clearances	* Economically ineffective	
	* Reduces differential vertical deflection problems	* Does not alter gauge length for decreasing strain due to horizontal movements		

Summary of Experience Nationwide

Past reflection cracking studies for the most part have been of an empirical nature with no concentrated research effort. Studies to estimate the life expectancy of each treatment have been neglected and adequate documented data is scarce. A major problem, in general is that there have not been adequate studies of the existing pavement prior to overlay; to determine existing conditions and to develop an answer to the following questions.

- What are the joint/crack movements as a function of temperature?
- What are the deflections either side of the joint/crack (differential deflection)?
- What are the existing crack patterns?
- What are the strengths and thicknesses of existing layers?

No one treatment is a cure for all situations; rather, the reported crack preventing methods should be integrated into an overlay design, directly tailored to the nature of distress (Ref. 16). Figure 2.1 shows a flow diagram which lists each type treatment that could be considered depending on the existing failure mechanism. The user proceeds downward in the chart to isolate the mechanism producing the distress, then one of several specific treatments may be selected. Figure 2.2 summarizes where the various techniques reviewed in the literature were used. Note that every state has used at least one technique while most states have tried several. Thus, the techniques have been exposed to a wide variety of environmental conditions. When using these charts, it should be kept in mind that careful evaluation and consideration should be given in selecting a treatment so that other distress mechanisms (rutting, disintegration, shoving, fatigue cracking, etc.) do not develop.

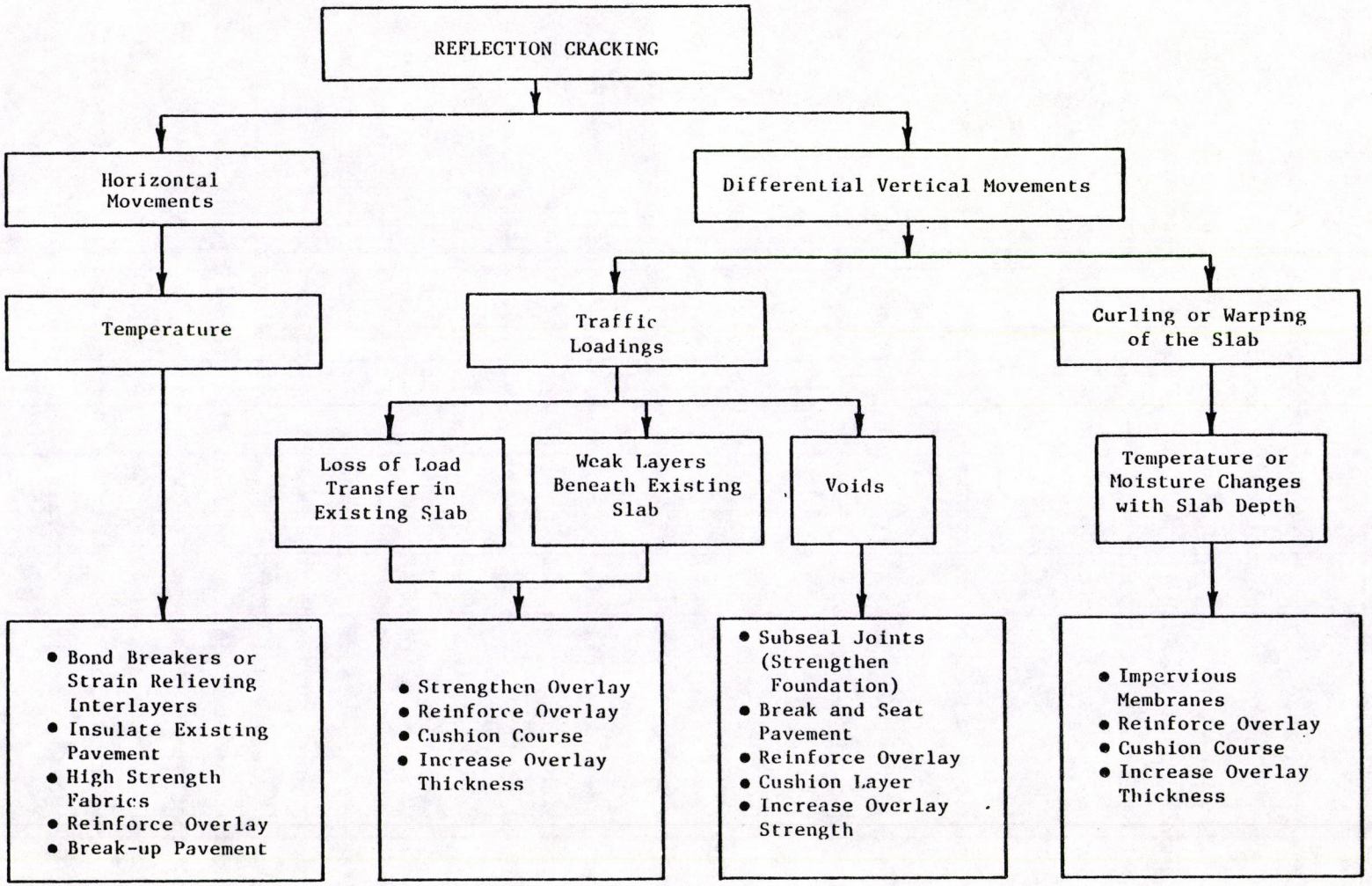

Figure 2.1. Flow diagram to determine a treatment which can be considered to reduce reflection cracking (after Ref. 1).

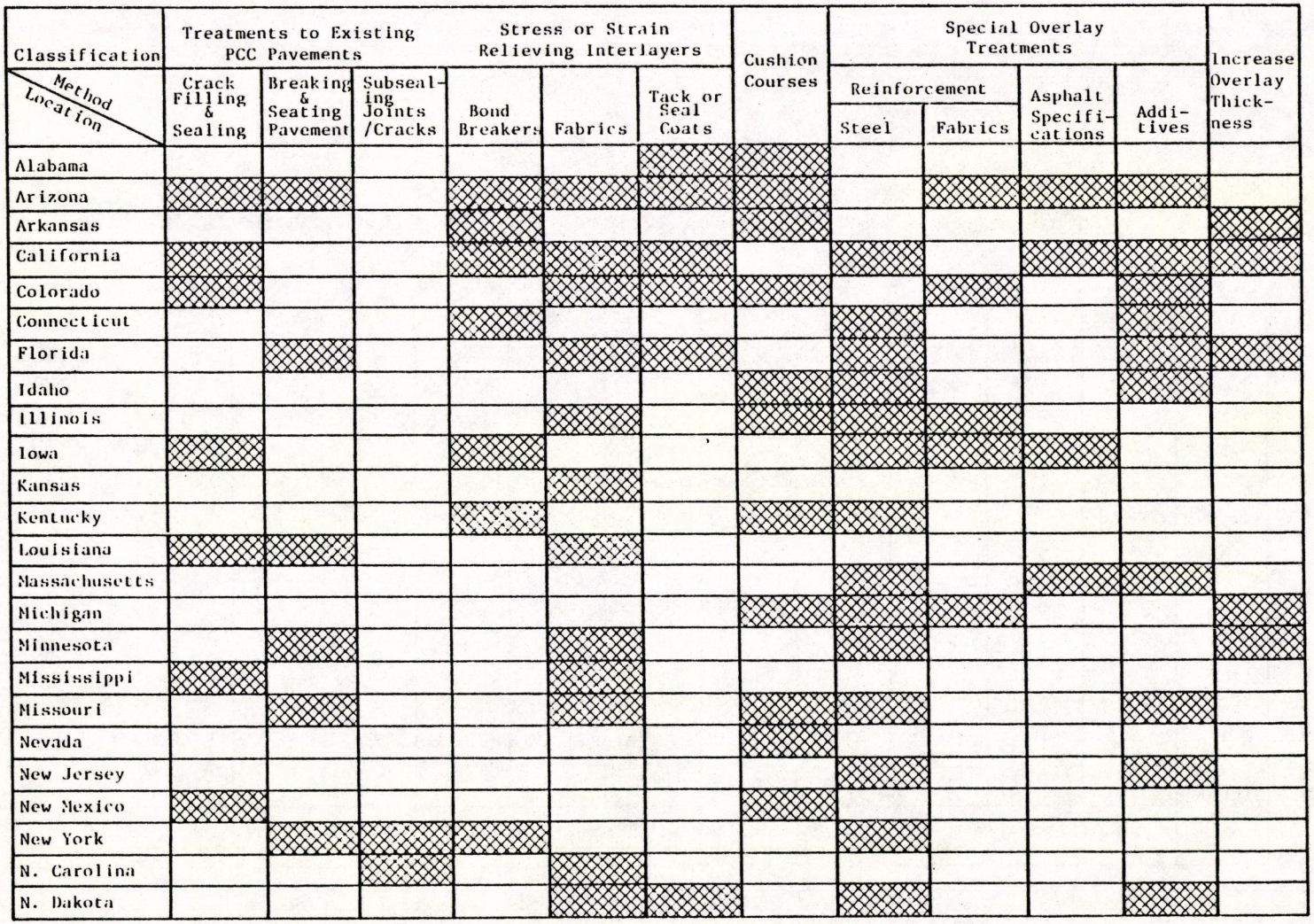

Figure 2.2. Various locations reviewed, where a method or type of treatment has been applied (after Ref. 1).

Classification	Treatments to Existing PCC Pavements			Stress or Strain Relieving Interlayers			Cushion Courses	Special Overlay Treatments				Increase Overlay Thickness
								Reinforcement		Asphalt Specifications	Additives	
Method / Location	Crack Filling & Sealing	Breaking & Seating Pavement	Subsealing Joints /Cracks	Bond Breakers	Fabrics	Tack or Seal Coats		Steel	Fabrics			
Oklahoma				▨	▨		▨					
Oregon			▨		▨							
Pennsylvania			▨	▨	▨			▨	▨		▨	
S. Carolina				▨	▨	▨	▨	▨				
S. Dakota					▨			▨				
Tennessee							▨					
Texas	▨	▨			▨	▨	▨	▨			▨	▨
Utah							▨				▨	
Vermont						▨		▨				
Virginia				▨	▨							
Washington			▨	▨			▨					
Wisconsin							▨	▨				
Wyoming	▨				▨		▨				▨	

Figure 2.2. (Continued) Various locations reviewed, where a method or type of treatment has been applied (after Ref. 1).

Summary of Experience in Arkansas

As Figure 2.2 and our discussions with AHTD engineers have indicated, Arkansas has experience with 1) the use of strain relieving interlayers, in particular the bond-breaker material known as SAMI, stress absorbing membranes interlayer, 2) the use of cushion courses, (including the asphalt treated open-graded course) and 3) conventional hot mix asphalt concrete overlays. Table 2.6 shows a listing of Arkansas highways where the various combinations of cushion courses, SAMI materials, and hot-mix asphalt concrete overlays have been used. There were a large number of sections constructed in 1978 and of particular significance were the experimental test sections located on Highway 70 and a section on I-30 which has a number of instrumented overlay measurement devices (Ref. 16) which were evaluated as a part of this study.

Various material combinations and thicknesses have been used and future monitoring of these sections will provide better information upon the performance of the various types of preventative measures implemented in Arkansas. Dantin indicates (Ref. 16) that there is seven years of experience using a 3-layer system, where a 3 inch top-size aggregate open-graded course is overlayed with binder and surface courses which has been 100% effective in eliminating reflection cracking.

CONCLUSIONS

The review of existing literature results in several conclusions which must be considered in the development of any procedure to analyze reflection cracking:

1) Both vertical and horizontal movements must be controlled to reduce or prevent reflection cracking.

Table 2.6. Examples of preventative measures which have been used in Arkansas.

Highway	Section	Cushion Courses			Stress Relieving Interlayer	Hot Mix Asphalt Concrete Overlay		
		ASTCSBS†	CSBCB	OGB	SAMI	HMBC	HMSC	PMS
71	16	*				*	*	
IH 40	51		*			*	*	
IH 55	11		*			*	*	*
US 65	19		*			*	*	*
70	20							*
70	20			*				*
70	20			*	*			*
70	20				*			*
US 67	18		*			*	*	*
IH 30	22		*			*	*	

† ASTCSBS - Asphalt Treated Crushed Stone Base Course
CSBCB - Crushed Stone Crack Relief Layer
OGB - Open Graded Base Course
SAMI - Stress Absorbing Membrane Interlayer
HMBC - Hot Mix Binder Course
HMSC - Hot Mix Surface Course
PMS - Plant Mix Seal

2) Some preventative measures may only be applicable to one of the two principle distress mechanisms, and therefore the use of these solutions as a universal cure-all is highly suspect.

3) There is no substitute for detailed measurement studies prior to an overlay and continuing throughout the life of the section.

The vast majority of experience in Arkansas to date is of a limited nature from a time standpoint since many of the techniques which have been tried have only been in place since 1978. It is hoped that a careful study will continue to be made of these sections so that available information can be gained as to how these sections are performing and used to further calibrate the analysis and design procedure developed in this study. It is recommended that any or all future experimental sections in Arkansas continue to be fully documented to ascertain existing cross-sectional characteristics prior to the construction of any experimental preventative method. The format and procedures for these measurements should take into account those required by the recommended design procedure.

CHAPTER 3

FIELD MEASUREMENTS AND DATA COLLECTION

With the methodology used in developing, calibrating and testing the new design procedure for minimizing reflection cracking in asphalt concrete overlays in Arkansas, it was necessary to obtain information of several different varieties. This chapter discusses the pertinent data that were collected and the field measurements that were made. Detailed discussion of the use and application of this information, however, is presented in the next chapter.

INSTRUMENTED OVERLAY SITES

Although the actual project for the development of the design procedure began in mid 1980, field data collection began much sooner (in 1977) through a cooperative effort between the Arkansas State Highway and Transportation Department (AHTD) and the University of Arkansas. The selection and construction of instrumented overlay sites as well as a considerable amount of the field data collected at the sites has already been documented by Dantin (Ref. 16). Consequently, only a summary of this information is presented here.

Two different sections of interstate highway were selected for instrumentation prior to and during overlay construction. One section consists of a 9-inch jointed concrete pavement (JCP) on I-30 near Benton, Arkansas. The other section consists of an 8-inch continuously reinforced concrete pavement (CRCP) located on I-40 near Forrest City, Arkansas. Three different sites were designated for instrumentation at both the I-30 and I-40 locations. Unfortunately, because of vandalism, the wiring at all the I-40 (CRCP) sites was destroyed and no data could be collected.

Basically, the instrumentation consisted of a network of Bison strain sensors placed on the surface of the original concrete pavement and within the different layers of the overlay structures. Their placement within

the three different sites (comprising the three overlay structures) is illustrated in the longitudinal pavement cross sections presented in Figure 3.1. Figure 3.2, on the other hand, provides a plan view of the pavement showing the sensor locations relative to the original slab joint.

Field data for different sensor combinations were obtained by exciting one sensor with a certain amount of current and then measuring the amount of current generated in an adjacent sensor. Since the amount of "feedback" current is proportional to the distance between the two sensors, it was possible to determine the spacing between adjacent sensors at different points in time. This provided the basis for determining the movements at the joint, both horizontally and vertically.

Horizontal Movements

Since the horizontal movements of the concrete slab are almost entirely attributable to changes in temperature, the measurements of horizontal slab movement were conducted for both daily and seasonal changes in temperature. These measurements were made during the initial AHTD - University of Arkansas study and are therefore documented in detail in the original Dantin report (Ref. 16). Figure 3.3 provides a plot of the apparent horizontal strain developed in the I-30 two-layer overlay structure at different transverse locations across the outside lane for a change in environmental conditions occurring between October 5, 1977 and February 2, 1978. As may be seen in the temperature profile provided in the lower part of the figure, the difference in temperature between the two dates is considerable, particularly at the interface between the PCC slab and the binder course. The strain diagram shown was generated using the relative sensor spacings obtained at the two temperature extremes. The dashed lines represent the theoretical tensile strains developed in the overlay as predicted by a computer program based on the finite element solution technique. As can be seen, there is relatively good consistency between the measured strains as well as good agreement between them and the theoretical finite element tensile strain.

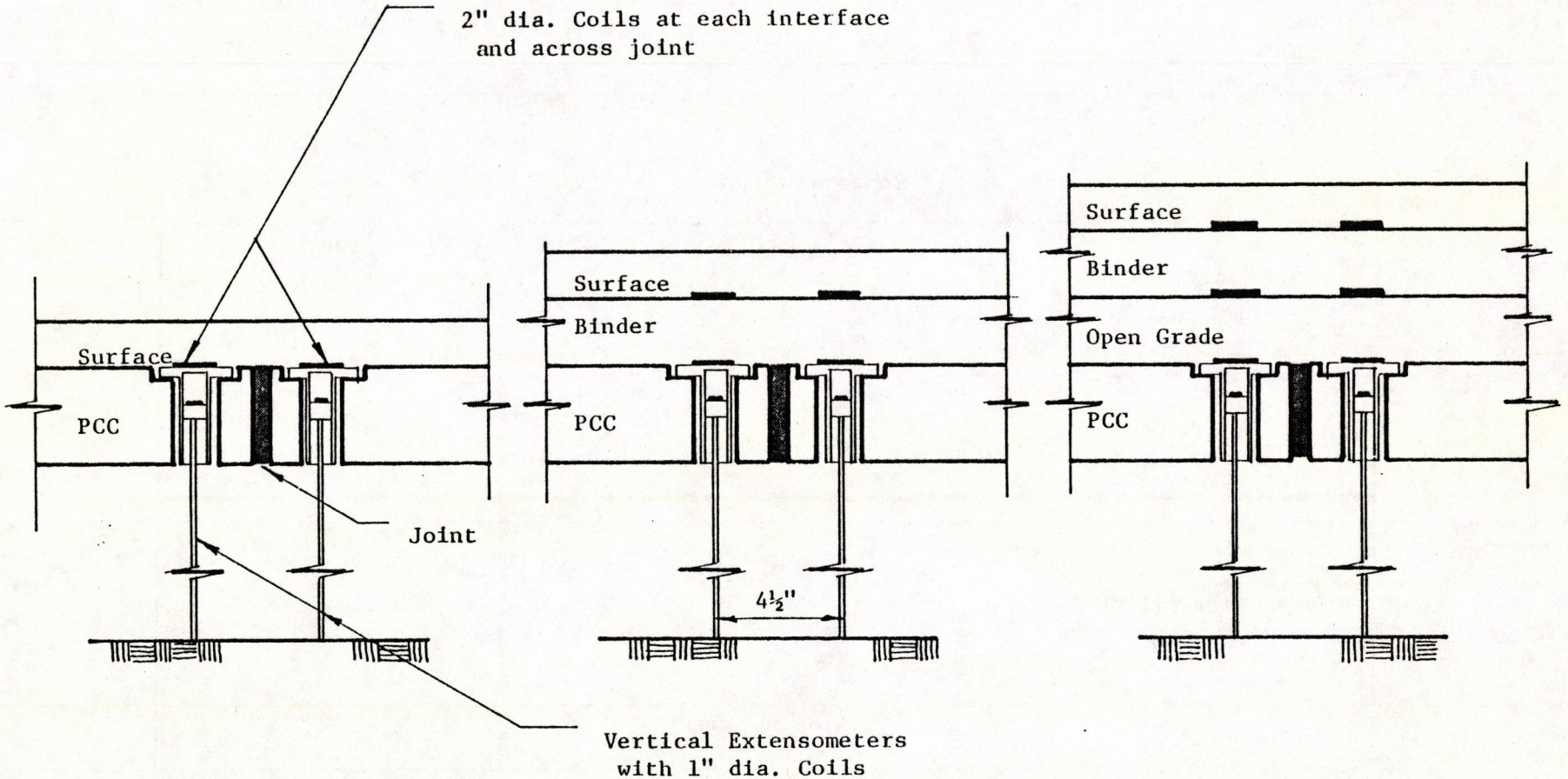

Figure 3.1. Typical Sensor Embedment Profiles for (a) One, (b) Two and (c) Three Layered Overlays (after Ref. 16).

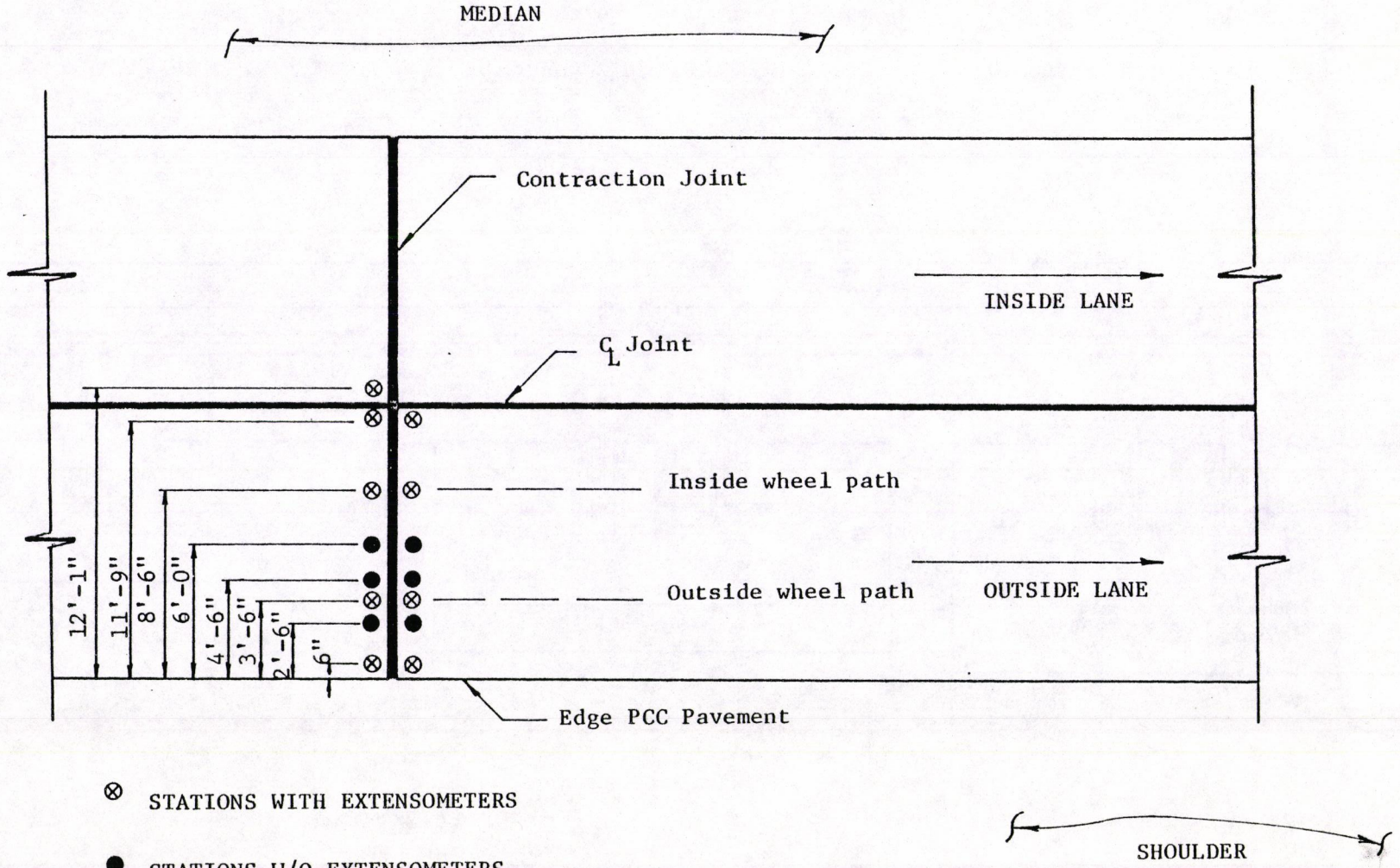

Figure 3.2. Typical Sensor edment Plan (after Ref. 16).

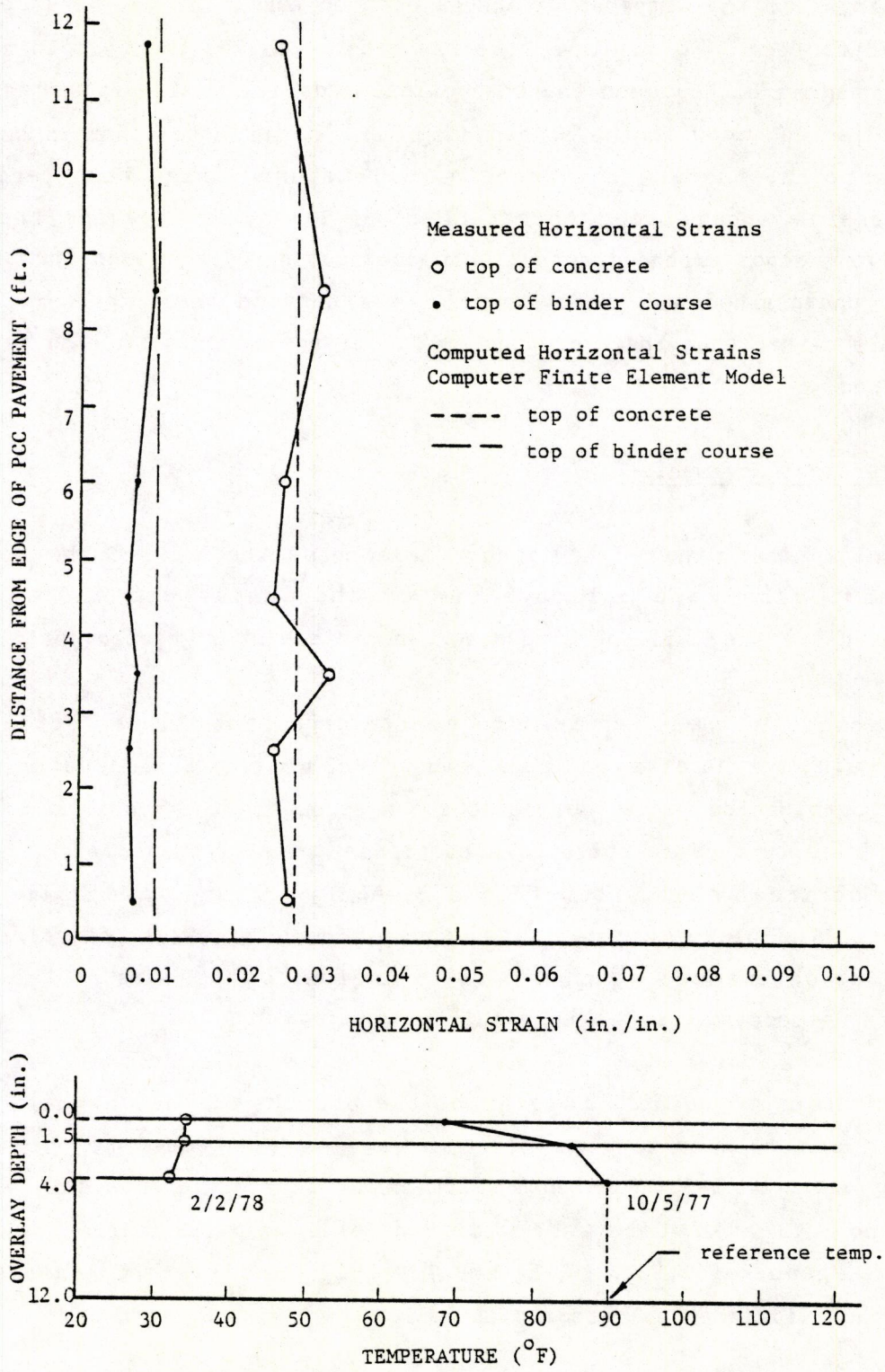

Figure 3.3. Horizontal tensile strains across the two-layer overlaid joint in the JRCP on I-30 near Benton (after Ref. 16).

In contrast, Figure 3.4 provides a similar plot of the strain resulting from the temperature change between April 15, 1977 and February 2, 1978 for the I-30 one-layer overlay site. Besides the fact that there is poor agreement between the theoretical and field values, there is one other discrepancy with the strain diagram. It indicates that in spite of the fact that there was a drop in temperature during that period, a compressive strain was generated in the overlay, meaning that the underlying slabs expanded rather than contracted. The reason for this is as yet unexplained and, unfortunately, the data in this figure represent the rule rather than the exception as far as the majority of the data are concerned.

Vertical Movements

Unlike the measured horizontal movements, the bulk of the vertical movement data were collected after the Dantin study (Ref. 16). Consequently, they will be discussed here in slightly greater detail.

Basically, these vertical movements represent the deflection of a given point in the pavement as a load travels over it. Depending on the sensor combination, these deflections can represent the vertical movement of the slab surface relative to a stationary point (extensometer reading) or the vertical movement within a given layer (e.g., the open-graded course or the binder course in the three-layer overlay structure). Thus, it can be determined which are the principal components of the total surface deflection.

In order to be able to examine the effects of load magnitude and vehicle speed, several measurements were made at the three different overlay sites on I-30 near Benton, Arkansas. Five different vehicles were used and deflection data were obtained for five different approximate vehicle speeds of 5, 20, 30, 55 and 70 mph. The different vehicles and their approximate axle loads are as follows:

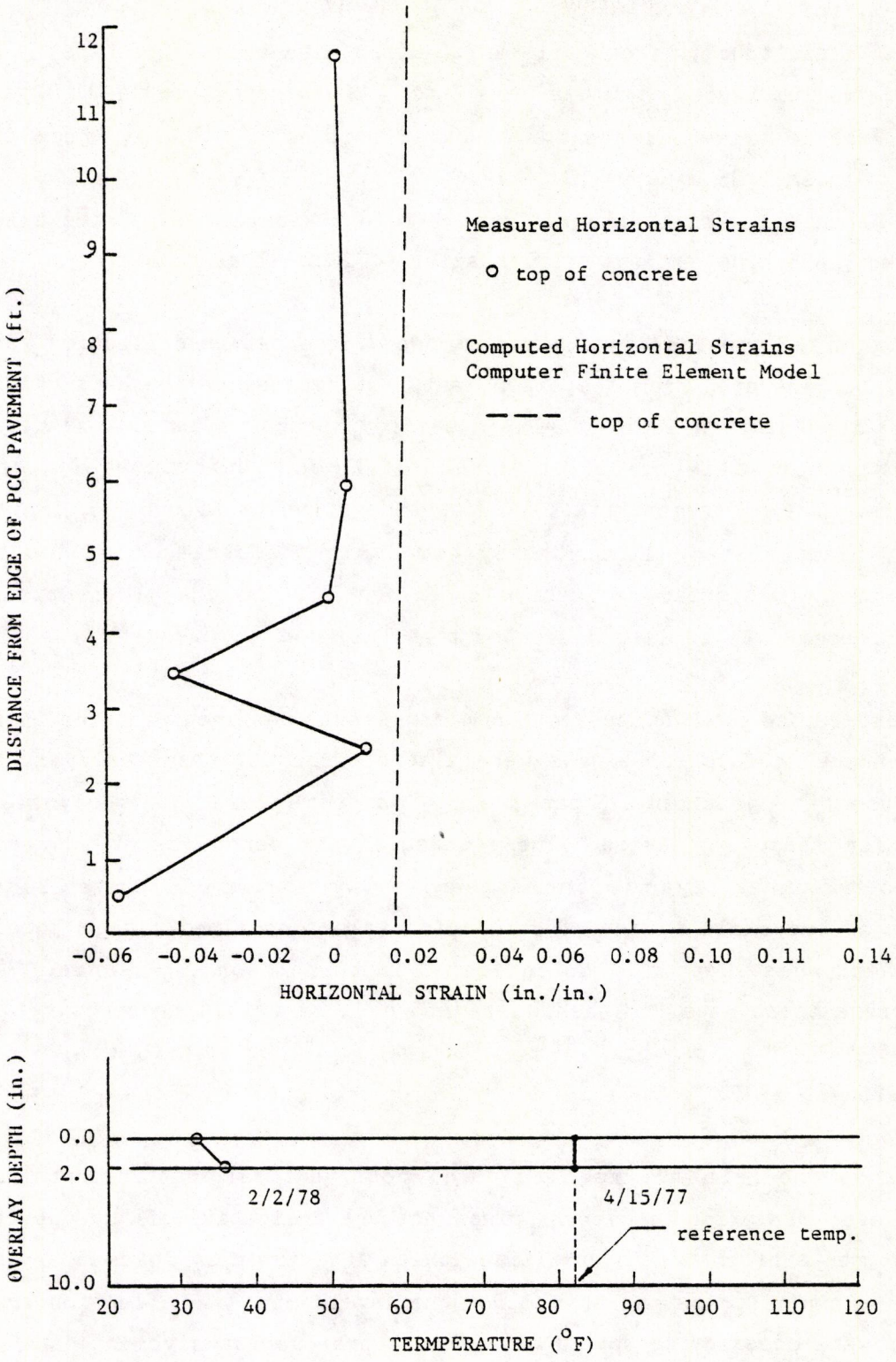

Figure 3.4. Horizontal tensile strains across the one-layer overlaid joint in the JRCP on I -30 near Benton (after Ref. 16).

1. full size automobile: front axle - 1.6 kips, rear axle - 1.6 kips;
2. small truck: front axle - 2.6 kips, rear axle - 5.2 kips;
3. medium truck: front axle - 5 to 7 kips, rear axle 14-21 kips;
4. three axle-tandem drive truck: front axle - 8 kips, rear drive axles - 35 kips;
5. tractor semi-trailer: front axle - 7 kips, tandem drive axles - 32-35 kips, tandem trailer axles - 32 to 37 kips.

Figure 3.5 provides an example of one of the better deflection versus time plots generated from the experiment. It represents the deflection of the PCC slab surface in a two-layer overlay structure during the passage of the tractor semi-trailer at a speed of 7 mph. Unfortunately, there were also many plots generated, such as that shown in Figure 3.6, in which "noise" that existed within the system during recording resulted in a significantly distorted deflection profile. Most of the plots obtained, however, seemed to be less distorted than this one.

Besides the maximum deflection measurements obtained from the in-situ coil sensors, deflection basins were also obtained at the overlay surface using the five geophones (spaced at 1-foot intervals) of the Dynaflect deflection measuring devise. These measurements were made at and around the two and three layer instrumented overlay sites on I-30 near Benton. Because of the small number of deflection values obtained, it is possible to present these data (in its entirety) in this report. Figures 3.7 and 3.8 present these data for the two and three layer sites, respectively.

NON-OVERLAYED RIGID PAVEMENTS

Since the relative magnitudes of both vertical and horizontal concrete movements prior to overlay placement are indicative of the potential for movements after overlay and since these after overlay movements represent the main distress mechanisms for the development of reflection cracking, it was necessary to obtain some actual pre-overlay movement data from

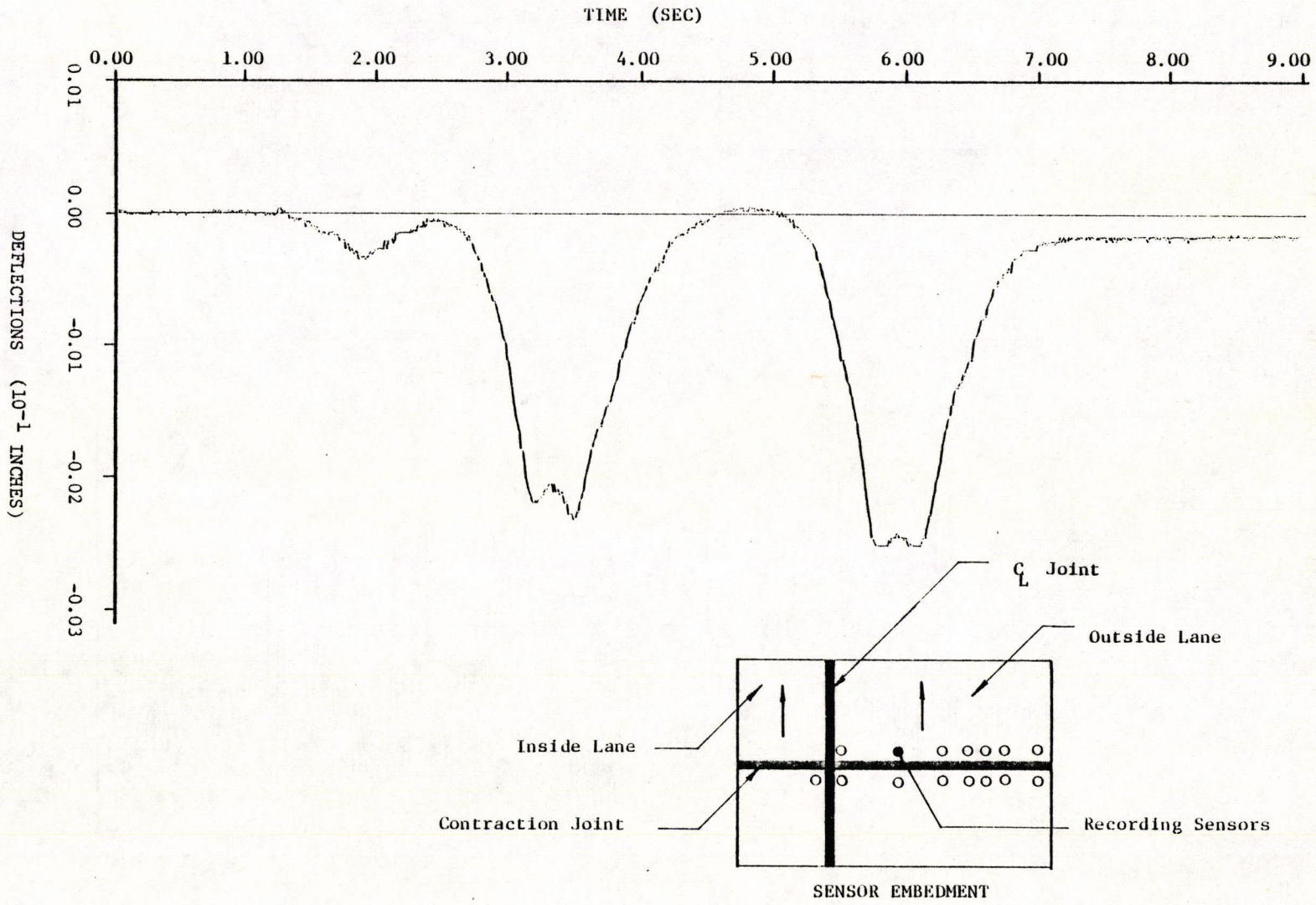

Figure 3.5. Plot of deflection of PCC slab surface versus time (extensometer reading) during the passage of the tractor semi-trailer combination at a speed of 7 m.p.h.

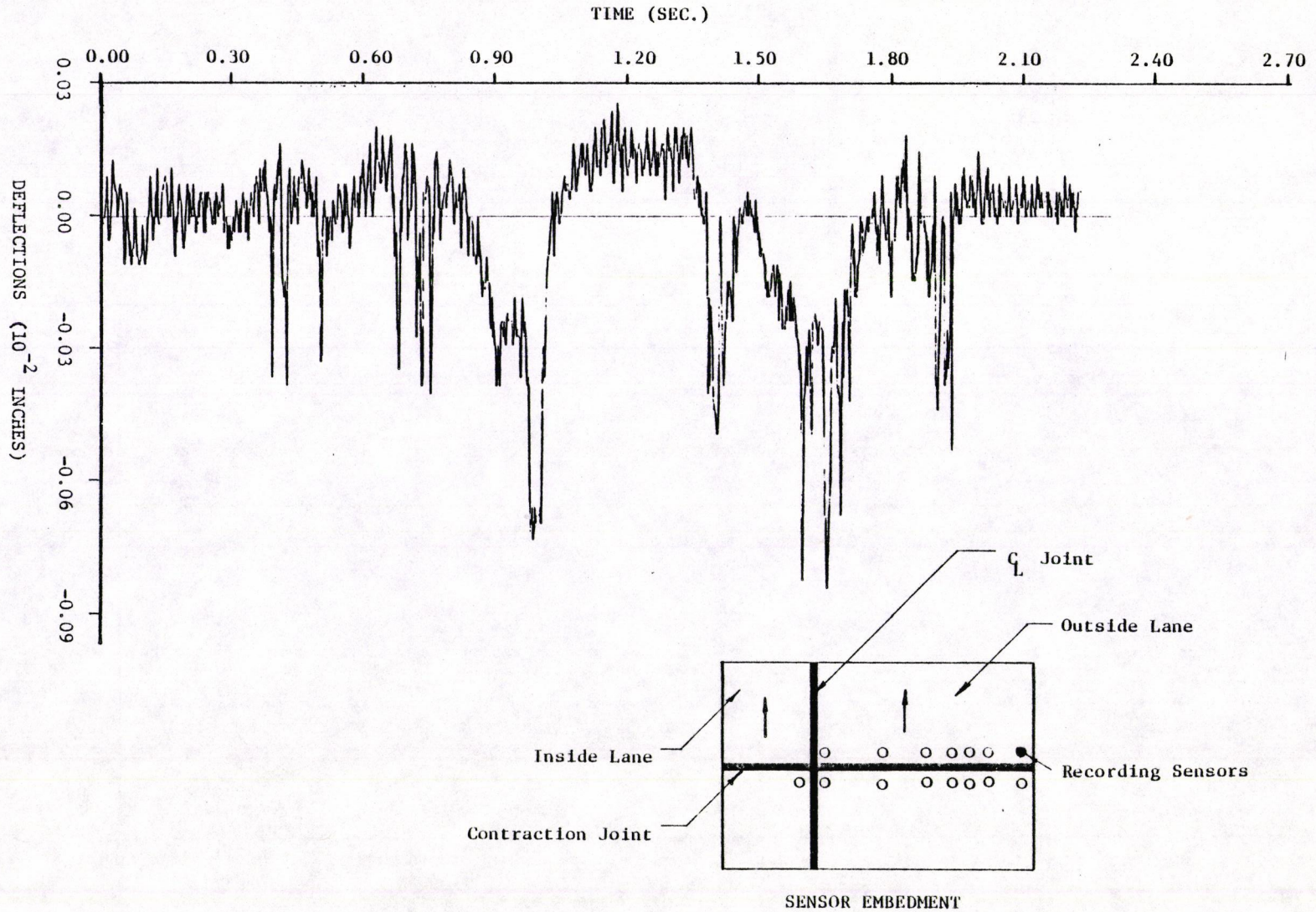

Figure 3.6. Plot of deflection of PCC slab surface versus time (extensometer reading) illustrating the presence of considerate "noise" in the system during the passage of the tractor semi-trailer combination at a speed of 28 m.p.h.

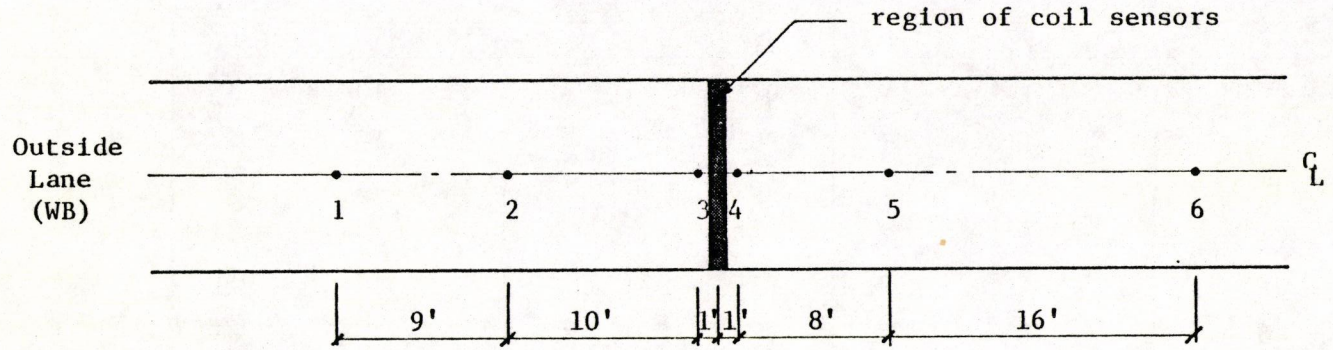

Dynaflect Readings (in milli-inches):

Location	W_1	W_2	W_3	W_4	W_5
1	.29	.23	.17	.14	.12
2	.28	.21	.16	.14	.12
3	.32	.23	.16	.12	.10
4	.30	.22	.15	.13	.12
5	.24	.18	.13	.11	.10
6	.29	.22	.15	.13	.11

Figure 3.7. Dynaflect deflection basin measurements for instrumented 3-layer overlay site on I-30 near Benton, Arkansas (81/8/12).

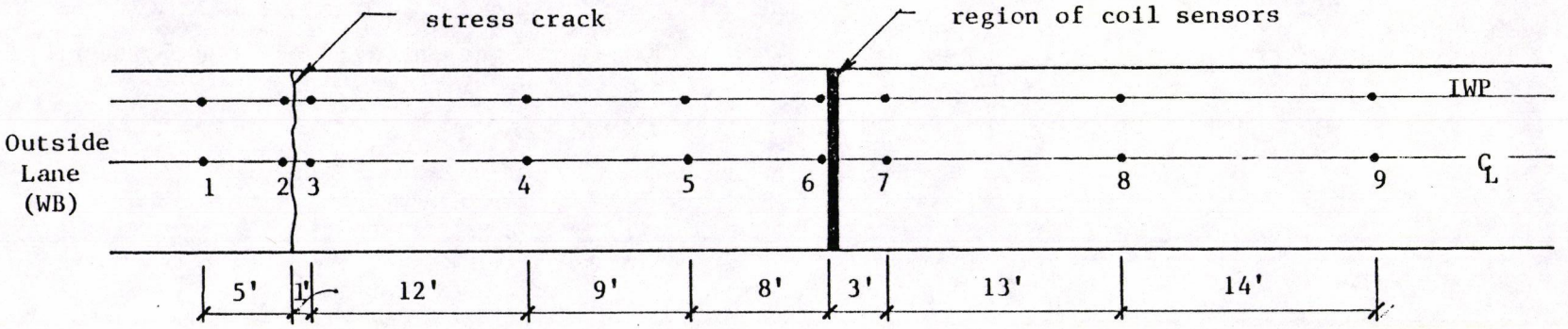

Dynaflect Readings (in milli-inches):

Location	Centerline of Lane (℄)					Inner Wheel Path (IWP)				
	W_1	W_2	W_3	W_4	W_5	W_1	W_2	W_3	W_4	W_5
1	.19	.14	.10	.09	.08	.23	.16	.11	.09	.08
2	.19	.14	.10	.09	.08	.24	.15	.10	.09	.08
3	.22	.14	.10	.10	.08	.23	.15	.10	.09	.08
4	.25	.18	.14	.12	.10	.26	.18	.13	.12	.10
5	.21	.16	.12	.11	.09	.25	.18	.12	.11	.09
6	.20	.17	.13	.11	.08	.22	.16	.12	.10	.08
7	.23	.18	.12	.10	.08	.22	.16	.12	.11	.09
8	.21	.18	.14	.12	.10	.30	.19	.13	.12	.10
9	.30	.25	.20	.17	.14	.26	.24	.18	.16	.14

Figure 3.8. Dynaflect deflections basin measurements for instrumented 2-layer overlay site on I-30 near Benton, Arkansas (81/8/12).

typical concrete pavements in Arkansas. These data were obtained by AHTD using methods similar to if not exactly the same as those which are recommended in the new design procedure. Once again for discussion purposes, these movement data is broken down into two categories, horizontal slab movements and vertical slab movements at the joint.

Horizontal Movements

As mentioned previously, horizontal movements of a concrete slab are almost entirely related to thermal contraction and expansion which occur during changes in temperature. Accordingly, a procedure was developed for measuring the movement of a slab along one to three daily temperature cycles. In this procedure, holes were drilled in specific locations of the concrete slab, brass bolts inserted and securely embedded with epoxy. The head of the brass bolts then served as the reference points for measurements of slab movement.

Figure 3.9 provides a diagram showing the locations of these brass bolts relative to the joint between two slabs. Using this pattern, it is possible to obtain the change in joint width at two transverse locations along the joint, A-B and C-D. Furthermore, with bolt E on the shoulder, it is possible to determine if one slab is moving more or less than the one adjacent to it.

Two non-overlayed jointed pavements were also prepared to obtain these measurements of horizontal slab movement. Both jointed pavements are located on I-30 near Benton. One had a 26-foot joint spacing, and the other, is the same type of JRCP underlying the instrumented overlay sites, i.e., 45-foot slabs with 15-foot warping joints. In the case of the 26-foot JCP, data were obtained from six consecutive joints. For the 45-foot slabs, ten consecutive joints (counting the warping joints) were outfitted and measured. The data obtained from the measurements on these two sections are presented in Tables 3.1 and 3.2, respectively.

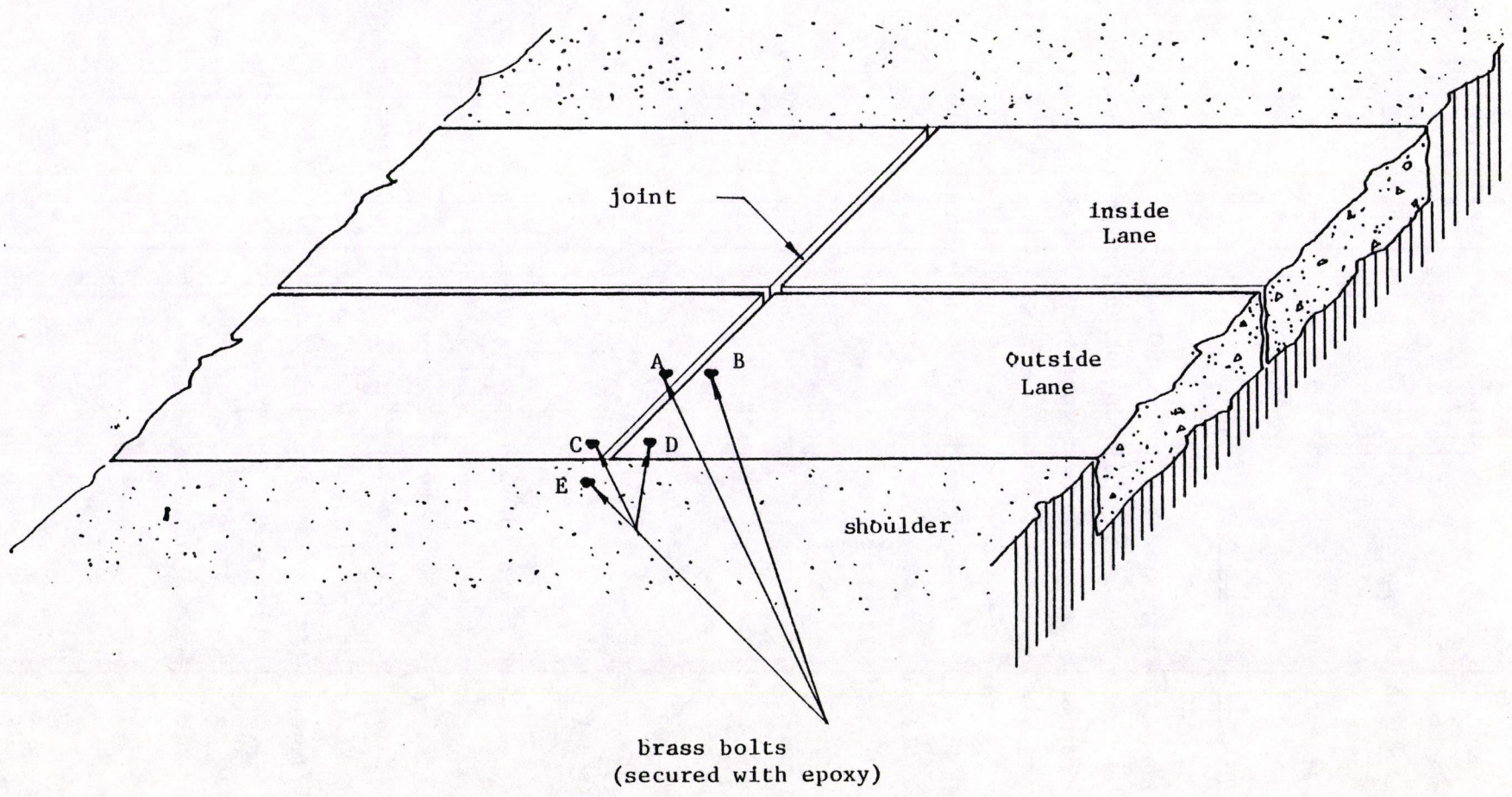

Figure 3.9. Diagram showing brass bolt locations relative to the slab joint and pavement shoulder.

Table 3.1. Field measurements of slab movement on a section of 26-foot JCP on I-30 near Benton, Arkansas.

DATE	JOINT 1			JOINT 2			JOINT 3			JOINT 4			JOINT 5			JOINT 6		
	Temp.	Edge	Int.	Temp.	Edge	Int.	Temp.	Edge	Int.	Temp.	Edge	Int.	Temp.	Edge	Int.	Temp.	Edge	Int.
8/19/80	86	8.0150	8.0200	86	8.0395	*7.96	86	8.0528	8.0605	86	8.0896	8.0905	88	8.0751	8.0566	88	8.0039	8.0359
	93	8.0050	8.0075	93	8.0204	*7.96	95	8.0379	8.0401	97	8.0684	8.0696	97	8.0700	8.0358	97	8.0060	8.0009
	122	8.0000	8.0035	100	8.0081	*7.94	102	8.0201	8.380	104	8.0686	8.0569	102	8.0642	8.0294	102	8.0005	8.0015
	126	*7.99	8.0040	104	8.0011	*7.94	106	8.0136	8.0140	104	8.0415	8.0508	108	8.0502	8.0161	109	8.0001	8.0088
				118	8.0171	*7.94	118	8.0038	8.0152	117	8.0325	8.022	117	8.0092	8.0061	117	*7.98	8.0071
				122	8.0012	*7.94	122	8.0100	8.0132	122	8.0483	8.0323	117	8.0041	8.0150	120	*7.98	8.0084
				124	8.0172	*7.90	122	8.0123	8.0204	124	8.0432	8.0445	122	8.0468	8.0101	122	*7.97	8.0041
8/20/80	100	8.0011	8.0003															
	104	8.0009	8.0005															
	122	8.0005	8.0001															
9/4/80	70	8.0252	8.0397	70	8.0609	8.0019	70	8.0778	8.0300	70	8.1194	8.0245	70	8.0915	8.0309	70	8.0530	8.0261
	117	8.0080	8.0012	117	8.0122	>8.00	117	8.0311	8.0367	117	8.0567	8.0579	117	8.0422	8.0196	117	8.0070	8.0238
9/8/80	108	8.0007	8.0000	115	8.0187	*7.99	115	8.0162	8.0269	115	8.0498	8.0402	115	8.0432	8.0102	115	8.0040	8.0151
9/9/80	68	8.0258	8.0334	68	8.0518	8.0174	68	8.00849	8.0315	68	8.1159	8.0998	68	8.1066	8.0771	68	8.0579	8.0807
9/24/80	70	8.0252	8.0471	70	8.0582	8.0102	70	8.0832	8.1042	70	8.1185	8.0239	70	8.1011	8.0720	70	8.0676	8.0705
1/5/81	25	8.1175	8.0887	25	8.1380	8.0804	25	8.1690	8.0741	25	8.1055	8.1829	25	8.1003	8.1628	25	8.1370	8.1572
1/12/81	57	8.0638	8.0700	57	8.1071	8.0576	57	8.1526	8.1525	57	8.1727	8.1663	57	8.1776	8.1475	57	8.1257	8.1342
1/13/81	28	8.0962	8.1108	28	8.1996	8.0961	28	8.1717	8.1756	28	8.1990	8.1880	28	8.1911	8.1758	28	8.1570	8.1570
	52	8.0477	8.0654	52	8.0948	8.0466	52	8.1436	8.1499	52	8.1733	8.1577	52	8.1605	8.1382	52	8.1091	8.1266

Table 3.2. Field measurements of slab movement on a section of 45-foot JRCP on I-30 near Benton, Arkansas.

Date	Surface Temp. (°F)	Joint 1 Formed		Joint 1a Sawed		Joint 1b Sawed		Joint 2 Formed		Joint 2a Sawed		Joint 2b Sawed	
		Edge	Int.	Edge	Int.	Edge	Int.	Edge	Int.	Edge	Int.	Edge	Int.
4- 1-81	110	8.0002	8.0000	8.0148	8.0479	8.0000	7.9999	8.0158	8.0207	8.0180	8.0666	8.0781	8.0075
4- 3-81	83	8.0073	8.0264	8.0355	8.0629	8.0033	7.99	8.0313	8.0357	8.0311	8.0745	8.1005	8.0119
4-15-81	77.5	8.0005	8.0168	8.0220	8.0668	8.0069	7.999	8.0271	8.0101	8.0333	8.0817	8.0882	8.0198
5-27-81	86	8.0005	8.0010	8.0106	8.0338	8.0005	7.99	8.0100	8.0331	8.0291	8.0680	8.0788	8.00
5-27-81	99.5	8.0022	8.0020	8.0195	8.0535	8.0095	7.99	8.0185	8.0218	8.0275	8.0648	8.700	8.0008
5-28-81	56	8.0025	8.0086	8.0165	8.0497	8.00	7.99	8.0186	8.0201	8.0161	8.0676	8.0731	8.0020
5-28-81	96	8.0	8.0	8.0	8.0174	8.00	7.99	8.0025	8.0194	8.0183	8.0585	8.0645	8.00
6-23-81	99.5	8.00	8.00	8.00	8.0406	7.99	7.99	8.00	8.0119	8.0122	8.0584	8.0434	8.00
6-23-81	80	8.00	8.00	8.00	8.0288	8.00	7.99	7.99	8.0253	8.0100	8.0517	8.0685	8.00
6-24-81	81	8.00	8.00	8.00	8.0452	8.00	7.99	8.00	8.0282	8.0111	8.0651	8.0309	8.00

Table 3.2. (continued) Field measurements of slab movement on a section of 45-foot JRCP on I-30 near Benton, Arkansas.

Date	Surface Temp. (^{o}F)	Joint 3 Formed		Joint 3a Sawed		Joint 3b Sawed		Joint 4 Formed	
		Edge	Int.	Edge	Int.	Edge	Int.	Edge	Int.
4- 1-81	100	8.0081	8.0155	8.0191	8.0200	8.0042	8.0076	8.0492	8.0089
4- 3-81	83	8.0188	8.0134	8.0230	8.0175	8.0248	8.0101	8.0662	8.0285
4-15-81	77.5	8.0069	8.0248	8.0391	8.0232	8.0269	8.0119	8.0810	Dest.
5-27-81	86	8.0020	8.0075	8.0155	8.0100	8.0141	8.0025	8.1145	-
5-27-81	99.5	8.0012	8.0070	8.0000	8.0105	8.0118	8.0000	8.1029	-
5-28-81	56	8.0000	8.0105	8.0191	8.0141	8.0085	8.0003	8.1211	-
5-28-81	96	8.0000	8.0000	8.0168	8.0069	8.0099	8.0000	8.1002	-
6-23-81	99.5	8.0000	8.0000	8.0000	8.0091	8.0271	8.0000	8.1028	-
6-23-81	80	7.99	8.0000	8.0044	8.0000	8.0055	8.0000	8.1040	-
6-24-81	81	8.0000	8.0000	8.0000	8.0080	8.0000	8.0000	8.1238	-

Figure 3.10 provides a typical example of one of the slab movement versus pavement surface temperature plots obtained from the 26-foot JCP. Likewise, Figure 3.11 provides an example plot for the 45-foot JRCP (with the 15-foot warping joints). In both graphs, data from both the interior and edge reference points (interior: A-B, edge: C-D) are plotted to determine if there is any difference between the movements at each location.

Inspection of the two figures indicates that measurements of slab movement on the 26-foot JCP (Figure 3.10) are quite consistent and can be considered useful for both analysis and design purposes. The typical slab movement plot for the 45-foot JRCP (Figure 3.11), however, is very inconsistent and probably inadequate for analysis. The reason for the scatter in this plot is probably because the measurements were taken over an extended period of time rather than within a two or three day cycle.

Vertical Movements

Once again, the use of vertical movements here refers to pavement deflection. In this case, however, they are taken directly on the surface of the concrete using the Dynaflect (as they will be for use in the recommended design procedure). The purpose of the measurements is to determine load transfer across the joint between two slabs. The magnitude of the load transfer, then, gives an indication of the shear forces that will be carried by the overlay.

The deflection data was obtained from the same two jointed pavements from which the horizontal slab movements were obtained, i.e., the 26-foot JCP and the 45-foot JRCP (with 15-foot warping joints) on I-30 near Benton, Arkansas. The measurements were made at two locations, at the joint and at midslab for a series of slabs. For the deflection measurements made at the joint, it was necessary to position the load wheels and the number 1 geophone of the Dynaflect on the upstream side of the joint, detach the number 2 geophone and place it on the downstream side of the joint directly across from geophone number 1. The difference

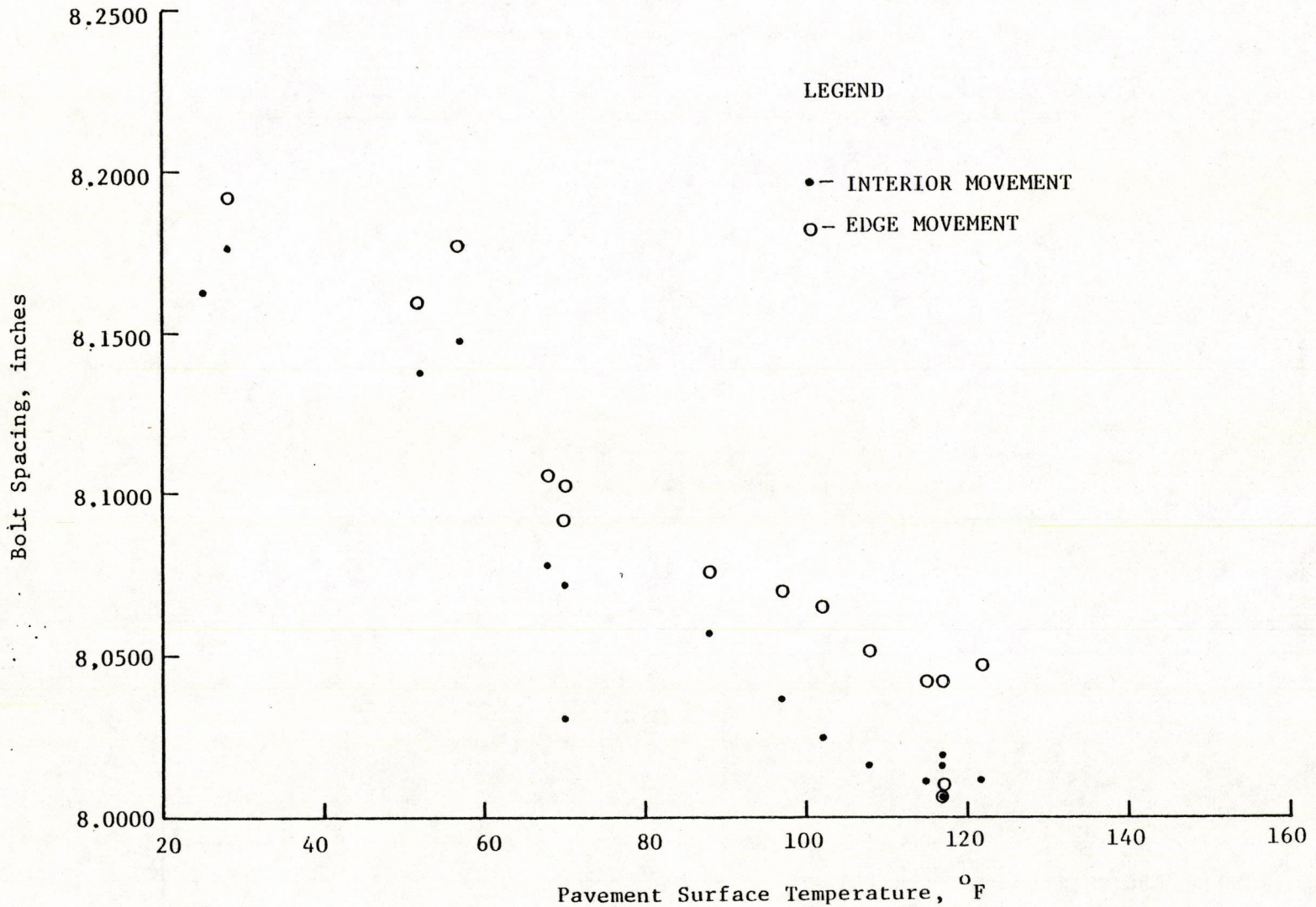

Figure 3.10. Typical plot of joint movement for 26-ft JCP on I -30 near Benton, Arkansas (Joint 5 in Table 3.1).

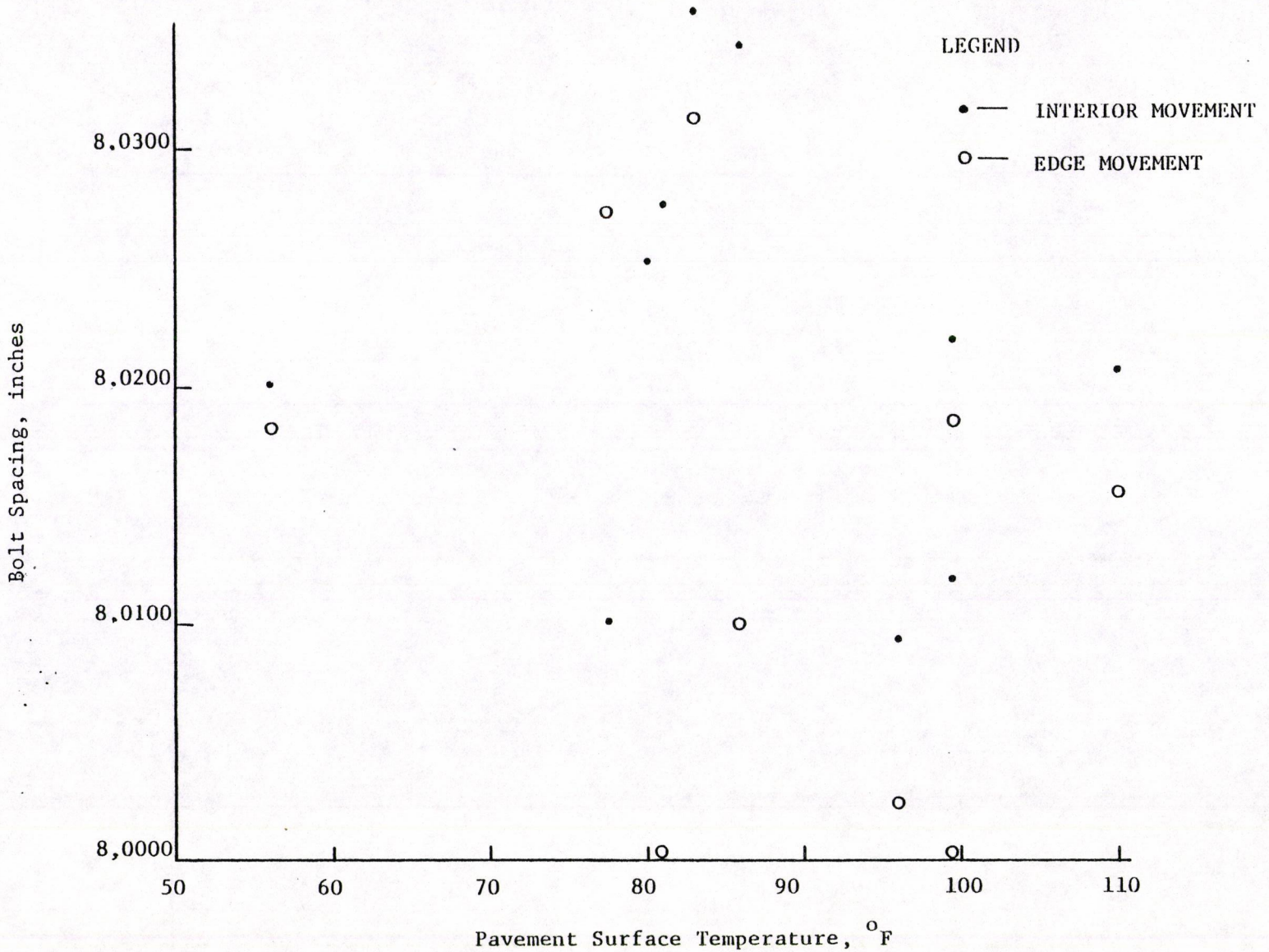

Figure 3.11. Typical plot of joint movement for 45-foot JRCP (with 15' sawed warping joints) on I -30 near Benton, Arkansas (Joint 2 in Table 3.2).

between the deflections obtained from the two geophones, then, is indicative of the load transfer at that joint.

The deflection measurements for both the 26-foot and 45-foot JRCP were obtained at two different times during the year, at the same locations. One period was during the spring (15 Apr. 81) and the other during the summer (13 Aug. 81). Figures 3.12 and 3.13 represent the deflection profiles of the 26-foot JCP during these two respective periods. Likewise, Figures 3.14 and 3.15 represent the deflection profiles for the 45-foot JRCP during these two periods. A quick inspection shows that the deflections for both pavements are considerably higher during the spring.

OVERLAY PERFORMANCE DATA

In order to provide a basis for calibrating the new overlay design procedure, it was necessary to obtain some actual field data on both the structure and performance of different overlayed pavements. Thanks to the efforts of AHTD and the Center for Transportation Research (CTR) at the University of Texas (Ref. 66) in both obtaining historic data and surveying pavements in their present condition, a considerable amount of data were collected. AHTD provided data from seven different overlay projects, while CTR was able to provide data from three overlay projects in Texas.

Arkansas Data

A summary of the pertinent data obtained from the seven Arkansas projects is presented in Table 3.3. Specific descriptions of these projects provided by AHTD are as follows:

1. Highway 71, Section 16, in Washington County was first built in 1931. The old 9"-6"-9" JRCP (edge-centerline-edge thickness) was jointed every 50 feet. We have no idea of what the base or subbase material is composed. In 1966, this section was first overlayed with 6 inches of,

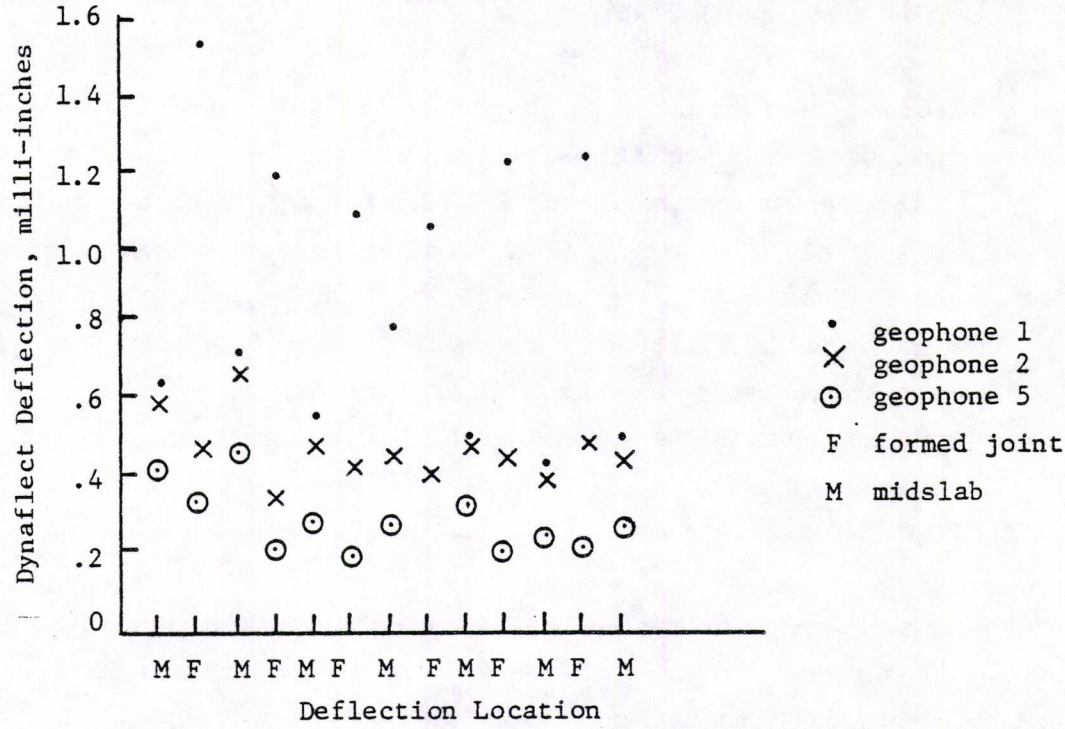

Figure 3.12. Spring Dynaflect deflection profile, 26-foot JCP on I-30 near Benton, Arkansas (15 April 1981).

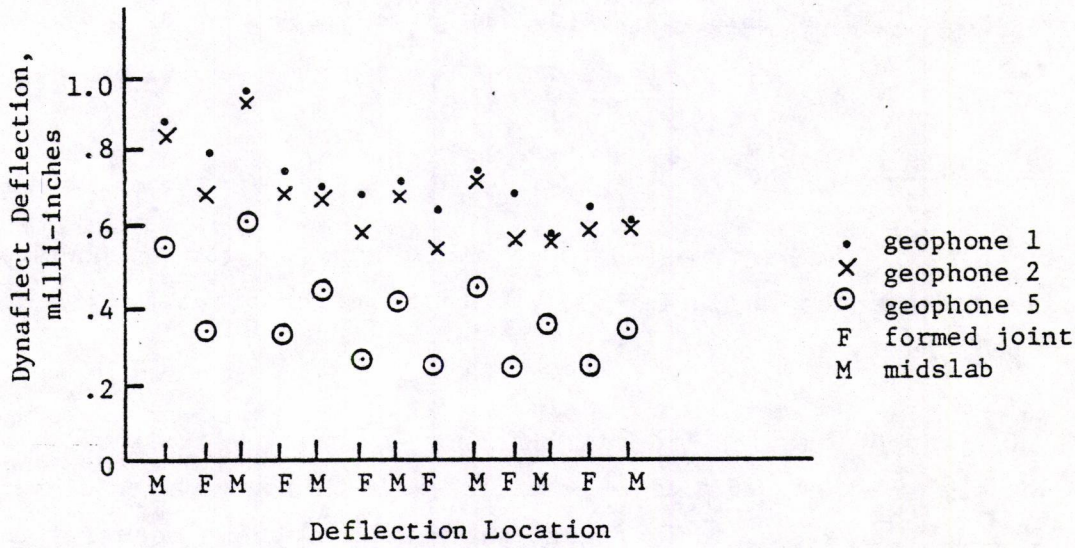

Figure 3.13. Summer Dynaflect deflection profile, 26-foot JCP on I-30 near Benton, Arkansas (13 August 1981).

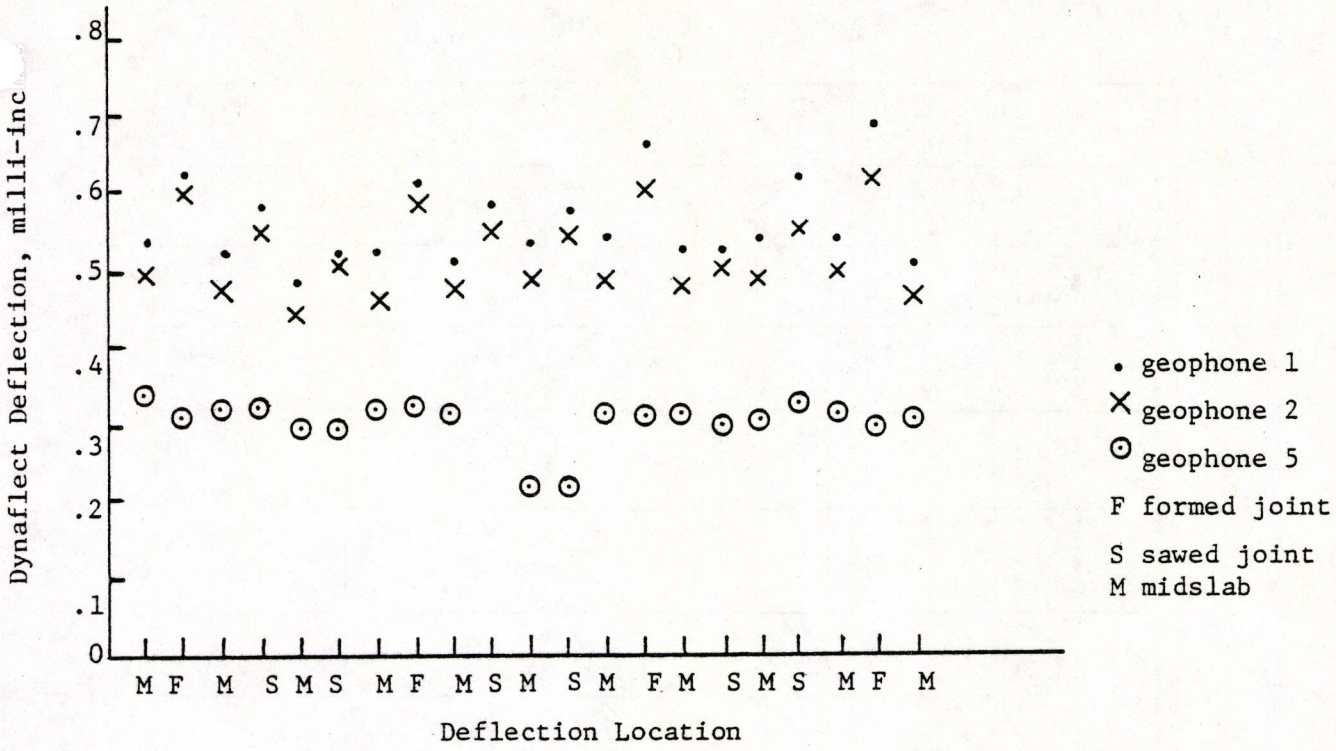

Figure 3.14. Spring Dynaflect deflection profile, 45-foot JRCP on I-30 near Benton, Arkansas (15 April 1981).

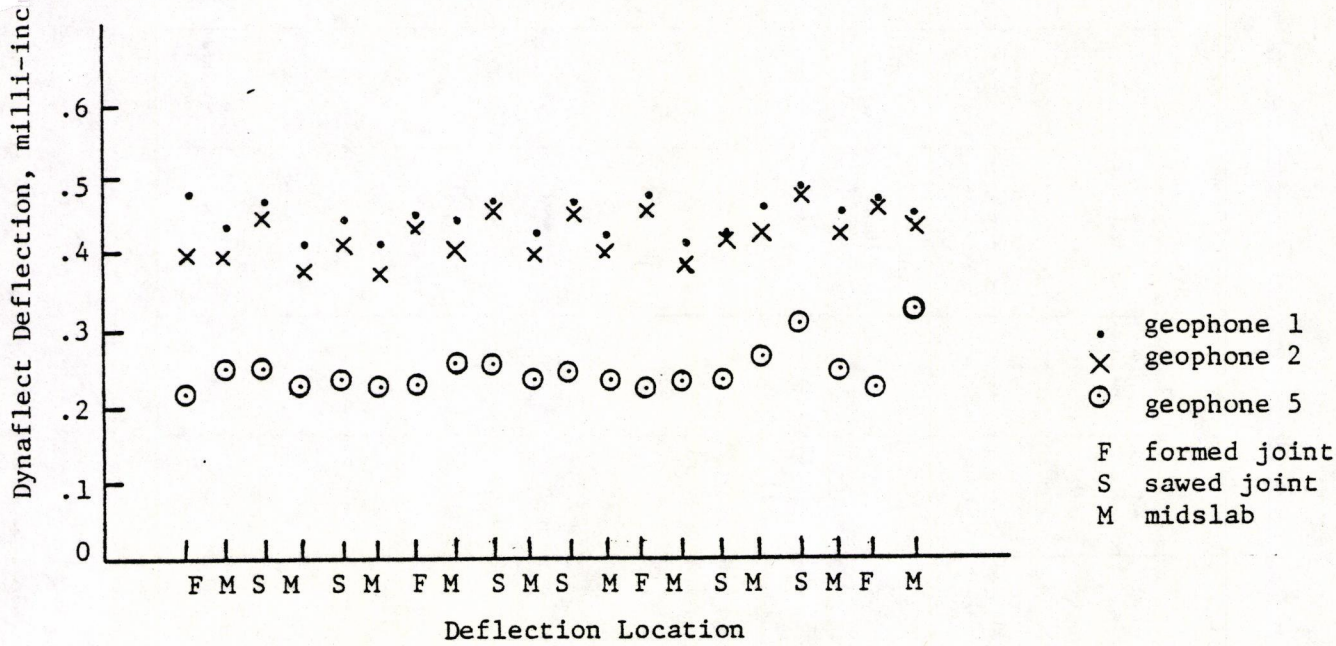

Figure 3.15. Summer Dynaflect deflection profile, 45-foot JRCP on I-30 near Benton, Arkansas (13 August 1981).

Table 3.3. Arkansas overlay performance data.

No.	Pav't Type	Joint/ Crack Spacing (feet)	Site Location	Coarse Aggregate Type	Subbase (or Base) Type	Slab Thickness (in.)	Longitudinal Steel Reinf.		Overlay Thickness (in.)			Survey Data		
							Bar Spacing (in.)	Bar Dia. (in.)	Open-Graded Course	Binder	Surface	Overlay Age (years)	Overlay Length (feet)	% Ref. Cracking
1.	JRCP	50	71/16	Sandstone	unknown	9-6-9	-	-	6.0	3.0	2.5	-	1300	100.
2.	CRCP	6	I-40/51	Terrace Sand/ Gravel[1]	gravel	8.0	4.0	.491	3.0	4.0	2.0	3	2000	none
3.	JRCP	45	I-55/11	River Gravel[1]	Unified Class SM-1	9.0	-	-	3.0	5.0	2.0	3	3000	4.5
4.	JRCP	45	65/19	River Gravel[1]	unknown	9-6-9	-	-	3.0	2.5 2.0	1.5 2.0	18 3	2200	86.
5a.	JRCP	50[2]	70/20	Chert River Gravel[1]	unknown	9-6-9	-	-			2.0 1.5	24 3	500	100.
5b.	JRCP	50	70/20	Chert River Gravel[1]	unknown	9-6-9	-	-	2.0		2.0 1.5	24 3	1000	15.
5c.	JRCP	50	70/20	Chert River Gravel[1]	unknown	9-6-9	-	-	2.0	SAMI[3]	2.0 1.5	24 3	1000	none
5d.	JRCP	50[2]	70/20	River Gravel[1]	unknown	9-6-9	-	-		SAMI[3]	2.0 1.5	24 3	700	100.
6.	JRCP	50[2]	67/18	Dolomite[1]	Unified Class SM-1	10.0	-	-	3.0	2.75	2.0	3	1100	100.
7.	JRCP	45	I-30/22	River Gravel	Crushed Gravel	9.0	0	0	4.0	4.0	2.0	4.3	1000	31.5

[1] Estimated concrete coarse aggregate type.

[2] Underlying slab may have some transverse cracks which may have reflected to the surface.

[3] Stress absorbing membrane interlayer placed prior to overlay surface c[illegible].

what was then called, asphalt treated crushed stone base course (this ASTCSBC is not our crack relief layer, but has a considerable amount of voids), 3 inches of binder and 1-3/4 inches of surface. The section was overlayed again in 1968 with 3/4 inches of a sand-asphalt overlay when the skid numbers of the surface became unacceptably low.

2. I-40, Section 51, Log Mile 262, in St. Francis County was built in 1968. The 8-inch CRCP was placed over a gravel base of approximately 12 to 18 inches. The subgrade was classified as an A-7 material. The section was overlayed in 1978 with 3 inches of CSBCB (crack relief layer), 4 inches of HMBC (binder) a 1-1/2 inches of HMSC (surface). Considerable rutting occurred in this section during the next year. Therefore, the top 2 inches was milled off in 1979 and 1-1/2 inches of surface was applied with a 1/2 inch plant mix seal course.

3. I-55, Section 11, in Crittenden County was constructed in 1959. The 9 inch JRCP was jointed every 45 feet with a warping joint every 15 feet. The subbase material thickness ranged from 6 to 12 inches of select material. The section was overlayed during September and October 1978 with 3 inches of CSBCB, 5 inches of HMBC, 1-1/2 inches of HMSC, and 1/2 inches of plant mix seal.

4. U.S. 65, north of McGehee in Desha County, was constructed in 1939 with the 9"-6"-9" JRCP (edge-centerline-edge thickness) with 50 foot slabs. The base or subbase material and thickness are unknown. The pavement was overlayed with 2-1/2 inches of HMBC and 1-1/2 inches of HMSC in 1962. The section was again overlayed in 1978 with 3 inches of CSBCBC, 2 inches of HMBC, 1-1/2 inches of HMSC, and 1/2 inch plant mix seal.

5. Highway 70 was originally constructed as a "9"-6"-9"" JRCP and was overlayed in 1957 with 2 inches of ACHM. This section was again overlayed in September of 1978 as part of a demonstration project. This project consisted of demonstrating several different methods of relieving reflection cracking. Although the study primarily focused on the use of

low modulus stress absorbing membrane interlayers (SAMI), the project also evaluated a smaller size crack relief layer and a control section (the gradation appears in the attachments). Four sections of the demonstration project were surveyed for reflection cracking data; these sections include:

1. 1-1/2 inches of surface
2. 2 inches of OGBC (open graded base course), 1-1/2 inches of ACHM
3. 2 inches of OGBC, 1/2 inch SAMI, 1-1/2 inches of ACHM
4. 1/2 inch SAMI, 1-1/2 inches ACHM

6. U.S. 67, Section 18, in Lawrence County near Alicia was constructed in 1952 with 10 inches JRCP at 50 foot intervals; however, the actual spacing may differ from the plans in this instance. The concrete was placed over 6 inches of select material (SM-1). The soil log for this job showed a subgrade classification as an A-7-6. In 1978, the section was overlayed with 3 inches of CSBCBC, 2-3/4 inches of ACHMBC, 1-1/2 inches of ACHMSC and 1/2 inches of plant mix seal.

7. The project on I-30 in Saline County is the one which contains the three instrumented overlay sites near Benton, Arkansas. The original 9 inch JRCP with the 45-foot joint spacing (and 15-foot sawed warping joints) was constructed in 1959. The Arkansas Mix Overlay (4 inch open graded course, 4 inch binder course, 1-1/2 inch surface course and 1/2 inch plant mix seal) was constructed during the period between May and October, 1977.

Texas Data

The overlay performance data obtained from Texas are presented in Table 3.4. All of the data are from sections of I-45 between Houston and Dallas. Though each original pavement is different in nature, all were constructed using the same type of subbase and concrete coarse aggregate

Table 3.4. Texas overlay performance data.

No.	Pav't Type	Joint/ Crack Spacing (feet)	Site Location	Coarse Aggregate Type	Subbase (or Base) Type	Slab Thickness (in.)	Longitudinal Steel Reinf.		Overlay Thickness (in.)			Survey Data		
							Bar Spacing (in.)	Bar Dia. (in.)	Open-Graded Course	Binder	Surface	Overlay Age (years)	Overlay Length (feet)	% Ref. Cracking
1.	JCP	15	I-45 Walker Co.	River Gravel	Granular	11	-	-	0	0	3.0	0.5	-	99.0
2.	JRCP	61.5	I-45 Mont. Co.	River Gravel	Granular	10	-	-	3.5	2.5	1.5	1.2	13,350	14.7
3a.	CRCP	2.5	I-45 Walker Co.	River Gravel	Granular	8	6.5	.625	0	0	2.5	6.0	2000	4.24
3b.	CRCP	1.85	I-45 Walker Co.	River Gravel	Granular	8	6.5	.625	0	0	6.0	6.0	500	0.37

type. The 15-foot JCP with an 11-inch slab was overlayed with 3-inches of ACHM and exhibited almost 100 percent reflection cracking in about half a year. The 61.5-foot JRCP with the 10-inch PCC slabs was overlayed using the Arkansas Mix Design procedure and exhibited approximately 15 percent reflection cracking in slightly more than one year. The CRC pavement shown in Table 3.4 (Nos. 3a and 3b) represents the experimental CRCP sections constructed in 1960 and 61 which have been monitored continuously over the years. The overlay sections shown were approximately 6 years old at the time they were last surveyed.

ARKANSAS TEMPERATURE DISTRIBUTION DATA

Recognizing that daily temperature changes are an integral part of the development of reflection cracking in asphalt concrete overlays, it became important that some type of temperature distribution data for the state of Arkansas be obtained for use in the study. Accordingly, the National Climatic Center (Ref. 65) was contracted to provide certain specific data.

Basically, the NCC was instructed to go through its historic temperature data and for any weather station in a given climatic station, obtain the following:

1. For each day of each available year, determine the maximum temperature drop (i.e., subtract the maximum temperature from minimum temperature observed during that day) and based upon the magnitude, assign that day to a particular temperature drop class of a frequency distribution. The temperature drop classes should be: 0-10°F, 11-20°F, 21-30°F, 31-40°F, 41-50°F, 61-70°F and above 71°F. Then, after this is done for each year considered, determine the average number of days per year for each temperature drop class.

2. For each day of each available year, subtract the minimum temperature from 50°F and once again, assign that day to a particular temperature drop class of a frequency distribution (the temperature drop classes are the same as above). If the minimum temperature is not below 50°F, then that day should not be counted. Finally, as before, the average number of days per year for each temperature drop class is determined.

Tables 3.5 and 3.6 respectively represent the results of 1) and 2) above for Alum Fork, a town in one of Arkansas' nine climatic regions. As can be seen, the data for this station (as well as that from the other eight) covers a period of seven years, 1974 through 1980. Summaries of the complete data set on Arkansas temperature distribution are presented in Tables 3.7 and 3.8. Figure 3.16 provides a map of Arkansas showing the nine different climatic regions and the locations of each of the representative climatic stations.

Table 3.5. Yearly distribution of maximum daily temperature drops for Alum Fork (Station 030130, Central region of Arkansas) for for period of 1974 - 1980. (National Climatic Center).

	Maximum Daily Temperature Drop Classes, ^{o}F *							
Year	1-10	11-20	21-30	31-40	41-50	51-60	61-70	>71
1974	56	70	27	3	0	0	0	0
1975	48	70	42	6	1	0	0	0
1976	62	64	39	6	3	0	0	0
1977	54	48	39	11	5	0	0	0
1978	58	50	39	25	0	0	0	0
1979	48	59	39	15	4	0	0	0
1980	76	64	30	14	0	0	0	0
TOTAL	402	425	255	80	13	0	0	0
AVERAGE	57	61	36	11	2	0	0	0

* CLASSES REPRESENT RANGES OF DIFFERENCES BETWEEN 50 DEGREES FAHRENHEIT AND THE DAILY MINIMUM TEMPERATURE.

Table 3.6. Yearly distribution of be 50°F daily temperature drops for Alum Fork (Station 030130, Central region of Arkansas) for period of 1974 - 1980. (National Climatic Center).

Year	Below 50°F Temperature Drop Classes, °F *							
	1-10	11-20	21-30	31-40	41-50	51-60	61-70	>71
1974	22	122	159	59	3	0	0	0
1975	13	105	184	61	2	0	0	0
1976	9	96	179	75	7	0	0	0
1977	19	81	195	66	4	0	0	0
1978	21	111	177	50	6	0	0	0
1979	21	131	159	50	4	0	0	0
1980	25	78	181	80	2	0	0	0
TOTAL	130	724	1234	441	28	0	0	0
AVERAGE	19	103	176	63	4	0	0	0

* CLASSES REPRESENT RANGES OF DIFFERENCES BETWEEN THE DAILY MAXIMUM AND THE DAILY MINIMUM TEMPERATURE IN DEGREES FAHRENHEIT.

Table 3.7. Summary of maximum daily temperature drop data for the nine climatic regions of Arkansas.

Climatic Region	Representative Station		Maximum Temperature Drop Class (^{o}F)						
			0-10^{o}	11-20^{o}	21-30^{o}	31-40^{o}	41-50^{o}	51-60^{o}	61-70^{o}
South-West	De Queen	Avg.	16 (days)	85	162	86	15	0	0
		Max.	23	102	176	128	26	1	0
		Min.	8	60	140	62	4	0	0
South-Central	Camden	Avg.	22	91	180	67	5	0	0
		Max.	37	108	186	84	11	0	0
		Min.	14	81	170	48	0	0	0
South-East	Dumas	Avg.	27	132	168	38	1	0	0
		Max.	31	176	188	51	2	0	0
		Min.	18	99	144	20	0	0	0
West-Central	Dardanelle	Avg.	24	112	154	66	10	0	0
		Max.	32	129	164	85	16	0	0
		Min.	17	95	139	43	3	0	0
Central	Alum Fork	Avg.	19	103	176	63	4	0	0
		Max.	25	131	195	80	7	0	0
		Min.	9	78	159	50	2	0	0
East-Central	Brinkley	Avg.	24	111	188	40	2	0	0
		Max.	35	165	223	57	2	0	0
		Min.	13	79	139	26	1	0	0
North-West	Eureka Springs	Avg.	20	94	187	62	3	0	0
		Max.	26	117	201	99	4	0	0
		Min.	6	72	164	45	0	0	0
North-Central	Calico Rock	Avg.	19	64	124	118	35	2	0
		Max.	32	77	151	145	58	6	0
		Min.	9	51	97	98	15	0	0
North-East	Corning	Avg.	26	114	170	54	2	0	0
		Max.	32	127	182	81	3	0	0
		Min.	11	99	152	39	0	0	0

Table 3.8. Summary of below 50° daily t[illegible]rature drop data for the nine climatic regions in Arkansas.

Climatic Region	Representative Station		Below 50°F Temp. Drop Class (°F)						
			0-10°	11-20°	21-30°	31-40°	41-50°	51-60°	61-70°
South-West	De Queen	Avg.	59 (days)	54	46	12	2	0	0
		Max.	66	65	55	15	0	0	0
		Min.	47	44	35	2	0	0	0
South-Central	Camden	Avg.	55	63	37	11	0	0	0
		Max.	70	72	51	18	3	0	0
		Min.	39	50	24	2	0	0	0
South-East	Dumas	Avg.	65	52	29	7	1	0	0
		Max.	74	62	46	11	2	0	0
		Min.	57	43	18	1	0	0	0
West-Central	Dardanelle	Avg.	60	57	46	14	2	1	0
		Max.	65	67	52	26	5	3	0
		Min.	51	43	36	3	0	0	0
Central	Alum Fork	Avg.	57	61	36	11	2	0	0
		Max.	76	70	42	25	5	0	0
		Min.	48	48	27	3	0	0	0
East-Central	Brinkley	Avg.	56	72	36	12	1	0	0
		Max.	67	91	41	24	4	0	0
		Min.	38	59	29	5	0	0	0
North-West	Eureka Springs	Avg.	56	58	38	18	8	3	0
		Max.	67	63	46	27	12	7	0
		Min.	47	46	34	12	5	0	0
North-Central	Calico Rock	Avg.	59	62	54	26	7	1	0
		Max.	68	74	67	39	11	4	1
		Min.	43	53	35	17	2	2	0
North-East	Corning	Avg.	60	62	40	16	5	1	0
		Max.	66	75	48	24	12	4	0
		Min.	51	47	27	9	0	0	0

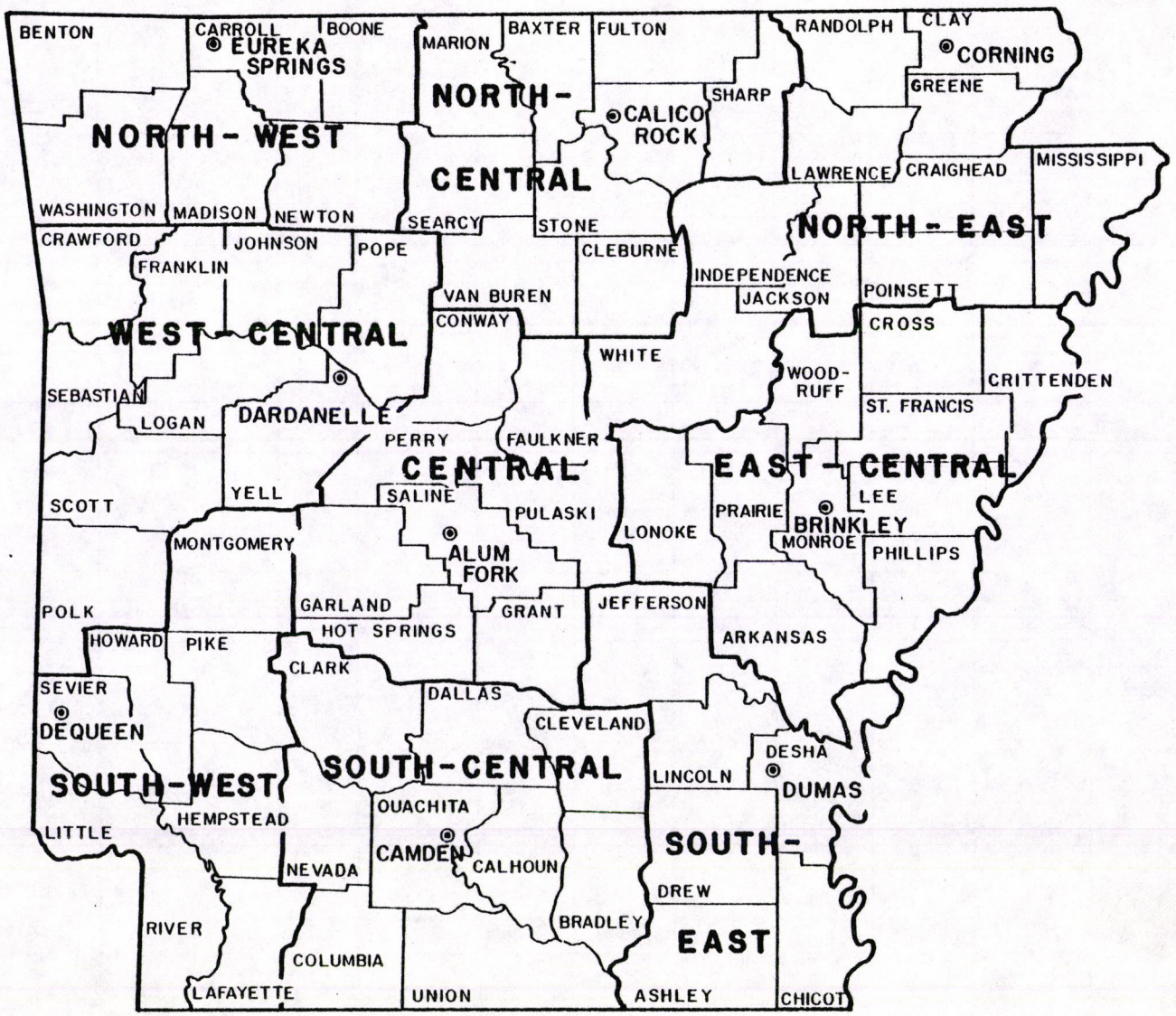

Figure 3.16. Nine climatic regions of A nsas (National Climatic Center).

CHAPTER 4
FIELD SAMPLING AND LABORATORY TESTING

This chapter summarizes the results of the laboratory testing conducted by Austin Testing Engineers Inc, on the asphalt and concrete core samples selected and taken by the Arkansas State Highway and Transportation Department (AHTD). The results of these tests are used to both calibrate the new overlay design procedure and provide a basis for the selection of appropriate design criteria.

SAMPLING PROGRAM

The materials that were tested were basically obtained during two different periods by AHTD. In the initial sampling period (April 7-9, 1981), cores were obtained from the different instrumented overlay sites on I-30 near Benton, Arkansas and on I-40 near Forrest City, Arkansas. In the second sampling period (April 24-May 6, 1981), cores were taken from several different concrete pavements across the state in an attempt to obtain a sampling of the different concrete coarse aggregate types used in the state.

Table 4.1 provides information on the location and description of each sample obtained from the instrumented overlay sites. The total number of these samples taken is twelve, since there are three different instrumented sites on both the I-30 (Benton) and I-40 (Forrest City) sections, and since two cores (bore holes) were taken at each site. Note that the three sites at each location correspond to different overlay cross-sections. It should also be noted that gravel makes up the coarse aggregate type used in all the PCC samples.

As for the fourteen core samples obtained during the second sampling period, an inventory of their locations and descriptions is presented in Table 4.2.

Table 4.1. Inventory of pavement samples taken from instrumented overlay sites on I-30 and I-40.

Bore Hole	Date of Boring	Location/ Identification	Material Description
B-1	4/7/81	I-30 westbound lane 1st sensor location Boring nearest sensors Benton	7" AC 1½" Open Graded Agg. w/binder 8" PCC 6" Granular Base Reddish brown silty clay
B-2	4/7/81	I-30 westbound lane 1st sensor location Boring farthest from sensors Benton	7" AC 1½" Open Graded Agg. w/binder 9" PCC 6" Granular Base Reddish brown silty clay
B-3	4/7/81	I-30 westbound lane Closest to overlay end Boring nearest sensors Benton	5½" AC 11" PCC 6" Granular Base Reddish brown silty clay
B-4	4/7/81	I-30 Westbound lane Closest to overlay end Boring closest to sensors Benton	5½" AC 10¼" PCC 6" Granular Base Reddish brown silty clay
B-5	4/8/81	I-30 Eastbound lane Mile marker 118 Boring closest to sensors Benton	2½" AC 10¼" PCC 6" Granular Base Reddish brown silty clay
B-6	4/8/81	I-30 Eastbound lane Mile marker 118 Boring farthest from sensors Benton	2¼" AC 10½" PCC 6" Granular Base Reddish brown silty clay
B-7	4/9/81	I-40 Widener Exit 247 Inside eastbound lane Inside hole - farthest from sensors	7" AC 4½" Open Graded Agg. w/binder 8¼" PCC 6" Granular Base Brown clay
B-8	4/9/81	I-40 Widener Exit 247 Inside eastbound lane Boring closest to sensors	7" AC 4½" Open Graded Agg. w/binder 8½" PCC 6" Granular Base Brown clay

Table 4.1. (cont.) Inventory of pavement samples taken from instrumented overlay sites on I-30 and I-40.

Bore Hole	Date of Boring	Location/ Identification	Material Description
B-9	4/10/81	I-40 Exit 260 eastbound Right side of inside lane Shell lake	6" AC 8½" PCC 6" Granular Base Brown clay
B-10	4/10/81	I-40 Exit 260 eastbound Left side of inside lane Shell lake	6" AC 8½" PCC 6" Granular Base Brown clay
B-11	4/13/81	I-40 inside lane ≈ LM 265 Right core hole	3/8" Chip Seal 1½" AC 8¼" PCC Brown clay
B-12	4/13/81	I-40 inside lane ≈ LM 265 Left core hole	3/8" Chip Seal 1½" AC 8¼" PCC 6½" CTS Brown clay

Table 4.2. Inventory of Arkansas PCC core samples.

	Date of Boring	Location	Slab Thickness	PCC Coarse Aggregate Type
1.	4/24/81	East Belt, Little Rock Sta. 452+00 - 452+30	11 in.	Syenite
2.	4/24/81	East Belt, Little Rock Sta. 452+00 - 452+50	10 3/4 in.	Syenite
3.	4/28/81	Hwy 63 bypass @ Willow Rd., SB	9 1/2 in.	Dolomite
4.	4/28/81	Hwy 63 bypass @ Willow Rd.	9 1/4 in.	Dolomite
5.	5/5/81	Hwy 71, Springdale	9 in.	Limestone
6.	5/5/81	Hwy 71, Springdale	9 in.	Limestone
7.	5/6/81	I-40, MM-104, EB rest stop	8 5/8 in.	Sandstone
8.	5/6/81	I-40, MM-104, EB rest stop	8 3/8 in.	Sandstone
9.	5/6/81	I-40, MM-8, Truck weight station parking	10 1/4 in.	Sandstone
10.	5/6/81	I-40, MM-8, Truck weight station parking	10 1/4 in.	Sandstone
11.	-	I-30, EB, log mile 99 (east of Malvern)	9 1/2 in.	Gravel
12.	-	I-30, EB, log mile 99 (east of Malvern)	9 1/4 in.	Gravel
13.	-	I-30, WB, log mile 23	7 1/2 in.	Gravel
14.	-	I-30, WB, log mile 23	7 1/2 in.	Gravel

TESTING PROGRAM

After all the cores were logged and examined, those from the overlay sites were further divided into individual specimens using a diamond saw. Selected specimens were then tested for thermal coefficient and then for dynamic modulus, creep modulus, and tensile strength using the indirect tensile apparatus.

The fourteen other concrete core samples from around the state were also tested in the laboratory, but in this case, only for thermal coefficient and compressive strength.

The results of all the testing is presented next, beginning with thermal coefficient (AC and PCC), continuing with the indirect tensile test results for dynamic modulus (AC and PCC), creep modulus (AC only) and tensile strength (PCC only), and ending with the PCC compression tests.

THERMAL COEFFICIENT TESTS

The thermal related shrinkage or shrinkage potential of a pavement material is believed to be a primary contributor to the development of reflection cracking in asphalt concrete overlays on PCC pavements. The thermal coefficient (which is also referred to as the coefficient of thermal expansion) is a property of a given material which is indicative of its potential for contracting with a drop in temperature.

Since the new reflection cracking analysis and overlay design procedure calls for specific values of thermal coefficient for the different pavement layers, it was considered essential that thermal coefficient tests be conducted on commonly used pavement materials in Arkansas. The materials tested include specimens of the binder/surface course used in the AHTD Overlay Mix Design as well as several PCC samples having different types of coarse aggregate. Because of the different thicknesses of the samples, however, it was necessary to use two different

test procedures for estimating thermal coefficient. Both procedures, however, are based on the following equation for calculating thermal coefficient.

$$\alpha = \frac{(\ell_1 - \ell_2) \; / \; \ell_1}{T_1 - T_2}$$

where: α = thermal coefficient (in./in./^{o}F)

ℓ_1 = sample gage length at high temperature (inches),

ℓ_2 = sample gage length at low temperature (inches),

T_1 = high temperature (^{o}F), and

T_2 = low temperature (^{o}F).

Thinner samples, such as the asphalt concrete overlay specimens, required the use of a micrometer to measure changes in gage length (in this case, diameter) with changes in temperature. These measurements were made in two orthogonal directions across the specimen (see Figure 4.1). On the other hand, the thick core samples, such as those taken from a thick layer (e.g., PCC slab), were measured using a Berry strain gage at three locations around the perimeter of the sample (see Figure 4.2). This procedure was more desirable since the Berry strain gage had the same precision as the micrometer (0.0001"), but was capable of measuring over a much longer gage length.

Micrometer Results

The results of testing using the micrometer to determine thermal coefficient are presented in Table 4.3. All samples shown are from the instrumented overlay sites near Benton and Forrest City. PCC samles were heated to 185^{o}F in an oven and then cooled to 25^{o}F in a freezer to achieve the greatest precision. AC samples were not oven-heated, however, to avoid the effects of viscoelasticity. Unfortunately, due to problems with obtaining perpendicular faces on the samples after sawing, only four asphalt concrete (AC) and four portland cement concrete (PCC) were tested. Also, because of some sample disturbances during testing, some of the measurements along the b-b axis were not available.

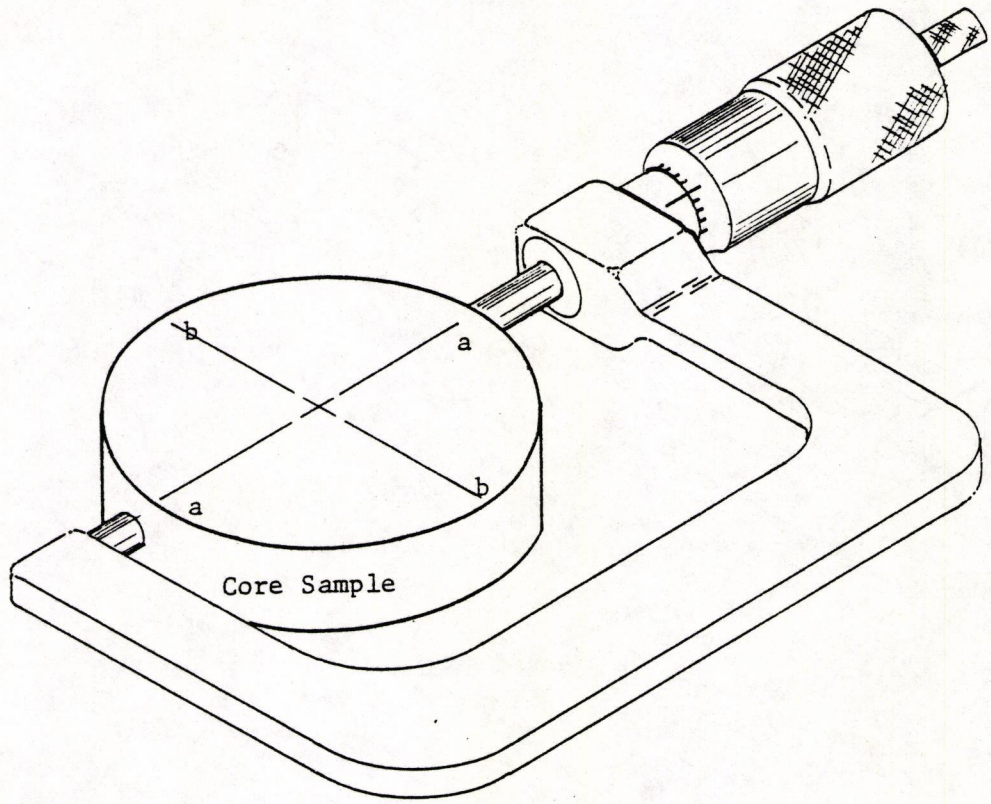

Figure 4.1. Illustration of thermal coefficient determining using micrometer.

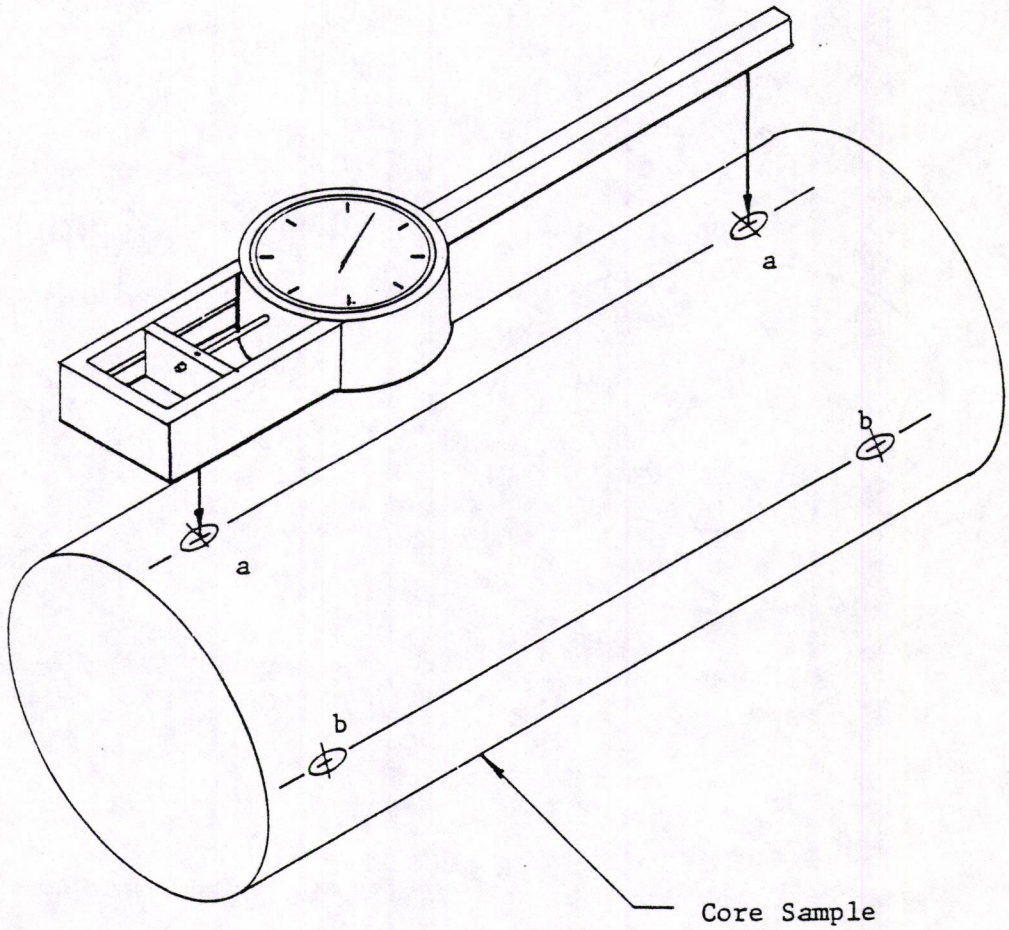

Figure 4.2. Illustration of thermal coefficient determination using Berry strain gauge.

Table 4.3. Thermal coefficients of AC binder c[illegible] and PCC slab at instrumental overlay sites (determined using micrometer).

Specimen No.	Material Type	Specimen Diameter, in.				Thermal Coefficient 10^{-6} in/in/^{o}F		
		ℓ_{1a}	ℓ_{1b}	ℓ_{2a}	ℓ_{2b}	α_a	α_b	α_{AVG}
2B	AC	4.0174	-	4.0143	-	15.7	-	15.7
6A	AC	4.0161	4.0170	4.0132	4.0143	14.7	13.7	14.2
8B	AC	4.0153	4.0142	4.0132	4.0124	10.7	9.1	9.9
10B	AC	4.0173	-	4.0133	-	20.3	-	20.3
2D	PCC	4.0074	4.0064	4.0032	4.0025	6.6	6.1	6.3
7F	PCC	4.0077	4.0137	4.0046	4.0097	4.8	6.2	5.5
8F	PCC	4.0088	-	4.0131	-	6.7	-	6.7
11E	PCC	4.0153	-	4.0109	-	6.8	-	6.8

Berry Strain Gauge Results

Besides using the Berry strain gauge to measure sample gage lengths, a more rigorous test procedure was used for the determination of the thermal coefficients of the remaining 14 concrete cores. This was accomplished by measuring the gage lengths of each sample at four different times along a temperature cycle. The sample was first measured at room temperature (RT_1), then it was placed in an oven for 24 hours and measured again at approximately 140°F (OT). Then, it was allowed to cool Finally, it was placed in a refrigerator and cooled to near freezing temperature (CT) and measured for the last time. The measurements recorded represented an average of 3 readings at each temperature.

Four separate thermal coefficients were then determined for four different periods of the cycle, RT_2 to OT, OT to RT_2, RT_2 to CT, and OT to CT. These results are presented in Table 4.4. (Note: RT_1=76.5°F, OT=140°F, RT_2=77°F, and CT=32°F for specimens 1, 5, 6, 7, and 8. RT_1=78.5°F, OT=145°F, RT_2=77°F, and CT=35°F for specimens 2, 3, 4, 9, 10, 11, 12, 13, and 14).

In order to combine these data logically and reduce the effect of poor measurements, a weighted average thermal coefficient was determined for each side of each specimen (also shown in Table 4.4). This was done by assigning weighting values of 2, 1, 1, and 4 (respectively) to the thermal coefficients determined for the different parts of the temperature cycle.

Examination of these test results indicate that in spite of the efforts to achieve good precision, there is still some error in the test procedure. However, the results do provide a good basis for the selection of appropriate design values for concrete thermal coefficient.

Table 4.4. Thermal coefficient of concrete for different types of coarse aggregate used in the State of Arkansas.

Coarse Aggregate Type	Specimen No.	Side	Berry Strain Gauge Readings (inches)				Thermal Coefficients (10^{-6} in/in/^{o}F)				
			@ RT_1	@ OT	@ RT_2	@ CT	RT_1-OT	OT-RT_2	RT_2-CT	OT-CT	Wt. Avg.
Syenite	1	a	8.0411	8.0441	8.0412	8.0397	5.87	5.72	4.15	5.06	5.23
		b	8.0383	8.0410	8.0391	-	5.29	3.75	-	-	4.52
	2	a	8.0396	8.0428	8.0411	-	5.98	3.11	-	-	4.55
		b	7.9612	7.9629	7.9605	7.9586	3.21	4.43	5.68	4.91	4.52
Dolomite	3	a	8.0597	8.0610	8.0598	8.0587	2.43	2.19	3.25	2.60	2.59
		b	8.0493	8.0513	8.0492	8.0478	3.74	3.84	4.14	3.95	3.91
	4	a	8.0603	8.0636	8.0609	8.0592	6.15	4.92	5.02	4.96	5.26
		b	8.0782	8.0805	8.0784	8.0768	4.28	3.82	4.72	4.16	4.22
Limestone	5	a	8.0304	8.0343	-	8.0302	7.64	-	-	4.73	5.70
		b	8.0286	8.0309	8.0285	8.0270	4.51	4.74	4.15	4.50	4.49
	6	a	8.0469	8.0489	8.0474	8.0459	3.91	2.96	4.14	3.45	3.59
		b	8.0850	8.0870	8.0852	8.0835	3.90	3.53	4.67	4.01	4.01
Sandstone	7	a	8.0260	8.0296	8.0263	8.0240	7.06	6.52	6.37	6.46	6.61
		b	8.0598	8.0625	8.0592	8.0571	5.27	6.50	5.79	6.20	5.95
	8	a	8.0628	8.0645	8.0616	8.0594	3.32	5.71	6.06	5.86	5.23
		b	7.9564	7.9589	7.9552	7.9526	4.95	7.38	7.26	7.33	6.73
		c	7.9651	7.9674	7.9648	7.9623	4.55	5.18	6.98	5.93	5.62
	9	a	8.0716	8.0738	-	8.0699	4.10	-	-	4.39	4.29
		b	8.0500	8.0524	8.0494	8.0472	4.48	5.48	6.51	5.87	5.55
	10	a	8.0285	8.0311	-	8.0259	4.87	-	-	5.89	5.55
Gravel-A	11	a	8.0330	8.0372	8.0331	8.0308	7.86	7.50	6.82	7.24	7.38
		b	8.0499	8.0535	8.0510	8.0499	6.72	4.57	3.25	4.06	4.69
	12	a	8.0487	8.0513	8.0481	8.0459	4.86	5.84	6.51	6.10	5.81
		b	8.0271	8.0290	8.0265	8.0240	3.56	4.58	7.42	5.66	5.22
Gravel-B	13	a	6.0640	6.0667	6.0642	6.0628	6.69	6.06	5.50	5.84	6.04
		b	6.0560	6.0585	6.0570	6.0553	6.21	3.64	6.68	4.80	5.24
	14	a	6.0546	6.0585	6.0534	6.0519	9.68	12.38	5.90	9.90	9.66
		b	6.0322	6.0353	6.0323	6.0300	7.72	7.31	9.08	7.98	7.97

INDIRECT TENSILE TESTS

The indirect tensile test is a relatively new test procedure whereby tension is induced into a core specimen indirectly so that its properties along the tensile axis can be determined. Figure 4.3 provides a schematic diagram of the test apparatus. The test procedure is documented by Kennedy and Anagnos (Ref. 67) and is presently being incorporated into ASTM Standards. The procedure used in this study to determine the dynamic moduli of the asphalt concrete and portland cement concrete specimens is exactly the same as that under ASTM consideration, however, a variation of the test was used to determine the creep moduli for the asphalt concrete materials.

Dynamic Moduli

Four asphalt concrete specimens from the instrumented overlay sites near Benton were tested for dynamic modulus under repetitive load conditions. The results of these tests for the four specimens (one of which was tested along two perpendicular axes) are presented in Figure 4.4. Note that the moduli were determined for different levels of applied stress in order to determine the sensitivity.

As can be seen, all but one of the specimens had a dynamic modulus in the range of 150,000 to 400,000 psi at a temperature of approximately 78-80°F (room temperature). The No. 7 specimen, seeming unusually stiff, had an elastic modulus of between 700,000 and 900,000 psi.

Creep Moduli

In order to determine the creep modulus of the pavement materials considered (only AC specimens from the I-30 instrumented overlay sites near Benton were tested), it was necessary to modify the indirect tensile test procedure. Instead of applying a repetitive dynamic load as in the previous tests, a constant load was applied and the time dependent

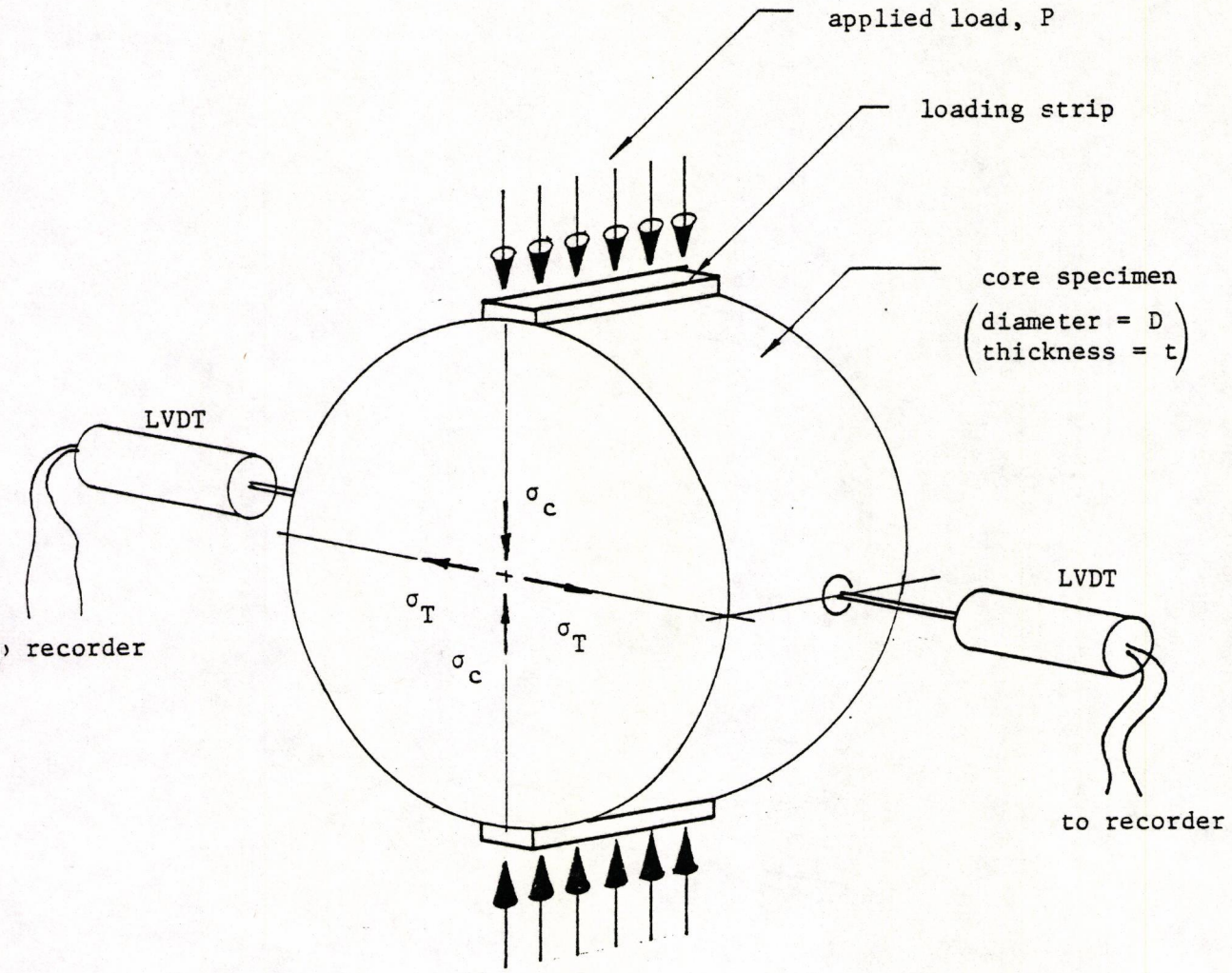

Figure 4.3. Schematic diagram of indirect tensile test.

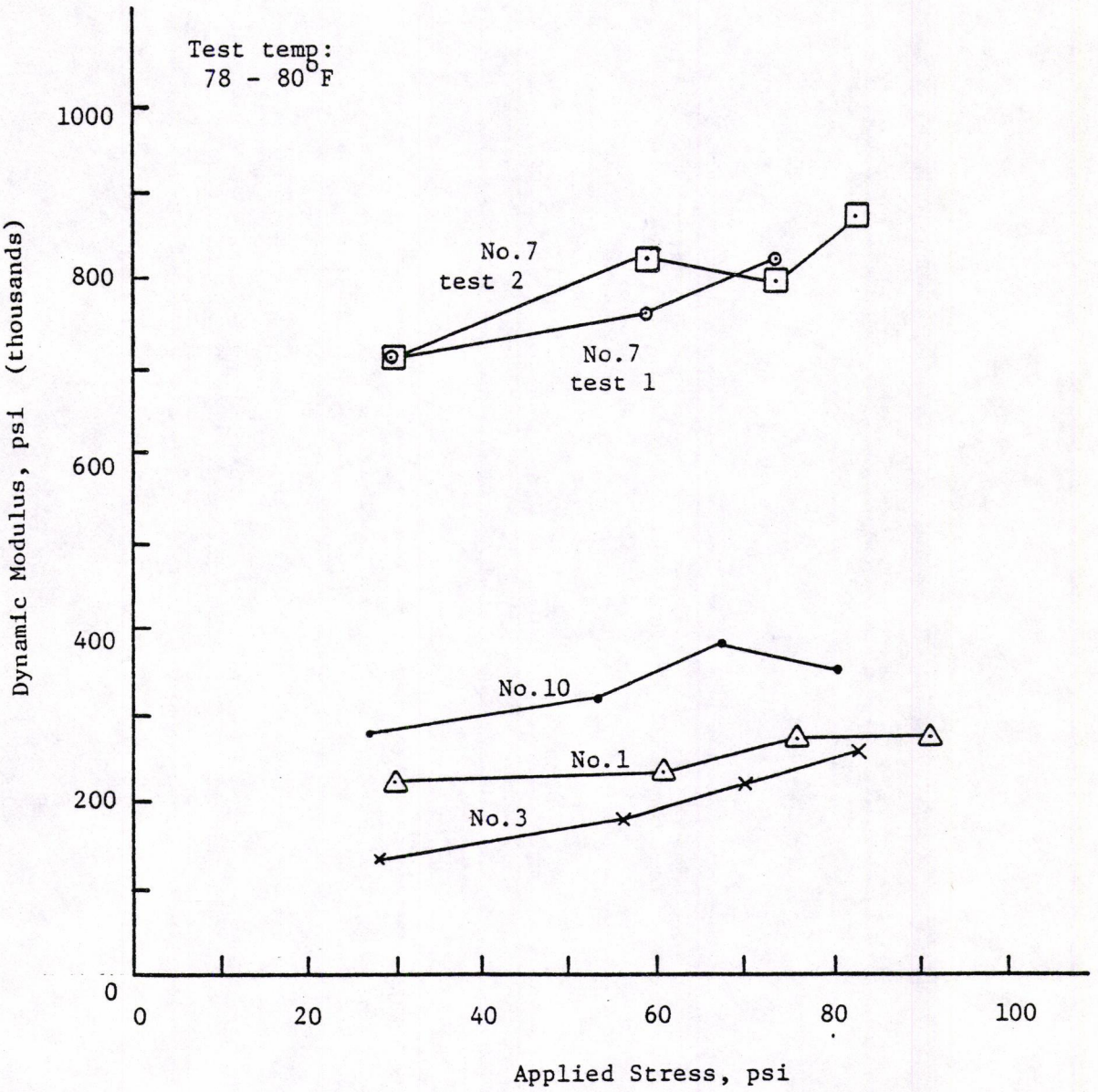

Figure 4.4. Indirect tensile test results for dynamic moduli on AC specimens from I-30 overlay near Benton, Arkansas.

deformation of the sample was recorded. These time dependent strains were then translated into the corresponding creep modulus depending on the applied stress level.

The same four samples tested for dynamic modulus were used in these tests to determine their creep moduli. The samples were tested at either a 30 psi or 60 psi applied load. One sample was tested at both stress levels. The results of these tests are presented in Figure 4.5.

The samples seemingly exhibited a wide range in resistance to creep deformation. It is believed that the samples exhibiting the greater resistance (i.e., specimen numbers 1 and 7) are more or less typical of the values that can be expected in the field.

COMPRESSION TESTS

Since it was not possible to accurately determine the dynamic modulus of the concrete samples using the indirect tensile apparatus, it became necessary to use the results of compression testing to estimate the modulus values. (Fortunately, the 14 concrete cores representing the different coarse aggregate types used around the state were not sawed for indirect tensile testing when the problem was discovered).

Basically, estimates of the concrete elastic moduli were determined by first determining the compressive strength of each cylinder-core (using standard compression test load cell). Then, the American Concrete Institute (ACI) equation, which correlates compressive strength to elastic modulus, was used to calculate the corresponding concrete elastic modulus. The ACI equation (Ref. 68) for normal weight concrete is as follows:

$$E_c = 57000 \, (f'_c)^{0.5}$$

The results of these compression tests are presented in Table 4.5. Note that since ratio of the height of the specimen to the diameter (h/D)

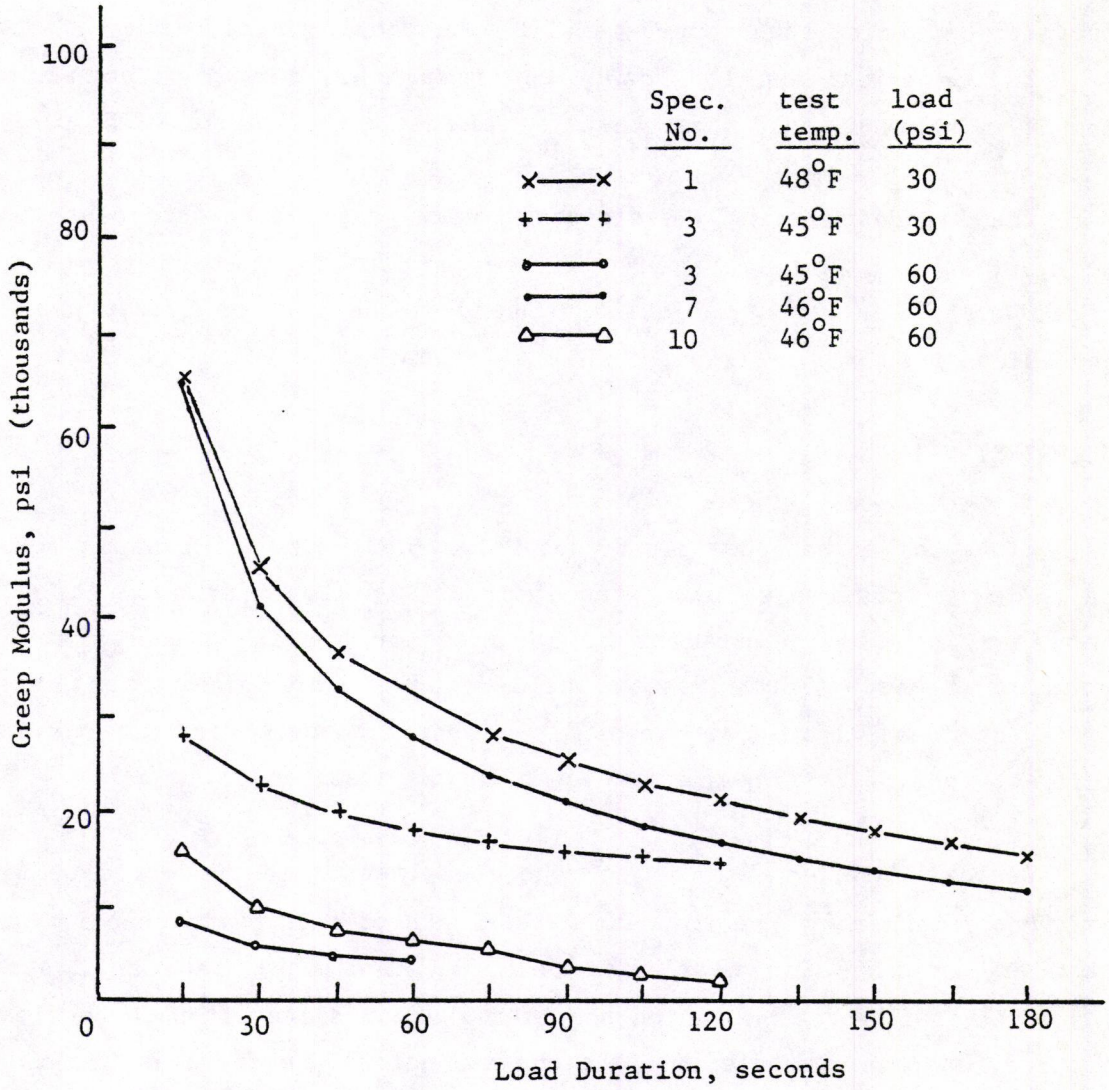

Figure 4.5. Indirect tensile test results for creep moduli on AC specimens from I-30 overlay near Benton, Arkansas.

Table 4.5. Results of concrete compression tests on 14 pavement cores representing the different aggregate types used in Arkansas.

Course Aggregate Type	Sample No.	Height, h (in)	Ratio* h/D	Max. Load, P(lb)	Compressive Strength, f'_c (psi)	Concrete Elastic Modulus E_c (psi)
Syenite	1	11.0	2.7	65,500	5160	4.09×10^6
	2	10.8	2.7	67,000	5280	4.14×10^6
Dolomite	3	9.5	2.4	69,000	5440	4.20×10^6
	4	9.3	2.3	72,500	5710	4.30×10^6
Limestone	5	9.0	2.2	71,500	5630	4.27×10^6
	6	9.0	2.2	66,000	5200	4.11×10^6
Sandstone	7	8.6	2.1	53,000	4180	3.68×10^6
	8	8.4	2.1	42,500	3350	3.29×10^6
	9	10.3	2.6	94,000	7410	4.90×10^6
	10	10.3	2.6	93,500	7370	4.89×10^6
Gravel - A	11	9.5	2.4	90,000	7100	4.80×10^6
	12	9.3	2.3	82,500	6500	4.59×10^6
Gravel - B	13	7.5	1.9	53,000	4180	3.68×10^6
	14	7.5	1.9	65,000	5120	4.07×10^6

*Note: The diameter, D, for all specimens was 4.02 inches.

is almost two or greater, no adjustment to the compressive strengths was necessary. Furthermore, note that based upon these test results, there is not any reason to believe that there is a significant difference between the elastic moduli of 14 different concrete samples.

SUMMARY

The purpose of this chapter was to summarize the field sampling and laboratory testing conducted on highway materials in Arkansas. The results are used to calibrate the new reflection cracking analysis and overlay design procedure developed as a part of this study for AHTD. The results are also used to provide appropriate design criteria to the user for the analysis of prospective overlay designs.

CHAPTER 5
DEVELOPMENT OF ARKANSAS REFLECTION CRACKING ANALYSIS AND OVERLAY DESIGN PROGRAM

The primary objective of this study was to develop a procedure capable of analyzing the potential for reflection cracking in an asphalt concrete overlay placed on an existing concrete pavement, thereby providing criteria for the selection of the most cost effective overlay strategy. The procedure was to be geared to conditions and current AHTD (Arkansas State Highway and Transportation Department) design practices. Based upon a review of the available literature on the practical design of asphalt concrete overlays for the prevention of reflection cracking, a design and analysis procedure (developed originally by ARE Inc) was selected for modification, calibration and adaptation in Arkansas. This chapter discusses the original procedure and the improvements made as a part of this study.

ORIGINAL ANALYSIS AND DESIGN PROCEDURE

The original reflection cracking analysis and overlay design method was developed in 1977 for the Federal Highway Administration (Ref. 1, 70). The main component of the original procedure was a computer program entitled RFLCR-1. Some minor coding errors were detected and corrected as a part of this study. This resulted in the second version of the program, RFLCR-2, which is conceptually identical to RFLCR-1. The general RFLCR methodology forms the basis for the new program, ARKRC-2, developed for Arkansas.

There are two main distress mechanisms which lead to reflection cracking. The first is due to the effects of thermal contraction of the overlay and the temperature-drop related movements of the underlying slab. The second is due to differential vertical movements which occur as a load moves across a joint or crack in the original pavement. These two distress mechanisms are illustrated in Figure 5.1. Note that the temperature-drop

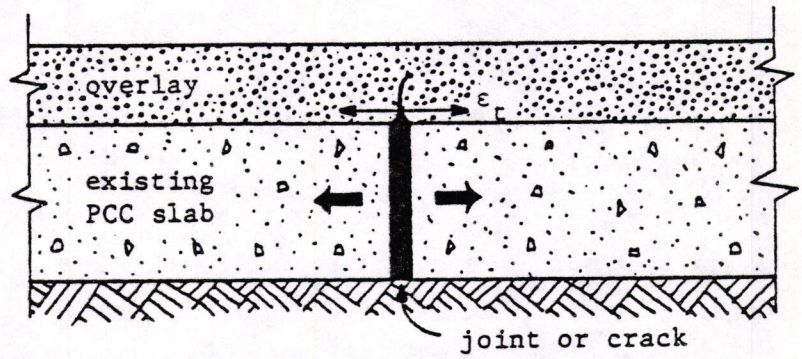

a) tensile strains induced in overlay due to temperature drop related movements in underlaying slab

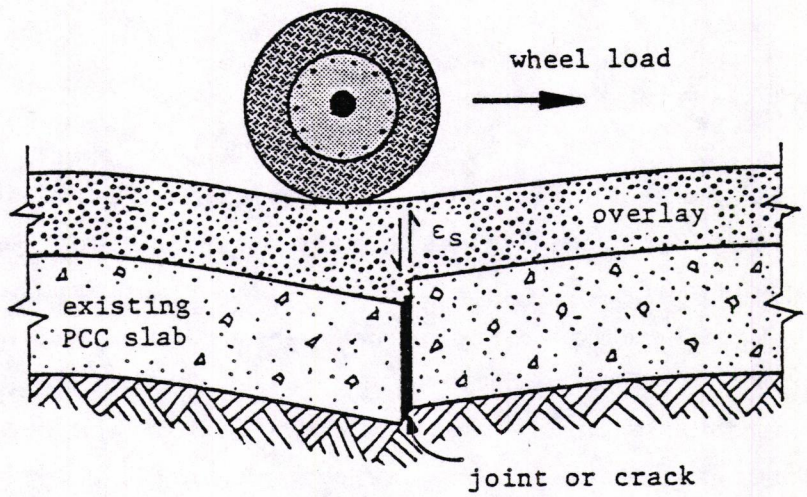

b) shear strain induced in overlay due to passing wheel load and poor load transfer

Figure 5.1. Major distress mechanisms which lead to reflection cracking.

related movements induce horizontal tensile strains in the overlay (as shown in Figure 5.1a) while differential vertical movements induce vertical shear strains in the overlay (as shown in Figure 5.1b). In order to minimize reflection cracking, the objective is to keep these two critical strains below some allowable level. The RFLCR-2 computer program uses several user-specified design values and the results of field observations of slab movements to predict these critical strains. A flowchart of the basic components of the program are shown in Figure 5.2 and are sequentially numbered by a Roman numeral.

Block I summarizes the collection and input of data required by the program. Blocks II through V summarize the method for predicting the horizontal tensile strain developed in an overlay when the underlying slab undergoes a severe temperature drop.

More specifically, block II summarizes the characterization of the horizontal movement of the existing slab for a change in temperature. Figure 5.3 provides an illustration of the movement along the slab for a given drop in the temperature. Note that maximum movement occurs at the crack or joint and zero movement at mid-slab. Figure 5.4 (part a) shows how the joint (or crack) width changes when changing from a high to a low temperature. Part b shows how this change in joint (crack) width is translated into a slab end movement. Part c, then, shows how this end movement is used to estimate the restraint coefficient, beta (β), which is indicative of the slab's movement relative to unrestrained thermal contraction. The result is a mathematical expression for the movement along the entire slab.

Block III of Figure 5.2 summarizes the part of the process where the slope of the friction force versus slab movement curve for the existing pavement is determined. This step is required in order to determine the influence slab-base friction after overlay. Figure 5.5 provides an illustration of the process for the simplest case, a jointed slab with no steel reinforcement. Decreases in slab temperature result in a potential for

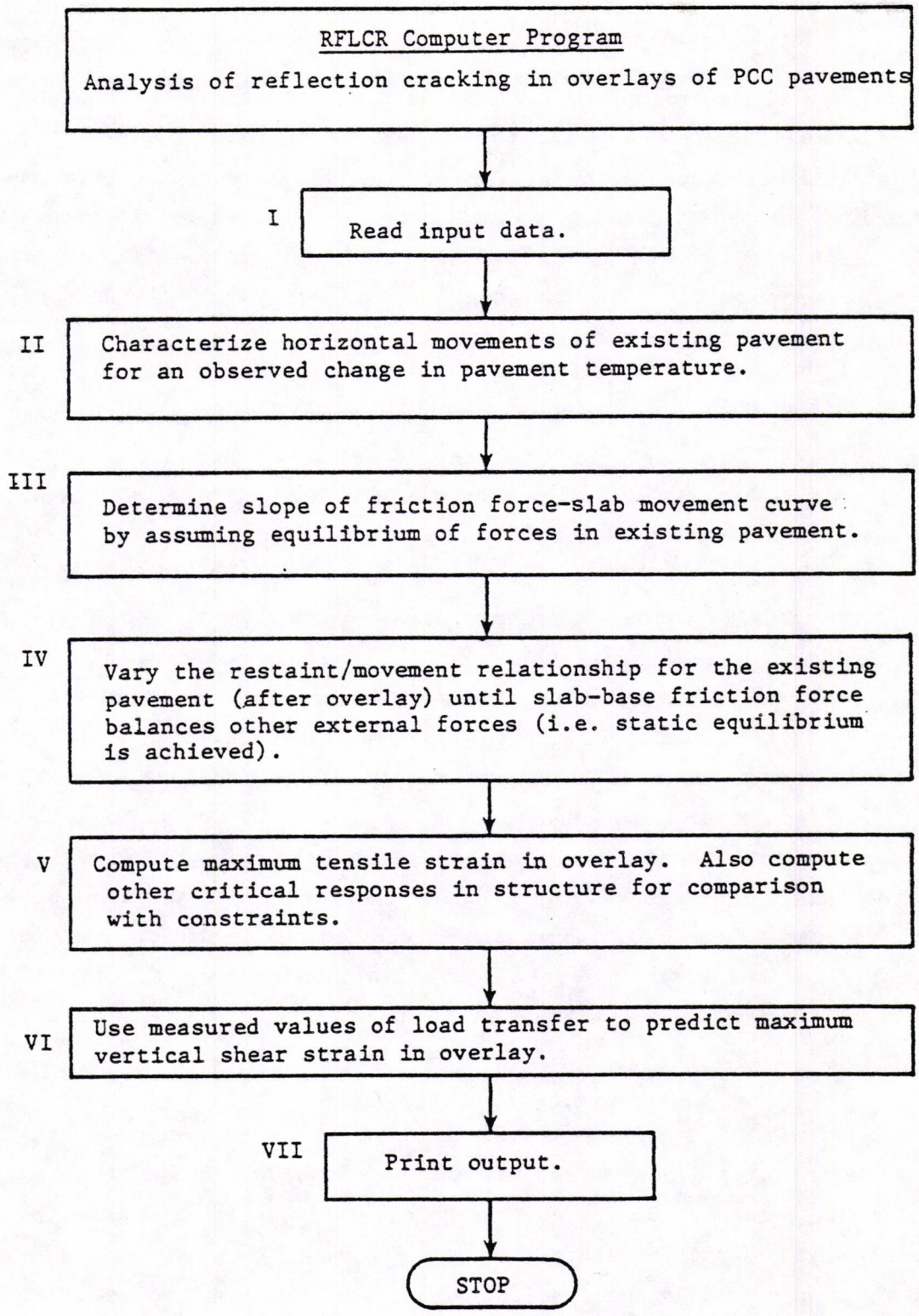

Figure 5.2. Flowchart of the major components of the reflection cracking analysis program, RFLCR.

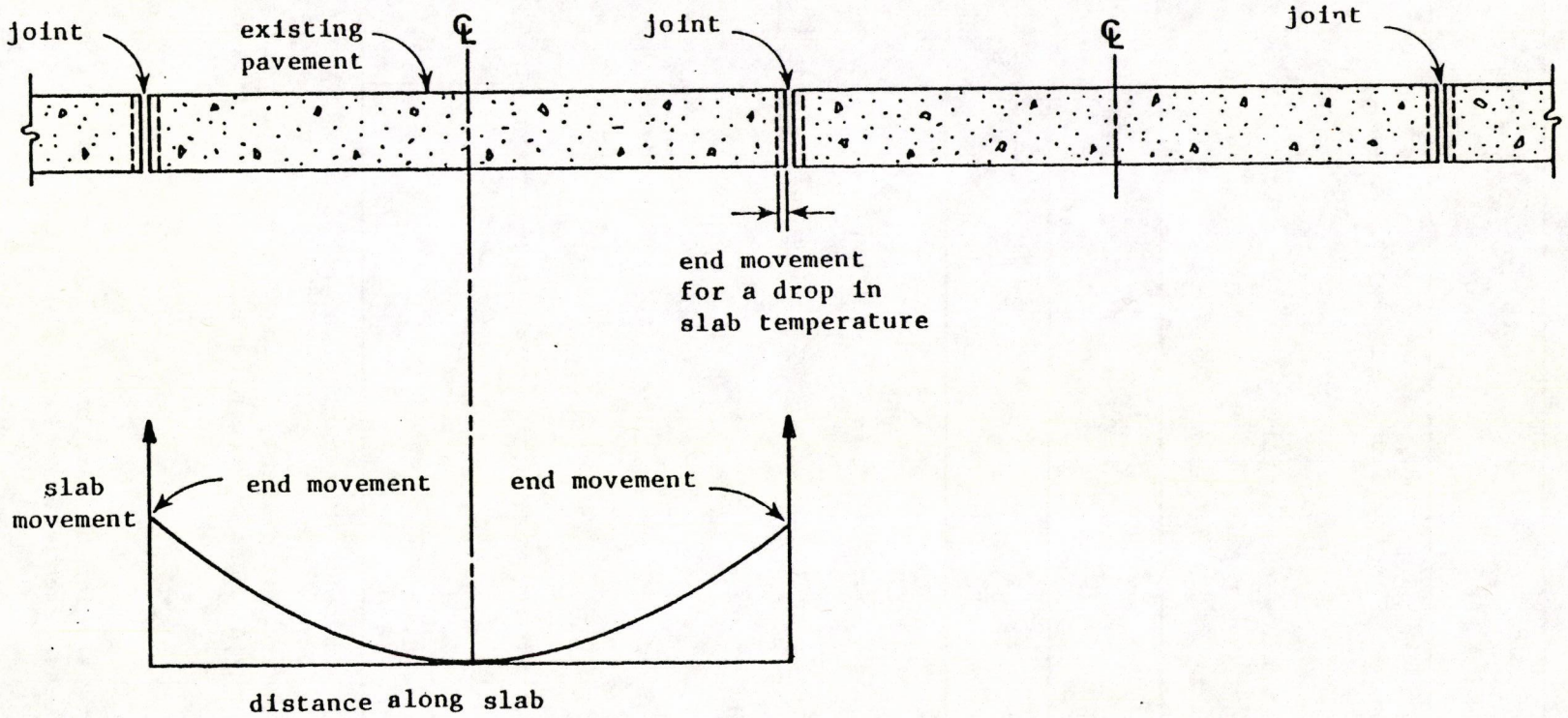

Figure 5.3. Illustration of movement along slab under a drop in temperature.

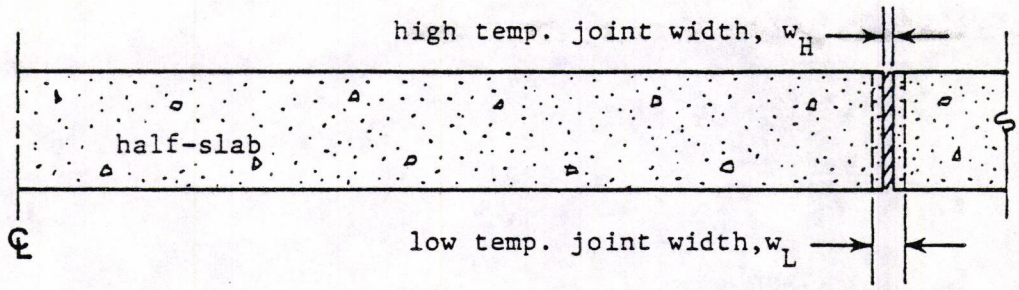

a) observed high and low temperature joint (or crack) widths

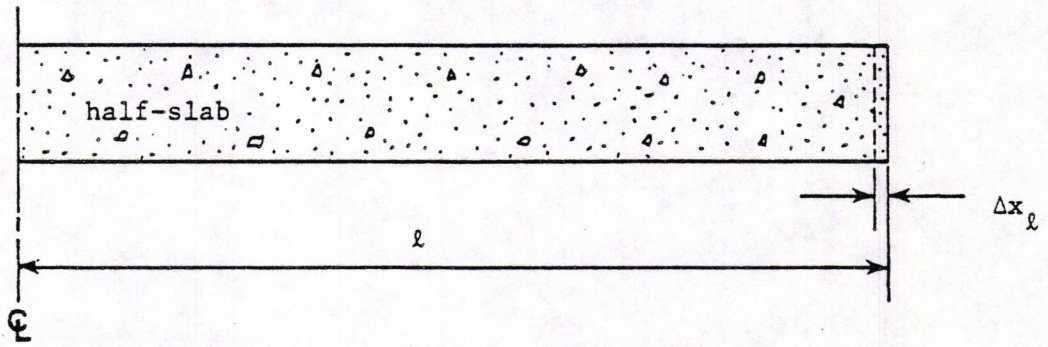

b) slab end movement due to drop in temperature ($\Delta T = T_H - T_L$):

$$\Delta x_\ell = \frac{w_L - w_H}{2}$$

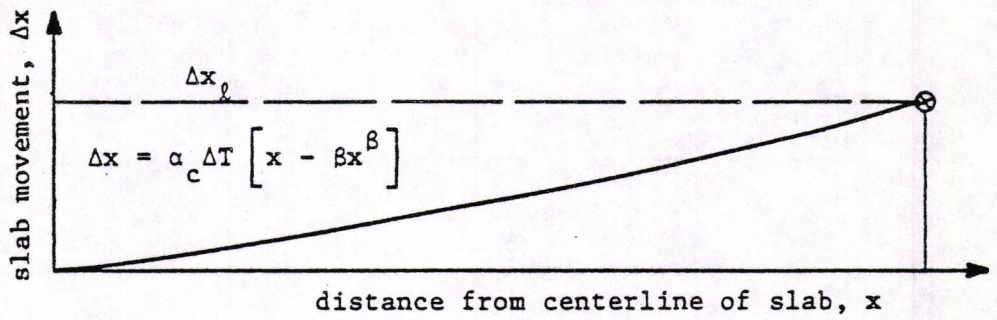

c) solve for restraint coefficient, β, in slab movement relationship using $x = \ell$, $\Delta x = \Delta x_\ell$ and α_c = concrete thermal coefficient

Figure 5.4. Characterization of horizontal slab movements from observed field measurements.

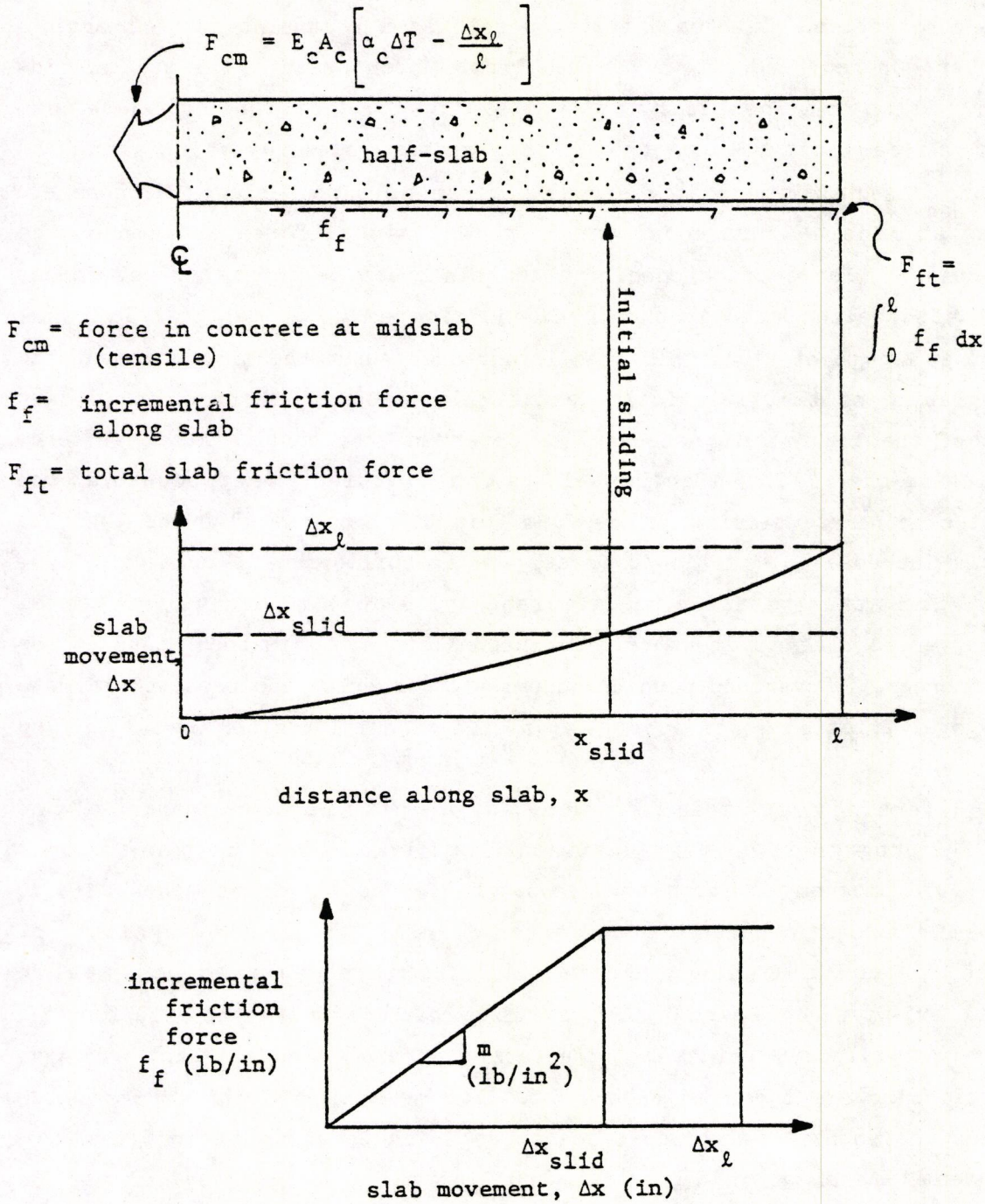

Figure 5.5. Illustration of the process for determining the slope of the friction curve, m.

slab contraction. Slab-base friction acts as a restraint to contraction, however, thereby inducing concrete forces which reach a maximum at mid-slab. Since it is necessary to maintain static equilibrium, these concrete forces must balance the frictional forces at any point along the slab. Consequently, in a free body diagram of a half-slab, the concrete force at midslab must equal the total frictional force applied on the underside. (For a crack condition in reinforced pavements, steel forces must also be included in the free body diagram). Since the frictional force at any point along this slab is dependent upon the slab movement, an integration of the restraint/movement relationship, (shown in the lower part of the figure), is necessary to determine the total frictional force acting on the slab. Unfortunately, a complication is introduced at the point of concrete sliding, since from this point to the slab end there is little increase in frictional force. Once equilibrium is achieved, however, it is then possible to calculate the slope, m, of the frictional force versus slab movement relationship. This slope is then adjusted for the increase in overburden which occurs after overlay and used to estimate the total friction force acting for a given condition after overlay.

Referring once again to Figure 5.2, the next major component of the RFLCR-2 program is contained within Block IV. In this part of the process, the program attempts to balance the forces which are generated due to temperature drops that occur after overlay. Since the magnitude of these forces is highly dependent upon concrete movement, static equilibrium is achieved by varying the restraint/movement relationship. Some of the forces which are affected by varying the restraint/movement relationship are shown in Figure 5.6. The most significant forces which affect the equilibrium process are those which occur in the original PCC pavement. As shown in Figure 5.6, equilibrium is achieved by varying the after overlay restraint coefficient, β_B, until these forces balance.

After equilibrium is achieved, the force, F_{oc}, which is carried by the overlay (at the joint or crack) is used to compute the maximum tensile strain, ε_t, generated in the overlay at the joint. This calculation

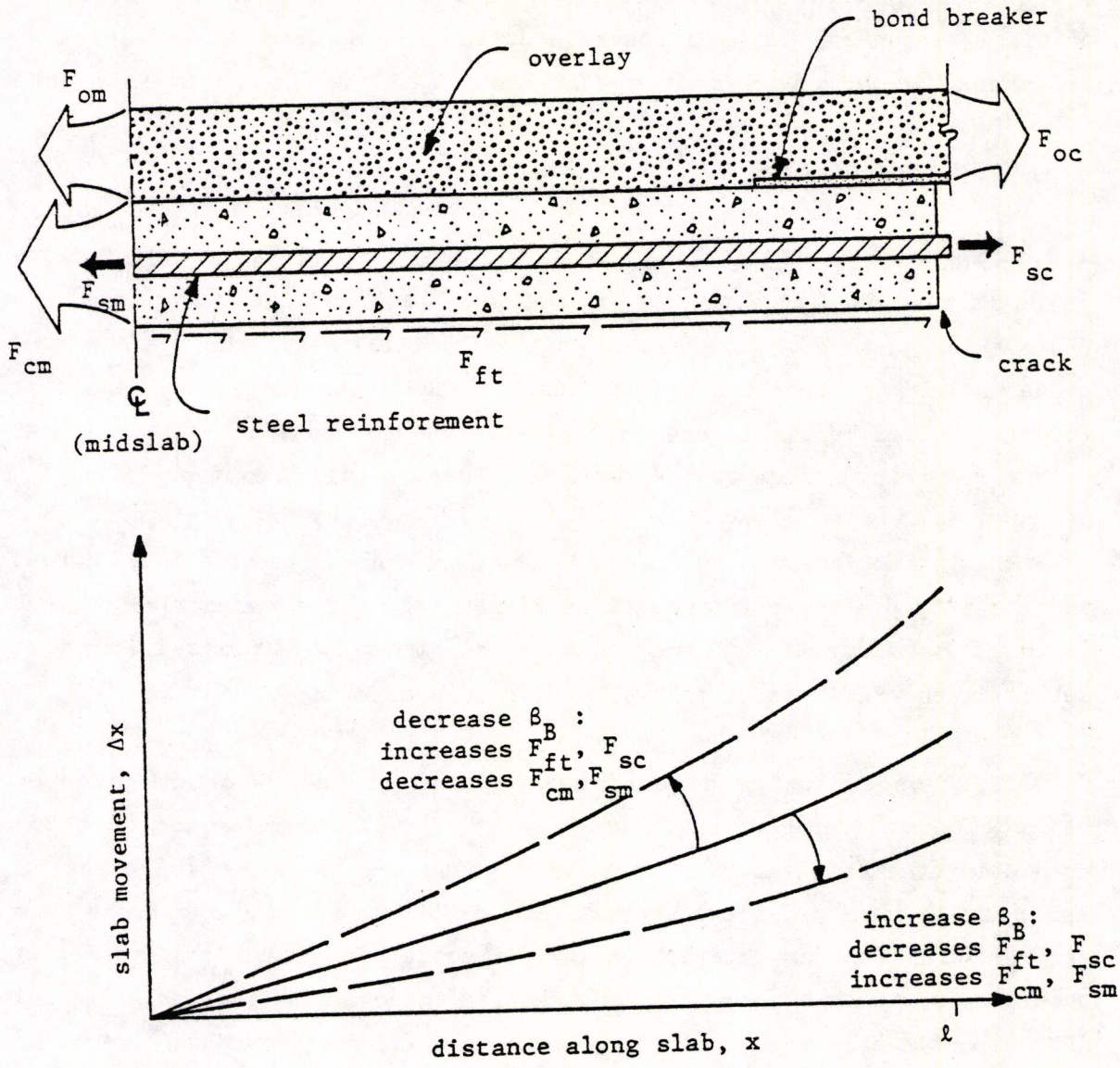

Figure 5.6. Illustration of the force balancing method used to achieve equilibrium in the pavement structure after overlay for the design temperature drop.

(illustrated in Figure 5.7) along with the calculation of the other critical responses, maximum concrete stress and maximum steel stress at the crack, is what is summarized by Block V of the flowchart in Figure 5.2.

Block VI of Figure 5.2 summarizes the use of field deflection measurements at joints (or cracks) to calculate load transfer, L_T. This value is then used to estimate the maximum vertical shear strain, γ, in the overlay just above the joint. Figure 5.8 illustrates this part of the procedure. It is important to note that the shear strain is very sensitive to differential vertical movements between the two adjacent slabs and may be the governing design factor for low values of load transfer.

The last major component of the flowchart summarizes the RFLCR output and its interpretation (Block VII in Figure 5.2). Like the collection and input of data for the program (Block II), this is discussed in great detail in the FHWA report and will not be discussed here.

This concludes the general description of the second version of reflection cracking analysis program, RFLCR-2, and its procedure for predicting the critical overlay strains conducive to reflection cracking. Appendix A, however, provides a detailed illustrative flowchart of the program with further description of the actual iterative processes. It should be noted that there are some changes in notation (from the original FHWA report) which were made in order to aid in interpretation.

ARKRC: ARKANSAS REFLECTION CRACKING PROGRAM

This section discusses all the improvements that were made to the original RFLCR-2 computer program in order to develop the new ARKRC-2 program which comprises the main component of the new Arkansas reflection cracking analysis and overlay design procedure. These improvements fall under the following headings:

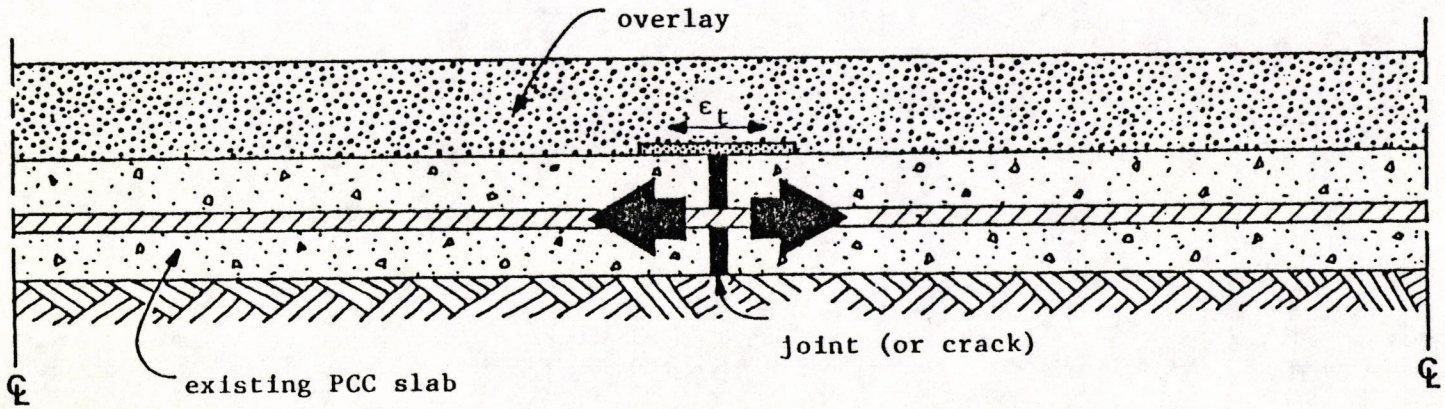

$$\varepsilon_t = \frac{F_{oc}}{E_o A_o}$$

where: ε_t = maximum tensile strain in overlay after design temperature drop,

F_{oc} = force in overlay at crack after design temperature drop,

E_o = ACP overlay stiffness at low temperature, and

A_o = cross-sectional area of overlay (width x thickness).

Figure 5.7. Calculation of the maximum horizontal tensile strain in an ACP overlay after the design temperature drop.

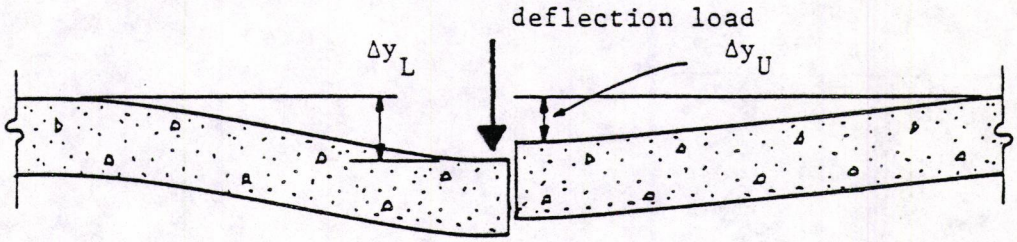

$$L_T = 1 - \frac{\Delta y_L - \Delta y_U}{\Delta y_L}$$

a) calculation of the fraction of load transfer, L_T, from field measurements of vertical motion.

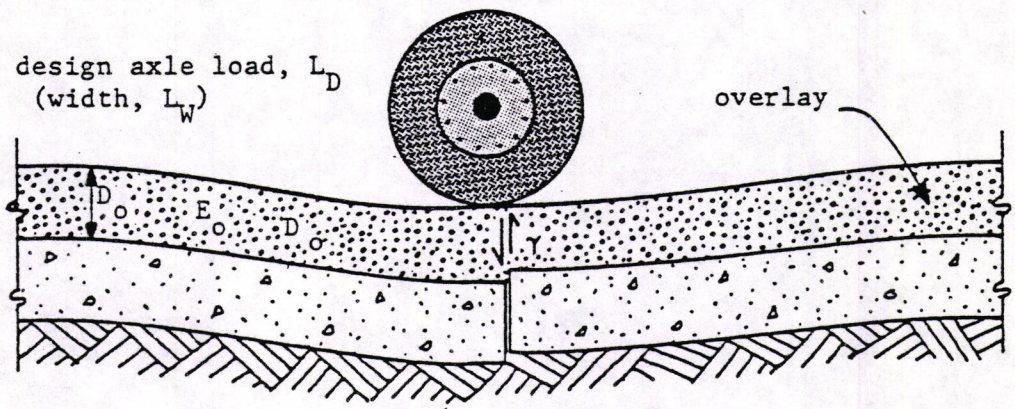

shear strain, $$\gamma = 2 \left[\frac{L_D (1 - L_T)}{E_o D_o L_W} \right] (1 + \upsilon_o)$$

where:

υ_o = overlay Poisson's ratio

b) calculation for maximum shear strain resulting from differential vertical motion at joint.

Figure 5.8. Illustration of the procedure for calculating the maximum shear strain in an overlay due to poor load transfer across a joint (or crack).

1. New restraint/movement relationship,
2. Effect of intermediate layer,
3. Fatigue damage model,
4. Development of tensile strain fatigue equation, and
5. Improved shear strain model.

The first four apply to the improvements made after considering the effects of temperature changes and the thermal related horizontal slab movements. The last improvement applies to the effects of differential vertical movements between adjacent slabs.

New Restraint/Movement Relationship

The restraint/movement relationship (beta function) is used in the reflection cracking program to define the temperature drop related movement at any point along a concrete slab. This relationship plays a significant role in the program in that the iterative force balance (equilibrium) process used depends on the movement profile defined by the function for different values of the restraint coefficient, beta (β).

The function used in the original RFLCR-1 (and RFLCR-2) reflection cracking program(s) had the following form:

$$\Delta x = \alpha_c \cdot \Delta T \, (x - \beta x^{\beta})$$

where:
α_c = concrete thermal coefficient (in/in/^{o}F),
ΔT = temperature change (^{o}F),
x = longitudinal point along slab measured from center-line or midpoint of slab (in), and
β = restraint coefficient (beta), and
Δx = movement at point x (in.)

The range of beta is from zero to one. A zero value implies that slab movement is unrestrained and a value of beta equal to one means that the

slab is completely restrained against thermal movements. Figure 5.9 provides a simple illustration of the effect of varying restraint on the forces acting on a concrete slab as it contracts due to a temperature drop. Increased restraint or a higher value of beta results in high tensile forces in the concrete at midslab (F_{cm}) and low frictional forces (F_{ft}) on the underside of the slab. Conversely, decreased restraint or a lower value of beta results in low concrete forces at midslab and higher frictional forces between the concrete and base layer due to higher relative movements between the two. This inter-relationship between movement and opposing forces provides the basis for the more complex equilibrium process used to solve overlayed pavements.

Although the original beta function seems to provide reasonable results, there are some problems with it. One is that it has inconsistent units. Another is that its form results in excessive iterations by the program before equilibrium is achieved. Lastly, and more importantly, its form does not accurately model actual slab movements under semi-restrained conditions. The equation predicts higher movements near midslab than are observed in the field. This, in turn, results in higher estimates of the frictional forces acting on the slab.

In order to remedy these problems, then, another equation with a slightly different form was developed and incorporated into the ARKRC-2 program:

$$\Delta x = \alpha_c \cdot \Delta T \cdot (1-\beta) \cdot x \cdot \left(\frac{x}{\ell}\right)^{\beta}$$

where all the variables are the same as before except, ℓ, the half-length of the slab (inches) has been introduced. This new equation has greater curvature and therefore, predicts equal or less movement all along the slab.

Figure 5.10 provides a normalized plot for comparing the two functions. The vertical axis represents slab movement which has been normal-

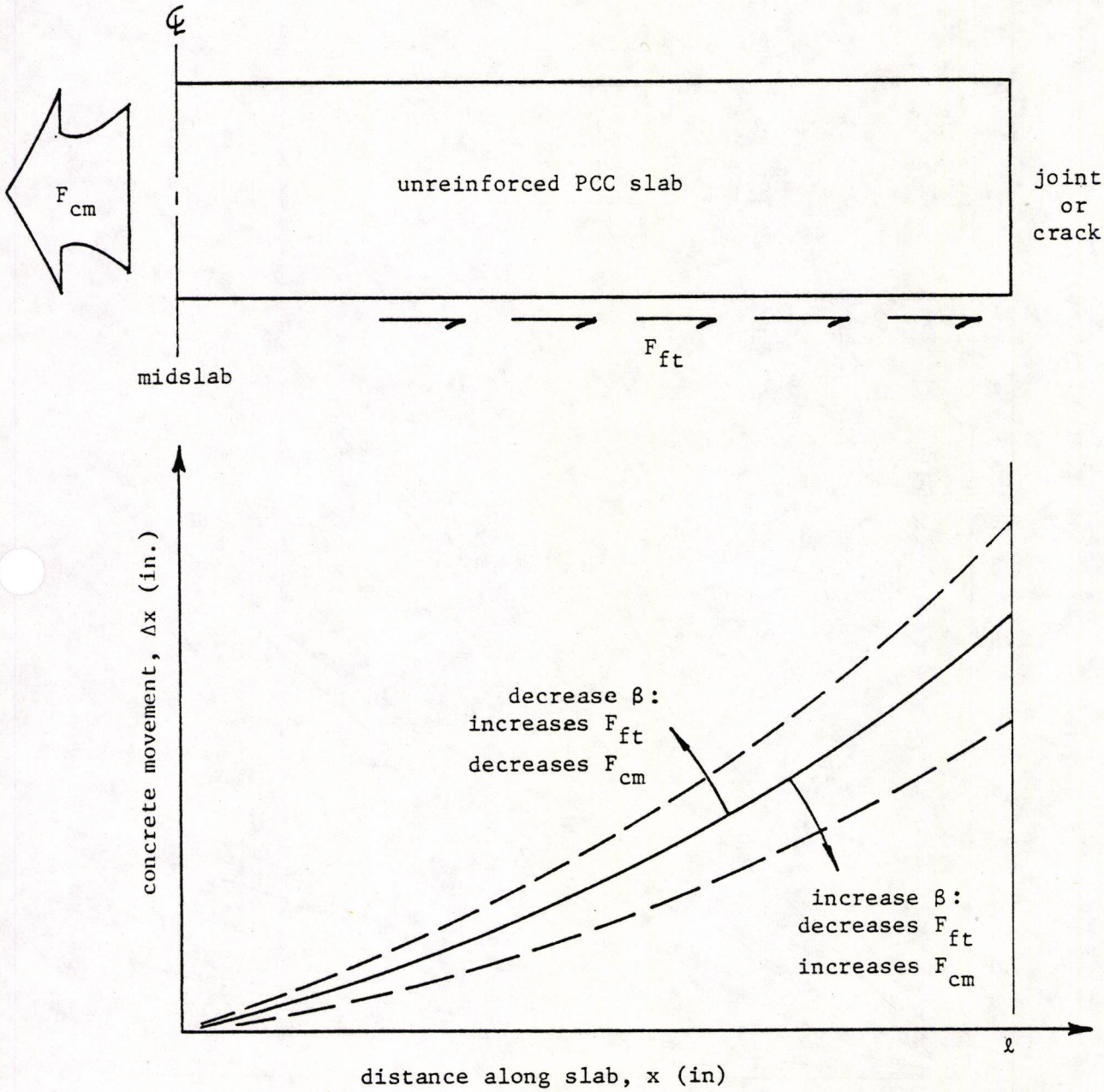

Figure 5.9. Illustration of the effect of varying restraint (β) on the primary forces acting in a concrete pavement under a given temperature drop.

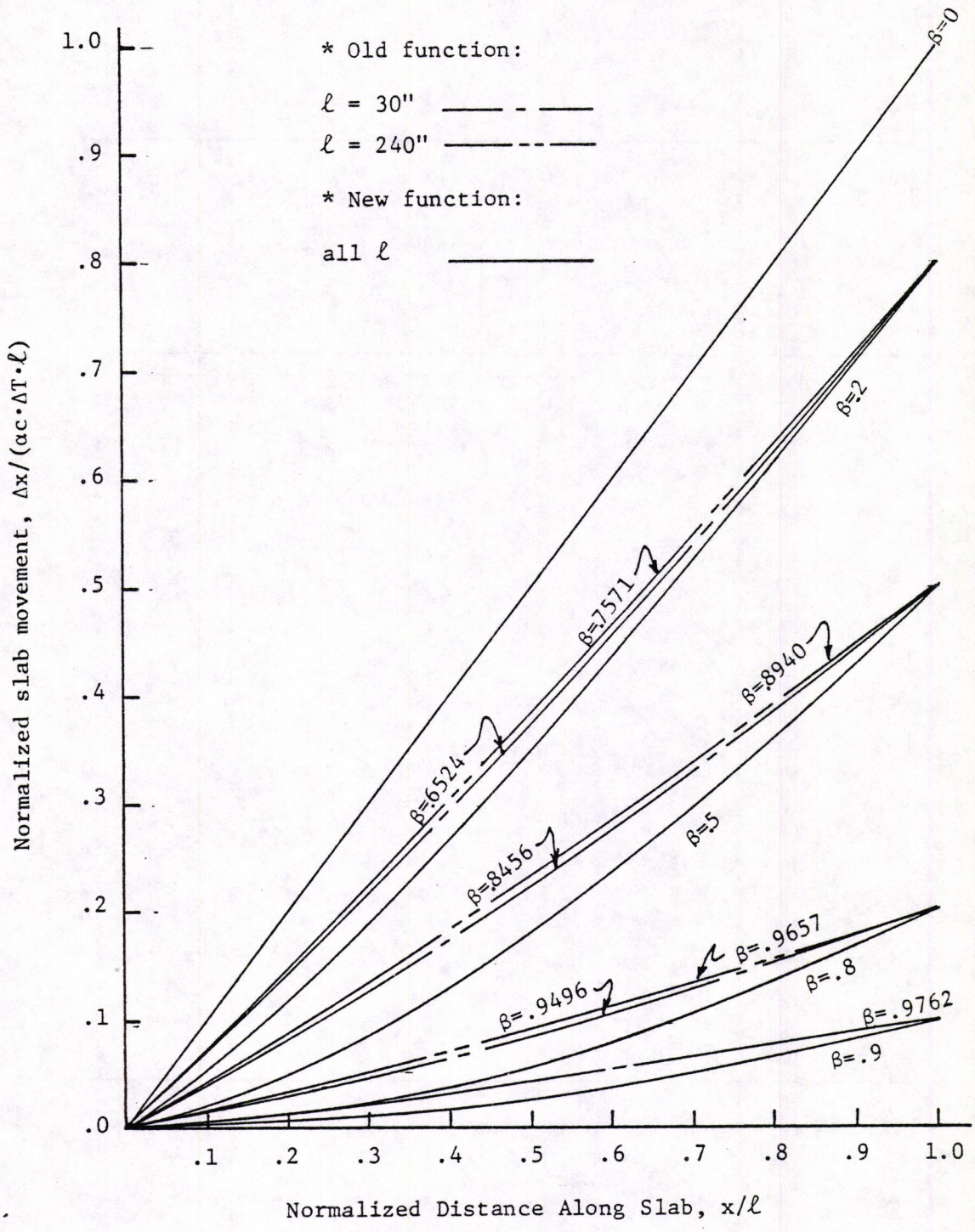

Figure 5.10. Normalized plot of slab movement versus distance along slab for comparison of new and old β functions.

ized relative to the maximum thermal movement that can occur at the slab end for unrestrained conditions. The horizontal axis represents normalized distance along the slab. Note that an additional advantage to the new function is that a certain amount of restraint corresponds to only one value of beta, regardless of slab length.

Effect of Intermediate Layer

The primary purpose of the intermediate layer is to reduce tensile strains in an asphalt concrete overlay which develop as a result of the temperature related horizontal movements of the underlying concrete slab. Unfortunately, the models used in the original RFLCR programs did not adequately consider the effects a low stiffness intermediate layer (e.g. the Arkansas open-graded course) has on reducing these tensile strains. Basically, the RFLCR programs do not consider the ability of such an intermediate layer to absorb some of these slab thermal movements before they reach the overlay. Although this inherent assumption is conservative, it was considered necessary to analyze the effects in more detail in this study since the open-graded course is frequently used in Arkansas as a deterrent to reflection cracking.

In order to be able to adequately predict the effects of an intermediate layer on reducing overlay tensile strain then, it was necessary to develop an equation which considered the primary characteristics of the layer (i.e. thickness and creep modulus). After considering alternative methods for developing this function, it was decided that the only practical means was the combined use of a finite element programs and regression analyses. The finite element computer program, SOLID SAP (Ref. 75), was selected because of the success experienced in using it for many other pavement analysis problems.

Figure 5.11 illustrates the difference between the maximum tensile strain, ε_{max}, developed in the intermediate layer and the strain that is

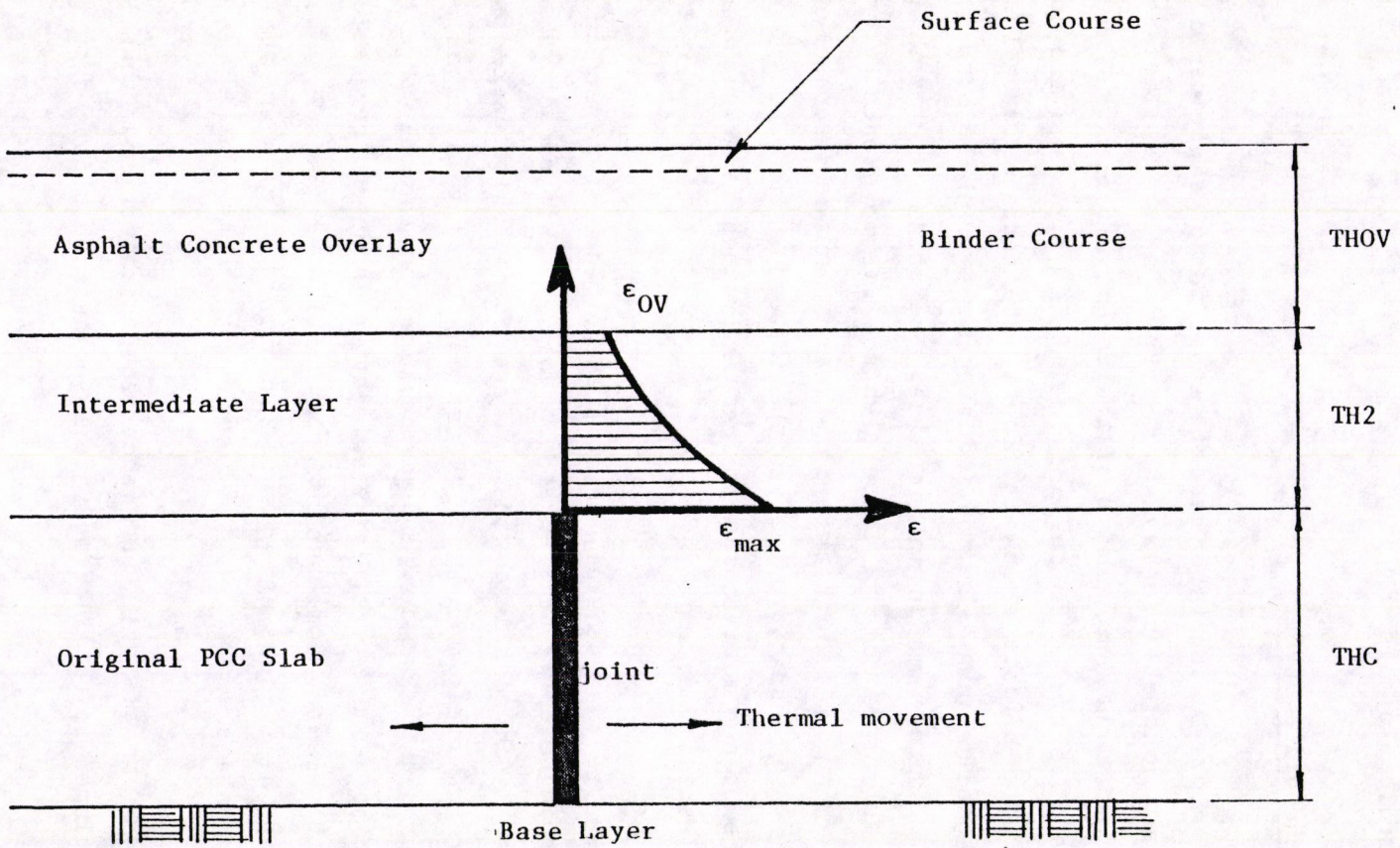

Figure 5.11. Illustration of the reduction (or absorption) of horizontal strain by a low stiffness intermediate layer.

transferred to the overlay, ε_{OV}. The equation used to estimate, ε_{OV} is of the form:

$$\varepsilon_{OV} = f_{IL} \cdot \varepsilon_{max}$$

where f_{IL} (the intermediate layer strain reduction factor) is a function of the layer thickness (THOV and TH2) and the layer creep moduli (EOV and E2).

The equation for f_{IL} was the result of a step-wise linear regression analysis of several SOLID SAP solutions. The two-dimensional finite-element overlay model used to generate the solutions is illustrated in Figure 5.12. The node load diagram shown is representative of the loading applied to the intermediate layer due to the thermal contraction of the slab. This loading was translated into equivalent node loads in order to generate the SOLID SAP solutions.

Several SOLID SAP runs were made in which values of the critical factors were in the following range:

1) Asphalt concrete overlay thickness, THOV: 1.5 - 6.5 inches
2) Asphalt concrete overlay creep modulus, EOV: 20,000 - 75,000 psi
3) Intermediate layer thickness, TH2: 2.0 - 6.0 inches
4) Intermediate layer creep modulus, E2: 5,000 - 10,000 psi

The equation for f_{IL} that resulted from the regression analysis of this data is as follows:

$$\ln(f_{IL}) = +5.9223 - 0.50742 \cdot \ln(TH2) - 5.5061 \cdot [\ln(EOV)/\ln(E2)] - 0.52215 \cdot [\ln(THOV) \cdot \ln(EOV)/\ln(E2)]$$

After the development of this equation, it was recognized that it was also necessary to consider the effect of strain reduction on both the intermediate layer and overlay forces calculated and used in the ARKRC-2

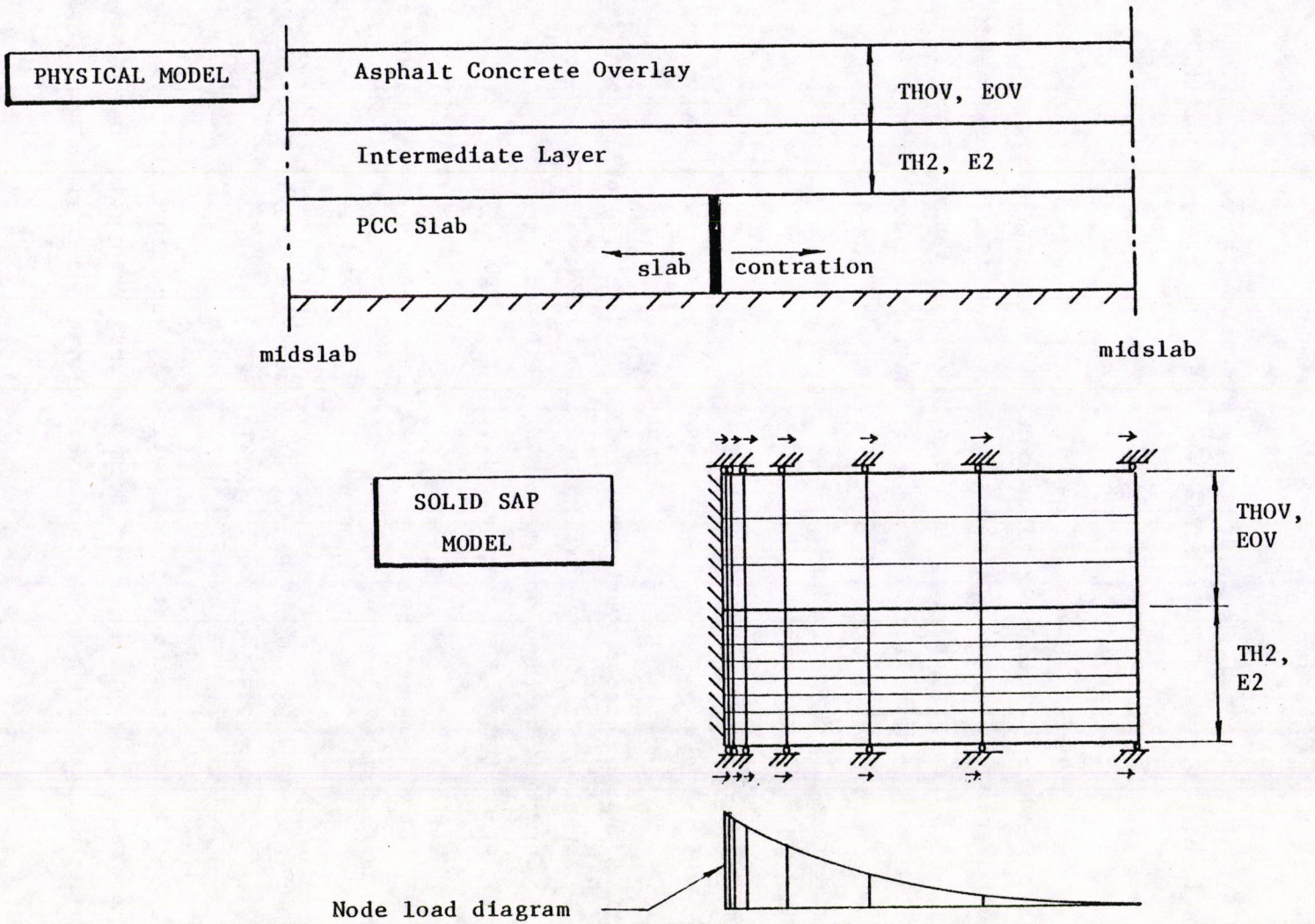

Figure 5.12. Illustration of two-deminsional SOLID SAP Model of intermediate layer and asphalt concrete overlay subjected to loading by underlying slab contraction.

computer program's iterative force balance (equilibrium) process. Consequently, a second equation was developed using the same finite-element program (SOLID SAP) solutions to estimate the ratio, f_{OV}, of the strain at the top of the overlay (ε_{TOP}) to the maximum overlay strain (ε_{OV}). The resulting equation for f_{OV} is as follows:

$$f_{OV} = 0.3362 + 0.3021 \cdot \ln(9-THOV)$$

[Note: If THOV greater than 9 inches, then $f_{OV} = 0$].

The strain at the top of the overlay could then be calculated using the following equation:

$$\varepsilon_{TOP} = f_{OV} \cdot \varepsilon_{OV}$$

Finally, in order to estimate the forces acting in these layers under a given temperature drop, a model was developed which integrates the tensile strain distribution function between the top and bottom of each layer. (A log-linear relationship was used to define each layer's distribution of strain between the maximum at the bottom and minimum at the top). It is important to note that the effects of strain reduction were considered to apply only to the strains developed due to underlying slab movements. They do not apply to each layer's thermal component of strain, since these are directly related to the temperature of the layer and not the movement of the slab.

Fatigue Damage Model

It has been pointed out that the tensile strains which induce reflection cracking come about as the result of both direct thermal stresses and the temperature drop related movements of the underlying slab. Since the purpose of the procedure is to provide criteria for the selction of long-lasting overlay design alternatives and since these tensile strains are cyclic in nature, the reflection cracking which develops in the overlay

must be attributed to fatigue or the accumulation of damage brought about by cyclic loading. Because of this, it was considered essential that the fatigue damage concept be incorporated into the ARKRC-2 analysis and design procedure.

The consideration of fatigue for a constant cyclic loading condition is very simple. A small complication is introduced, however, when the effects of a variable cyclic load (such as that resulting from varying low-temperature drops) are considered. This consideration of variable load effects requires the assumption that Miner's linear damage hypothesis is applicable to the analysis of fatigue in flexible overlays. This is not a bad assumption and has, indeed, been used in several other problems dealing with the analysis and design of highway pavements.

Aside from the ARKRC program improvements already discussed, the modifications required to incorporate the new fatigure model were minimal. The basic iterative force balance (or equilibrium) process is still used to estimate the maximum tensile strain in the overlay under the maximum temperature drop conditions. New computer code was added, however, to allow the computation of the lesser tensile strains which are developed under less severe temperature drop conditions. Additionally, a new subroutine (called OVLIFE) was incorporated into the program to convert these strains into an estimated overlay life (in years).

Information on the distribution of daily temperature drops for Arkansas was obtained from the National Climatic Center (see Chapter 3). This information was collected from a seven year period (1974 - 1980) for both the maximum daily temperature drop and the difference between 50°F and the minimum daily temperature. The latter data were obtained because a study conducted at the Texas Transportation Institute (Ref. 72) indicated that the primary temperature related damage suffered by asphalt concrete occurs when the temperature is below 50°F. The results of the fatigue equation development (discussed later) verified this observation for conditions in Arkansas, and therefore, 50°F was selected as a

reference temperature for calculating the overlay tensile strains. Inspection of the Arkansas temperature data shows that the differences between 50°F and the daily minimum temperature are divided into 10 degree frequency ranges (classes) which identify the average number of days during the year that the temperature drops a certain magnitude below 50°F. The total number of days from each range (class) for a given region is never equal to the total number of days in a year (365) since days in which the temperature stays above 50°F are not counted. The seven temperature drops and corresponding minimum temperature frequency ranges (classes) considered are as follows:

	Range of Temperature Drop (°F)	Range of Minimum Temperature (°F)	Average Temperature Drop Below 50°F
1.	1 to 10	49 to 40	5
2.	11 to 20	39 to 30	15
3.	21 to 30	29 to 20	25
4.	31 to 40	19 to 10	35
5.	41 to 50	9 to 0	45
6.	51 to 60	- 1 to -10	55
7.	61 to 70	-11 to -20	65

The average temperature drops (below 50°F) shown are used by the program to estimate the corresponding overlay tensile strains. For the procedure used by the program, it is assumed that each layer of the pavement (i.e., AC overlay, intermediate layer and original PCC slab) undergoes this same average temperature drop. Although this is not always true, it is a conservative assumption.

After these tensile strains $(\varepsilon_T)_i$ are determined for each average temperature drop, a fatigue relation (discussed in the next section of this chapter) is used to estimate the allowable number of cycles, $(N_T)_i$, of a given strain the overlay can carry before it cracks. Next, the

incremental damage, d_i, accrued each year by each given strain level is determined using the following equation:

$$d_i = \frac{n_i}{(N_T)_i}$$

where: n_i = average number of days during the year in which the overlay is subjected to a given strain level $(\varepsilon_T)_i$.

Note: Since each strain level corresponds to a particular average temperature drop, n_i can be determined from the Arkansas temperature distribution data discussed previously.

Next, the yearly damage due to each individual strain level is accumulated according to Miner's hypothesis:

$$D = \sum_{i=1}^{7} d_i = \sum_{i=1}^{7} \frac{n_i}{(N_T)_i}$$

where D represents the total damage experienced by the overlay during the course of one year.

Since by definition, "failure" occurs when D is equal to 1.0, the number of years, Y_T, the overlay will last can finally be determined using the following simple equation:

$$Y_T = 1.0/D$$

This leaves only one detail to be discussed about the new procedure, the development of a fatigue relation used to estimate the allowable number of cycles, $(N_T)_i$, of each overlay strain level.

Development of Tensile Strain Fatigue Equation

Because of the need to predict the occurrence of reflection cracking using the fatigue approach, it was necessary to develop a tensile strain fatigue equation compatible with the ARKRC analysis model. This was accomplished by calibrating the ARKRC-2 program based on the field performance of overlays in Arkansas and Texas. As discussed in Chapter 3, AHTD conducted the surveys and provided the data on the performance of ten separate overlay sections in Arkansas (Table 3.3), while the University of Texas' Center for Transportation Research provided data on four overlay sections in Texas (Table 3.4). Unfortunately, because of one or a combination of reasons, eight of the ten Arkansas sections could not be considered in the calibration process, which is why it was necessary to use the available data from Texas. Section 1 could not be considered because the type of subbase was not known and neither was the age of the overlay. Section 2 was not considered because it exhibited no reflection cracking. Section 4 could not be considered because of an unknown subbase type and the presence of multiple overlays. Sections 5a, 5b, 5c and 5d were not considered because of an unknown subbase type and the presence of multiple overlays. Furthermore, the presence of cracks in sections 5a and 5d and the use of an unknown width SAMI (stress-absorbing membrane interlayer) in sections 5c and 5d made the data from these sections questionable. Section 6 was not considered because of the lack of survey data on cracking in the original PCC pavement prior to overlay. This left only two Arkansas JRCP sections (No. 3 and No. 7 in Table 3.3) and the four Texas sections (two CRCP, one JCP and one JRCP with the Arkansas mix design overlay) left for use in developing the fatigue equation and calibrating the ARKRC-2 program.

Fatigue equations for asphalt concrete tensile strain are generally of the form:

$$N_T = a_1(\varepsilon_T)^{a2}$$

where a_1 and a_2 represent calibration (or regression) coefficients and N_T

and ε_T are as defined previously. Shahin and McCullough (Ref. 76) conducted a study for the prediction of low-temperature and thermal-fatigue cracking in flexible pavements which provided a basis for initial calibration. They indicated that the coefficients a_1 and a_2 are dependent upon the modulus of the asphalt concrete. Figure 5.13 shows their fatigue curves corresponding to extreme values of asphalt concrete modulus, E_{AC}. Log-linear interpolation was recommended to estimate a_1 and a_2 for E_{AC} values between these extremes.

In order to calibrate the program, then, it was necessary to determine the appropriate input values for each section, define the fatigue coefficients and then see how well the program predicted the observed reflection cracking. Appendix B summarizes the input data used in the calibration process. (These data were selected based mostly on criteria provided in the User's Manual presented in Chapter 6).

As a final step before the iterative calibration procedure, it was necessary to define a common basis for the overlay performance data. Consequently, the age of each overlay section when it exhibited 50 percent reflection cracking was estimated using a relationship which assumes that the distribution of reflection cracking is log-normally distributed:

$$y_{50} = y/SD^z$$

where: y_{50} = overlay age at 50 percent reflection cracking (years),
y = overlay age at time of survey (years),
SD = standard deviation of log-normal distribution (our experience with fatigue relationships indicates $\log_{10}SD = 0.20$), and
z = standard normal variate (in this case z depends on the percentage of reflection cracking actually observed in overlay section).

With these conversions, several trial and error iterations were conducted where the fatigue coefficients were assumed, the program run on each

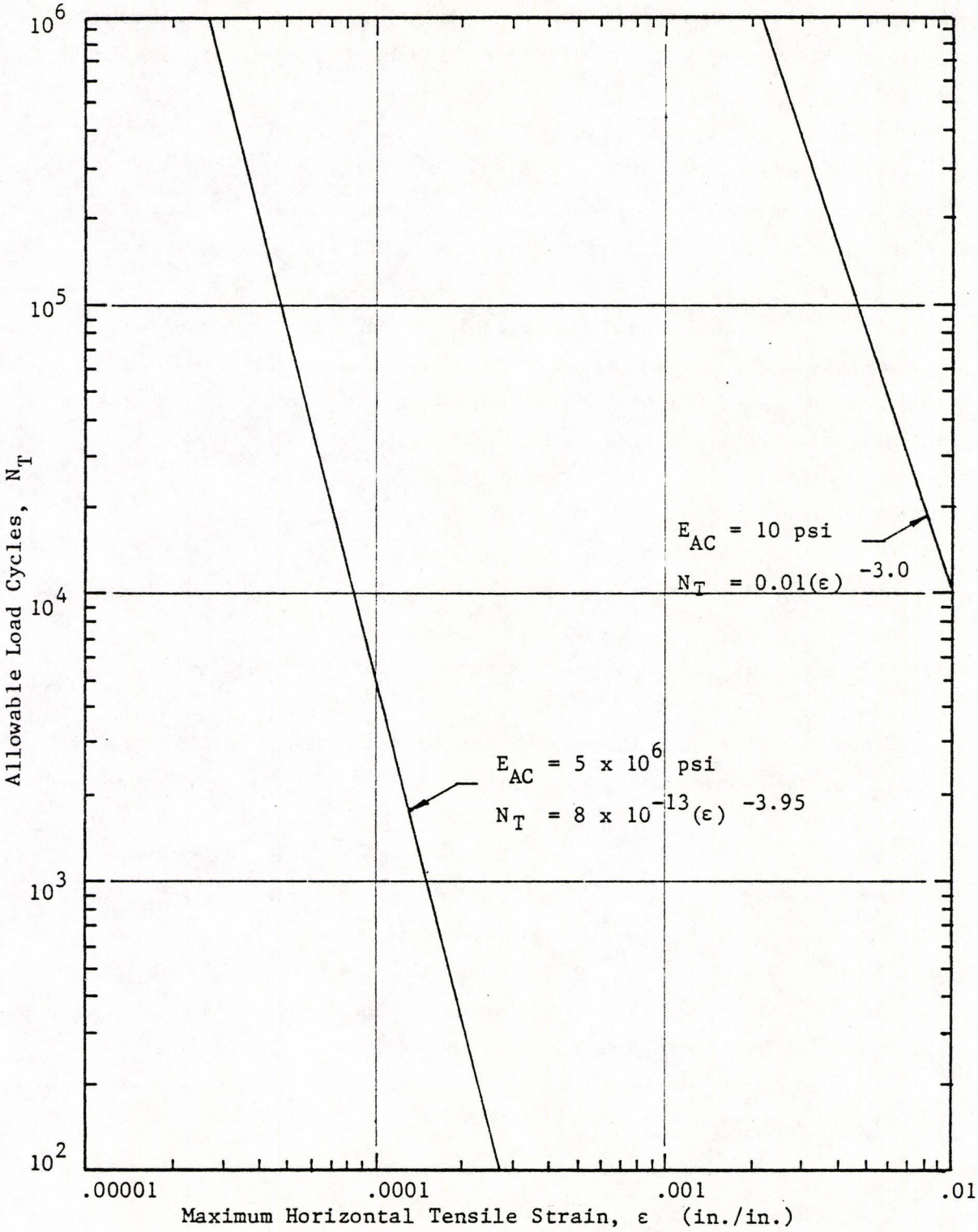

Figure 5.13. Asphalt concrete fatigue relationships for thermally induced tensile strains.

section and the results examined. The result was a tensile fatigue equation that was not too different from the Shahin-McCullough equation (Ref. 76).

Basically, it was determined that the fatigue coefficient, a_1, was still dependent upon the creep modulus of the overlay, but somewhat different from the value estimated by the Shahin-McCullough equation. On the other hand, the remaining fatigue coefficient, a_2, which represents the slope of the line was determined to be relatively independent of the overlay modulus, but almost identical to the value predicted by the Shahin-McCullough equation for the range of overlay moduli considered. The fatigue coefficients are as follows:

$$a_2 = -3.70$$

$$a_1 = 8.072 \times 10^{-4} (EOV)^{-1.118}$$

where: EOV = asphalt concrete overlay creep modulus, psi.

Table 5.1 shows the comparison between the actual overlay age, y, at the time of the survey and the value, Y, predicted by the procedure. Also shown is the y_{50} to Y_{50} comparison, where Y_{50} represents the number of years predicted by the program to 50 percent reflection cracking. Note that the comparisons are excellent for all but one of the sections (Texas 3a). It was not considered worthwhile to sacrifice the accuracy of prediction for the five other sections when the "outlying" section (a 6-year old 2-1/2 inch overlay with less than 5 percent reflection cracking) appeared to be performing much better than can normally be expected.

Improved Shear Strain Model

In the development of the original shear strain model (Ref. 1), some simplifying assumptions were made in order to estimate the overlay shear strain. These assumptions are acceptable, given that the resultant shear

Table 5.1. Comparison between actual and predicted overlay ages for the Arkansas and Texas calibration sections.

State	Section Number	Survey Data		Actual Overlay Age Adjusted for 50% Reflection Cracking, Y_{50} (years)	Overlay Age Predicted by ARKRC-2 for 50% Reflection Cracking, Y_{50} (years)	ARKRC-2 Overlay Age Adjusted for Actual Reflection Cracking, Y (years)
		Percent Reflection Cracking	Overlay Age, y (years)			
Arkansas	3.	4.5	3.0	6.5	6.5	3.0
	7.	31.5	4.3	5.4	5.4	4.3
Texas	1.	99.	0.5	0.2	0.2	0.5
	2.	14.7	1.2	2.0	2.0	1.2
	3a.	4.24	6.0	13.3	3.6	1.6
	3b.	0.37	6.0	20.6	21.4	6.2

strain need only be compared against some minimum allowable strain criteria. They are not considered acceptable, however, in the more rigorous method required for the Arkansas design procedure.

The primary improvement made in the shear strain model was in the estimation of the maximum shear strain given the applied load and joint (crack) deflections made prior to overlay. The new improvement recognizes some theoretical boundary conditions which result in a higher maximum overlay shear strain than that determined by assuming that the shear strain is distributed evenly throughout the overlay. This new improvement will be discussed within the reformulated model presented in the following paragraphs.

Since overlay shear stresses develop primarily as a result of differential vertical movements at joints (or cracks) between adjacent slabs, it is important that some field measurements be made prior to overlay to characterize this distress mechanism. The best way to do this is: for a number of joints (or cracks) within a given design section, load one side of the joint and measure the deflection on both the loaded and unloaded sides. A light load is desirable so that the differential deflections measured will simulate those after overlay.

The Dynaflect deflection device is well suited for this measurement and is recommended for use in Arkansas. Figure 5.14 provides an illustration of the location of the Dynaflect load and geophones required to give the loaded and unloaded deflection values, w_ℓ and w_u. Note that in order to have geophones 1 and 2 so close together, it is necessary to unstrap geophone 2 from its support and manually position it directly across the joint from geophone 1.

With these deflection values, it is possible to estimate the amount of shear force, V_o, that will be carried by the overlay layers. This can be illustrated with the aid of Figure 5.15. The deflections w_ℓ and w_u on either side of a joint due to a load P (Figure 5.15a) can be simulated by

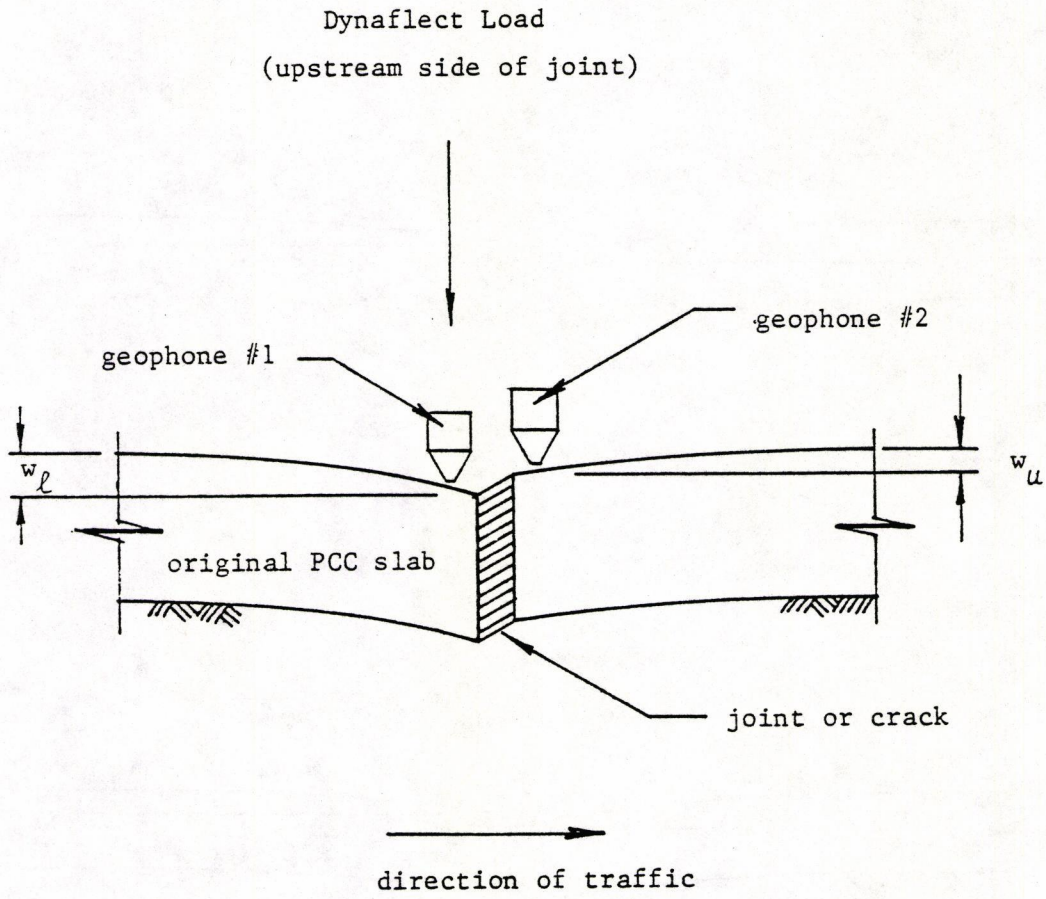

Figure 5.14. Illustration of Dynaflect deflection load and geophone configuration for determining required deflection values.

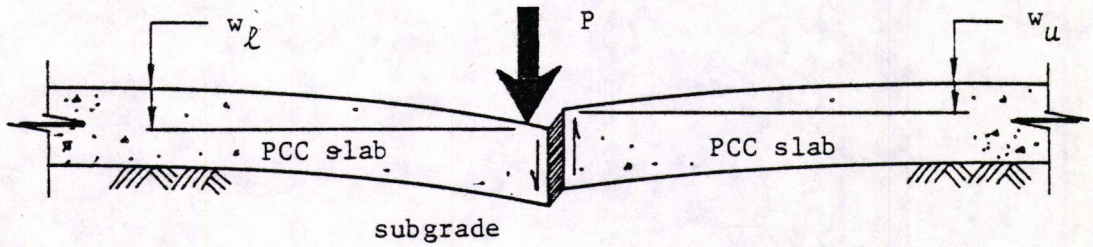

a) illustration of actual mechanism of load transfer

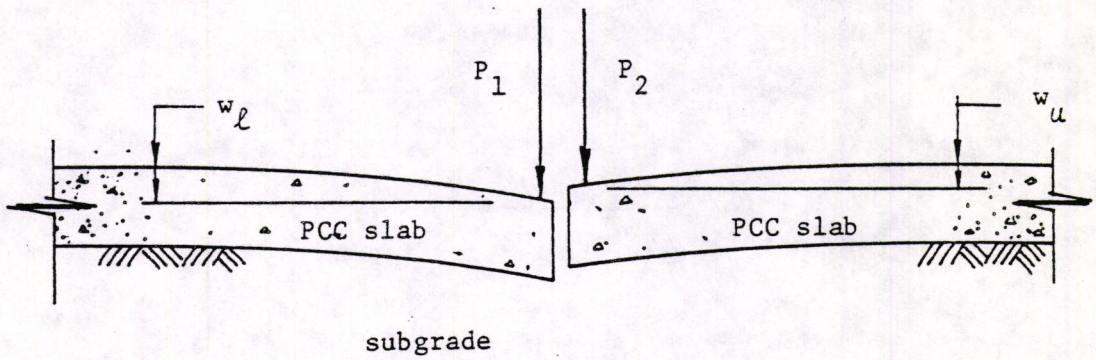

b) model showing effective forces P_1 and P_2, which result in identical deflections

Figure 5.15. Load transfer diagrams.

two forces, P_1 and P_2, acting separately (Figure 5.15b). From the Westergaard theory (Ref. 73) and slab theory, we know that the magnitude of a slab's deflection is directly proportional to the load applied, therefore:

$$\frac{P_1}{P_2} = \frac{w_\ell}{w_u}$$

Since the total force which causes the deflection on both sides, P, is equal to $P_1 + P_2$ and since the shear force after overlay V_o, is equal to $P_1 - P_2$, the equation can be rearranged to solve for V_o:

$$V_o = P \left[\frac{w_\ell - w_u}{w_\ell + w_u} \right]$$

This equation represents a significant change from the equation used in the original procedure (i.e., $V_o = P \cdot w_\ell / w_u$) which did not recognize that both w_ℓ and w_u are the result of the total load, P.

The next step in the determination of the maximum shear strain is to estimate the shear moduli of the overlay layer(s). This is accomplished using the following equation:

$$G = \frac{E}{2(1 + \upsilon)}$$

where:

G = shear modulus, psi (G_{OV} for overlay, G_2 for intermediate layer,

E = design dynamic modulus of the layer during critical temperature conditions, psi, and

υ = Poisson's ratio for the layer (0.30 recommended for

ACHM overlay, 0.35 for open-graded course intermediate layer).

These shear moduli are then used to determine an effective overlay thickness, D_e:

$$D_e = THOV + \left[\frac{G_2}{G_{OV}}\right] TH2$$

where THOV and TH2 are the thicknesses (in inches) of overlay and intermediate layers, respectively.

Next, the maximum shear stress in the overlay layers is determined using the improved procedure pointed out earlier. If a section, A-A, is taken out of the ovelay in the region where the shear force acts, then the distribution of shear stress along that section will be as illustrated in Figure 5.16. The general equation below defines the shear stress at any location along the face:

$$\tau = \frac{VQ}{Ib}$$

where:

τ = shear stress, psi
V = shear force, lb.
Q = first moment of the area above (or below, depending on the position of the neutral axis) the location where strain desired, $in.^3$
I = moment of inertia, $in.^4$, and
b = width of section, in.

Note that for equilibrium of a small element taken at the top (or bottom) of the section, the shear stress must be zero. (The original assumption

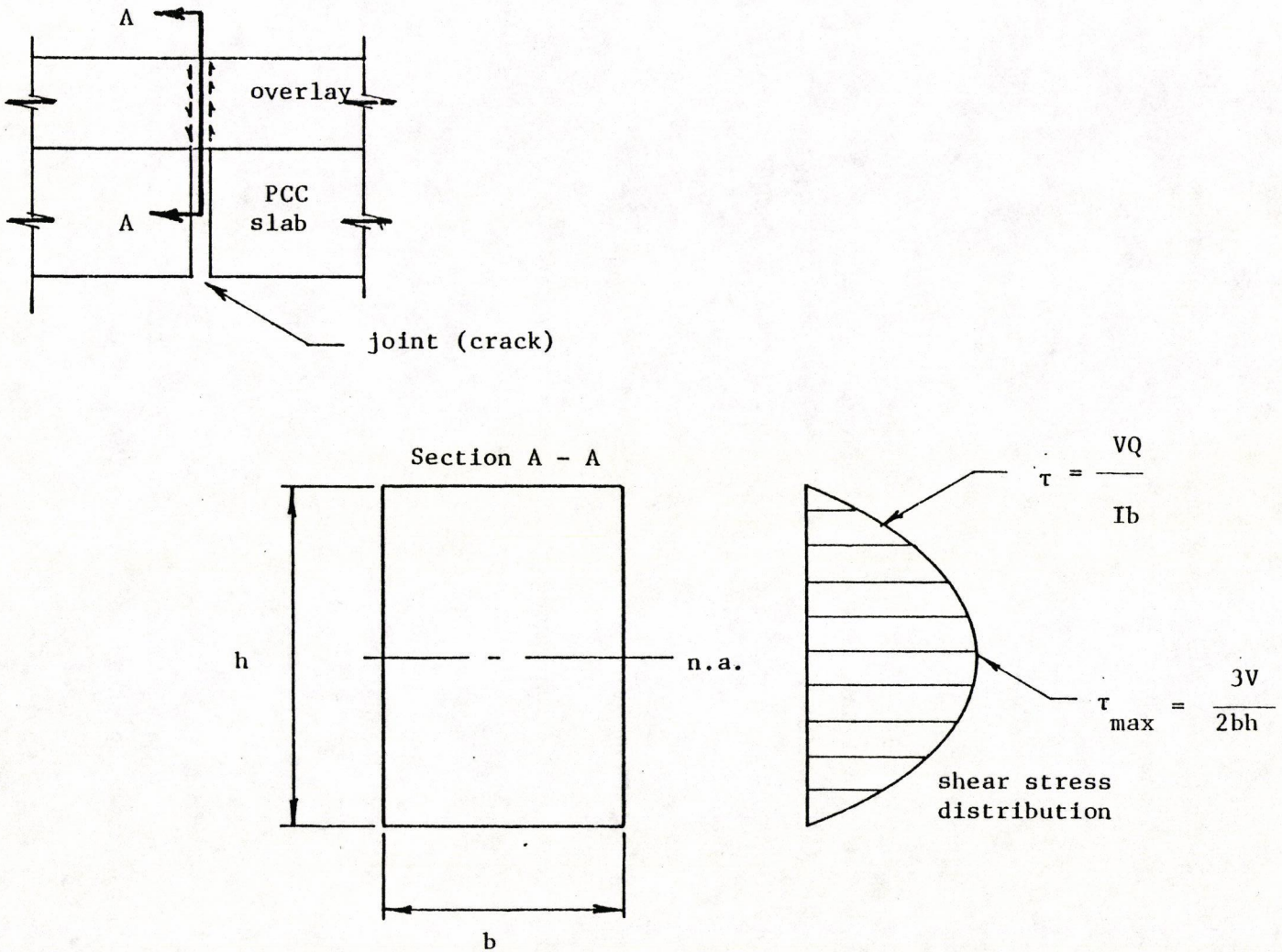

Figure 5.16. Distribution of shear stresses in the overlay.

of an equal distribution of shear stress violates this boundary condition).

A simplification of this equation can be used to estimate the maximum shear stress at the neutral axis cross-section.

$$\tau_{max} = \frac{3V}{2bh}$$

where: $V = V_o$, overlay shear force, lb.,
b = width of the section, in. (for purposes of the overlay shear calculations, this value should be the width of the region of shear, which is approximately 25 inches for dual tired axle), and
h = height of cross-section, in. (or the effective overlay thickness, D_e, for overlay shear calculations).

Note that this equation represents a 50 percent increase in maximum shear stress over the original method which estimated the average shear stress.

Next, the maximum shear strain in the overlay γ_{OV}, is determined using the following equation:

$$\gamma_{OV} = \frac{\tau_{OV}}{G_{OV}}$$

where: $\tau_{OV} = \tau_{max}$, the maximum shear stress in the overlay, psi, and
G_{OV} = overlay shear modulus, psi.

Finally, the overlay life for a given shear strain should be determined using a fatigue-type relationship based on asphalt shear strain. Unfortunately, the available literature did not provide a relationship which could be used effectively in the model. Therefore, it

was necessary to adapt the overlay tensile strain equation (developed in this study) to consider the effects of shear strain. This was accomplished using known relationships between tensile and shear stresses in the indirect tensile test and between normal and shear moduli:

$$\tau = 2 \cdot \sigma_T = 2 \cdot EDV \cdot \varepsilon_T \qquad \text{(Ref. 67)}$$

$$G_{OV} = EDV/[2 \cdot (1 + \upsilon_{OV})] \qquad \text{(Ref. 74)}$$

where: υ_{OV} = Poisson's ratio for overlay.

Thus, overlay tensile strain can be converted to shear strain using the following equation:

$$\varepsilon_T = \gamma_{OV}/[4(1 + \upsilon_{OV})]$$

Then, when this is substituted into the tensile strain fatigue equation and rearranged to solve for allowable overlay shear strain, the result is the following equation which assumes a value of 0.30 for Poisson's ratio of the overlay material:

$$\gamma_{OV} = 0.7587 \cdot (EDV)^{-0.3022} \cdot (N_T)^{-0.2703}$$

where: N_T = DTN18, the design 18-kip equivalent single axle applications that will be carried by the overlay prior to the development of reflection cracking, and

EDV = dynamic modulus of the overlay material, psi.

This section has thus far described the logical development of the reformulated shear strain model. The design model incorporated into the ARKRC-2 program is based on the same concepts, but is formulated in reverse order. The user specifies a design 18-kip ESAL traffic and a possible overlay strategy and the program back-calculates a critical

deflection factor, F_W. This factor can then be used to single out the joints (or cracks) which are particularly damaging and may require structural maintenance to reduce its potential for generating reflection cracking after overlay. Thus, if the F_W value for a given joint (crack) calculated using the equation:

$$F_W = \frac{w_\ell - w_u}{w_\ell + w_u}$$

is greater than the critical F_W determined by the ARKRC-2 program, then it is probably necessary to underseal that joint or crack prior to placing the overlay. This is discussed in further detail in the ARKRC-2 User's Manual (see Chapter 6).

SUMMARY

This chapter has discussed the original reflection cracking program (RFLCR) developed for the FHWA (Ref. 1) and the modifications made as a part of this study to improve and calibrate the procedure for use in Arkansas. The improvements are both design and analysis oriented and have been incorporated into the new version of the program, now called ARKRC-2. A listing of this program is provided in Appendix E. The next chapter, the ARKRC-2 User's Manual, discusses the use of the new procedure for the analysis and design of asphalt concrete overlays.

CHAPTER 6
ARKRC-2 USER'S MANUAL

A program has been developed for the analysis of reflection cracking in asphalt concrete overlays of existing Portland Cement Concrete pavements in Arkansas. This program (ARKRC-2) is intended to aid the Arkansas State Highway and Transportation Department (AHTD) in the design and selection of overlay strategies which minimize the occurrence of future overlay reflective cracking. The manual presented here provides all the documentation necessary for operating the new program, including a detailed input guide, a discussion of the use and meaning of all data and input variables, and a discussion of how to interpret the program output.

ARKRC-2 PROGRAM

ARKRC-2 was developed with the aid of a Radio Shack TRS-80 Model II Minicomputer. It has, however, been checked and examined thoroughly according to ANSII standards to insure transportability to other computer systems. The program is written in Fortran IV computer language and is the result of an extensive study for the modification, improvement and calibration of the original RFLCR-1 program developed under the sponsorship of the Federal Highway Administration (Ref. 1). This new program is intended for direct application by AHTD for Arkansas conditions.

COLLECTION OF FIELD DATA

The initial step of the analysis and design procedure is the collection of the field data necessary for characterizing the existing pavement. The other categories of data required by the program are covered later under the heading of Data Selection.

In the ARKRC procedure, the adequacy of a given overlay strategy to withstand reflection cracking is established based on two types of failure criteria: overlay shear strain and overlay tensile strain. Shear strains

are basically the result of the potential for differential vertical movements between adjacent slabs underlying the overlay. Tensile strains, on the other hand, are the result of thermal stresses and horizontal movements of the underlying slab. Because these two types of distress mechanisms are both associated with the existing concrete pavement, it is possible to estimate the amount of influence they will have (on the development of reflection cracking) by making some field measurements of concrete movement prior to overlay placement.

Deflection Measurements

For the case of the vertical shear strain criteria, it is necessary to obtain deflection measurements at several joints (of a JCP or JRCP) or cracks (of a CRCP) in the existing pavement. The required measurements can be obtained easily using the AHTD Dynaflect.

Figure 6.1 illustrates the recommended positioning of the Dynaflect and its geophones within the lane and with respect to the joint or crack. Note that the deflection measurements are taken in the outside wheelpath of the outside lane. Note also that the load wheels and geophone no. 1 are located on the upstream side of the joint while geophone no. 2 must be detached from the mounting bar and placed on the downstream side of the joint, directly across from geophone no. 1. Readings from the other geophones may be recorded, but are not required. Henceforth, the deflections from geophones 1 and 2 (when in this configuration) will be designated as w_ℓ (loaded side) and w_u (unloaded side), respectively.

It is recommended that the deflections be obtained during a period representative of the base support conditions after overlay. In other words, measurements should not be made during spring thaw or after a significant rainfall since the overlay will act as moisture sealant and help improve load transfer conditions during these wet periods. Late spring, summer and autumn are probably the best times to obtain these deflection measurements.

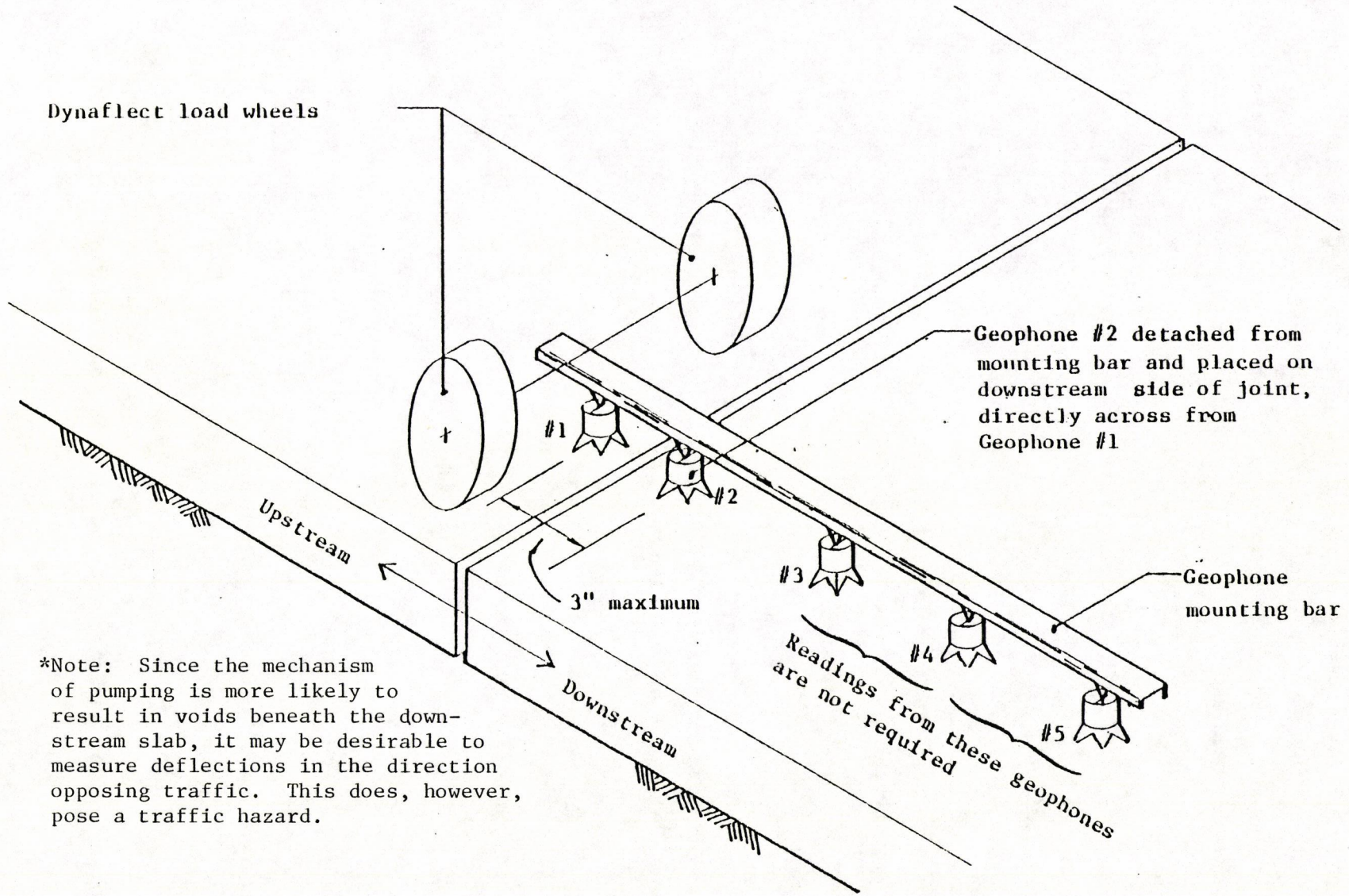

Figure 6.1. Required positioning of Dynaflect load wheels and geophones for load transfer deflection measurements.

In order to achieve good reliability in the results, it is also important to obtain a good sample of deflection measurements. The number of measurements recommended is dependent upon the spacing between the joints (or cracks) and the possibility of the use of some type of undersealant to improve poor load transfer areas.

For the case of jointed concrete pavements (JCP or JRCP), it is desirable to obtain measurements at every construction joint. This is especially true if an undersealant is being considered, since certain criteria will be provided later for the selection of which joints to underseal. If an undersealant is not considered and the joint spacing is less than 25 feet, it is probably adequate to obtain measurements at every other joint, so long as there are not any apparent problems with joint pumping.

For the case of continuously reinforced concrete pavements (CRCP), it is recommended that the deflection measurements be obtained for a series of 3 to 5 cracks at approximate 200-foot intervals. 100-foot intervals are recommended if an undersealant is to be considered in areas where pumping is observed.

After the data has been recorded, processing should begin by computing the deflection factor, F_W, for each joint (or crack) using the following equation:

$$F_W = \frac{w_\ell - w_u}{w_\ell + w_u}$$

where: w_ℓ = deflection on loaded side of joint and
w_u = deflection on unloaded side

This data reduction is probably best accomplished with the aid of a computer. After the data are reduced, it is then useful to prepare a

longitudinal profile plot of F_w versus distance along the roadway for later analysis.

Slab Horizontal Movements

In order to predict the effects of cyclic temperature changes, it is necessary to collect measurements of slab movement as a function of pavement temperature. The recommended procedure for doing this is to install metal reference points on both sides of several joints (or cracks) in the existing PCC pavement, and then measure the spacing between these points (using a Berry Strain Gauge) over a range of pavement temperature. In order to avoid some of the other external effects, it is recommended that these measurements be obtained at the rate of 5 different temperatures per day (min. 30°F range) for a minimum of 2 consecutive days.

The installation procedure recently used by AHTD to obtain these measurements was to first drill holes on both sides of a joint (crack) and securely glue brass bolts into these holes to act as reference points. The bolts had tiny drilled holes on their heads which functioned as seats for the Berry Strain Gauge. Figure 6.2 provides an illustration of the placement of these brass bolts. Note that the bolts are placed out of the wheelpaths (preferably 12-18 inches from the pavement edge) to minimize wheel load disturbance.

Like the deflection measurements, it is important to obtain a good sample of horizontal movement data from several joints (or cracks) in the existing PCC pavement. Unfortunately, it is not as easy or as safe to obtain horizontal movement data. Consequently, it is up to the user or highway engineer to determine the number of joints (or cracks) which should be measured. It should be recognized, however, that the procedure calls for the joint (crack) movement occurring over a drop in air temperature, and the more locations that are measured, the more likely it is that joints (or cracks) with a high reflection cracking potential will be considered. For continuously reinforced concrete pavements, the

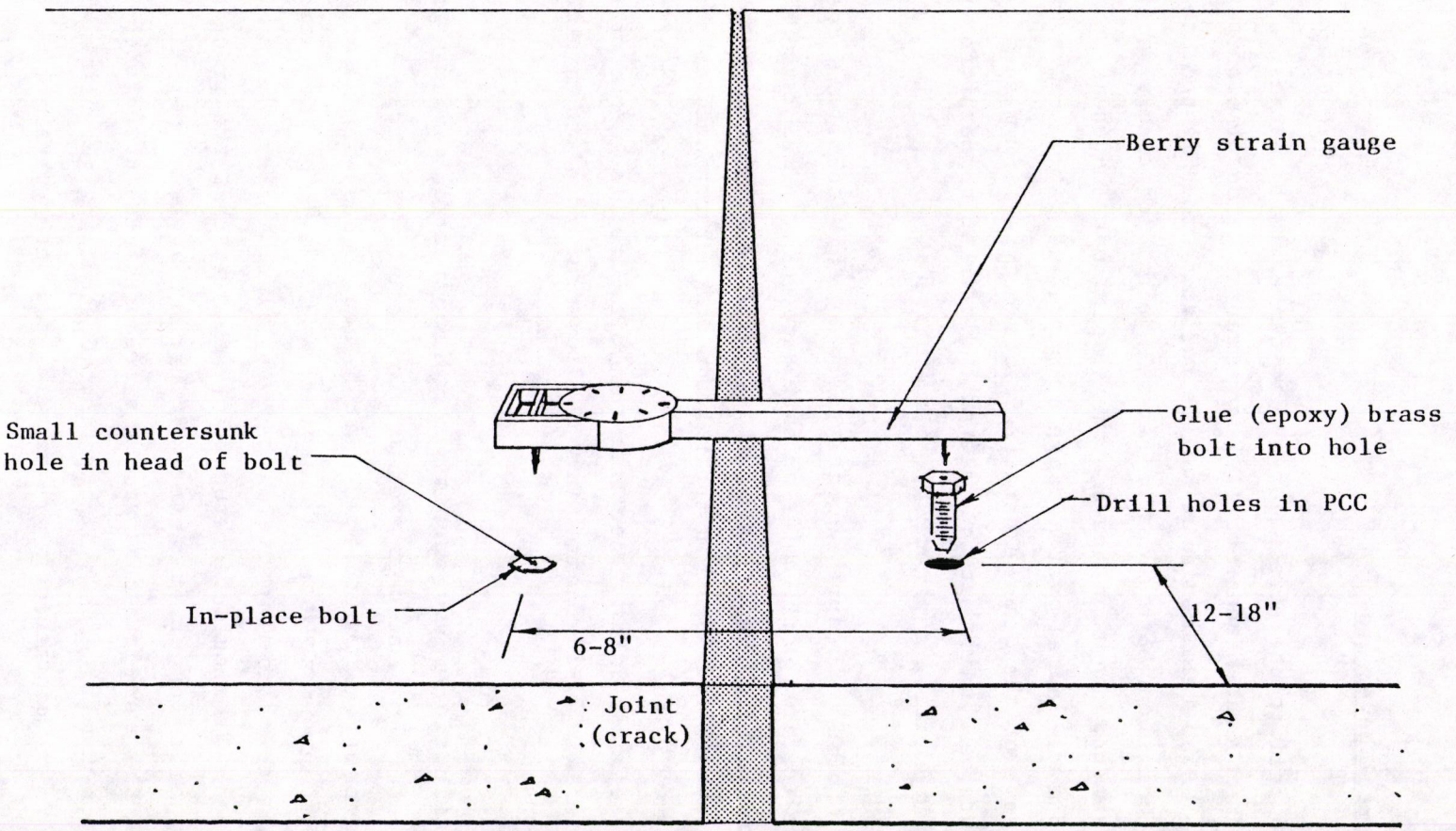

Figure 6.2 Placement of brass bolts for measurement of horizontal slab movement.

measurements must be made in areas which exhibit the average crack spacing for the overlay design section.

Table 6.1 provides a sample form for collection of the horizontal movement data from a single joint (crack). The grid at the bottom of the table is provided to allow the user to plot the data after it has been recorded. These plots will be used later as aid in selecting design movement data.

DATA SELECTION

This section describes, in detail, the selection of appropriate values for use in the ARKRC-2 computer program for analyzing an asphalt concrete overlay design for Arkansas conditions. A guide for coding the data for input into the ARKRC-2 program is provided in Appendix B. The variable descriptions used in the input guide are very brief, however, and should only be used after the user becomes familiar with the detailed discussion provided here in the User's Manual.

The inputs to the program have been divided into eight different categories:

1. Problem description,
2. Existing concrete pavement,
3. Existing pavement reinforcement,
4. Existing pavement movement characterization,
5. Asphalt concrete overlay characteristics,
6. Intermediate layer characteristics,
7. Design traffic, and
8. Yearly frequency of minimum temperatures.

The order shown is also the same as the order or the input data cards required by the program. The individual variables have been assigned a keyword name (shown in capitals) for ease of discussion and identification of the input guide.

Table 6.1. Sample form for collecting horizontal movement data.

REFLECTION CRACKING ANALYSIS DATA
HORIZONTAL SLAB MOVEMENTS

Project: _____
Location: _____
Joint/crack No. _____ Recorder _____
Slab Lengths: Upstream side _____ Downstream side _____

Measurement Number	Date	Time of Day	Pavement Temperature °F	Joint/Crack Width (inches)
1				
2				
3				
4				
5				
6				
7				
8				
9				
10				
11				
12				
13				
14				
15				

Joint/Crack Width, inches

Pavement Temperature, °F

1. Problem Description

This category of data basically refers to a description of the problem. IPROB defines the number of the problem while PRODES represents descriptive information provided by the user about the problem. This should include the project location, the limits, the date, the user's initials and any other relevant information.

2. Existing Concrete Pavement

This category represents the characteristics and/or properties of the existing concrete pavement.

2.1 PVTYPE identifies the existing pavement type, either plain jointed (JCP), jointed reinforced (JRCP) or continuously reinforced (CRCP) concrete pavement.

2.2 UC refers to the condition of the existing concrete pavement, either cracked (C) or uncracked (U). CRC pavements should always be considered cracked, while jointed pavements should be considered uncracked unless most of the slabs exhibit transverse cracking.

2.3 SPACE defines the spacing between the joints of a jointed pavement or the average spacing between the cracks of a continuous pavement. If CRCP, then the average crack spacing can be determined by counting the number of cracks in a section of the highway of known length and then dividing the section length by the number of cracks. It is important to note that this information is used in conjunction with the horizontal movement data which should have been recorded from areas which exhibited the average joint or crack spacing.

2.4 THC is the variable that defines the thickness (in inches) of the concrete slab. In cases where the thickness of the slab varies transversely across the width of the pavement, the value that should be

input is the thickness near the pavement edge, where the measurements of horizontal slab movement are made. It is desirable to use a thickness determined from averaging the depth of several cores. However, as-built plan thicknesses are adequate for specifying THC since the results of the procedure are not very sensitive to slab thickness.

2.5 EC defines the elastic modulus (in psi) of the existing concrete under long term loading (creep) conditions. This creep modulus is generally significantly lower than an elastic modulus determined under short term or dynamic loading conditions. Neville (Ref. 69) conducted tests that indicate that the elastic modulus under creep conditions is approximately 80 percent of the modulus determined under short term loading conditions for concretes with a compressive strength greater than 3000 psi.

Based on these results, the following procedure is recommended for estimating the concrete creep modulus for use in the ARKRC-2 procedure.

Obtain several 4-inch diameter cores of the concrete in the existing pavement and determine their compressive strength, f'_c (in psi), using the standard compression test (ASTM C 116-60T). Next, estimate the average elastic modulus of the concrete core specimens using the ACI formula (Ref. 68):

$$E_c = 57000\ (f'_c)^{0.5}$$

Then, estimate the creep modulus, EC, by multiplying the average elastic modulus, E_c, by 0.80 (or 80 percent) or by using this equation:

$$EC = 45{,}600\ (f'c)^{0.5}$$

Alternatively, if it is not possible to obtain pavement cores for testing, Table 6.2 may be used to obtain an approximate estimate of the concrete creep modulus. This table is based on tests of concrete from

Table 6.2. Elastic moduli, creep moduli, and thermal coefficients for various concretes used in Arkansas.

Concrete Coarse Aggretate Type	Approximate Location	Average PCC Elastic Modulus (psi)	Average PCC Creep Modulus (psi)	Average PCC Thermal Coefficient (in/in/^{o}F)
Syenite	East Belt, Little Rock, Sta. 452+00	4.1×10^{6}	3.3×10^{6}	4.7×10^{-6}
Dolomite	Hwy. 63 Bypass at Willow Road	4.3×10^{6}	3.4×10^{6}	4.0×10^{-6}
Limestone	Hwy. 71 Springdale	4.2×10^{6}	3.4×10^{6}	4.4×10^{-6}
Sandstone	I-40 MM-104 I-40 MM-8	3.5×10^{6} 4.9×10^{6}	2.8×10^{6} 3.9×10^{6}	6.1×10^{-6} 5.3×10^{-6}
Gravel - A	I-30, log mile 99	4.7×10^{6}	3.8×10^{6}	5.8×10^{-6}
Gravel - B	I-30, log mile 23	3.9×10^{6}	3.1×10^{6}	7.2×10^{-6}

different highway pavements in Arkansas having different types of coarse aggregate.

2.6 ALFC is the variable which represents the thermal coefficient of the existing concrete (in/in/°F). Its value can be estimated from concrete cores obtained from the existing pavement (in the same manner discussed in Chapter 4). If PCC cores are not available, then the estimate can be based on the thermal coefficient information provided in Table 6.2, especially if the user knows that the concrete coarse aggregate used in his pavement is the same as that used at the locations shown in the table. Also, it is useful to point out that there is an inverse relationship between the elastic modulus and thermal coefficient of the concrete, as exhibited in Table 6.2. In other words, as the modulus of the concrete increases, its thermal coefficient decreases.

2.7 DENSC represents the density or unit weight (in pcf) of the existing concrete and is used to account for the effect of the increased overlay overburden on the friction between the base layer and the slab. A value of 145 pcf is recommended for normal weight concrete.

2.8 DS identifies the point on a slab-base friction force versus movement curve where sliding occurs. (This is the point where the slab-base frictional force due to relative movement at the interface becomes almost constant, regardless of the amount of additional movement). Some criteria for the selection of an appropriate value based on the type of base or subbase material underlying the slab is provided in Table 6.3. In cases where the subbase or base material is unknown, it is recommended that a lower value of DS be used (0.02 inches), since this is more conservative for design purposes.

3. Existing Pavement Reinforcement

This category represents the characteristics and properties of the longitudinal reinforcing steel in the existing concrete pavement.

Table 6.3. Movement between the concrete slab and underlying layer at which sliding or constant friction force occurs (Ref. 70).

Material	Movement at Sliding, inches
Polyethylene Sheeting	0.02
Granular Subbase[1]	0.25
Sand	0.05
Sand Asphalt	0.02
Plastic Soil[1]	0.05
Sandstone	0.02
Limestone	0.25
Gravel	0.25

[1]Moisture dependent

This data is required only if the existing pavement is a CRCP or if the longitudinal reinforcement is continuous across the joints where the critical concrete movements occur. An example is a pavement which has continuous steel and joints sawed at regular intervals.

For the case of the 45-foot JRC pavements (with 15-foot sawed warping joints) used in Arkansas, the critical joints are the construction joints which do not have any reinforcing steel across them. Therefore, these pavements should be considered as if they did not have any reinforcement.

3.1 BARD defines the diameter of the longitudinal reinforcing bars (in inches) used in the existing pavement. Again, this applies only to the reinforcement which is continuous across the joint under consideration.

3.2 BARS refers to the average interior spacing (in inches) between the longitudinal reinforcing bars.

3.3 ES defines the elastic modulus (in psi) of the steel reinforcement. The program assumes a default value of 30 million psi if ES is undefined.

3.4 ALFS defines the thermal coefficient of the steel reinforcement (in/in/^{o}F). Table 6.4 provides some criteria for the selection of ALFS based on the type of steel.

3.5 SMU is the variable which defines the bonding stress (in psi) between the concrete and steel. Two equations are recommended (Ref. 70) for calculating this value. The first is for the case when cracking in the existing pavement is primarily thermal and/or shrinkage related:

$$SMU = \frac{f_t \times THC \times 12}{\left[\frac{12 \times SPACE}{2}\right] \times BARD}$$

Table 6.4. Thermal coefficients for different types of steel (after Ref. 70).

Types of Steel	Thermal Coefficient (10^{-6} in/in/^{o}F)
Steel (1020)	6.5
Steel (1040)	6.3
Steel (1080)	6.0
Steel (18Cr-8N: stainless)	5.0

which reduces to:

$$SMU = 0.637 \times \left[\frac{f_t \times THC}{SPACE \times BARD} \right]$$

where: f_t = concrete tensile strength (in psi) as determined in accordance with ASTM C-496-71.

All other variables are as defined previously.

If, on the other hand, there is a significant amount of fatigue cracking in the existing concrete pavement, then the bonding stress should be determined using the second equation:

$$SMU = \frac{9.5 \ (f'_c)^{0.5}}{BARD}$$

where: f'_c = compressive strength of concrete (in psi) determined in accordance with ASTM C 116-60T.

4. Existing Pavement Movement Characterization

This category covers the information that is used to characterize the thermally related horizontal movements of the existing concrete pavement. The collection of the field data required here was discussed previously. Therefore, the discussion here will assume that these data have already been collected.

For each joint (or crack) measured and recorded in the form shown in Table 6.1, the user should determine slope of the "best-fit" straight line through the data. Based upon inspection of the slope values for each line, the user should select a data set or series of data sets for use in analyzing the potential for reflection cracking in the section

characterized by the data set(s). This means that for some overlay projects, it may be necessary to identify and design different overlay sections. In selecting these sections, the user should recognize that those having the highest slope values will have the greatest potential for reflection cracking (at least from the standpoint of tensile strain). The user should note too, that the slope value is the most important characteristic of the data and that it is not necessary to separate sections which have approximately the same slope but different intercepts.

For each design section, then, the user should select two coordinates which define the "best-fit" line through the data. This information can then be used as input into the ARKRC procedure for characterizing the horizontal movement of the existing concrete pavement.

4.1 TH represents the temperature axis coordinate or abscissa (in ^{o}F) of the selected point on the best fit line having the higher temperature.

4.2 WH represents the joint (crack) width axis coordinate or ordinate (in inches) of the best fit line corresponding to the high temperature.

4.3 TL represents the temperature axis coordinate (in ^{o}F) of the selected point on the best fit line having the low temperature.

4.4 WL represents the joint (crack) width axis coordinate (in inches) of the best fit line corresponding to the low temperature.

4.5 T1 is a variable which identifies the minimum temperature that the existing concrete pavement has experienced since its construction. The variation of this variable for conditions in Arkansas has very little effect on the results of the design procedure; therefore, it is recommended that a value of $0^{o}F$ be used for all problems.

5. Asphalt Concrete Overlay Characteristics

The purpose of this category of data is to define the properties and characteristics of the asphalt concrete overlay in a particular design alternative.

5.1 THOV defines the thickness (in inches) of the asphalt concrete overlay and represents one of the factors that can be varied in the selection of an adequate design for minimizing reflection cracking. THOV should consist of the combined thickness of all binder and surface courses which are considered to increase the load carrying capacity of the pavement structure. This variable should not include the thickness of any intermediate or strain-absorbing layers (such as an open-graded course).

It is recommended that THOV only be considered a factor in the overlay design if the thermal related tensile strains are predicted to be a probable cause of premature cracking. Although increased overlay thickness is somewhat effective in reducing shear strain, it is recommended that it not be considered a factor for the case of shear strain criteria because of the availability of more cost effective methods, such as undersealing, for reducing excessive overlay shear strains. This will be discussed later in the User's Manual.

5.2 EOV is the variable used to define the effective creep modulus of the combined asphalt concrete binder and surface overlay layers. If the indirect tensile test apparatus is available, it is recommended that the value of EOV be determined using the procedure described in the section on laboratory testing provided in this report (Chapter 4). It is probably best to run these tests on core samples from overlay sections already constructed with the same mix design, however, it is also acceptable to conduct the tests on laboratory compacted samples. The temperature at which the test is conducted should be based upon the location of the overlay site. Table 6.5 and Figure 6.3 should provide the necessary criteria for selecting the appropriate test temperature. Since

Table 6.5. Design asphalt concrete mix test temperatures for the nine different regions of Arkansas.

Arkansas Region	Recommended Test Temperatures*	
	^{o}F	^{o}C
South - West	34	1.1
South - Central	35	1.6
South - East	36	2.3
West - Central	34	0.9
Central	35	1.4
East - Central	35	1.4
North - West	32	0.0
North - Central	32	-0.2
North - East	33	0.7

* Weighted average temperature of days in which temperature dropped below $50^{o}F$.

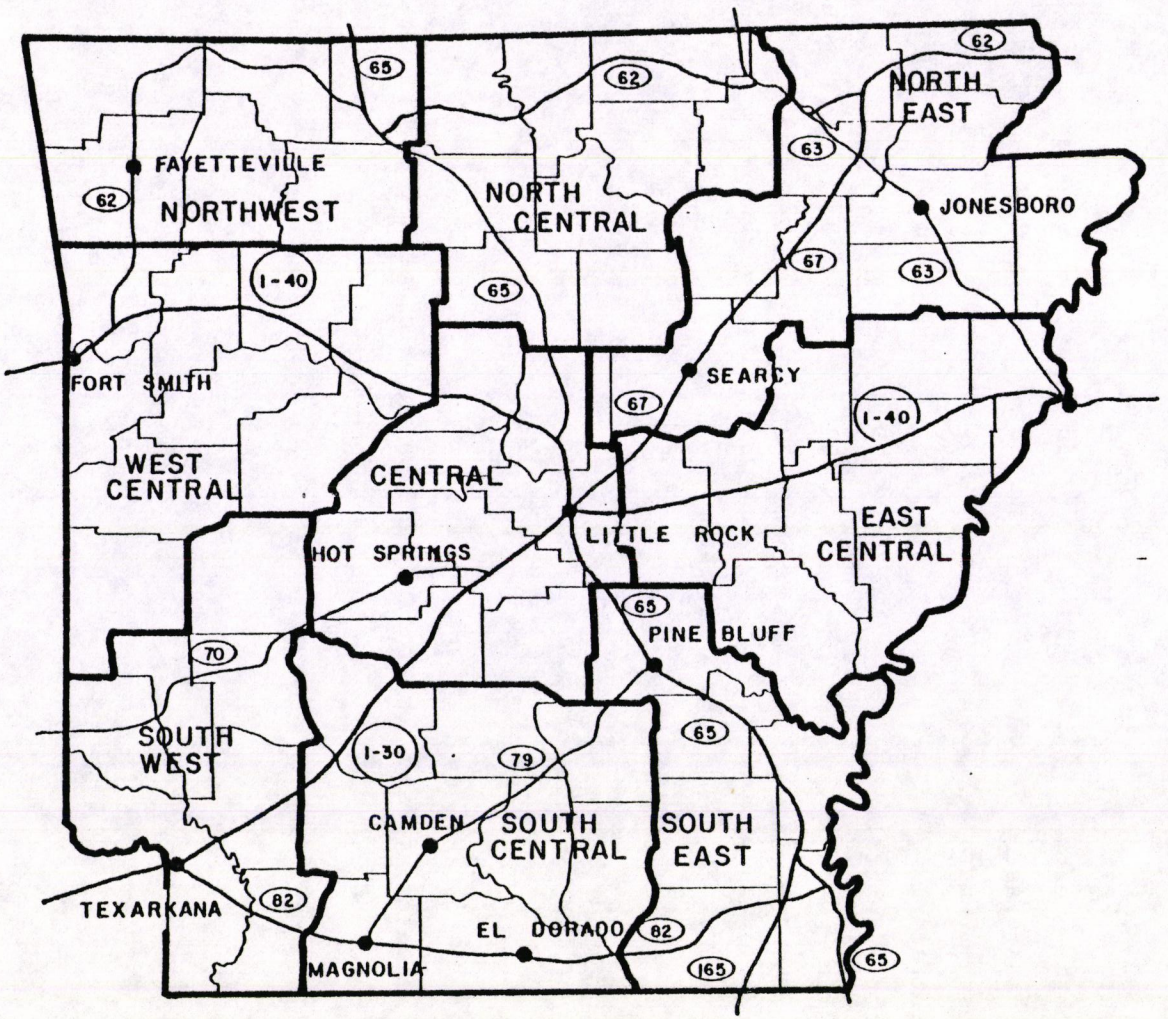

Figure 6.3. Nine climatic regions of Arkansas (After Ref. 65).

the creep modulus is dependent upon load magnitude loading time, it is recommended that the long term indirect tensile test be run at an indirect tensile stress of 30 psi for a period of 3 hours or until the creep modulus stops decreasing significantly.

An alternative procedure for estimating EOV calls for the user to conduct two different laboratory tests on the asphalt bitumen that will be used in the overlay mix. The tests are known as the Ring and Ball Softening Point Test (ASTM D 36) and the Standard Penetration Test (ASTM D 5). The ring and ball softening point temperature, $T_{R\&B}$, the penetration value, PEN, and the penetration test temperature, T, are then used along with Figure 6.4 to estimate the asphalt penetration index, PI.

Next, it is necessary to determine the stiffness of the asphalt bitumen at the design temperature, T_{DES}, for the particular region in Arkansas. (T_{DES} can be determined from the table of test temperatures presented in Table 6.5). The stiffness modulus of the asphalt bitumen, S_{ac}, can then be determined with the aid of the Heukelom and Klomp nomograph presented in Figure 6.5. Once again, a loading time of 3 hours (10,800 seconds) is recommended in estimating S_{ac}.

The last step of the alternative method is to estimate the overlay creep modulus, EOV, as the stiffness modulus of the asphalt mix, S_{MIX}, under the same asphalt bitumen loading time and temperature conditions. This can be done by estimating C_v, the volume concentration of the aggregate in the mix and then using the nomograph presented in Figure 6.6. Note that to use this nomograph, the units of S_{ac} (estimated from Figure 6.5) must be converted from kg/cm^2 to psi by multiplying by 14.223. Also note that percentage of air voids was assumed to be approximately 3 percent in order to generate the curves. If the actual air voids that will be pesent in the mix is significantly greater, then the following correction factor developed by Van Draat and Sommer (Ref. 71) may be applied to determine an adjusted C_v value:

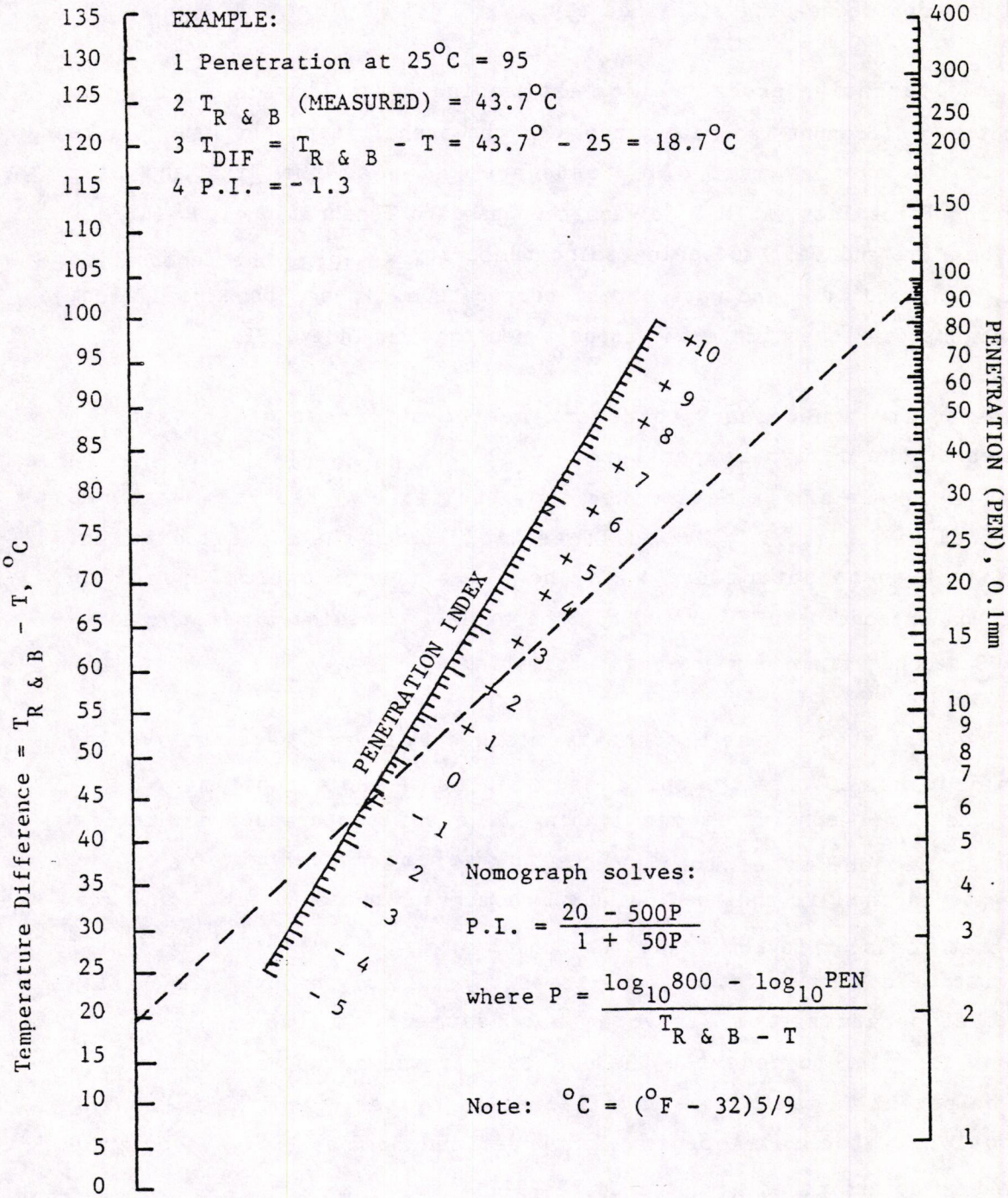

Figure 6.4. Nonomgraph for determining Pfeiffer and Van Dorrmaal's Penetration Index (Ref. 70).

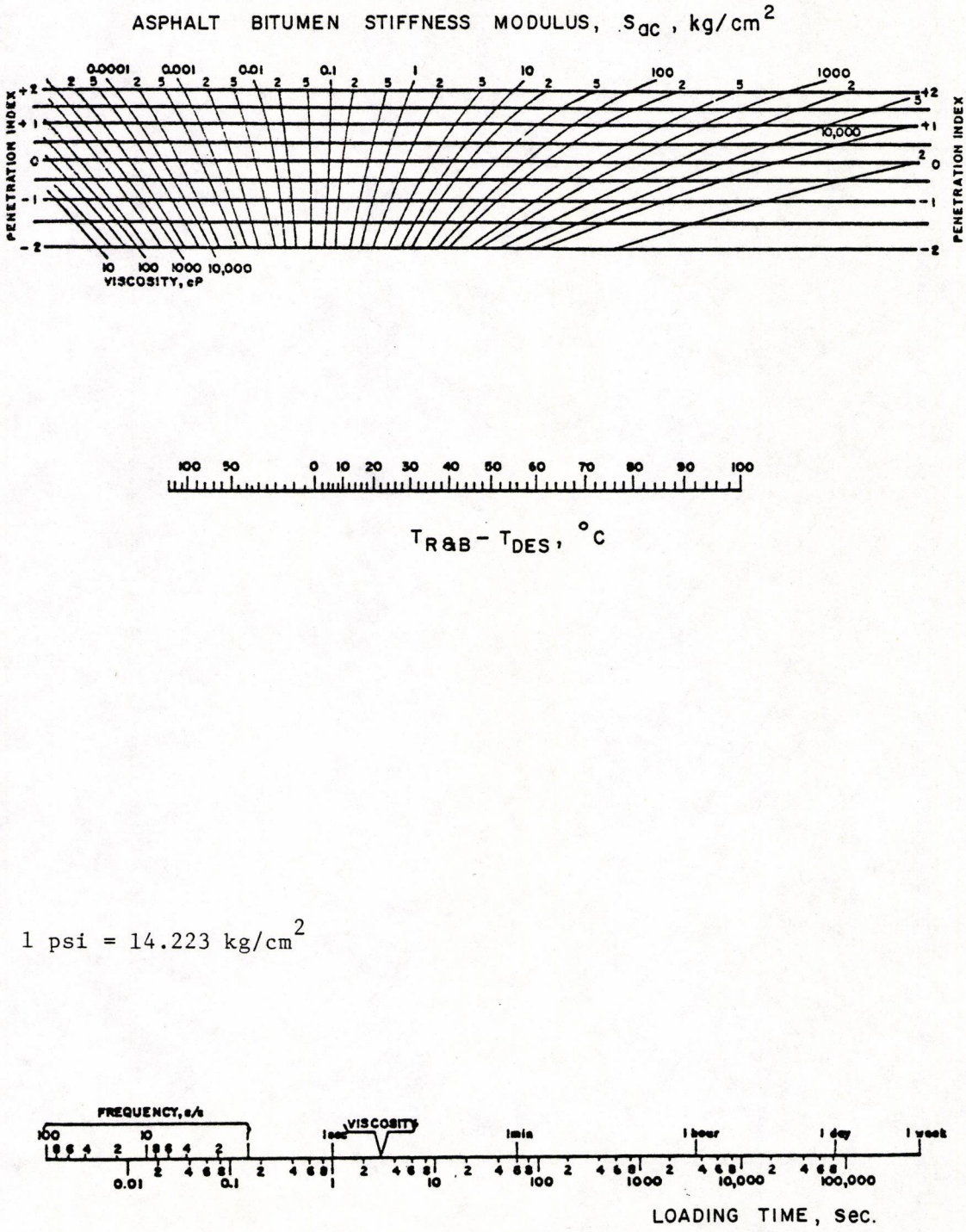

1 psi = 14.223 kg/cm^2

Figure 6.5. Nomograph for predicting the stiffness modulus of asphaltic bitumens, after Heukelom and Klomp (Ref. 70).

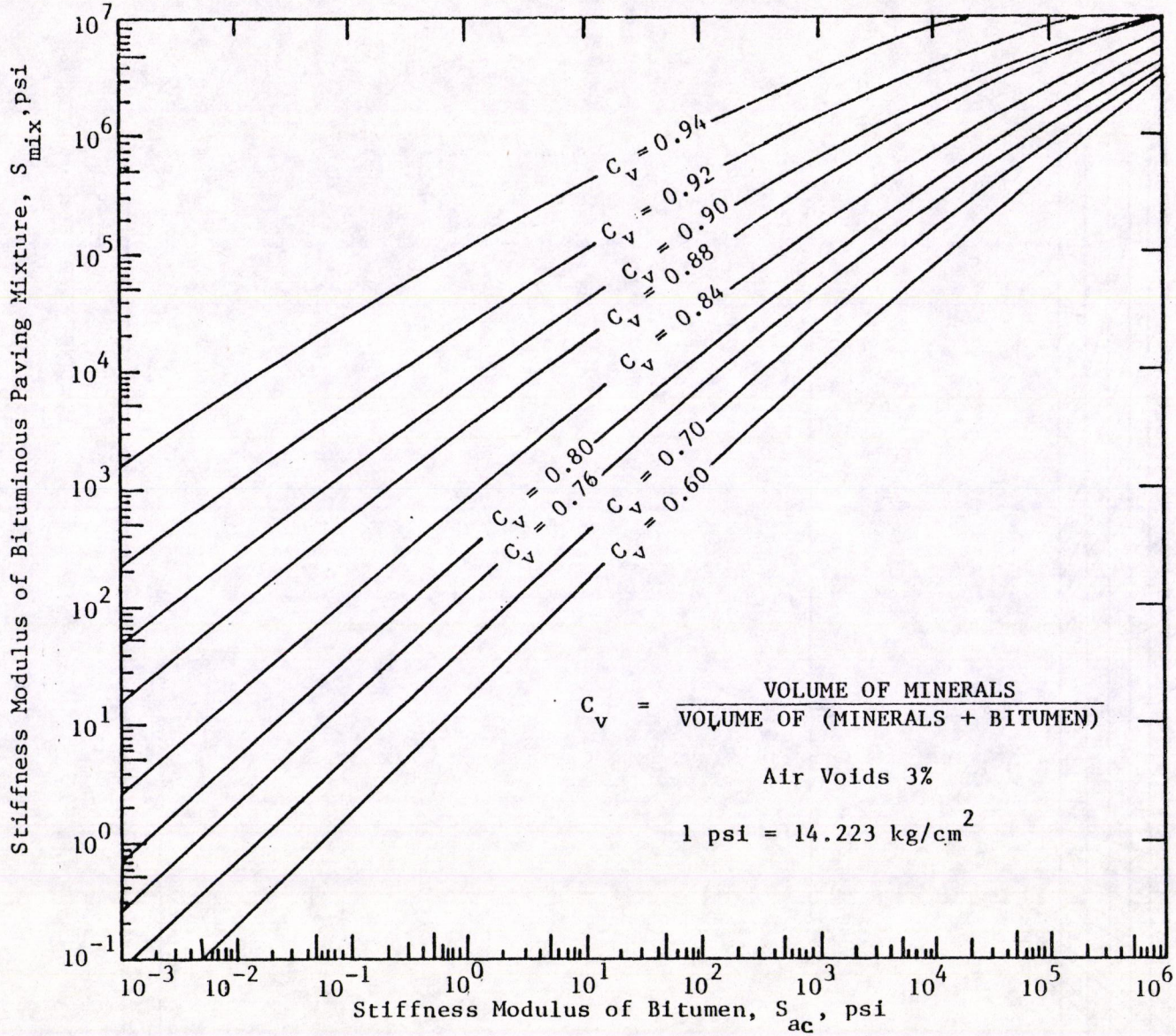

Figure 6.6. Relationships between m li of stiffnes of asphalt cements and paving mixtures contain the same asphalt cements (Based on Hukelom and Klomp) (Ref. 70).

$$C_{v(new)} = \frac{C_v}{1 + H}$$

where: H = actual fraction of air voids in the mix minus 0.03.

The new C_v value can then be used in the nomograph in Figure 6.6.

5.3 EDV represents the dynamic modulus of the asphalt concrete overlay to be used in the analysis of overlay shear strain. This value is generally in the range of 400,000 to 800,000 psi for conditions in Arkansas but may be as high as 2,000,000 psi for dense mixes containing stiff asphalts. High values can also be expected for areas which experience sustained cool temperatures.

It is recommended that EDV be determined using the same alternative test procedure used for estimating EOV, which requires the Ring and Ball Softening Point Test (ASTM D 36) and the Standard Penetration Test (ASTM D 5). The only differences are that the determination of EDV requires a shorter loading time (1 second recommended), and the use of higher design temperature, T_{DES}, corresponding to the year round average temperature for the region.

5.4 ALFV is the variable which represents the thermal coefficient (in/in/°F) of the asphalt concrete. This value can be determined with a micrometer and 4-inch diameter core (from an overlay having the same asphalt concrete mix design) using a thermal coefficient test procedure similar to that described in the section on labroatory testing (Chapter 4) presented in this report.

If thermal coefficient tests cannot be performed, then a value of 14.0×10^{-6} in/in/°F is suggested based on the tests performed on the asphalt concrete specimens obtained from the overlay on I-30 near Benton, Arkansas.

5.5 DENSOV refers to the density or unit weight (in pcf) of the asphalt concrete overlay. The magnitude of this value is not very significant, therefore a value of 140 pcf is recommended.

5.6 OVBS defines the overlay to existing concrete surface bond-slip stress (in psi). In the case where an intermediate or strain-absorbing layer will be used, however, OVBS defines the bond-slip stress between the intermediate layer and the concrete surface. Table 6.6 provides some criteria for the selection of an appropriate value for OVBS. A value of 250 psi was used in the calibration of the program and is recommended for pavements which are not transversely grooved or roto-milled prior to overlay construction. For the latter conditions, a value of 1000 psi is suggested.

5.7 BBW is the variable which defines the width (in feet in the longitudinal direction) of a bond breaker placed over the existing joint (or crack) prior to overlay. This bond breaker is assumed to be a thin layer of material which will keep the bond from forming between the overlay and existing concrete surface. Because of this bond separation, then, there is an increased overlay gauge length over which the strains induced by underlying slab movements can occur.

Conceptually, bond breakers should be very cost effective. Unfortunately, they are not always as efficient as intended. Some materials such as plastic sheeting may be too thin and pliable such that they may allow some surface bearing to occur between the two layers, thereby resulting in greater strains in the overlay. Although there is no such thing as an ideal bond breaker which is completely frictionless, it is recommended that the user strive to use a material which will allow as much relative movement as possible.

Table 6.6. Recommended Values of Asphaltic Overlay Bonding Stress (Ref. 70).

Condition of Existing Surface	Average Bonding Stress, psi
Smooth; polished surface; no exposed coarse aggregate	50
Rough; same as for smooth surface but some of the as-constructed texture remains; small amount of coarse aggregate exposed	500
Very rough; worn surface with exposed coarse aggregate; contains aggregate popout; contains surface texture	1200
Jagged; grooves present; numberous aggregate popouts; coarse aggregate highly exposed	semi-infinite

6. Intermediate Layer Characteristics

An intermediate layer represents a material of certain thickness placed prior to overlay to help minimize reflection cracking brought about by underlying slab movements. The layer is different from a bond breaker layer in that it is designed to internally absorb some of the underlying slab movements before they reach the overlay layers. It is not very effective in reducing reflection cracking brought about by poor load transfer across joints or cracks.

In Arkansas, the most commonly used type of intermediate layer is an open-graded course with low asphalt content (approximately 3 percent) and with roughly 98 percent of the aggregate particles in the range of 3/8 to 2 1/2 inches (68 precent greater than 1 1/2 inches). When placed and compacted properly, it can be very effective, however, it is possible that in cases where there is considerable heavy truck traffic and/or poor compaction of the open-graded course, there can be problems with excessive rutting.

6.1 TH2 is the variable which defines the thickness (in inches) of the intermediate layer that will be placed prior to overlay (TH2 equals zero if no intermediate layer). In the analytical method incorporated into the ARKRC-2 program, TH2 can have a large effect on the critical tensile strain developed in the asphalt concrete overlay, particularly if the creep modulus (discussed next) is low. The strain-absorbing open-graded course used in Arkansas is such a material, however, it does have its thickness limits. It can not be less than 3 inches since some of the aggregate particles are as large as 2 1/2 inches. Also, because of the rutting and compaction problems discussed earlier, the open-graded course thickness should not be greater than 5 or 6 inches. Consequently, if the user intends to use some other type of intermediate layer, care should be taken to insure that its possible thickness limits are considered.

6.2 E2 defines the creep modulus (in psi) of the intermediate layer. In general, this value should range between 3000 and 12000 psi for a true strain-absorbing layer.

Because of its loosely bound nature, it is very difficult to determine the creep modulus of the Arkansas open-graded material in the same way that it was determined for the overlay material. Consequently, a value of 5000 psi (which was used in the program calibration) is recommended for use in design. A higher value of creep modulus should be used if a similar type open-graded material is used which has a greater density due to smaller size aggregates and fewer voids.

6.3 ED2 represents the dynamic modulus (in psi) of the intermediate layer to be used in the analysis of vertical shear strain criteria. Because an intermediate layer is designed to absorb horizontal movements of the underlying slab, it is relatively ineffective in reducing the reflection cracking associated with poor load transfer at joints or cracks. Consequently, a value of 20,000 psi is recommended for the standard open-graded base course used in Arkansas.

For an intermediate layer material which is capable of carrying shear strains (i.e., materials which have much fewer voids than the Arkansas open-grade course), however, it is recommended that ED2 be determined using the same procedure as that recommended for EDV (variable 5.3).

6.4 ALF2 defines the coefficient of thermal expansion for the intermediate layer. A value of 20 x 10^{-6} in/in/°F is recommended for the open-graded course material used in Arkansas. The use of some other intermediate layer material requires either a laboratory or some other field type determination of ALF2.

6.5 DENS2 is a variable which defines the density or unit weight (in pcf) of the intermediate layer material. Its variation (within practical

limits) is also relatively insignificant, therefore a value of 120 pcf is recommended for the Arkansas open-graded course material.

7. Design Traffic

Only one variable, DTN18, is required for this category of data. DTN18 represents the design 18-kip equivalent single axle load applications (ESAL) before the overlay reaches a certain level of reflection cracking inherent in the vertical shear strain criteria. Consequently, it is recommended that the user estimate DTN18 as the number of 18-kip ESAL that can be expected in the design lane in the overlay direction for the design period. Subsequently, the ARKRC-2 program will generate a critical deflection factor which can be used in conjunction with the deflection factor plots (discussed in the previous section on the Collection of Field Data) to determine which joints (cracks) have load transfer problems. Based on this, it is recommended that the user design the overlay for the horizontal tensile strain criteria and then improve the condition of the poor performing joints (cracks) by undersealing them.

8. Yearly Frequency of Minimum Temperatures

This category of data is required in order to define the primary climatic factors (i.e. low temperature drops) which result in reflection cracking in asphalt concrete overlays on portland cement concrete pavements. Research at the Texas Transportation Institute (Ref. 72) showed that asphalt concrete is particular susceptible to cracking at temperatures below 50°F. For this reason, 50°F was used as a reference temperature for developing and calibrating the ARKRC-2 program for Arkansas conditions. Thus, it is necessary for the user to provide information on the yearly frequency of these critical low temperatures. DAY_i represents an array of variables which define the average number of days per year (frequency) in which the minimum daily temperature falls into a certain frequency range. Table 6.7 provides criteria for the selection of appropriate DAY_i values for the nine different climatic

Table 6.7. Average days per year (DAY_1) in which minimum daily temperature falls into specified frequency range for nine climatic regions in Arkansas (after Ref. 63).

Arkansas Climatic Region	Ranges of Minimum Daily Temperature, ^{o}F						
	49-40	39-30	29-20	19-10	9-0	-1 - -11	-11 - -20
	DAY_1	DAY_2	DAY_3	DAY_4	DAY_5	DAY_6	DAY_7
South-West	59	54	46	12	2	0	0
South-Central	55	63	37	11	0	0	0
South-East	65	52	29	7	1	0	0
West-Central	60	57	46	14	2	1	0
Central	57	61	36	11	2	0	0
East-Central	56	72	36	12	1	0	0
North-West	56	58	38	18	8	3	0
North-Central	59	62	54	26	7	1	0
North-East	60	62	40	16	5	1	0

regions in Arkansas. For example, for the Central Region, DAY_1 = 57, DAY_2 = 61, DAY_3 = 36, DAY_4 = 11, DAY_5 = 2, DAY_6 = 0 and DAY_7 = 0.

INTERPRETATION OF ARKRC-2 OUTPUT

After the ARKRC-2 program is executed with appropriate data, it will generate a two-page print out for each problem considered. The first page and a half consists of an echo-print of the input data. The last half-page contains the critical shear and tensile strain criteria. It is important for the user to recognize that the overlay life projected using the two criteria will not necessarily be the actual life of the overlay. There may be other distress mechanisms which are not considered by the ARKRC procedure (such as rutting) which may cause the overlay to "fail" sooner. This is a very important point since in some cases the ARKRC procedure may predict an overlay life of 15 or more years when practically, the overlay will have a considerably shorter life expectancy. The implication of such a long predicted life is that the overlay has been designed such that reflection cracking will be minimized.

Of the critical shear strain criteria, the maximum deflection factor is the most important as it can be used to detect joints with poor load transfer that can cause premature reflection cracking in the overlay design being considered. If this maximum deflection factor is plotted on the graph of field deflection factor (F_w) versus distance along the roadway discussed earlier in the section on Collection of Field Data), then the poor performing zones which may require undersealing will appear as any point or series of points which exceed the horizontal line defined by the ARKRC-2 maximum deflection factor. This is illustrated in Figure 6.7 for example measurements from a 50-foot jointed pavement. Based on this, the joints between 1000 and 1350 feet should be undersealed prior to overlay placement.

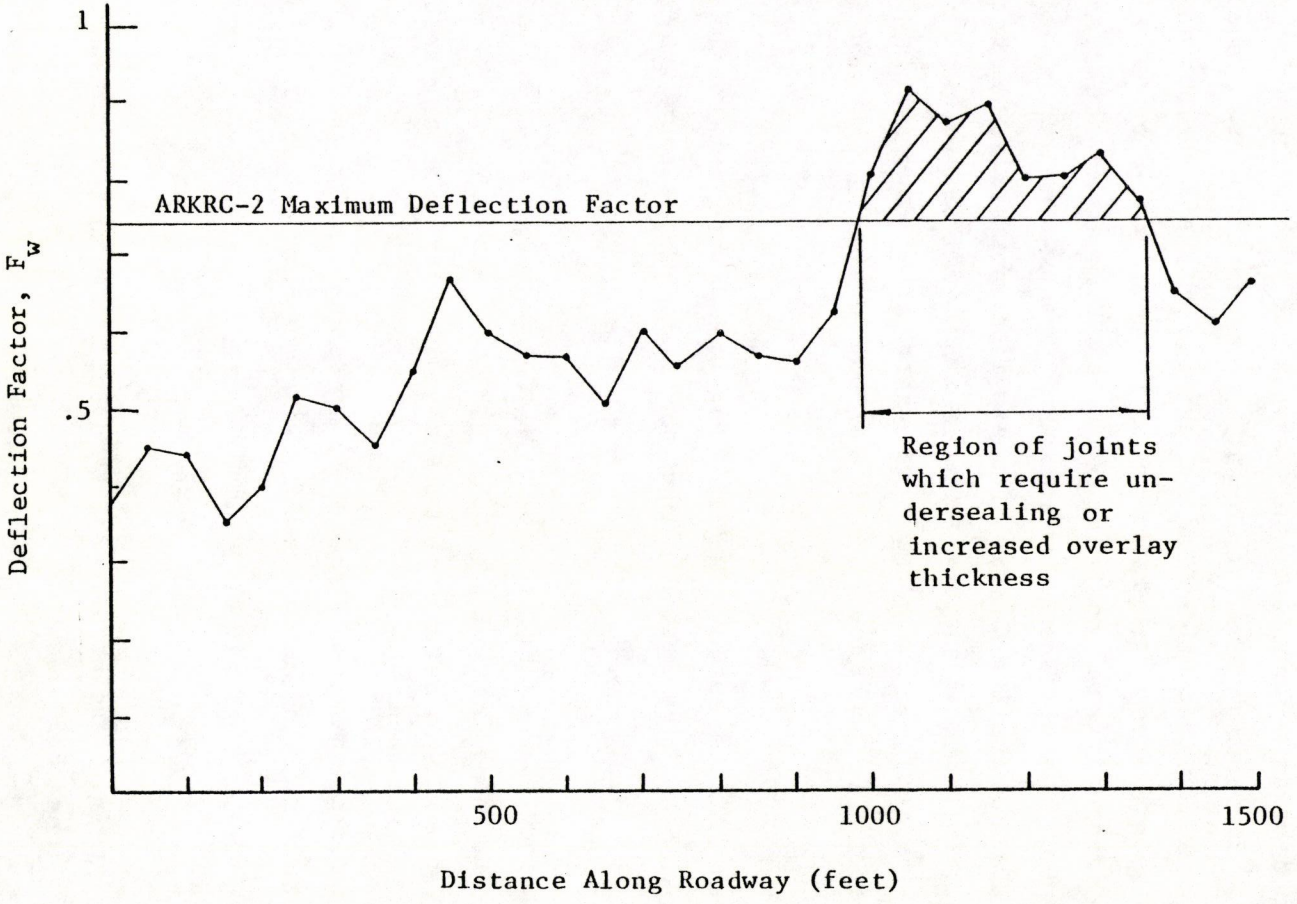

Figure 6.7. Graph of field deflection factors for 50-foot JCP illustrating application of ARKRC-2 maximum deflection factor in detecting joints which will cause premature reflection cracking in the overlay design considered.

Tensile Strain Criteria

Like the shear strain model, the model used for tensile strain is based on a fatigue type analysis. However, it is different in that the loading is separated into different categories and not combined into equivalent loading such as the 18-kip equivalent single axle load applications. The model was reformulated this way in order to account for the increased damage suffered by the overlay at lower temperatures. Because of this, it is possible to consider the differences in the distribution of temperature between different climatic regions. The ARKRC-2 output (for the tensile strain criteria) contains a table which shows the yearly damage inflicted by the different levels and frequency of minimum daily temperature. The cumulative damage of these is expressed as the total yearly damage in the ARKRC-2 output. The reciprocal of this total yearly damage, then, represents the number of years after the overlay is constructed before it will reach the failure criteria (50 percent reflection cracking).

If the user is interested in estimating when different levels of reflection cracking will be reached, then the folowing procedure may be applied:

1. Select the level of reflection cracking considered as a limit. This will range anywhere from 5 to 99%.
2. Use Table 6.8 to determine the z-value corresponding to the selected reflection cracking level.
3. Solve for the number of years, Y, corresponding to the desired level of reflection cracking using the following formula:

$$Y = 1.585^{z} \times Y_{50}$$

where: Y_{50} = number of years before 50% reflection cracking is reached (from ARKRC-2 output)

Table 6.8. z-values corresponding to different levels of reflection cracking.

Percent Reflection Cracking	z-values
1	-2.330
5	-1.645
10	-1.282
15	-1.037
20	-0.841
25	-0.674
30	-0.524
35	-0.385
40	-0.253
45	-0.126
50	0.000
55	0.126
60	0.253
65	0.385
70	0.524
75	0.674
80	0.841
85	1.037
90	1.282
95	1.645
99	2.330

It should be pointed out that the accuracy of this prediction decreases for very high or very low levels of reflection cracking.

SUMMARY

This chapter has provided detailed discussion on the use, application and interpretation of the ARKRC-2 reflection cracking analysis and overlay design procedure. The procedure calls for the analysis and overlay design to be based on two criteria, 1) overlay shear strain resulting from the potential for differential vertical movement between adjacent slabs at a joint or crack and 2) overlay tensile strain resulting from thermal stresses and temperature related horizontal movements of the underlying slab. Based on the field measurements and laboratory testing, the analysis of the above two criteria and the possible use of different methods for minimizing reflection cracking, the user should be able to select the one which is most cost effective.

In order to help incorporate the new ARKRC-2 procedure into AHTD practice, an implementation example was prepared and is presented in Chapter 8. This chapter may also be helpful to the user if he has any difficulties with the procedure as discussed previously.

CHAPTER 7
DEVELOPMENT OF OVERLAY DESIGN NOMOGRAPHS

As a supplement to the ARKRC-2 computer program, nomographs have been developed as an aid in the design of asphalt concrete overlays for conditions in Arkansas. This chapter discusses the development of these nomographs for both the tensile and shear strain criteria, while Appendix D discusses their application and use in an asphalt concrete overlay design procedure. Appendix D is designed to "stand alone," therefore it may, in some cases, repeat some of the information provided here.

NOMOGRAPHS BASED ON OVERLAY TENSILE STRAIN CRITERIA

In order to develop a nomograph, it is first necessary to have a deterministic equation which provides a direct solution. Unfortunately, because of the iterative procedure followed by the ARKRC-2 program to solve for the critical tensile strains in the overlay, it is not possible to derive an equation which can provide an exact solution for all the factors considered by the program. For this reason, it is necessary to use several analytical and statistical techniques to arrive at approximate equations which can then be converted into nomographs. The following is a summary of the procedure used to develop equations and nomographs for the overlay tensile strain criteria:

1. select the conditions to be covered by each equation,
2. select the mathematical model and the desired inference space for each equation,
3. select the significant constant factors which are to be considered for each equation,
4. select the appropriate constant values to use for less significant factors,
5. select appropriate high, medium and low levels for the significant factors selected,
6. select the fractional factorial experiment design for generating

observations,

7. generate observations for each required treatment combination,
8. screen data and remove any treatment combination which has an observation outside the desired inferencespace of each equation.
9. conduct a sums of squares type analysis to determine significant main effects and two-factor interactions to use in each model,
10. conduct a regression analysis and generate the coefficients for each equation, and
11. prepare nomographs.

These steps are discussed next in greater detail.

Select Conditions for Equations

Because of the large amount of effort required to generate a single equation and corresponding nomograph, it was necessary to limit the number developed, yet still provide for most of the design conditions that may be encountered. Accordingly, four equations (and nomographs) were developed, two for continuously reinforced concrete pavements (CRCP) and two for plain jointed or jointed reinforced concrete pavements (JCP or JRCP). The equations were designed to cover two of five composite regions in Arkansas. The first (Region B) represents a combination of the central, east-central and south-central regions of Arkansas. The second (Region D) represents the combined north-west and north-east regions. The five composite regions (A through E) are illustrated in Figure 7.1 The regions were combined based on an equation of the yearly temperature distributions in the original nine climatic regions (see Chapter 3). Therefore, the yearly temperature distribution in each composite region represents the average of the yearly temperature distributions of the original climatic regions that were combined.

A review of the temperature distributions for each composite region shows that Regions A has the mildest climate (as far as the development of reflection cracking is concerned), while Region E has the most severe.

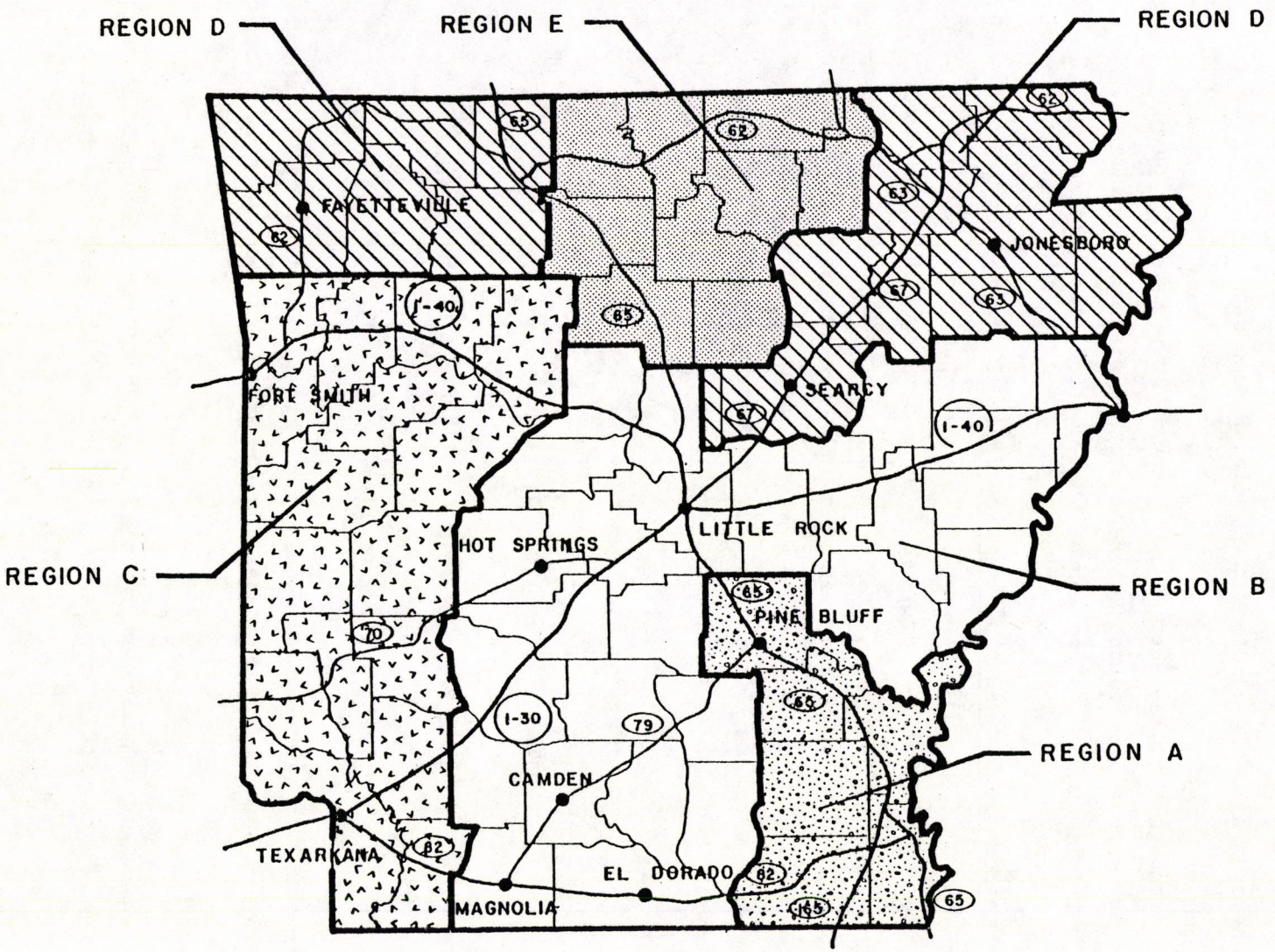

Figure 7.1. Five composite Arkansas regions.

Thus, with the selection of Regions B and D for developing the design equations and nomographs; overlays in Region A can be conservatively designed using the Region B nomograph. Furthermore, overlays for Region C can be designed by interpolating between the results of designs for both Regions B and D. Region E can be designed by applying a factor of safety to the overlay designed using the Region D nomograph.

Although this may seem to cover most of the bases for overlay design, it should be recognized that there are other assumptions made later which may still limit the application of the equations and nomographs.

Mathematical Model and Inference Space

Since the ARKRC-2 program predicts the life of the overlay (in years), it was decided that overlay life, Y_T, would be the dependent variable in the mathematical model for the equations. Additionally, experience with the program indicated that a log-transform of Y_T would provide a more precise model. Consequently, the selected model is as follows:

$$\ln(Y_T) = b_o + b_1x_1 + b_2c_2 + b_3x_3 + \ldots + b_nx_n$$

$$+ b_{11}x_1x_1 + b_{12}x_1x_2 + b_{13}x_1x_3 + \ldots + b_{1n}x_1x_n$$

$$+ b_{22}x_2x_2 + b_{23}x_2x_3 + \ldots + b_{2n}x_2x_n$$

$$+ b_{33}x_3x_3 + \ldots + b_{3n}x_3x_n$$

where the x's represent the selected significant factors (independent varibles) and the b's represent the coefficients to each term in the model.

Since highway pavements, in general, are never designed to last more than 30 years, an inference space of 0.5 to 30 years was selected for

screening the observations. It should be recognized, however, that an asphalt concrete overlay placed over a PCC pavement will generally last much less than 20 years, because of reflection cracking or the development of some other type of distress (e.g. rutting, loss of skid resistance, etc.).

Significant Factors

For jointed concrete pavements, six significant factors (independent variables) were selected:

1. joint spacing (SPACE),
2. slab thickness (THPCC),
3. concrete movement at sliding (DS),
4. restraint coefficient (BP),
5. overlay thickness (THOV), and
6. intermediate layer thickness (TH2).

Although there are other factors (such as concrete thermal coefficient and creep modulus) which can significantly affect the results, they were not included because it was determined that their variation (observed in laboratory tests or field data) was not as significant. Also, one of the design parameters that can be considered by the ARKRC-2 program, bond breaker width, was not considered significant here because of its limitd use by AHTD.

For continuously reinforced concrete pavement, only four significant factors were selected:

1. crack spacing (SPACE),
2. restraint coefficient (BP),
3. overlay thickness (THOV), and
4. intermediate layer thickness (TH2).

Slab thickness was not considered because most CRC pavements in Arkansas are 8 inches thick. Movement at sliding was not included since experience showed that it was not significant for CRC pavements. Once again, other factors were not considered because of their apparent small variation in Arkansas.

It should be pointed out, however, that the restraint coefficient used for both pavement types, is dependent upon the measured slab movement over a change in temperature (i.e., the slope of the movement versus temperature curve).

Appropriate Values for Less Significant Factors

Table 7.1 presents the selected values for the less significant factors used in developing the JCP/JRCP and CRCP equations. Both the creep modulus and thermal coefficient of the concrete in the existing pavement were selected based on an average of the laboratory test results. No steel reinforement was used for the jointed pavements since they are considered unreinforced. The steel reinforcement characteristics used for the CRC pavements, on the other hand, are based on the standard AHTD design for CRCP. As can be seen, the overlay creep modulus is dependent upon the region. The values were selected based on a weighted average temperature (during the critical below 50°F days) and the properties of the asphalt concrete overlay at the instrumented overlay sites on I-30 near Benton, Arkansas. The rest of values presented in Table 7.1 were selected based on the recommendations provided in the ARKRC-2 User's Manual (Chapter 6).

Finally, the composite frequency days for the average below 50°F temperature drop classes in both regions are presented in Table 7.2.

Table 7.1. Values selected for the less significant factors used in developing the JCP/JRCP and CRCP equations and nomographs.

FACTOR		JCP	CRCP
Slab thickness, inches		signif. factor	8
PCC creep modulus, psi		3.4×10^6	
PCC thermal coefficient, in./in/^oF		5.0×10^{-6}	
PCC unit weight, pcf		145	
Movement at sliding, in.		signif. factor	0.02
Bar diameter, in.		-	0.625
Bar spacing, in.		-	6.25
Steel elastic modulus, psi		-	30×10^6
Steel thermal coefficient, in./in./^oF		-	5×10^{-6}
Steel concrete bond stress, psi		-	500
Minimum temperature observed, ^oF		0	
Overlay creep modulus, psi	Region B	29000	
	Region D	35000	
Overlay thermal coefficient, in./in./^oF		14×10^{-6}	
Overlay unit weight, pcf		140	
Overlay bond-slip stress, psi		250	
Intermediate layer creep modulus, psi		5000	
Intermediate layer thermal coefficient, in./in./^oF		20×10^{-6}	
Intermediate layer unit weight, pcf		120	
Bond breaker width, ft.		0	

Table 7.2. Frequency days (per year) for the different temperature drop classes in Arkansas' composite Regions B and D.

Average Temperature Drop Below 50°F	Frequency Days Per Year	
	Region B	Region D
5°F	56	58
15°F	65	60
25°F	36	39
35°F	12	17
45°F	1	7
55°F	0	2
65°F	0	0

Levels of Significant Factors

Tables 7.3 and 7.4 present the selected levels of the significant factors for the jointed and CRC pavements, respectively. Note that the levels are spaced at equal intervals to allow the use of orthogonal polynomials in the sums of squares analysis.

Fractional Factorial Experiment Designs

Since there are six factors, each at three levels, for the JCP/JRCP experiments, the total number of computer solutions that are required for a full factorial is 3^6 or 729. This represents a number that is more than required for the mathematical model selected. Therefore, a one-third replicate or one-third fractional factorial experiment design recommended by Connor and Zelen (Ref. 78) was used to define the appropriate treatment combinations. This resulted in 243 observations and a corresponding number of computer runs.

Since only four factors (or independent variables) were selected for the CRCP equations, a full factorial would require only 3^4 or 81 program runs to generate the observations. Although a full factorial is not required by the mathematical model, 81 program solutions were not considered prohibitive and the full factorial experiment design was selected.

Generate Observations

The observations required for each of the four equations were generated by running the ARKRC-2 program for each required treatment combination. The data for each equation were then stored in the computer for later analysis.

Table 7.3. Levels of significant factors used for developing JCP/JRCP equations and nomographs.

FACTOR	Levels		
	Low	Medium	High
1. Joint spacing, SPACE (ft.)	10	35	60
2. Slab thickness, THC (in.)	8	10	12
3. Concrete movement at sliding, DS (in.)	0.01	0.13	0.25
4. Restraint coefficient, BP	0.1	0.4	0.7
5. Overlay thickness, THOV (in.)	1.0	3.5	6.0
6. Intermediate layer thickness, TH2 (in.)	0.0	3.0	6.0

Table 7.4. Levels of significant factors used for develpoing CRCP equations and nomographs.

FACTOR	Levels		
	Low	Medium	High
1. Crack spacing, SPACE (ft.)	3	6	9
2. Restraint coefficient, BP	0.1	0.4	0.7
3. Overlay thickness, THOV (in.)	1.0	3.5	6.0
4. Intermediate layer thickness, TH2 (in.)	0.0	3.0	6.0

Data Screening

The data analysis process was initiated by first screening all the observations generated for each equation. Then, those which had a predicted overlay life, Y_T, outside the selected inference space (0.5 to 30 years) were removed from data. This resulted in 147 remaining observations for Region B - JCP/JRCP equation, 145 for the Region D - JCP/JRCP equation, 52 for the Region B-CRCP equation and 58 for the Region D-CRCP equation.

Sums of Squares Analyses

This part of the data analysis process was conducted to determine which terms in the mathematical model explain most of the variation. This was carried out using a program called SUMSQ2 (Ref. 79).

As it turns out, two of the factors originally thought to be significant for jointed pavements were found to explain very little of the variation observed in the data. Therefore, they, along with many other insignificant 2-factor interactions, were removed from consideration in the mathematical model. The terms which remained in the model turned out to be the same for all four equations: BP (restraint coefficient), SPACE (joint or crack spacing), $SPACE^2$, TH2 (intermediate layer thickness), $TH2^2$, THOV (overlay thickness) and $THOV^2$.

Regression Analyses

The purpose of the regression analyses is to determine the coefficient (b's) of the significant terms left in the mathematical model. This was carried out a computer program called STEP-01 (Ref. 80) which performs a step-wise type linear regression analysis. Table 7.5 presents the results of this step for the four different design equations. Recall that the equations are designed to predict the natural log of the overlay

Table 7.5. Four equations developed for predicting overlay life (ln Y_T) for jointed (JCP/JRCP) and continous (CRCP) pavements in two composite regions in Arkansas.

Equation Term	JCP/JCRP Equations		CRCP Equations	
	Region B	Region D	Region B	Region D
Intercept (b_o)	-5.0066	-4.9458	-2.2651	-2.3409
BP	+3.1000	+2.7394	+2.8380	+2.4262
SPACE	-0.10153	-0.087205	-0.50998	-0.43589
$(SPACE)^2$	+0.00076267	+0.00063024	+0.022764	+0.020168
TH2	+1.6177	+1.5017	+1.3970	+1.2939
$(TH2)^2$	-0.13733	-0.12972	-0.11578	-0.11144
THOV	+1.3625	+1.2643	+1.2575	+1.1116
$(THOV)^2$	-0.10344	-0.096610	-0.10073	-0.088139
Coefficient of Determination	0.985	0.976	0.990	0.986
Average Percent Error	20	24	16	18

life in years, therefore the actual overlay life, Y_T, must be calculated using the following relation:

$$Y_T = e^S$$

where S represents the summation of the intercept, b_o, and all the terms (b's times x's) in the equation. The BP (beta) term in the equation is calculated using the observed slab movement, ΔC, over a range in temperature, ΔT, for a given joint or crack spacing, SPACE:

$$BP = 1 - \left[\frac{\Delta C / \Delta T}{6 \cdot 10^{-5} \cdot SPACE} \right]$$

This relationship is applicable to the use of all four of the equations developed.

As a final note on the information provided in Table 7.5, it should be recognized that although each equation has a relatively high coefficient of determination (r^2 are all greater than 0.97), their accuracy of prediction (in comparison with the ARKRC-2 predictions) is somewhat less than may be apparent. Basically, the average error is about 20 percent for each equation. This means that if the ARKRC-2 program predicts an overlay life of ten years, the appropriate regression equation would, on the average, be off by two years.

Develop Nomographs

Standard principles of nomography were used to develop the nomographs from the four equations presented in Table 7.5. In order to avoid repetition, they are presented only in Appendix D of this report.

NOMOGRAPHS BASED ON OVERLAY SHEAR STRAIN CRITERIA

Unlike the equations developed for the overlay tensile strain criteria, the equations for shear strain criteria are deterministic and can easily be converted into a form suitable for developing nomographs. The last section of Chapter 5 described the improved shear strain model, consequently, its development will not be presented here. By making appropriate substitutions into the various equations that were developed, however, an expression for the maximum allowable deflection factor, F_w, can be derived:

$$F_w = 7.123 \times 10^{-3} \cdot \gamma_{OV} \cdot (EDV \cdot THOV + 0.963 \cdot ED2 \cdot TH2)$$

where four of the five input variables are as defined and used in other sections of this report:

EDV = overlay dynamic modulus, psi,
THOV = overlay thickness, inches,
ED2 = intermediate layer dynamic modulus, inches, and
TH2 = intermediate layer thickness, inches.

The remaining input variable, allowable overlay shear strain (γ_{OV}), must be determined using the fatigue relationship which was also discussed in the last section of Chapter 5:

$$\gamma_{OV} = 0.7587 \cdot (EDV)^{-0.3022} \cdot (DTN18)^{-.02703}$$

where: DTN18 = design 18-kip equivalent single axle load applications.

It should be pointed out that both of these equations assume that Poisson's ratio for the overlay material is 0.30. Futhermore, the first equation assumes 18-kip single axle loading and that Poisson's ratio for the intermediate layer is 0.35.

Thus, with the nomographs developed from the above two equations (see Appendix D), the user should be able to estimate the allowable deflection factor (F_W) to use in judging whether or not a given joint needs undersealing. (This is discussed in both Chapter 6 and Appendix D).

SUMMARY

This chapter discussed the procedure followed in developing the necessary equations required to generate the nomographs. Considerable effort and the use of advanced statistical techniques were required to develop the equations for the overlay tensile strain criteria. Because of the nature of the shear strain model, however, the equations required for generating the nomographs for overlay the shear strain criteria were derived much easier. Standard techniques of nomography were used to translate these equations into nomographs. Appendix D presents these nomographs and discusses their use and application in overlay design.

CHAPTER 8
IMPLEMENTATION EXAMPLE

The purpose of this chapter is to help illustrate the new reflection cracking analysis and overlay design procedure (ARKRC-2) and to provide an initial basis for its implementation into AHTD practice. Accordingly, a section of highway pavement in Arkansas was selected and the new procedure applied (according to the User's Manual presented in Chapter 6) to determine an optimum overlay design alternative. By following the recommended procedure step-by-step, this example application should also help to answer any questions the user may have about the use of the procedure.

PROJECT LOCATION

The project selected for this implementation example was one for which AHTD had collected field measurements of slab movement during the course of the study. The project is basically a plain jointed concrete pavement with a 26-foot joint spacing and is located on a section of I-30 near Benton, Arkansas.

FIELD DATA COLLECTION

The two types of field data required by the design procedure are joint (or crack) deflection measurements and field measurements of slab movement with changes in temperature. These data and a discussion of their collection are presented in Chapter 3.

The deflection data were obtained by AHTD using the Dynaflect deflection measuring device. Although, not required by the procedure, these data were obtained during two different seasons of the year, spring and summer (see Figures 3.12 and 3.13). The effect of temperature and moisture are readily apparent when comparing these data and provide an interesting test for the shear strain component of the design procedure.

The slab horizontal movement data were collected on this jointed concrete pavement for a series of six joints over a range in pavement temperature from 25°F to 120°F (see Table 3.1). It should be pointed out here, however, that it is not normally necessary to obtain the data to the extent shown in Chapter 3; slab edge movements over a shorter period of time would have been adequate for the purposes of the design procedure. After tabulating the data, the joint movements from midslab (interior) and from the slab edge were plotted versus pavement temperature for each joint according to the recommended procedure. Figure 3.10 provided an example of one of these joint movement versus pavement temperature plots.

PAVEMENT CHARACTERIZATION AND OVERLAY DESIGN DATA

In order to determine the optimum overlay alternative for this project using the ARKRC-2 program, it is necessary to select appropriate values for all the input data required by the program. Unfortunately, as may often be the case in certain design situations, it was not possible to obtain pavement samples and conduct all the desired laboratory tests. Consequently, it was necessary to make some assumptions about the properties of the different materials. These assumptions were primarily based on the results of the testing that was conducted in this study on pavement materials from other locations in Arkansas. The remaining input data were selected based on recommendations provided in the User's Manual (Chapter 6). Table 8.1 summarizes the data that were held constant in the analysis. The table also shows which design variables were considered, although it does not show their magnitudes (these are presented later in the results of the analysis).

Existing Concrete Pavement

EC (concrete creep modulus) has a value of 3.4×10^6 psi, which represents 80 percent of a static elastic modulus value of 4.2×10^6 psi. This seemed to be the average value of the elastic moduli determined for the different types of concrete used in Arkansas (see Chapter 4).

Table 8.1. Constants used in overlay design for 26-foot JCP.

VARIABLE DESCRIPTION	VARIABLE NAME	VALUE USED
Existing Concrete Pavement		
Type	PVTYPE	JCP
Condition	UC	"U"
Joint spacing, ft.	SPACE	26
Slab thickness, in.	THC	10
Concrete creep modulus, psi	EC	3.4×10^{6}
Concrete thermal coefficient, in./in./^{o}F	ALFC	7.5×10^{-6}
Unit weight of concrete, pcf	DENSC	145
Movement at sliding, in.	DS	.02
EXISTING PAVEMENT REINFORCEMENT (none)	-	-
Existing Pavement Movement Characterization		
High Temperature, ^{o}F	TH	84
Joint width at high temperature, in.	WH	.0650
Low temperature, ^{o}F	TL	34
Joint width at low temperature, in.	WL	.1700
Minimum temperature observed, ^{o}F	T1	0
Asphalt Concrete Overlay Characteristics		
Thickness (binder + surface), in.	THOV	var.*
Creep modulus, psi	EOV	29,000
Dynamic modulus, psi	EDV	614,000
Thermal coefficient, in./in./^{o}F	ALFV	14×10^{-6}
Unit weight, pcf	DENSOV	140
Maximum bond stress, psi	OVBS	250
Bond breaker width, ft	BBW	var.*
Intermediate Layer Characteristics		
Thickness, in.	TH2	var.*
Creep modulus, psi	E2	5,000
Dynamic modulus, psi	ED2	20,000
Thermal coefficient, in./in./^{o}F	ALF2	20×10^{-6}
Unit weight, pcf	DENS2	120
Design Traffic, 18-kip ESAL	DTN18	10×10^{6}

*design variable, see Table 8.2

The ALFC value (concrete thermal coefficient) used was 7.5×10^{-6} in/in/°F. Even though this value is well within the range of the values determined from laboratory testing of the Arkansas PCC samples, it represents a value that is significantly higher than that of the concrete used at the instrumented overlay sites nearby. It was necessary to use this value however, after it was determined that the horizontal movements measured at the site were considerably larger than the theoretical thermal movement of a slab with a lower concrete thermal coefficient of say, 6.0×10^{-6} in/in/°F. Unfortunately, this high value of ALFC precluded the use of the design tensile strain nomographs (Appendix D), which assume a value 5.0×10^{-6} in/in/°F.

Work on developing the nomographs (Chapter 7) indicated that DS (concrete movement at sliding) did not have a significant affect on the procedure, consequently, a conservative value of 0.02 inches was used for design.

Existing Pavement Reinforcement

Since the project consists of plain JCP, there are no steel reinforcing bars across the joints. Therefore, all existing pavement reinforcement parameters required by ARKRC-2 procedure were set to zero.

Existing Pavement Movement Characterization

The selection of values for the existing pavement movement characterization were based on an analysis of the field horizontal movement data discussed previously. The movement versus temperature slope values were determined for each of the six joints measured. Inspection of the slope values showed that Joint 5 (see Figure 3.10) had the steepest slope (-0.0021 in/°F) and, therefore, the greatest potential for slab movement. Consequently, two coordinates of the "best-fit" line through the data in Figure 3.10 were used to define the TH, WH, TL and WL values.

Asphalt Concrete Overlay Characteristics

In order to design the overlay, it was necessary to assume that its properties would be the same as that of the overlay constructed on the 45-foot JRCP on I-30 nearby (i.e., where the instrumented overlay sites are located). Appendix B described the estimation of all these values except overlay dynamic modulus, EDV. Basically, this value was determined in the same way that the creep modulus, EOV, was. The same penetration index (PI = -1.0) and Ring and Ball Softening Point Temperature ($T_{R\&B}$ = 51.8°C) were applied to the Heukelom and Klomp nomograph (Chapter 6) along with an assumed year round average temperature of 60°F (15.6°C) and dynamic loading time of one second. This resulted in a dynamic modulus or mix stiffness of 614,000 psi.

Intermediate Layer Characteristics

All the intermediate layer characteristics were selected based on the recommendations provided in the User's Manual for an open-graded course.

Design Traffic

In order to insure that the development of distress in the overlay will not be related to excessive differential vertical movements at the joints between adjacent slabs, a value of DTN18 (18-kip equivalent single axle load traffic) of 10 million was used for design.

Yearly Frequency of Critical Minimum Temperatures

Since this project is located in the Central region of Arkansas. The recommended frequency days for the different classes of temperature drop below 50°F are (according to Table 6.7: DAY_1 = 57, DAY_2 = 61, DAY_3 = 36, DAY_4 = 11, DAY_5 = 2, DAY_6 = 0, and DAY_7 = 0.

ARKRC-2 SOLUTIONS

In generating possible solutions for this example, three design factors were considered, overlay thickness, THOV, intermediate layer (open-graded course) thickness, TH2, and bond breaker width, BBW. Three levels of open-graded course thickness (TH2 equal 0, 4 and 5 inches) and two levels of bond breaker width (BBW equal 0 and 1 foot) were considered. Although wide bond breakers are theoretically very effective at reducing overlay tensile strains developed from slab movements, they can result in severe "pop-outs" of unbonded sections. For this reason, the maximum bond breaker width considered was one foot.

For the combinations of TH2 and BBW considered, four levels of overlay thickness (THOV equal 3, 4, 5 and 6 inches) were run. Figure 8.1 provides an illustration of the ARKRC-2 output for the first problem. The rest of the results are summarized in Table 8.2. Recall that Y_T is the predicted life of the overlay (in years) before 50 percent reflection cracking can be expected. Also recall that F_W is the maximum allowable deflection factor to use in establishing whether or not a certain joint needs undersealing or whether increased overlay thickness is required.

ANALYSIS OF RESULTS

Inspection of the results presented in Table 8.2 shows, first of all, that the standard Arkansas Mix Design (4-inch open-graded course, 6-inch overlay) can only be expected to last approximately three and a half years before the overlay will exhibit 50 percent reflection cracking. This is not surprising as the field measurements indicated a large potential for horizontal slab movement.

Further inspection of the table shows that, by themselves, the varying thickness open-graded course and the placement of a 1-foot wide strip of bond breaker over the joints are not effective in minimizing reflection cracking. However, when used in combination, a marked increase

```
ARKRC - ARKANSAS REFLECTION CRACKING ANALYSIS AND OVERLAY
        DESIGN PROGRAM - VERSION 2.0 - NOVEMBER 1981

 )BLEM   1 DESCRIPTION                                          PAGE 1
ARKRC2 EXAMPLE PROBLEM, 26-FT JCP ON I-30 NEAR BENTON ARKANSAS

                          ******************
                          * INPUT VARIABLES *
                          ******************

    EXISTING CONCRETE PAVEMENT
          TYPE                                                    JCP
          CONDITION                                         UNCRACKED
          JOINT SPACING, FT                                     26.00
          SLAB THICKNESS, IN.                                   10.00
          CONCRETE CREEP MODULUS, PSI                         3400000.
          CONCRETE THERMAL COEFFICIENT, IN/IN/F              .00000750
          UNIT WEIGHT OF CONCRETE, PCF                          145.0
          MOVEMENT AT SLIDING, IN                               .0200

    EXISTING PAVEMENT REINFORCEMENT
          BAR DIAMETER, IN.                                     0.000
          BAR SPACING, IN.                                      0.000
          ELASTIC MODULUS OF STEEL, PSI                      30000000.
          THERMAL COEFFICIENT OF STEEL, IN/IN/F             0.00000000
          MAXIMUM BOND STRESS, PSI                                 0.

    EXISTING PAVEMENT MOVEMENT CHARACTERIZATION
          HIGH TEMPERATURE, DEGREES F                           84.0
          JOINT/CRACK WIDTH AT HIGH TEMPERATURE, IN.         .0650000
          LOW TEMPERATURE, DEGREES F                            34.0
          JOINT/CRACK WIDTH AT LOW TEMPERATURE, IN.          .1700000
          MINIMUM TEMPERATURE OBSERVED, DEGREES F                0.0

    ASPHALT CONCRETE OVERLAY CHARACTERISTICS
          THICKNESS (BINDER + SURFACE), IN.                     3.00
          CREEP MODULUS, PSI                                  29000.
          DYNAMIC MODULUS, PSI                               614000.
          THERMAL COEFFICIENT, IN/IN/F                       .00001400
          UNIT WEIGHT, PCF                                      140.0
          MAXIMUM BOND STRESS, PSI                              250.
          BOND BREAKER WIDTH, FT.                               0.00

    INTERMEDIATE LAYER CHARACTERISTICS
          THICKNESS, IN.                                        4.00
          CREEP MODULUS, PSI                                  5000.
          DYNAMIC MODULUS, PSI                               20000.
          THERMAL COEFFICIENT, IN/IN/F                       .00002000
          UNIT WEIGHT, PCF                                      120.0

    DESIGN TRAFFIC (18-KIP ESAL)                            10000000.
```

Figure 8.1. Example print-out of ARKRC-2 program for first problem of overlay design for 26-foot JCP in Arkansas.

ARKRC - ARKANSAS REFLECTION CRACKING ANALYSIS AND OVERLAY
DESIGN PROGRAM - VERSION 2.0 - NOVEMBER 1981

PROBLEM 1 DESCRIPTION
ARKRC2 EXAMPLE PROBLEM, 26-FT JCP ON I-30 NEAR BENTON ARKANSAS

YEARLY FREQUENCY OF CRITICAL MINIMUM TEMPERATURES

TEMP. CLASS	MINIMUM TEMPERATURE RANGE (DEG F)	NO. OF DAYS PER YEAR
1	+49 TO +40	57.
2	+39 TO +30	61.
3	+29 TO +20	36.
4	+19 TO +10	11.
5	+ 9 TO 0	2.
6	- 1 TO -10	0.
7	-11 TO -20	0.

****
* ARKRC OUTPUT *
****

BETA VALUES

BEFORE OVERLAY	.10256
AFTER OVERLAY (UNBONDED REGION)	.17089
AFTER OVERLAY (BONDED REGION)	.20439

DESIGN SHEAR STRAIN CRITERIA

MAXIMUM OVERLAY SHEAR STRAIN	.000173
MAXIMUM DEFLECTION FACTOR	.237

FATIGUE LIFE (TENSILE STRAIN CRITERIA)

TEMP. CLASS	NO. OF DAYS PER YEAR	OVERLAY TENSILE STRAIN (IN/IN)	ALLOWABLE FATIGUE CYCLES	YEARLY DAMAGE
1	57.	.0003878	34681.	.0016
2	61.	.0011635	595.	.1025
3	36.	.0019391	90.	.4003
4	11.	.0027147	26.	.4248
5	2.	.0034904	10.	.1957
		TOTAL YEARLY DAMAGE		1.1249

NO. OF YEARS BEFORE FAILURE CRITERIA IS REACHED .9

Figure 8.1. (continued) Example print-out of ARKRC-2 program for first problem of overlay design for 26-foot JCP in Arkansas.

Table 8.2. Summary of ARKRC-2 results for asphalt concrete overlay design on 26-foot JCP on I-30 near Benton, Arkansas.

Problem Number	Bond Breaker Width, BBW (ft.)	Open-Graded Course Thickness, TH2 (in.)	Overlay Thickness, THOV (in.)	Overlay Life, Y_T (years)	Allowable Deflection Factor, F_w
1	0	4	3	.9	.24
2			4	1.6	.31
3			5	2.4	.39
4			6	3.4	.46
5		5	3	1.3	.24
6			4	2.3	.32
7			5	3.5	.39
8			6	4.7	.47
9	1	0	3	.1	.23
10			4	.2	.30
11			5	.2	.38
12			6	.2	.46
13		4	3	26.2	.24
14			4	38.1	.31
15			5	49.9	.39
16			6	61.3	.46

in overlay life is observed. In fact, use of the 1-foot bond breaker with minimum levels of both open-graded course thickness and overlay thickness (i.e., Problem No. 13: BBW = 1 foot, TH2 = 4 inches, and THOV = 3 inches) results in a projected life of about 26 years before 50 percent reflection cracking or about 12 years prior to 5 percent cracking (based on z value equal to -1.645 as discussed in the ARKRC-2 User's Manual). This is an interesting outcome of the research used to develop this procedure, as the combined use of a bond breaker with an open-graded course has rarely been tried. Arkansas overlay performance Section 5C (see Table 3.3) on Highway 70 provides an example of a 2-inch OGBC, 0.5-inch SAMI and a 1.5-inch ACHM experimental section which seems to have performed well during its 3 years of service, as it exhibits no reflection cracking (compared to 100 percent cracking in Sections 5a and 5d and 15 percent in Section 5b).

The allowable defelction factor, F_w, calculated by the ARKRC-2 program for the recommended optimum design alternative (Problem No. 13) is 0.24. (The determination of this value is also illustrated in the nomographs based on shear strain in Appendix D). Thus, when plotted on the graph of field deflection factors, (Figure 8.2) it can be seen that none of the joints would need undersealing since their summer deflection factors are all below the allowable. If, on the other hand, the values during spring were used as criteria, all would need undersealing (or increased overlay thickness). Spring deflection factors are not recommended however, since they represent a short term condition whose moisture environment will be somewhat improved by the placement of the overlay.

SUMMARY

The purpose of this chapter was to provide an example problem which can be used to demonstrate and help implement the new ARKRC reflection cracking analysis and overlay design procedure in Arkansas. A 26-foot jointed concrete pavement on I-30 near Benton (for which field measurement data were available) was selected and the procedure followed until an

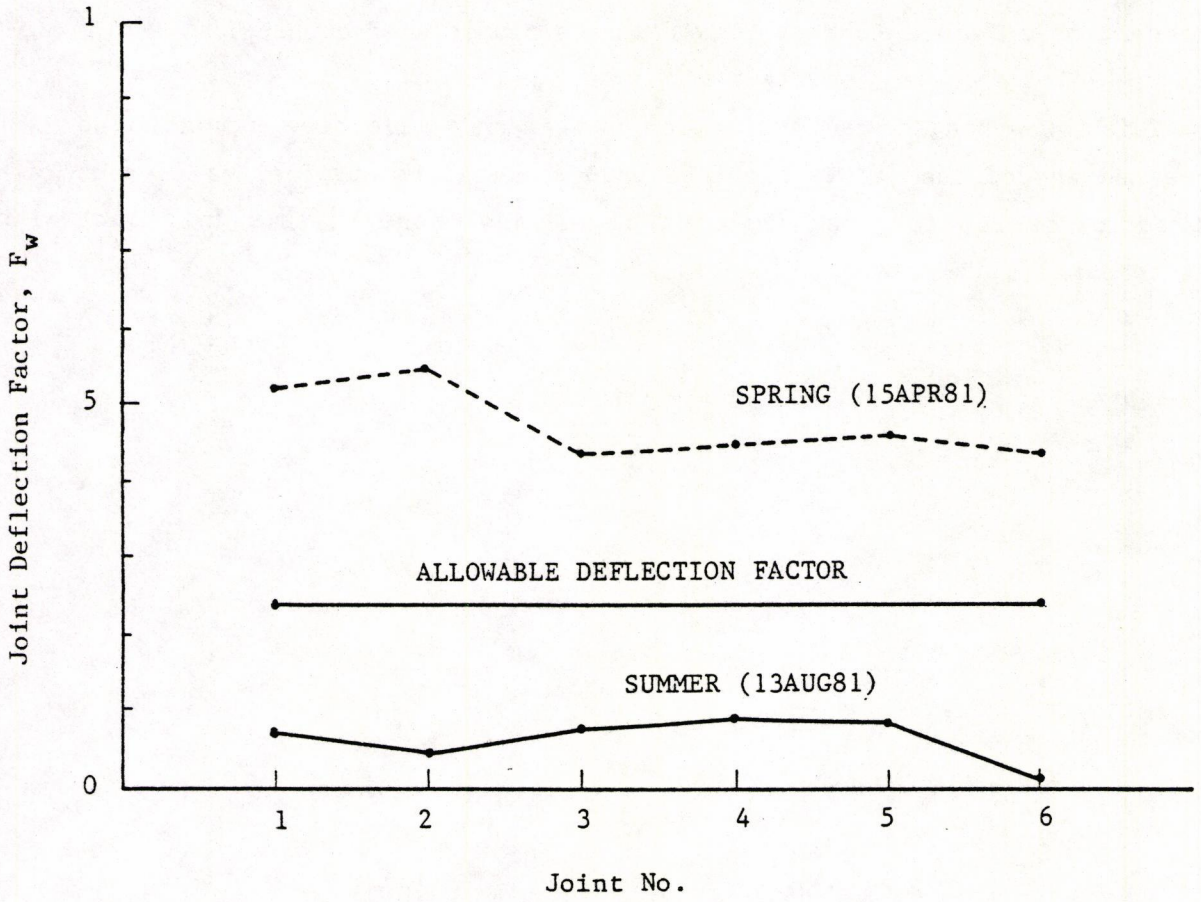

Figure 8.2. Deflection factor plot for asphalt concrete overlay design on 26-foot JCP on I-30 near Benton, Arkansas.

optimum overlay design alternative was derived. The results indicated that the optimum overlay design alternative consisted of a combination of two reflection cracking control methods: 1) the placement of a 1-foot bond breaker layer over each joint, and 2) the use of a 4-inch open-graded base course (Arkansas mix). Both of these would be placed prior to the placement of a 3-inch ACHM overlay (surface plus binder courses).

This "two-pronged" recommendation (which may have been extended to three had any of the joints required undersealing) is atypical of current methods of reflection cracking control and may represent a significant breakthrough in this area.

CHAPTER 9
CONCLUSIONS AND RECOMMENDATIONS

CONCLUSIONS

Based upon the final outcome of this research effort, a reflection cracking analysis and asphalt concrete overlay design procedure for rigid pavements in the State of Arkansas, the following conclusions can be made:

1. The development of overlay reflection cracking can be considered to be primarily the result of two failure mechanisms, differential vertical slab movements as well as the environmental stresses resulting from temperature drops and thermal related slab movements.

2. It is very important to characterize the potential for slab movements in the design process by making field measurements of both vertical and horizontal slab movements.

3. It is possible to go from a highly analytical and computerized design procedure to a much more simplified set of equations and design charts (nomographs) so long as certain assumptions and conditions are recognized.

4. The use of a single method to control or limit the development of reflection cracking may not be sufficient for pavements which exhibit a great potential for movement. For these, it may be necessary to combine two or even three control methods (e.g., open graded course, bond breaker and undersealing) in order to achieve the desired overlay performance.

Since the development of the analysis and design procedure has only recently been completed, it is difficult at this time to make any other

conclusions relative to how it will perform. However, the procedure does represent a significant advancement in the design to control reflection cracking and its extensive use should ultimately provide a basis for further conclusions about its adequacy.

RECOMMENDATIONS

Several areas of further work were recognized after the completion of the ARKRC analysis and design procedure. Most of these would be of additional benefit to the design procedure ultimately incorporated into the AHTD Highway Design Manual. The others may be considered more long-range type work which will provide a basis for verifying and/or re-calibrating the procedure.

1. In order to more exactly determine the significance of the input variables, it is recommended that a sensitivity analysis of the ARKRC-2 program be conducted. This would ultimately allow the user to put more emphasis on input data which has a great influence on the results and less emphasis on that data which is less significant.

2. Since it was determined that the combined use of a bond breaker layer and open-graded base course is effective in reducing overlay strains, it is recommended that more overlay design charts (nomographs) be developed to include the possible use of a bond breaker.

3. Additionally, since nomographs were only developed for the two primary composite regions in Arkansas, it may be desirable to develop more for the three regions not considered.

4. Since it was necessary to adapt the tensile strain fatigue equation developed in this study to a separate equation for shear strain fatigue, it is recommended that a study be conducted to

verify or modify the model so that accurate criteria can be provided for the selection of joints or cracks requiring undersealing or increased overlay thickness.

5. Because of the importance of the concrete thermal coefficient and the level of effort required for its determination, it is recommended that a more extensive field sampling and thermal coefficient testing project be conducted. This would provide the design engineer with a means of selecting appropriate values of thermal coefficient based solely on the type and source of the coarse aggregate used in the concrete.

6. Finally, for any project constructed using the new design procedure, it is recommended that a program of periodic surveys be conducted in order to monitor the performance of these projects and to provide feedback on the adequacy of the procedure as well as a basis for re-calibration. Also, for selected projects, it would also be beneficial to instrument several joints (or cracks) using the University of Arkansas method (but with fewer sensors per location and more locations) and obtain more data on slab movements after overlay.

REFERENCES

1. Austin Research Engineers Inc, "Overly Design and Reflection Cracking Analysis for Rigid Pavement, Volume 1 - Development of New Design Criteria", Report FHWA-RD-77-66, August 1977.

2. Sherman, George B., "Reflection Cracking," Pavement Rehabilitation: Proceedings of a Workshop, Report No. FHWA-RD-74-60, Federal Highway Administration, June 1974.

3. Jackson, Ralph D., "Use of Fabrics and Other Measures For Retarding Reflective Cracking of Asphaltic Concrete Overlays," Report FFA-RD-80-8, U.S. Army Engineer Waterways Experiment Station, Geo-technical Laboratory, Vicksburg, Mississippi, March 1980.

4. HRB Special Report 113, "Standard Nomenclature and Definitions for Pavement Components and Deficiencies," Highway Research Board, Washington, D. C., 1970.

5. "Preventing Reflection Cracks With An Asphalt Crack - Relief Layer," Construction Leaflet No. 16, The Asphalt Institute, December 1976.

6. Bone, A. J., and L. W. Crump, "Current Practices and Research on Controlling Reflection Cracking," Highway Research Board Bulletin 123, Highway Research Board, 1956.

7. Bone, A. J., and L. W. Crump, and V. J. Roggeven, "Control of Reflection Cracking in Bituminous Resurfacing over Old Cement-Contrete Pavements." Proceedings, Highway Research Board, Vol. 33 (1954).

8. Davis, M. M., Reflection Cracks in Bituminous Resurfacing. Report 12, Ontario Joint Highway Research Programme, University of Toronto, July 1960.

9. Finn, F. N., K. Nair, and J. Hilliard, "Minimizing Premature Cracking of Asphalt Concrete Pavements," Prepared for 1976 Annual Meeting of the AAPT, Woodward-Clyde Consultants, February 1976.

10. "Pavement Rehabilitation: Materials and Techniques," NCHRP Synthesis of Highway Pracitce No. 9, Highway Research Board (1972).

11. McCullagh, Frank R., "Reflection Cracking of Bituminous Overlays on Rigid Pavements," Special Reort 16, Engineering Research and Development Bureau, New York State Department of Transportation, February 1973.

12. Way, George, "Prevention of Reflection Cracking in Arizona Minnetonka-East (A Case Study)," Federal Highway Administration Report No. FHWA-AZ-HPR-224, Arizona Department of Transportation-Phoenix, Arizona, May 1976.

13. Kanarowski, Stanley M., "Study of Reflection Cracking in Asphaltic Concrete Overlay Pavements - Phase I," Report No. AFWL-TR-71-142, U.S. Army Engineer Construction Engineering Research Laboratory, Air Force Weapons Laboratory Kirtland AFB, New Mexico, March 1972.

14. Safford, Mark and Phil McCabe, "Reflection Cracking in Bituminous Overlays," Interim Report No. CDOH-P&R-R&SS-72-1, Colorado Division of Highways - Denver, Colorado, December 1971.

15. Way, George, "Prevention of Reflective Cracking, Minnetonka-East (1979 Addendum Report)," Arizona Department of Transportation, 1979.

16. Dantin, Terry J., "Movements in an ACHM Overlay in the Vicinity of Overlaid Joints in a PCC Pavement," Dissertation submitted to the University of Arkansas, December 1978.

17. Minkarah, I., J. P. Cook, J. F. McDonough, "Magnitude of Horizontal Movement in Jointed Concrete Pavements," Department of Civil Engineering, University of Cincinnati, paper presented 60th Annual Meeting TRB, Washington, D. C., January 1981.

18. McGhee, K. H., "Efforts to Reduce Reflective Cracking of Bituminous Concrete Overlays of Portland Cement Concrete Pavements," Virginia Highway & Transportation Research Council, VHTRC 76-R20, November 1975.

19. Brownridge, F. C., "An Evaluation of Continuous Wire Mesh Reinforcement in Bituminous Resurfacing," AAPT Proceedings, Vol. 33 (1964).

20. Tons, E., Bone, A. J., and V. J. Roggeveen, "Five year Performance of Welded Wire Fabric in Bituminous Resurfacing," Highway Research Board Bulletin 290, Highway Research Board, 1961.

21. Roggeveen, V. J., and E. Tons, "Progress of Reflection Cracking in Bituminous Concrete Resurfacing," Highway Research Board Bulletin 290, Highway Research Board, 1956.

22. McGhee, Ken H., "Efforts to Reduce Reflective Cracking of Bituminous Concrete Overlays of Portland Cement Concrete Pavements," Virginia highway and Transportation Research Council, VHTRC 79-RP3, Charlottesville, Virginia, December 1978.

23. Wood, William A., "Methods of Minimizing Reflection Cracking in Bituminous Overlays," FHWA Notice N 5140.9, A paper presented at the 34th annual meeting of SASHTO - Myrtle Beach, South Carolina, January 1976.

24. Ludwig, A. C., and L. N. Pena, Jr., "The Use of Sulphur to Control Reflective Cracking," Air Force Civil Engineer, Volume 10, No. 4, November 1969.

25. Kipp, O. L., and C. R. Preus, "Minnesota Practices on Salvaging Old Pavements by Resurfacing," Proceedings, Highway Research Board, Vol. 30 (1950).

26. Lyon, J. W., "Heavy Pneumatic Rolling Prior to Overlay: A 10-Year Project Report," Highway Research Record No. 327, Highway Research Board, 1970.

27. Korfhage, G. R., "The Effect of Pavement Breaker-Rolling on the Crack Reflectance of Bituminous Overlays," Highway Research Record No. 327, Highway Research Board, 1970.

28. Allen, Harvey S., "Crack Reflectance of Bituminous Overlaid PCC Pavement," Investigation No. 641, Office of Research and Development, Minnesota Department of Transportation, 1980.

29. Lyon, James W., Jr., "Slab Breaking and Seating on Wet Subgrade With Pneumatic Roller," Highway Research Record 11, Highway Reseearch Board, 1963.

30. Smith, L. L., and W. Gartner, "Welded Wire Fabric Reinforcement for Asphaltic Concrete," Highway Research Board Bulletin No. 322, Highway Research Board, 1962.

31. Velz, P. G., "Effect of Pavement Breaker Rolling on Crack Reflectance in Bituminous Overlays," Highway Research Board Bulletin No. 290, Highway Research Board, 1961.

32. Stackhouse, J. L., "Seating Old Pavements with Heavy Pneumatic-Tired Rollers Before Resurfacing," Highway Research Board Record 11, Highway Research Board, 1963.

33. Billingsley, N. A., "Salvaging Old Pavements by Resurfacing," Highway Research Circular 43, 1966.

34. Vicelja, J. L., "Methods to Eliminate Reflection Cracking in Asphalt Concrete Resurfacing Over Portland Cement Concrete Pavements," Proceedings, AAPT, Vol. 32 (1963).

35. Perry, B. F., "Subsealing of Concrete Pavements," HRB Bulletin No. 322, Highway Research Board, 1962.

36. "Specifications for Undersealing Portland Cement Concrete Pavements With Asphalt," Specification Series No. 6, The Asphalt Institute, December 1966.

37. "Mudjacking-Slabjacking-Limejacking-Subsealing," Maintenance Aid Digest, MAD 2, Federal Highway Administration, April 1971.

38. Fahnestock, T. V., and R. L. Davis, "A New Approach to Subsealing," Highway Research Record No. 11, Highway Research Board, 1963.

39. Slater, Don, "Washington's Shoulder Mud-Jacking Rescues Depressed Pavements," Rural and Urban Roads, january 1977.

40. Carey, Donald E., "Evaluation of Synthetic Fabrics for the Reduction of Reflective Cracking," Report No. 70-1B (B), Research and Development Section, Louisiana Department of Highways - Baton Rouge, Louisiana, April 1975.

41. McDonald, E. B., "Reduction of Reflective Cracking by Use of Impervious Membrane," South Dakota Department of Highways - Pierre, South Dakota.

42. "Reinforcing Fabric For Bituminous Seal Coat," Research Project No. 73-20 (2), Bureau of Materials, Testing and Research, Pennsylvania Department of Transportation.

43. Morris, Gene, and Charles McDonald, "Asphalt-Rubber Stress Absorbing Membranes and Recycled Tires," Rural and Urban Roads, August 1976.

44. Galloway, B. M., "Use of Rubber Aggregate in a Stress Relieving Interlayer for Arresting Reflection Cracking of Asphalt Concrete Pavements," Proceedings, International Symposium on Use of Rubber in Asphalt Pavements, 1971.

45. Copple, F., and L. T. Oehler, "Michigan Investigation of Soil Aggregate Cusions and Reinforced Asphaltic Concrete for Preventing or Reducing Deflection Cracking of Resurfaced Pavements," Highway Research Record No. 239, Highway Research Board, 1968.

46. Stackhouse, J. L., "Preparing Old Pavements for Resurfacing with 50-Ton Compactor," HRB, Proceedings, Vol. 38 (1959).

47. Johnson, Robert D., "Thin Overlay Bituminous Macadam for the Control of Reflex Cracking," Highway Research Record 150, Highway Research Board, 1966.

48. Zube, E., "Wire Mesh Reinforcement in Bituminous Resurfacing," Highway Research Board Bulletin 131, Highway Research Board, 1956.

49. Bushing, H. W., E. H. Elliott, and N. G. Reyneveld, "A State of the Art Survey of Reinforced Asphalt Paving," Proceedings, AAPT Vol. 39 (1970).

50. "Wire Mesh Reinforcement of Bituminous Concrete Overlays," Bur. of Phys. Res., Res. Report 66-1, New York State Dept. of Public Works, October 1966.

51. Chastain, W., Jr., and R. H. Mitchess, "Evaluation of Welded Wire Fabric in Bituminous Concrete Resurfacing," Highway Research Record No. 61, Highway Research Board, 1963.

52. Smith, Richard D., "Prevention of Reflection Cracking in Asphalt Overlays with Structofors, Petromat, and Cerex," Project HR-158, Iowa Highway Research Board, May 1977.

53. Tuckett, G. M., G. M. Jones, and G. Littlefield, "The Effects of Mixture Variables on Thermally Induced Stresses in Asphalt Concrete," Proceedings, AAPT, Vol. 39 (1970).

54. Roberts, S. E., "Cracks in Asphalt Resurfacing Affected by Cracks in Rigid Bases," Proceedings, Highway Research Board, Vol. 33 (1954).

55. Wortham, G. R., and L. M. Hatch, "Asbestos Fiber as a Filler in a Plant-Mix Pavement," Research Project No. 24, Idaho Department of Highways, December 1969.

56. Mellott, Dale B., "Asbestos Fibers in ID-2A Bituminous Concrete - Phase II, Research Project No. 70-12, Pennsylvania Department of Transportation, Bureau of Materials, Testing and Research, October 1975.

57. Blackhurst, M. W., J. A. Foxwell, and J. H. Kietzman, "Performance of Asbestos Asphalt Pavement Surface Courses with High Asphalt Contents," Highway Research Record 24, Highway Research Board, 1963.

58. Zuehlke, G. H., "Marshall and Flexural Properties of Bituminous Pavement Mixtures Containing Short Asbestos Fibers," Highway Research Record 24, Highway Research Board, 1963.

59. James, J. G., "A Full Scale Road Experiment with Rubberized Asphalt on Concrete Using Expanded Metal Over the Concrete Joints," Road Research Laboratory Note 3511.

60. Carroll, J. A., and D. G. Diller, "Use of Rubberized Asphalt to Control Reflection Cracking in Asphalt Concrete Overlays," Proceedings, International Symposium on Use of Rubber in Asphalt Pavements, 1971.

61. Gould, V. G., "Summarized Committee Report 1948-1960: Salvaging Old Pavements by Resurfacing," HRB Bulletin No. 290, Highway Research Board, 1961.

62. Van Breeman, William, "Discussion of Possible Designs of Composite Pavements," Highway Research Record 37, Highway Research Board, 1963.

63. Housel, William S., "Design, Maintenance and Performance of Resurfaced Pavements at Willow Run Airfield," Highway Research Board Bulletin 322, Highway Research Board, 1962.

64. Schnitter, O., W.R. Hudson and B.F. McCullough, "A Rigid Pavement Overlay Design Procedure for Texas SDHPT," Research Report 177-3, Center for Transportation Research, University of Texas at Austin, May 1978.

65. National Climatic Center, Federal Building, Asheville, North Carolina, 28801.

66. Center for Transportation Research, Ernest Cockrell Hall, Suite 2.4, University of Texas at Austin, Austin, Texas, 78712.

67. Anagnos, James N., and Thomas W. Kennedy, "Practical Method of Conducting the Indirect Tensile Test," Research Report No. 98-10, Center for Highway Research, University of Texas at Austin, August 1972.

68. American Concrete Institute, Building Code Requirements for Reinforced Concrete, (ACI 318-77).

69. Neville, A.M., Properties of Concrete, reprinted 1975, Pitman Publishing Ltd., London.

70. Austin Research Engineers, Inc, "Overlay Design and Reflection Cracking Analysis for Rigid Pavements, Volume 2 - Design Procedures," Report No. FHWA-RD-77-76, August 1977.

71. Van Draat, W.E.F. and P. Sommer, "Ein Gerat zue Bestimmung der Dynamischen Elastizitattsmoduln von Asphalt," Strasse und Autobahn, Volume 35, 1966.

72. Chang, Hang-Sun, Robert L. Lytton and Samuel H. Carpenter, "Prediction of Thermal Reflection Cracking in West Texas," Research Report 18-3, Texas Transportation Institute, Texas A & M University, March 1976.

73. Yoder, E.J. and M.W. Witczak, Principles of Pavement Design, second edition, Wiley and Sons, 1975.

74. Timoshenko, S.P. and J.M. Gere, Mechanics of Materials, D. Van Nostrand, 1972.

75. Wilson, Edward L., "SOLID SAP, A Static Analysis Program for Three-Dimensional Solid Structures," Structural Engineering Laboratory, University of California at Berkeley, 1971.

76. Shahin, Mohamed Y. and B. Frank McCullough, "Prediction of Low-Temperature and Thermal-Fatigue Cracking in Flexible Pavements," Research Report No. 123-14, The Center for Highway Research, University of Texas, August 1972.

77. Ma, James, "CRCP-2, An Improved Computer Program for the Analysis of Continuously Reinforced Concrete Pavements," Master of Science Thesis, The University of Texas at Austin, August 1977.

78. Connor, W.S. and Marvin Zelen, Fractional Factorial Experiment Designs for Factors at Three Levels, National Bureau of Standards Applied Mathematics Series 54, May 1959.

79. Potter, David and Stephen Seeds, SUMSQ2 - Computer program for the analysis of variance (sums of squares) of 3-level orthogonal factorial experiments. Unpublished computer program (version 2), Center for Transportation Research, University of Texas at Austin, June 1979.

80. "STEP-01 - Statistical Computer Program for Stepwise Multiple Regression," Center for Transportation Research, University of Texas at Austin.

APPENDIX A

DETAILED FLOWCHART OF THE RFLCR-2 PROGRAM

This appendix provides a detailed and illustrative flowchart of the reflection cracking analysis program, RFLCR-2. This version is basically the same as the first version of the program, RFLCR-1 (Ref 1, 70), but with some improvements which were made to correct obvious coding errors. The information contained within the detailed flowchart was summarized by the flowchart presented in Figure 5.2 (Chapter 5).

The detailed flowchart is divided into three main routines, RFLCR, BNDOV, and VERTM for ease of discussion. The main routine, RFLCR, performs the task of inputting data and printing the results. Its more important tasks, however, are the characterization of the existing pavement and the control of the other two branches of the program. Of the other two routines, the second, BNDOV, handles the part of the process for predicting the maximum overlay tensile strain while the third, VERTM, handles the part of the process for predicting the maximum overlay shear strain.

RFLCR Routine

As mentioned earlier, this is the main routine and its first task shown in Block 1 is the reading and printing of the input data.

Block 2 shows how the restraint coefficient, β, is determined using the restraint/movement relationship, half of the slab length, ℓ, the concrete thermal coefficient, α_c, and field measurements of slab end movements, Δx_ℓ, under observed changes in temperature, ΔT. The restraint/movement relationship (with known β) can then be used to define the concrete movement, Δx, at any point along the slab. Note, however, that problems will be encountered in determining ℓ if the measured movement, Δx_ℓ, is greater than that accounted for by thermal motion ($\Delta x_\ell = \alpha_c \cdot \Delta T_c \cdot \ell$).

Block 3, which is shown as a diamond, represents a fork in the flow of the program. If the amount of longitudinal steel, A_s, in the existing pavement is zero, then the pavement will be characterized as a plain jointed pavement (JCP). If the amount of steel is greater than zero, then the pavement wil be characterized as a continuous pavement (CRCP) and flow is transferred to Block 8. Note that if the longitudinal steel is not continuous across a joint, then it does not provide any restraint and the existing pavement should be characterized as a plain JCP by specifying A_s equal to zero.

Block 4 begins the branch on characterization of a plain JCP. It illustrates how the maximum concrete force, Fc_{max}, at midslab can be computed from the observed temperature change, ΔT, the measured concrete end movement, Δx_ℓ, slab thickness, D_c, half-slab length, ℓ, concrete stiffness, E_c, and thermal coefficient, α_c. Note that Fc_{max} is actually a change in the force at midslab due to the change in temperature. Note also that here and throughout the program, a 12-inch (1 foot) unit width of concrete is used for the calculations.

Block 5 illustrates how the location, x_{slid}, of the concrete movement at sliding, Δx_{slid}, is determined using the restraint/movement relationship. Block 5 also illustrates the significance of x_{slid}. Between this point and the slab end, the friction force per unit length remains constant even though conrete movement continues to increase.

Block 6 shows how the slope, m, of the friction force-slab movement curve can be determined. Since the friction force is dependent on the slab movement, an integration with respect to x is required to determine the total friction force applied to the underside of the slab. The integral is only valid up to the point of sliding, however, since the friction force per unit length remains constant beyond that point. A_p, then, represents the area under the restraint/movement curve which may be used to calculate the slope of the friction force-slab movement curve.

Note also that for static equilibrium, the maximum concrete force, Fc_{max}, at midslab must be equivalent to the total friction force, F_F.

Block 7 shows how the concrete and steel stresses at midslab are computed. Recognize that these stresses are due only to the measured change in temperature. Note that since the area of steel, A_s, was defined to be zero, the steel stress is equal to zero.

As shown by the flowchart, flow is transferred from Block 7 to Block 22, since the characterization of the existing plain JCP is complete. Block 8 then, begins the characterization of an existing CRCP.

In Block 8, the slab end movement, Δx_ℓ, is first determined using the restraint/movement relationship and the maximum temperature drop, ΔT_1. This temperature drop (which is the difference between the high temperature corresponding to measured high temperature joint width and the minimum temperature the pavement has experienced) is used since it would have produced the maximum length of bond-slip region between the steel and concrete.

Block 10 is the first block in an iterative loop where the current estimate of the slippage point, x_{slip}, is used to predict the movement at slippage, Δx_{slip}. The ultimate objective of the iterative process is to obtain an x_{slip} such that equilibrium of forces in the existing PCC will be achieved.

Block 11 shows how the total force, F_{sc}, in the steel at the crack is computed for the maximum temperature drop, ΔT_1. Note that the gauge length over which the strain in the steel occurs includes the slippage. Note also that F_{sc} is a total force in the steel and not a change in steel force due to the change in temperature.

In block 12, the amount of bond force, U, transferred between the steel and concrete is computed using the user-defined value of the

concrete to steel bond stress and the surface area of steel in the bond-slip zone.

In block 13, the force in the steel, F_{ss}, at x_{slip}, the force in the concrete, F_{cs}, at x_{slip} and the total frictional force, F_{fs}, beyond the slippage point are computed. Note that F_{ss} is simply the difference between the force in the steel, F_{sc}, at the crack and the bond slip force, U, transferred to the conrete. Also note that F_{cs}, is simply a function of the strain a x_{slip}. For equilibrium then, F_{fs} must be the difference between F_{cs} and U.

Block 14 shows how this frictional force applied to the underside of the slab in the bond slip region is translated into a slope, m, of the friction curve. The method of calculation is similar to that shown in Block 6 except that the forces occur over a short element near the end of the slab.

Block 15 shows the equations used to compute the forces in the steel, F_{sc}', at the crack and in the concrete, F_{cm}', at midslab which correspond to the high temperature joint width. These are the forces in the existing pavement prior to the temperature drop.

Block 16 shows how the forces at midslab, in the concrete (F_{cm}) and in the steel (F_{sm}) are computed for the maximum temperature drop conditions.

Block 17, then, illustrates how the total friction force F_{ft}, applied to the underside of slab can be computed given the restraint/movement function, the initial location, x_{slid}, of sliding between the concrete and base, and the slope, m, of the friction force-slab movement curve.

Block 18 summarizes all the forces which are acting on the half-slab model of the existing pavement after the maximum temperature drop. The unbalanced force, F_u, is the sum of all these forces in the x-direction. For static equilibrium, F_u should be equal to zero, but the program does allow some tolerance in the iteration process. Therefore, in block 19, if the F_u is less than the allowable unbalance, then equilibrium is achieved and flow is transferred to Block 21. If, on the other hand, F_u is greater than the allowable, then flow is transferred to Block 20, where x_{slip}, the initial location of slippage between concrete and steel is adjusted and another iteration is initiated back at Block 10.

Once static equilibrium is achieved (in a CRC existing pavement), then the maximum concrete and steel stresses experienced by the pavement for the maximum temperature-drop conditions can be computed. This completes the characterization of an existing CRCP.

In Block 22, the program branches to the bonded overlay routine, BNDOV, where calculations are made for conditions after overlay. Note that it is assumed that the overlay is at least partially bonded to the existing pavement since the solution to the unbonded overlay case is trivial. (RFLCR can handle the unbonded overlay case; it is just not shown in this flowchart.) In BNDOV, the maximum horizontal tensile strains developed in the overlay (due to underlying horizontal slab movements) are computed. Upon return from BNDOV, flow continues with Block 23.

In Block 23, the program branches to the VERTM routine where overlay vertical shear strains are computed. These shear strains are due to differential vertical movements which occur in the underelying pavement as an axle load moves across a joint or crack. Upon return from VERTM, flow continues with Block 24.

Block 24, then, summarizes the printing of the results of the reflection cracking analysis. Block 25 represents the completion of the analysis for a single problem.

BNDOV Routine

Block 26 begins the bonded overlay routine, BNDOV. As pointed out earlier in Block 22, it is assumed that the overlay is at least partially bonded.

The first significant task performed by the routine (shown in block 27), is to calculate the slope, m_o, of the friction force-slab movement curve for the overlayed structure. This is done by adjusting the slope, m determined for the existing or original pavement structure. The slope is increased by the ratio of the new overburden to the old overburden. Note that this adjustment is only performed if required by the user, since there is some uncertainty in adjusting by this ratio.

Blocks 28 and 29 show how the forces in the steel, F_{sc}', at the crack and in the concrete, F_{cm}', at midslab are computed for the high temperature joint width condition during the observation of slab movements. These calculations were previously performed in Block 15, but must be performed again for use in BNDOV.

Block 30 represents a fork in the flow of the program where flow is transferred to Block 41 if no bond breaker is to be considered. If, on the other hand, a bond breaker will be considered, flow is transferred to Block 31.

In Block 31, an estimate is made of the restraint coefficient, β_u, for the unbonded portion of the overlay. In the iterative process that follows, β_u, will be determined for the case of a completely unbonded

overlay. After β_u is determined then, it is assumed that it can be used to estimate concrete movement in the unbonded portion of a pavement which is not entirely unbonded.

Block 32 illustrates how the concrete movements Δx_ℓ and x_{slip} (at slab end and at the initial point of slippage, respectively) are computed for the totally unbonded overlay. Note that the restraint/movement relationship and the current estimate of β_u are used and note also that the movement depends on a user-defined design concrete temperature drop, ΔT_c.

Block 33 shows how the total concrete force, F_{cm}, at midslab is computed using the calculated end movement, Δx_ℓ, and the design concrete temperature-drop, ΔT_c.

Block 34 shows how the new location of the initial point of concrete sliding, x_{slid}, is computed for the current estimate of β_u and the known value for the movement at sliding, Δx_{slid}. Note that the restraint/movement relationship must be rearranged to solve for x_{slid}.

Block 35 illustrates how the total friction force, F_{fT}, is computed for the unbonded overlay case. The calculation is similar to that illustrated in block 17 except that 1) this is for the unbonded overlay case and 2) the adjusted slope, m_o, of the friction curve is used. The shaded area, A_{ft}, represents the integral of the restraint/movement function (up to the point of slippage) plus the rectangular area between ℓ and x_{slip} and under Δx_{slid}.

Block 36 shows how the force, F_{sm}, in the steel at midslab is computed using the design concrete temperature-drop, ΔT_c.

Block 37 illustrates how the force, F_{sc}, in the steel at the crack is computed for the design concrete temperature-drop, ΔT_c. Note that the

gauge length over which the steel strain occurs includes the bond-slip region.

Block 38 provides an illustration of the forces acting in the original concrete pavement. Since the overlay is totally unbonded, no forces are transferred between it and the original concrete, consequently, overlay forces are not considered in the equilibrium process. ΣF represents the summation of the forces which are considered.

Block 39 represents a fork in the flow of the program where if ΣE is less than the tolerance, then equilibrium is achieved, β_u is determined and flow is transferred to Block 41. If, on the other hand, ΣF is greater than the tolerance, the β_u is adjusted (Block 40) and flow is transferred back to Block 30 for another iteration.

In Block 41, an initial estimate is made of the restraint coefficient, β_B, for the bonded portion of the overlay. β_B is then used as the focus (iteration factor) towards reaching equilibrium in which the overlay is either fully or at least partially bonded to the existing concrete pavement.

Block 42 represents the initial iterative step towards reaching equilibrium in the pavement structure in which the overlay is either fully or partially bonded. Block 42 illustrates the determination of the concrete movement at the edge of the bond breaker (if there is one) for the design concrete temperature-drop, ΔT_c.

Block 43 illustrates how the concrete movement, Δx_{slip}, is computed at the initial point of slippage between the steel and concrete. Since the concrete movement at this point is dependent upon its location with respect to the bond breaker, two equations are required. The first is for movement in the bonded overlay region while the second is for movement in the unbonded overlay region.

Block 44 illustrates how the force, F_{cm}, in the concrete at midslab, the force, F_{sm}, in the steel at midslab and the force, F_{sc}, in the steel at the crack and also shows how they are computed from the information generated previously.

Block 45 provides an illustration of how the total friction force, F_{ft}, is computed using the restaint/movement relationship, the movement at sliding, Δx_{slid}, and the adjusted slope, m_o, of the friction curve. The method is the same as that used earlier.

Block 46 represents a fork in the flowchart where if full friction exists in the bonded overlay zone, then flow is transferred to Block 53. If slippage can occur between the overlay and existing surface, then flow continues with Block 47.

Block 47 shows how the force, F_{UZ}, which is transferred to the overlay through the bond-slip region, is computed. Note that it is simply the force which is not balanced by the other forces acting in the existing concrete pavement.

Block 48 illustrates the region of bond-slip between the overlay and existing concrete. It also shows how the length of the bond-slip region, x_{UZ}, is computed. Note that the user-defined value for the overlay to concrete bond stress, σ_{oc}, is used in the calculation. Note also that the 12-inch unit width also comes into the calculation.

Block 49 represents another fork in the flow of the program. If the length, x_{UZ}, over which overlay slippage occurs is negative or greater than the length, x_B, which is bonded to the existing pavement, then β_B is adjusted (as shown in Block 50) and flow is transferred back to Block 42. If x_{UZ} is greater than zero but less than x_B, then flow is transferred to Block 51.

Block 51 shows the calculation of the length, x_{BZ}, in the bonded region where there is full friction between the overlay and the existing concrete surface. Note that this region occurs near midslab where there is less potential for differential relative movements between the overlay and concrete.

Block 52 illustrates the location of this full-friction region and the force, F_{UZ}, acting in the bond-slip region. Block 52 also shows the calculation of the concrete movement, Δx_{BZ}, at the edge of the full-friction bonded region.

Block 53 represents another fork in the flow of the program where if an intermediate or cushion layer is placed along with the overlay, then flow is transferred to Block 57. If an intermediate layer is not placed along with the overlay, then flow continues with Block 54.

Since no intermediate layer is considered in this limb of the flowchart, Block 54 shows that its forces, both at midslab and at the crack, are set equal to zero.

Block 55 shows how the force F_{om}, in the overlay at midslab is calculated. Note that F_{om} is a function of the concrete force at midslab, F_{cm}, the difference between the overlay and concrete thermal coefficients, α_o and α_c, and the difference between the design temperature change, ΔT_o and ΔT_c, for both layers.

Block 56 shows how the force, F_{oc}, in the overlay at the crack is computed. Note that the equation used depends on whether or not slippage occurs in the bonded region of the overlay. From here, flow is transferred to Block 60 (to skip the branch where an intermediate layer is considered).

Block 57 represents the beginning of the branch where the placement of an intermediate or cushion layer (along with the overlay) is

considered. Block 57 shows how the force, F_{2m}, in the intermediate layer at midslab is computed. It is important to realize that the presence of this layer has no effect on the previous methods of calculation which ignored it.

Block 58 shows how the force, F_{2c}, in the intermediate layer at the crack is computed. Once again, this force is dependent upon whether or not slippage occurs in the bond region, which in turn means that two equations are required.

Block 59 shows how the forces in the ovelay at midslab, F_{om}, and at the crack, F_{oc}, are computed given that an intermediate layer was placed along with the overlay.

Block 60 shows how forces in the overlay reinforcement (if it exists) are computed. The program considers overlay reinforcement in an attempt to account for any type of wire mesh or fabric type reinforcement which may be used in the overlay. Like the presence of an intermediate layer, the presence of overlay reinforcement has no effect on the previous methods of calculation which ignored it.

Block 61 provides an illustration of all the possible forces which are considered by the RFLCR-2 program. F_u , then, represents the summation of all these forces (or the unbalanced forces).

In Block 62, a test is made to see if F_u is below the allowable unbalanced force (tolerance). If not, β_B is adjusted (Block 63) and flow is transferred back to Block 42 for another iteration. If F_u is less than the allowable unbalanced force, then equilibrium is achieved and flow is transferred to Block 64.

In Block 64, the equations for calculating the critical pavement responses are shown. These responses include the horizontal tensile strain in the overlay at the crack (or joint), the maximum steel stress

in the existing reinforcement, the strain in the intermediate layer at the crack and the strain in the overlay reinforcement at the crack.

Block 65 summarizes the end of the BNDOV routine and the return of control to the main routine, RFLCR.

VERTM Routine

Block 66 begins the overlay vertical shear strain routine, VERTM.

Block 67 illustrates how the load transfer, L_T, at a joint (or crack) is computed. Basically the deflection load is placed on one side of the joint while deflection measurements are made on both sides. Load transfer, then, is ratio of the deflection on the unloaded side to the deflection on the loaded side.

Block 68 shows how P_o, the shear force that must be carried by the overlay, is computed using the load transfer, L_T, and half of the design axle load, L_D.

Block 69 illustrates how the amount of overlay reinforcement, the intermediate layer thickness and the overlay thickness are translated into an effective thickness of overlay, D_e, for shear strain calculations.

Block 70 illustrates how the overlay shear stress, τ_o, is computed given the effective overlay thickness, D_e, the shear force, P_o, that must be carried by the overlay and the width, L_W, over which the shear force is spread.

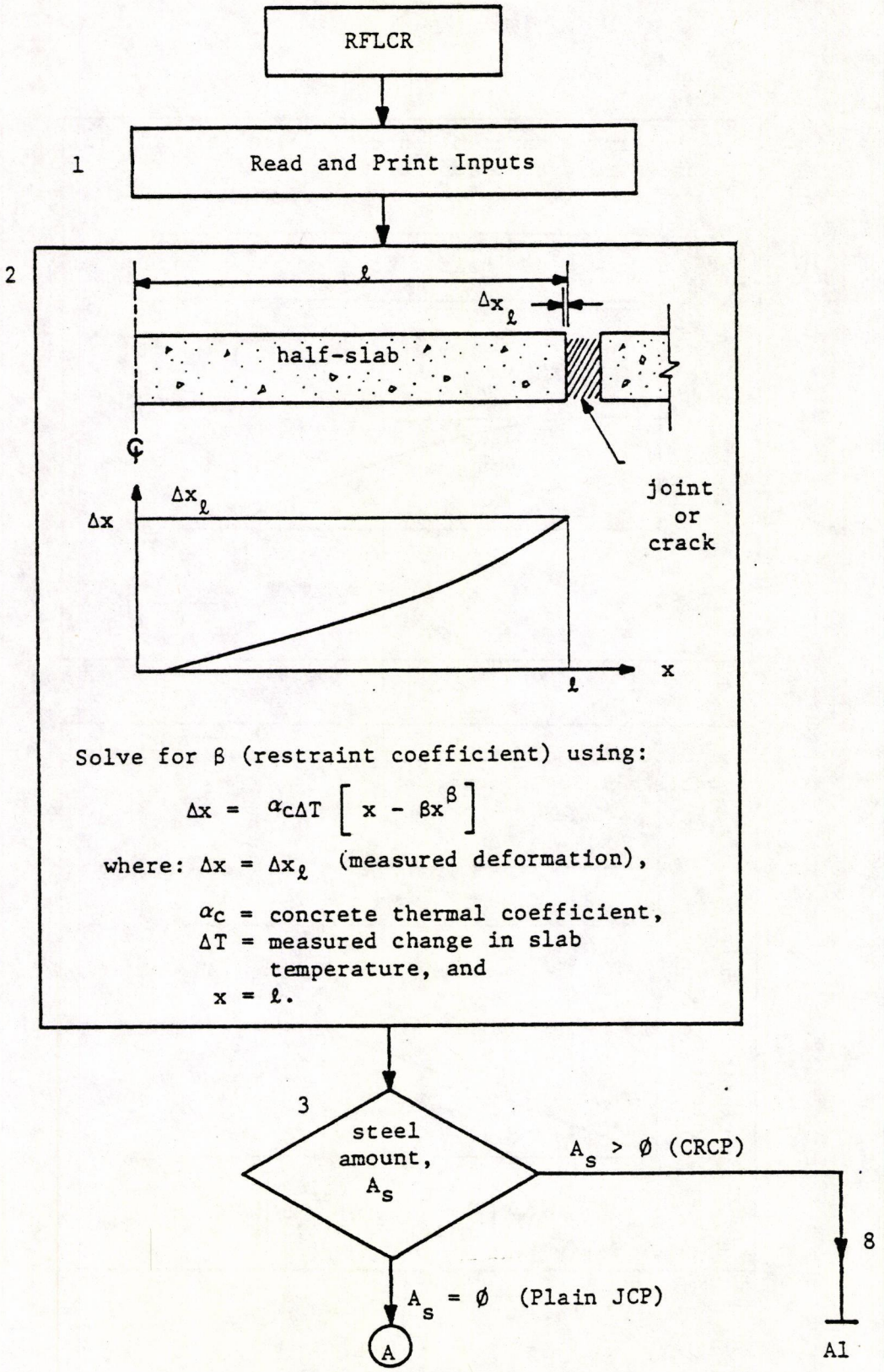
RFLCR
1
Read and Print Inputs
2
ℓ
Δx_ℓ
half-slab
joint
or
crack
Δx
Δx_ℓ
x
ℓ
Solve for β (restraint coefficient) using:
Δx = α_c ΔT [x - βx^β]
where: Δx = Δx_ℓ (measured deformation),
α_c = concrete thermal coefficient,
ΔT = measured change in slab temperature, and
x = ℓ.
3
steel amount, A_s
A_s > Ø (CRCP)
8
A_s = Ø (Plain JCP)
A
A1

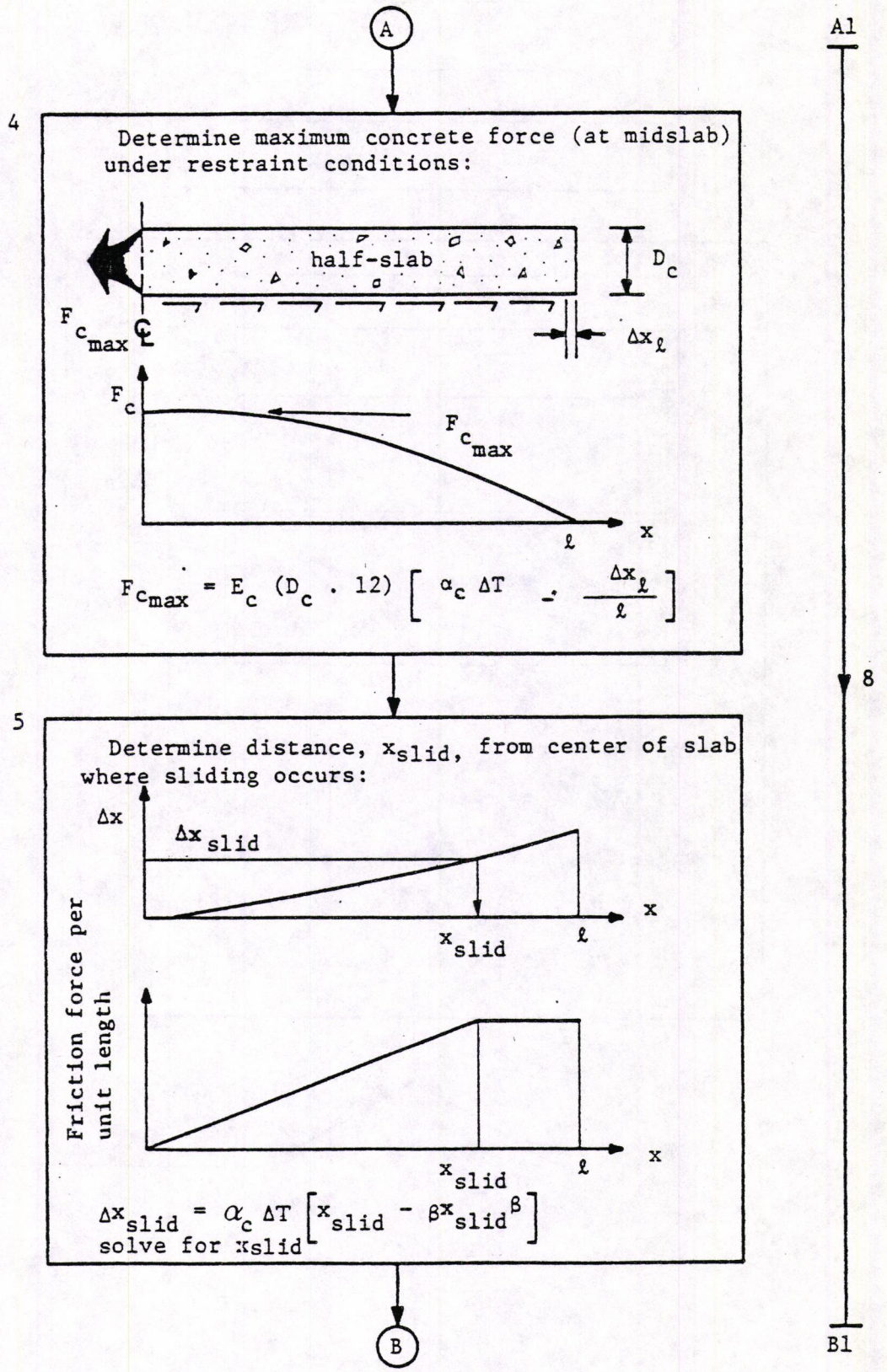
A
A1
4
Determine maximum concrete force (at midslab) under restraint conditions:
half-slab
D_c
$F_{c_{max}}$
℄
Δx_ℓ
F_c
$F_{c_{max}}$
x
ℓ
$F_{c_{max}} = E_c\ (D_c \cdot 12) \left[\alpha_c \Delta T - \frac{\Delta x_\ell}{\ell} \right]$
8
5
Determine distance, x_{slid}, from center of slab where sliding occurs:
Δx
Δx_{slid}
x
x_{slid}
ℓ
Friction force per unit length
x
x_{slid}
ℓ
$\Delta x_{slid} = \alpha_c \Delta T \left[x_{slid} - \beta x_{slid}^{\beta} \right]$
solve for x_{slid}
B
B1

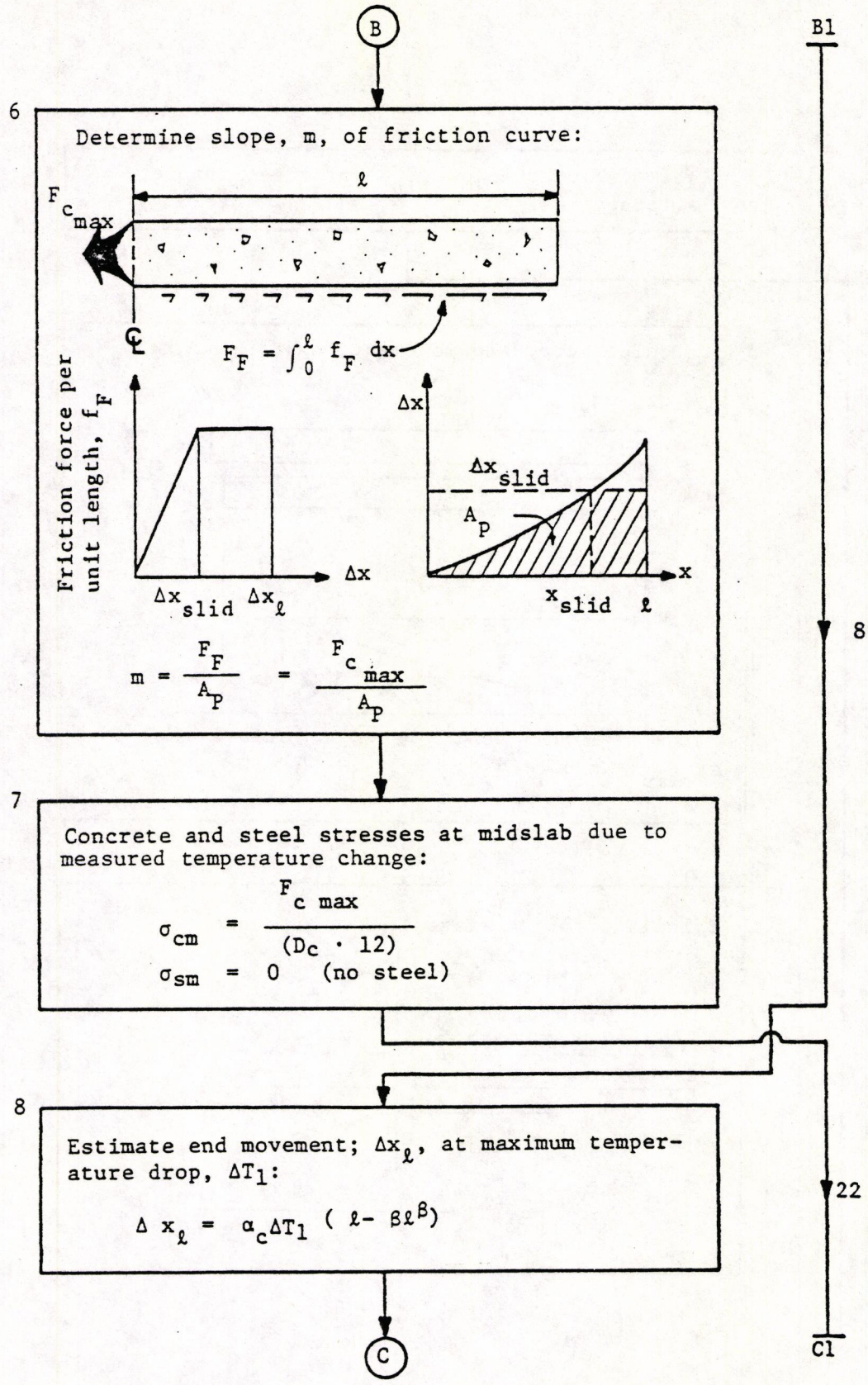
B
B1
6
Determine slope, m, of friction curve:
$F_{c\,max}$
ℓ
℄
$F_F = \int_0^{\ell} f_F\, dx$
Friction force per unit length, f_F
Δx
Δx_{slid}
Δx_ℓ
A_P
x
x_{slid}
ℓ
$m = \frac{F_F}{A_P} = \frac{F_{c\,max}}{A_P}$
8
7
Concrete and steel stresses at midslab due to measured temperature change:
$\sigma_{cm} = \frac{F_{c\,max}}{(D_c \cdot 12)}$
$\sigma_{sm} = 0$ (no steel)
8
Estimate end movement; Δx_ℓ, at maximum temperature drop, ΔT_1:
$\Delta x_\ell = \alpha_c \Delta T_1 (\ell - \beta \ell^\beta)$
22
C
C1

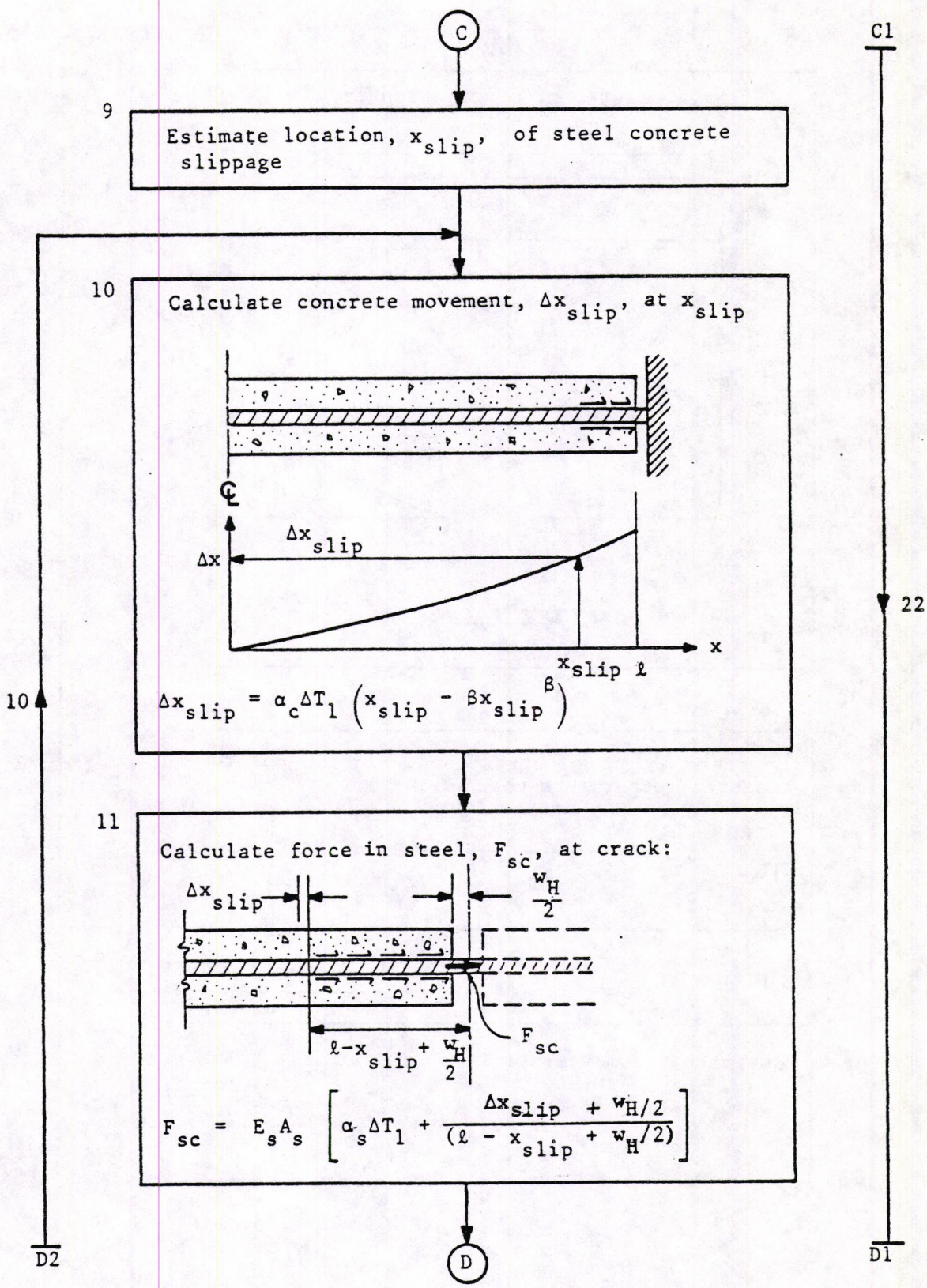
C
C1
9
Estimate location, x_{slip}, of steel concrete slippage
10
Calculate concrete movement, Δx_{slip}, at x_{slip}
Δx_{slip}
Δx
x
x_{slip} ℓ
$\Delta x_{slip} = \alpha_c \Delta T_1 \left(x_{slip} - \beta x_{slip}^{\beta} \right)$
22
10
11
Calculate force in steel, F_{sc}, at crack:
Δx_{slip}
$\frac{w_H}{2}$
F_{sc}
$\ell - x_{slip} + \frac{w_H}{2}$
$F_{sc} = E_s A_s \left[\alpha_s \Delta T_1 + \frac{\Delta x_{slip} + w_H/2}{(\ell - x_{slip} + w_H/2)} \right]$
D2
D
D1

D2

D

D1

12 Compute bond force transfer, U, between steel and concrete in region of slip.

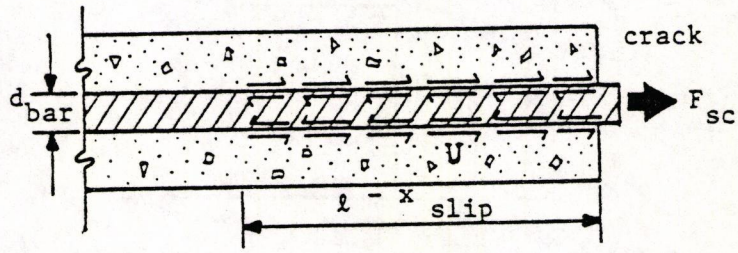

$$U = \sigma_{CB} \cdot (n \pi d_{bar}) \cdot (\ell - x_{slip})$$

where:

σ_{CB} = concrete to steel bond stress,

n = number of steel bars per foot width of concrete, and

πd_{bar} = perimeter of steel bar.

10

22

13 Compute force in steel, F_{ss}, and force in concrete, F_{cs}, at point of slippage and friction force, F_{fs}, in slip region.

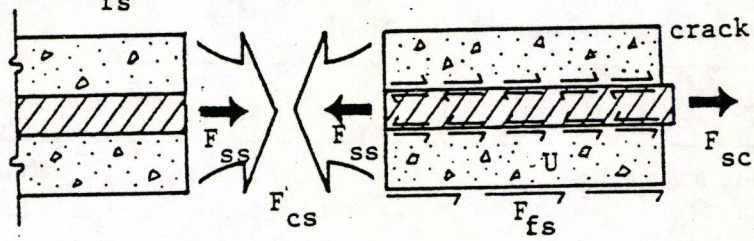

$$F_{ss} = F_{sc} - U$$

$$F_{cs} = E_c A_c \left[\frac{F_{ss}}{E_s A_s} + \alpha_c \Delta T_1 - \alpha_s \Delta T_1 \right]$$

$$F_{fs} = F_{cs} - U$$

E

E2

E1

E2

E

E1

14 Determine slope, m, of friction curve:

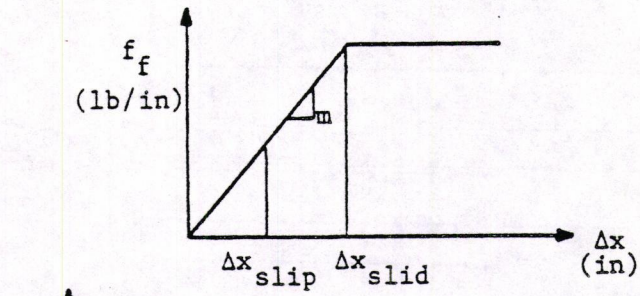

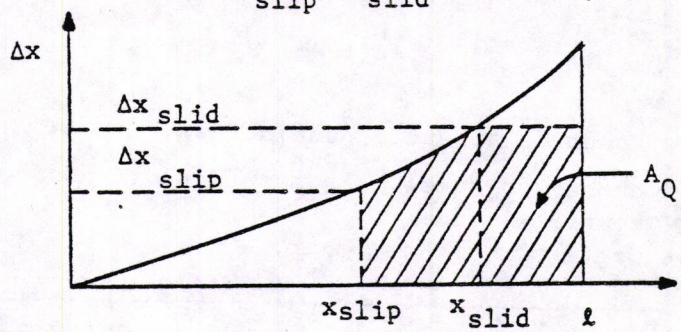

If $x_{slid} > x_{slip}$, $m = \dfrac{F_{fs}}{A_Q}$

If $x_{slip} > x_{slid}$, $m = \dfrac{F_{fs}}{\Delta x_{slid} (\ell - x_{slip})}$

10

22

15 Determine initial forces (at measured high temp.) in steel (at crack), F_{sc}', and concrete (at mid-slab), F_{cm}':

$$F_{sc}' = E_s A_s \frac{\frac{1}{2} w_H}{(\ell - x_{slip} + \frac{1}{2} w_H)}$$

$$F_{cm}' = F_{sc}' \Big/ \left[1 + \frac{E_s A_s}{E_c A_c} \right]$$

F2

F

F1

F2

F

F1

16 Compute forces in concrete, F_{cm}, and steel, F_{sm}, at midslab after maximum temperature drop:

$$F_{cm} = E_c A_c \left[\alpha_c \Delta T_1 - \frac{\Delta x_{\ell}}{\ell} \right] + F'_{cm}$$

$$F_{sm} = E_s A_s \left[\frac{F_{cm}}{E_c A_c} + \alpha_s \Delta T_1 - \alpha_c \Delta T_1 \right]$$

17 Compute total friction force, F_{ft}:

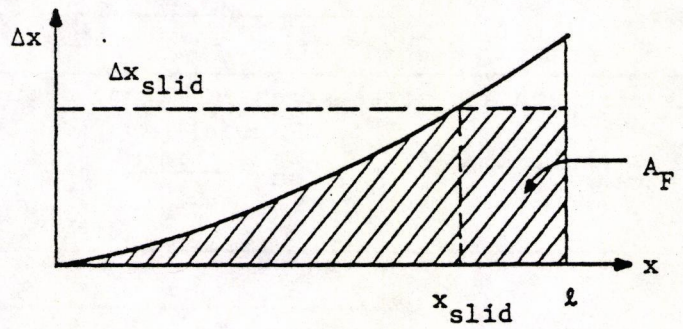

$$F_{ft} = m \cdot A_F$$

10

22

18 Compute unbalanced force, F_u:

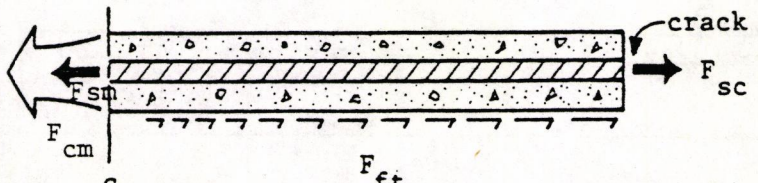

$$F_u = F_{sm} + F_{cm} - F_{ft} - F_{sc}$$

G2

G

G1

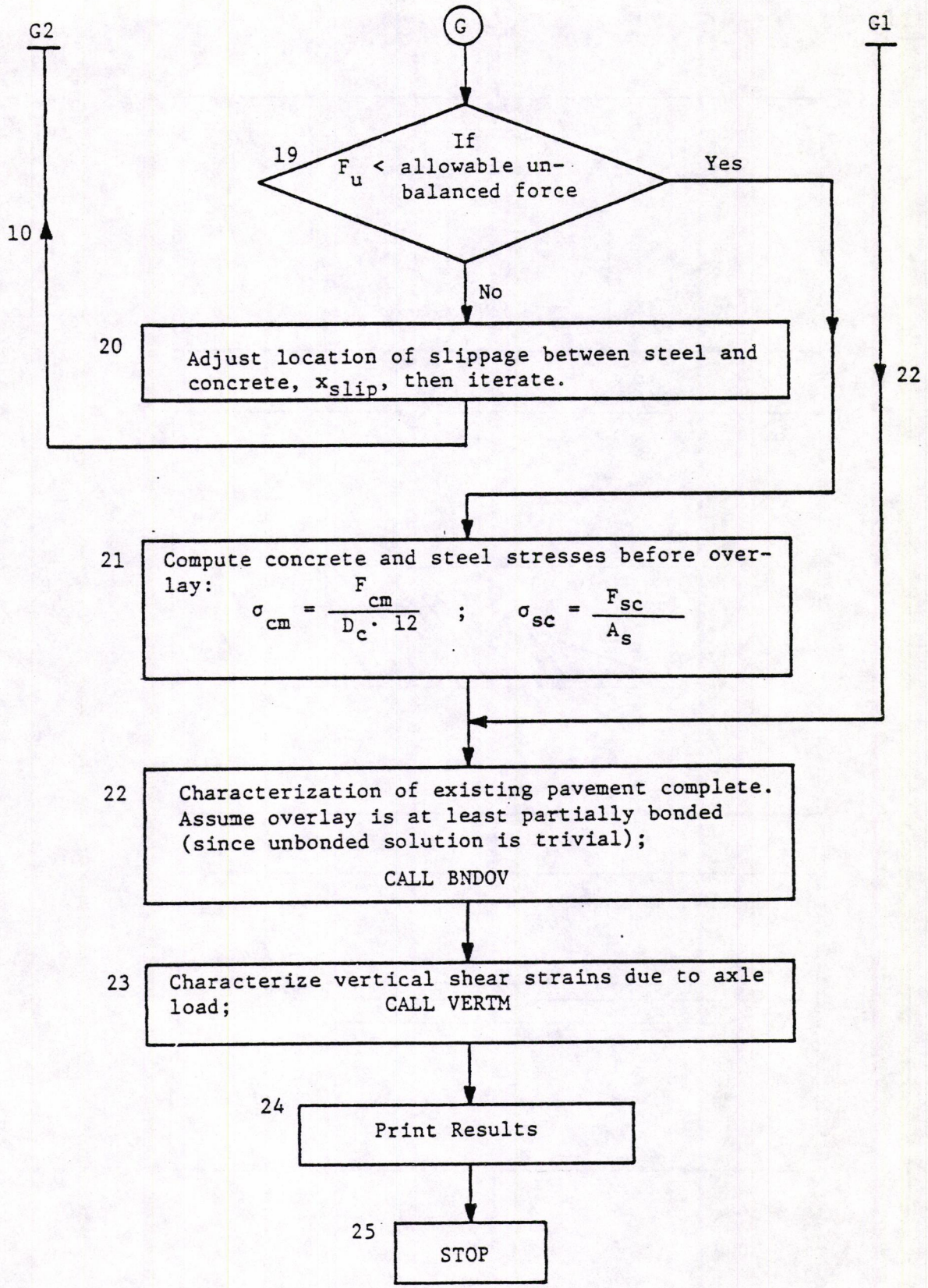
G2
G
G1
19
If
F_u < allowable un-balanced force
Yes
No
10
20
Adjust location of slippage between steel and concrete, x_{slip}, then iterate.
22
21
Compute concrete and steel stresses before overlay:
$\sigma_{cm} = \frac{F_{cm}}{D_c \cdot 12}$; $\sigma_{sc} = \frac{F_{sc}}{A_s}$
22
Characterization of existing pavement complete. Assume overlay is at least partially bonded (since unbonded solution is trivial);
CALL BNDOV
23
Characterize vertical shear strains due to axle load; CALL VERTM
24
Print Results
25
STOP

26 BNDOV

27 Adjust slope of friction curve to account for increase in overburden after overlay.

$$m_o = m\left[1 + \frac{D_o \gamma_o}{D_c \gamma_c}\right]$$

where: m = slope for existing pavement,
D_o = overlay thickness,
γ_o = overlay unit weight,
D_c = existing concrete thickness, and
γ_c = existing concrete unit weight.

note: $m_o = m$ (if no adjustment desired)

28 Compute force in steel at crack, F_{sc}', at measured high temperature:

$$F_{sc}' = E_s A_s \left[\frac{\frac{1}{2} w_H}{\ell - x_{slip} + \frac{1}{2} w_H}\right]$$

where: x_{slip} = distance from midslab where steel-concrete slippage begins (computed by calling routine).

29 Compute force in concrete at midslab, F_{cm}', corresponding to measured high temperature:

$$F_{cm}' = \frac{F_{sc}'}{\left[1 + \frac{E_s A_s}{E_c A_c}\right]}$$

H

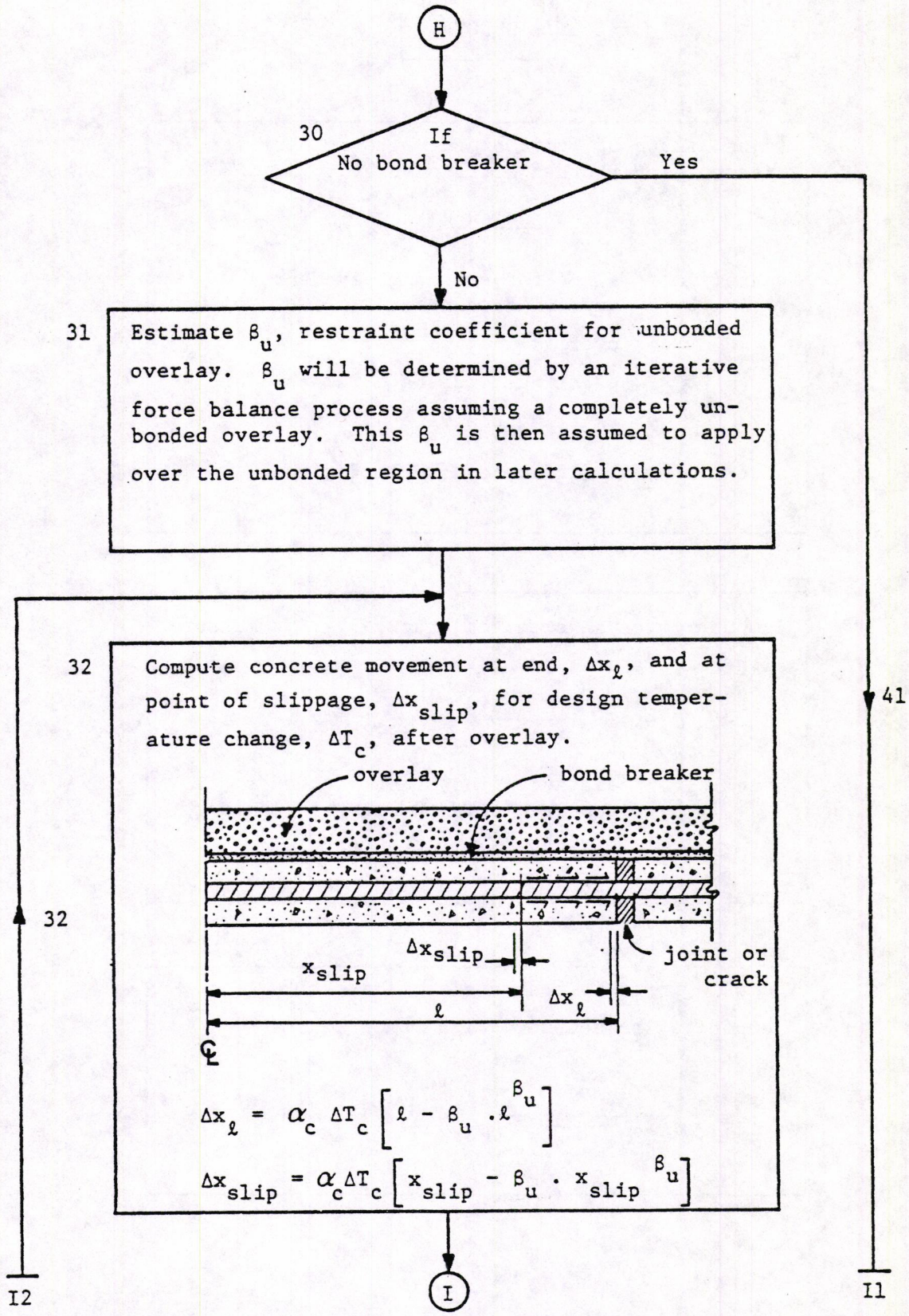
H
30
If
No bond breaker
Yes
No
31
Estimate β_u, restraint coefficient for unbonded overlay. β_u will be determined by an iterative force balance process assuming a completely unbonded overlay. This β_u is then assumed to apply over the unbonded region in later calculations.
32
Compute concrete movement at end, Δx_ℓ, and at point of slippage, Δx_{slip}, for design temperature change, ΔT_c, after overlay.
overlay
bond breaker
joint or crack
x_{slip}
Δx_{slip}
Δx_ℓ
ℓ
$\Delta x_\ell = \alpha_c \Delta T_c \left[\ell - \beta_u . \ell^{\beta_u} \right]$
$\Delta x_{slip} = \alpha_c \Delta T_c \left[x_{slip} - \beta_u . x_{slip}^{\beta_u} \right]$
32
41
I2
I
I1

I2

I

I1

33 Estimate force in concrete at midslab, F_{cm}, due to design temperature change, ΔT_c. (Assume totally unbonded overlay.)

$$F_{cm} = E_c A_c \left[\alpha_c \Delta T_c - \frac{\Delta x_\ell}{\ell} \right] + F_{cm}'$$

34 Calculate new location of sliding, x_{slid}, using this equation and estimate of β_u.

$$\Delta x_{slid} = \alpha_c \Delta T_c \left[x_{slid} - \beta_u \cdot x_{slid}^{\beta_u} \right]$$

where: Δx_{slid} = concrete movement at sliding.

32

41

35 Compute total friction force, F_{ft}, at interface between concrete and subbase.

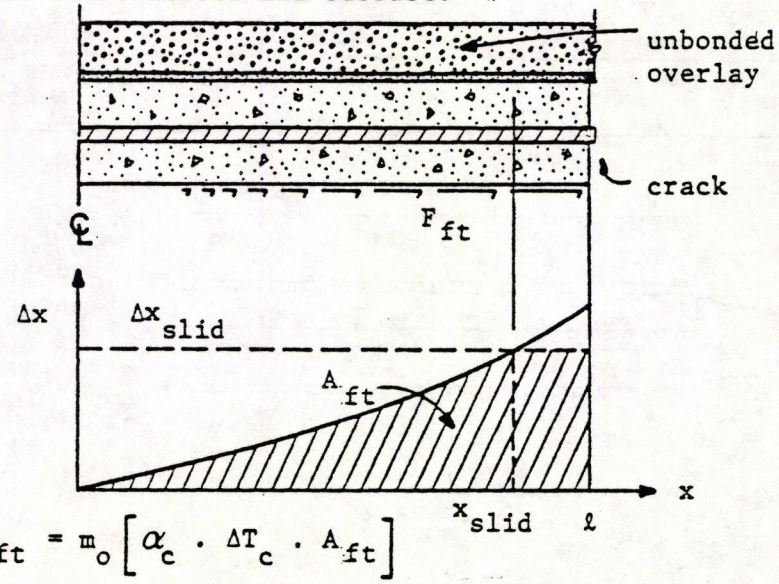

$$F_{ft} = m_o \left[\alpha_c \cdot \Delta T_c \cdot A_{ft} \right]$$

J2

J

J1

J2

J

J1

36 Compute force in steel at midslab, F_{sm}, due to design temperature drop, ΔT_c.

$$F_{sm} = E_s A_s \left[\frac{F_{cm}}{E_c A_c} + \Delta T_c \, (\alpha_s - \alpha_c) \right]$$

37 Calculate force in steel at crack, F_{sc}, after temperature drop.

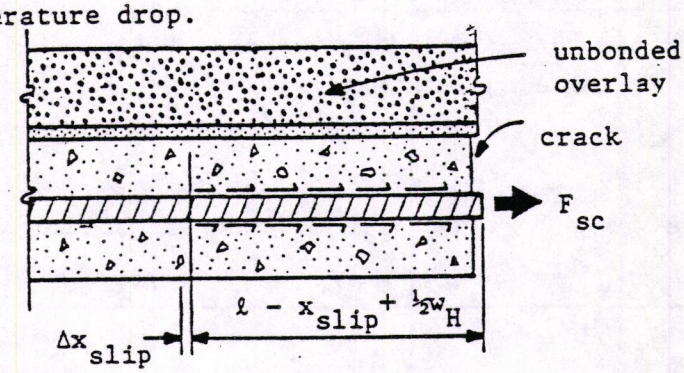

$$F_{sc} = E_s A_s \left[\alpha_s \Delta T_c + \frac{\Delta x_{slip} + \frac{1}{2} w_H}{\ell - x_{slip} + \frac{1}{2} w_H} \right]$$

32

41

38 Sum of forces, ΣF:

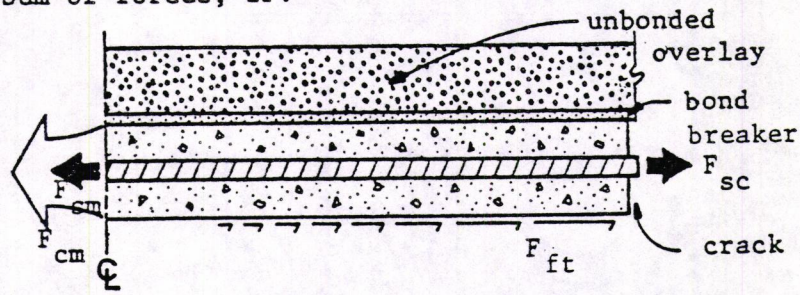

$$\Sigma F = F_{sc} + F_{ft} - F_{sm} - F_{cm}$$

K2

K

K1

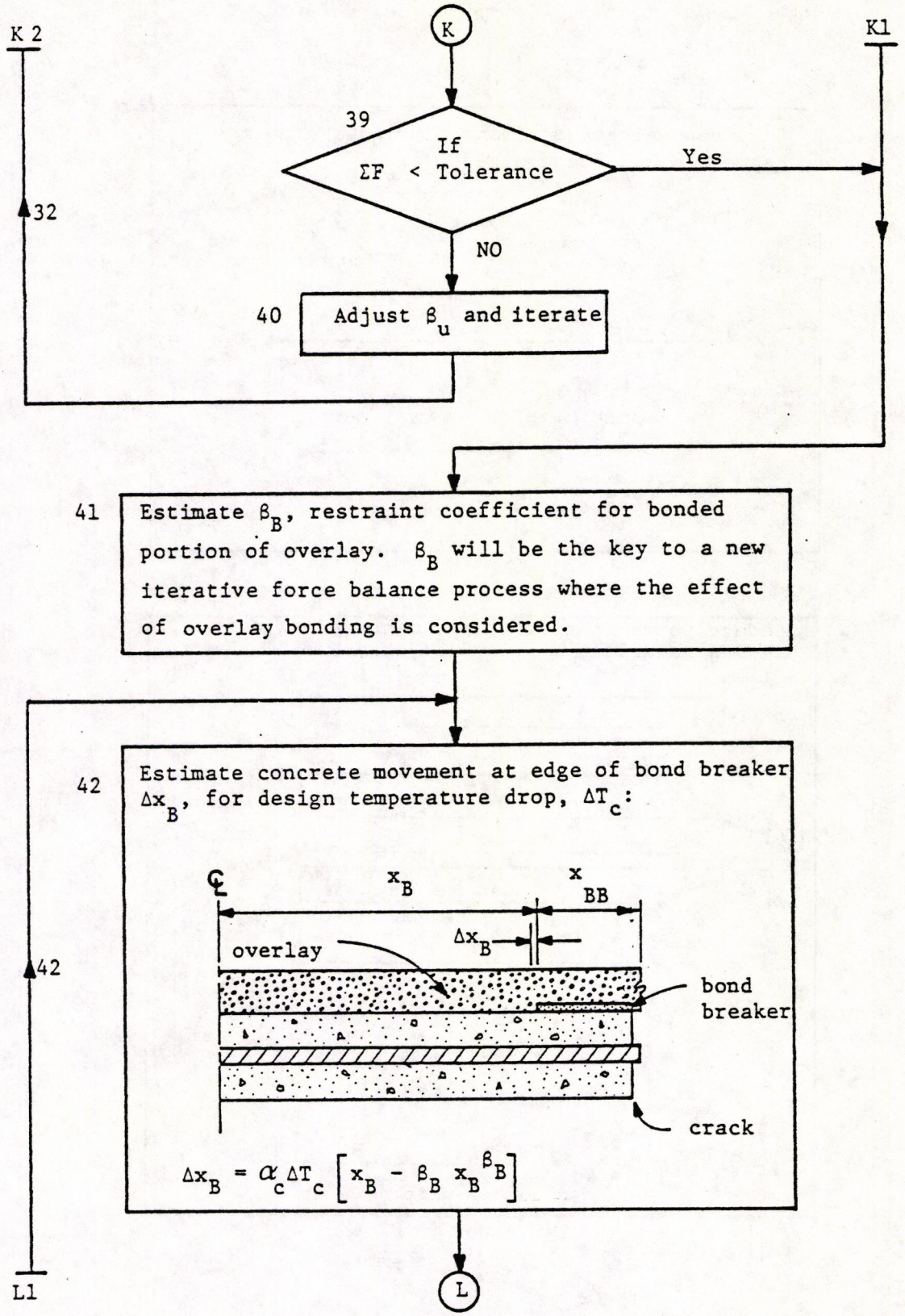
K 2
K
K1
39
If
ΣF < Tolerance
Yes
32
NO
40
Adjust β_u and iterate
41
Estimate β_B, restraint coefficient for bonded portion of overlay. β_B will be the key to a new iterative force balance process where the effect of overlay bonding is considered.
42
Estimate concrete movement at edge of bond breaker Δx_B, for design temperature drop, ΔT_c:
x_B
x_{BB}
Δx_B
overlay
bond breaker
crack
$\Delta x_B = \alpha_c \Delta T_c \left[x_B - \beta_B x_B^{\beta_B} \right]$
42
L1
L

L1

L

43 Compute concrete movement at slippage point between steel and concrete, Δx_{slip}:

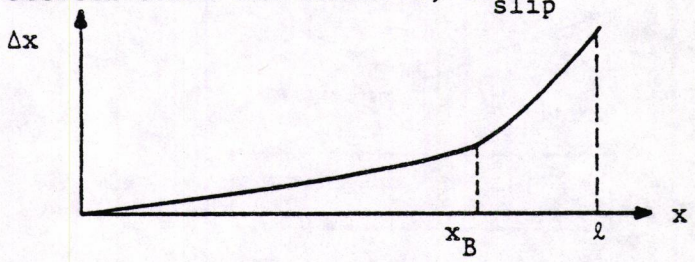

If $x_B \geq x_{slip}$:

$$\Delta x_{slip} = \alpha_c \Delta T_c \left[x_{slip} - \beta_B \, x_{slip}^{\beta_B} \right]$$

If $x_B < x_{slip}$:

$$\Delta x_{slip} = \Delta x_B + \alpha_c \Delta T_c \left[(x_{slip} - x_B) - \beta_B \, (x_{slip} - x_B)^{\beta_B} \right]$$

42 44 Compute force in concrete at midslab, F_{cm}, in steel at midslab, F_{sm}, and at crack, F_{sc}:

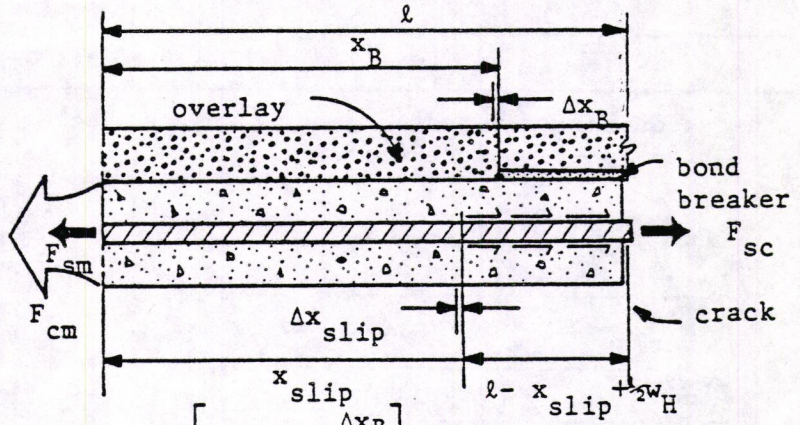

$$F_{cm} = E_c A_c \left[\alpha_c \Delta T_c - \frac{\Delta x_B}{x_B} \right] + F_{cm}'$$

$$F_{sm} = E_s A_s \left[\frac{F_{cm}}{E_c A_c} + \alpha_s \Delta T_c - \alpha_c \Delta T_c \right]$$

$$F_{sc} = E_s A_s \left[\alpha_s \Delta T_c + \frac{\Delta x_{slip} + \frac{1}{2} w_H}{\ell - x_{slip} + \frac{1}{2} w_H} \right]$$

M

M1

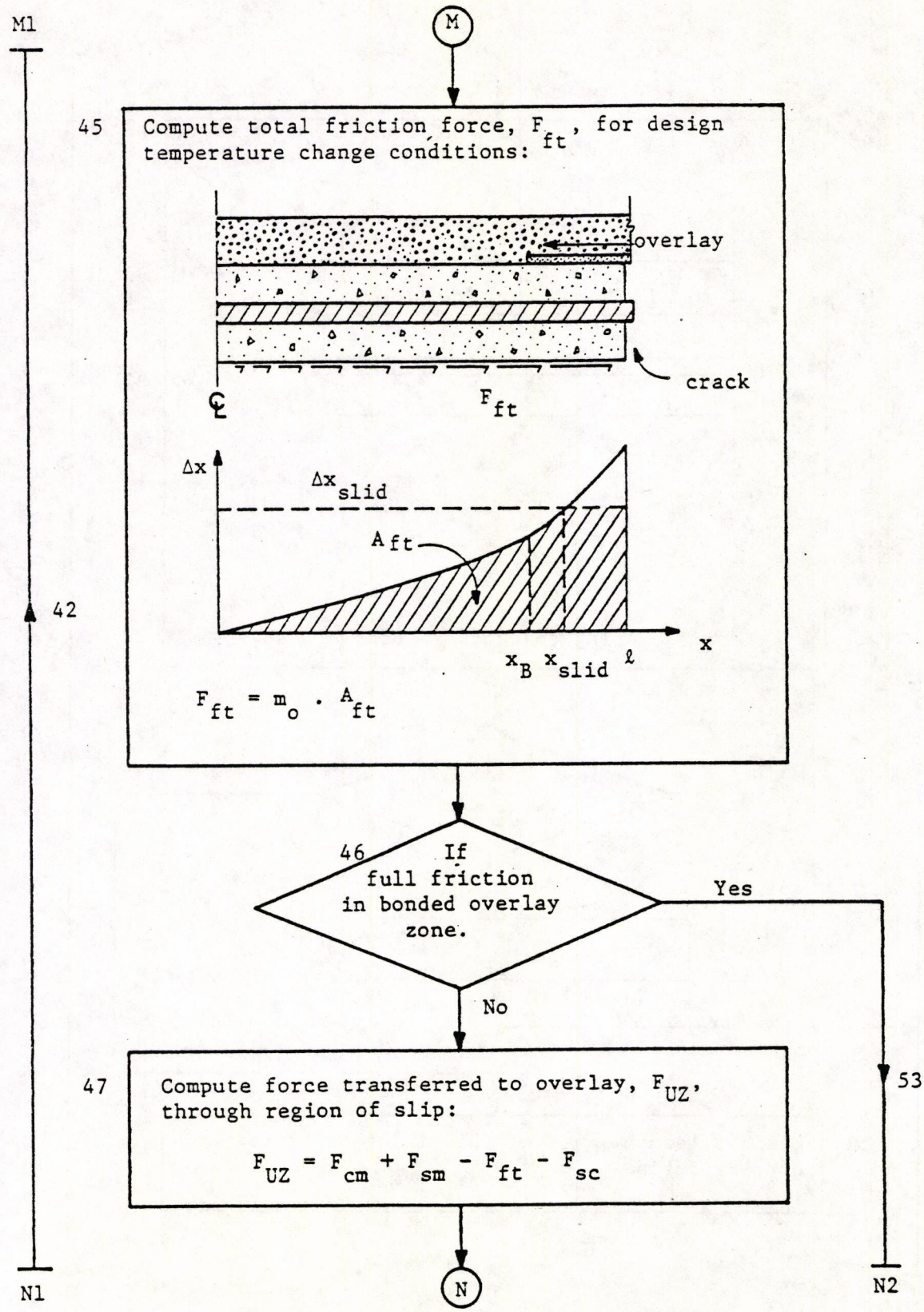
M1
M
45
Compute total friction force, F_{ft}, for design temperature change conditions:
overlay
crack
℄
F_{ft}
Δx
Δx_{slid}
A_{ft}
x
x_B x_{slid} ℓ
$F_{ft} = m_o \cdot A_{ft}$
42
46
If full friction in bonded overlay zone.
Yes
No
47
Compute force transferred to overlay, F_{UZ}, through region of slip:
$F_{UZ} = F_{cm} + F_{sm} - F_{ft} - F_{sc}$
53
N1
N
N2

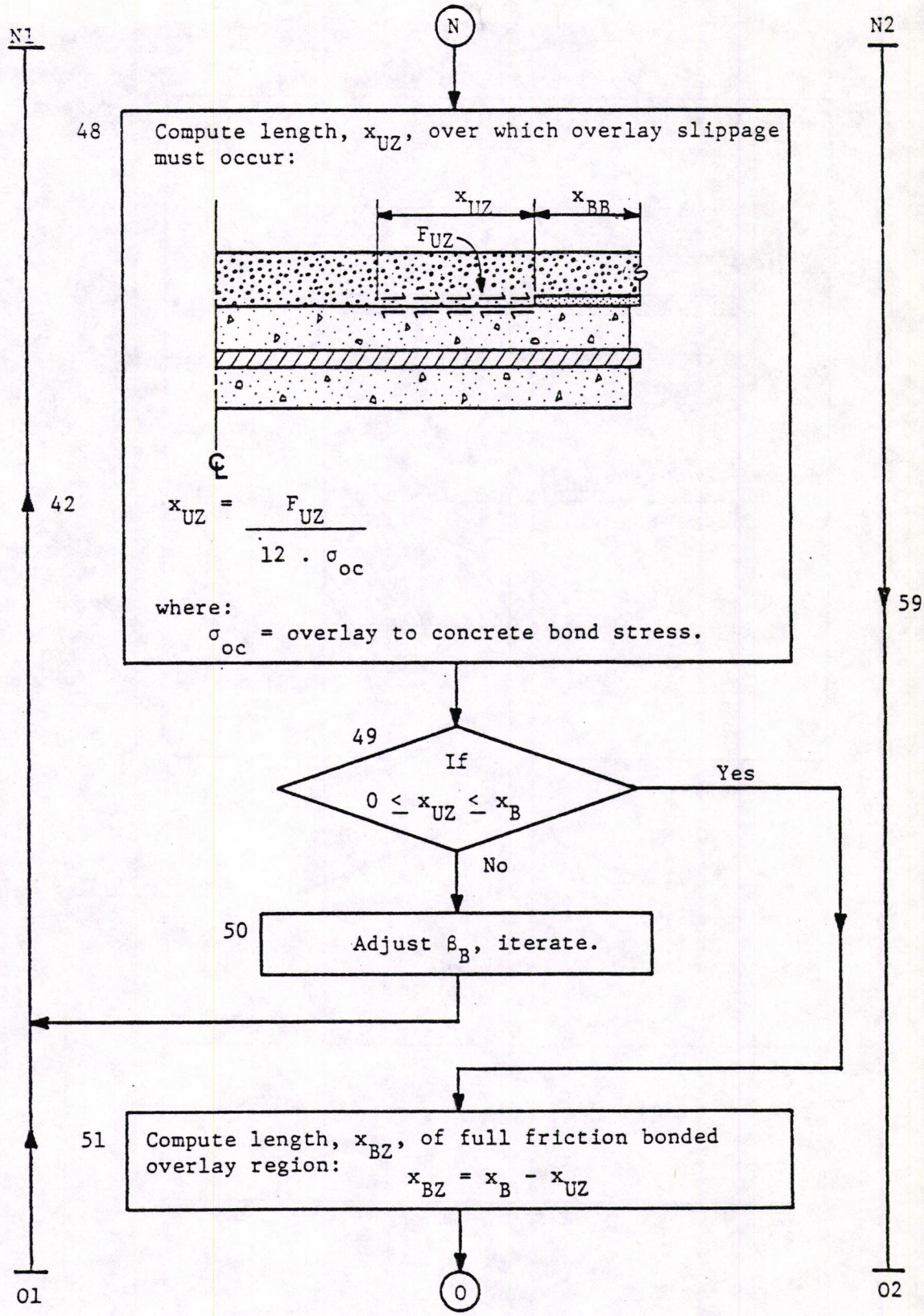
N1
N
N2
48
Compute length, x_{UZ}, over which overlay slippage must occur:
x_{UZ}
x_{BB}
F_{UZ}
$x_{UZ} = \frac{F_{UZ}}{12 \cdot \sigma_{oc}}$
where:
σ_{oc} = overlay to concrete bond stress.
42
59
49
If
$0 \leq x_{UZ} \leq x_B$
Yes
No
50
Adjust β_B, iterate.
51
Compute length, x_{BZ}, of full friction bonded overlay region:
$x_{BZ} = x_B - x_{UZ}$
O
O1
O2

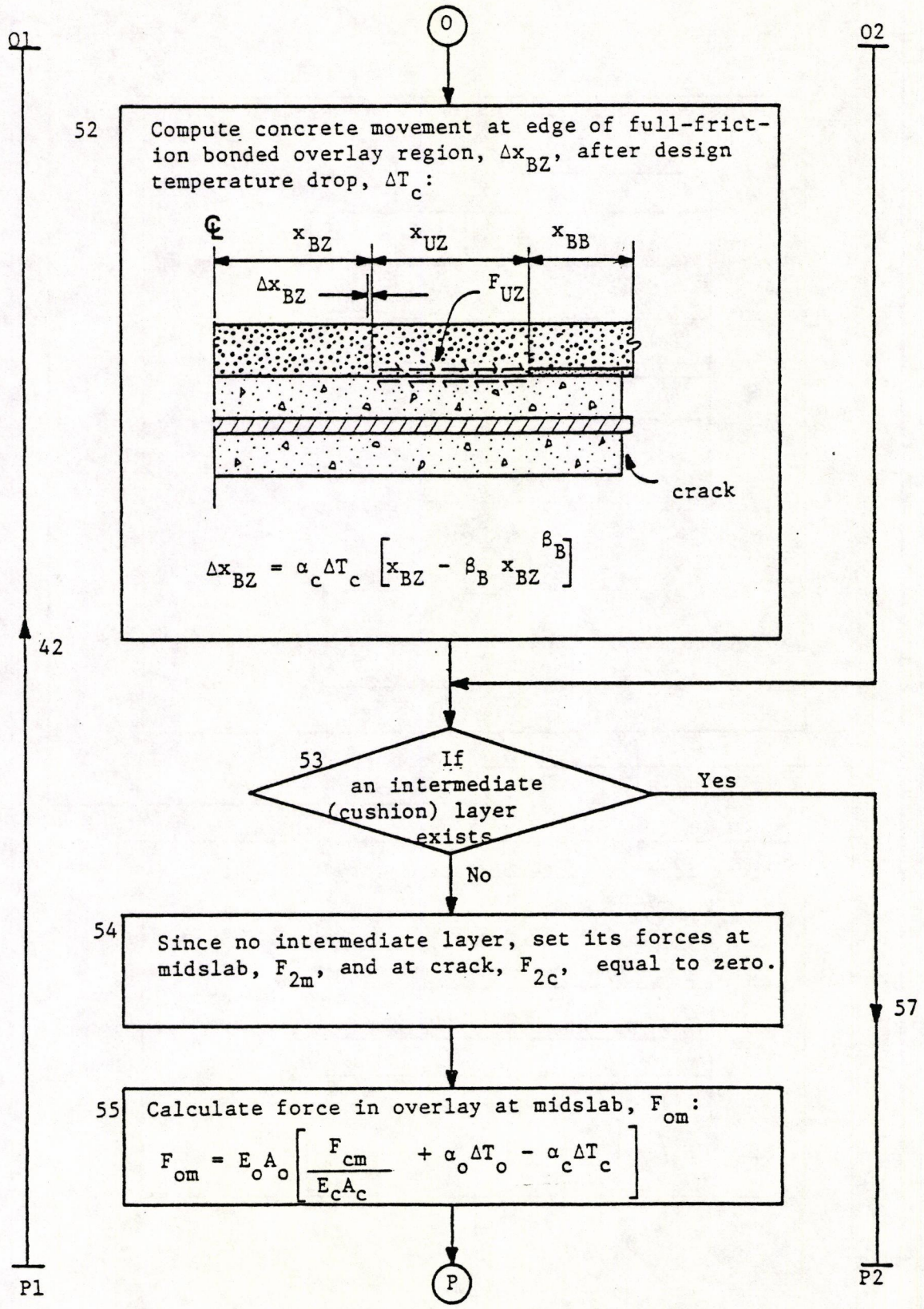
O1
O
O2
52
Compute concrete movement at edge of full-friction bonded overlay region, Δx_{BZ}, after design temperature drop, ΔT_c:
℄
x_{BZ}
x_{UZ}
x_{BB}
Δx_{BZ}
F_{UZ}
crack
$\Delta x_{BZ} = \alpha_c \Delta T_c \left[x_{BZ} - \beta_B x_{BZ}^{\beta_B} \right]$
42
53
If an intermediate (cushion) layer exists
Yes
No
54
Since no intermediate layer, set its forces at midslab, F_{2m}, and at crack, F_{2c}, equal to zero.
57
55
Calculate force in overlay at midslab, F_{om}:
$F_{om} = E_o A_o \left[\frac{F_{cm}}{E_c A_c} + \alpha_o \Delta T_o - \alpha_c \Delta T_c \right]$
P1
P
P2

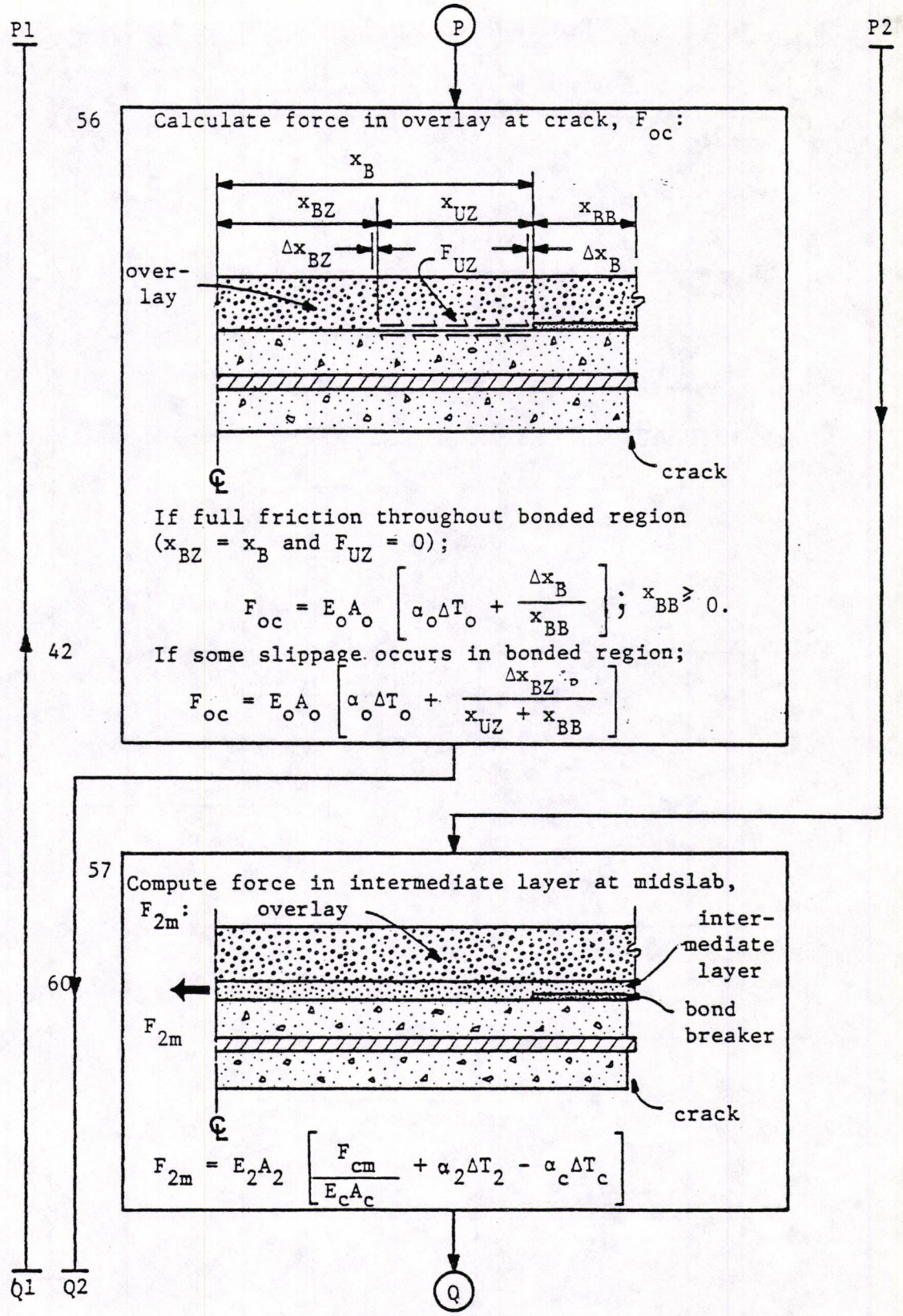
P1
P
P2
56
Calculate force in overlay at crack, F_{oc}:
x_B
x_{BZ}
x_{UZ}
x_{BB}
Δx_{BZ}
F_{UZ}
Δx_B
over-
lay
crack
If full friction throughout bonded region
($x_{BZ} = x_B$ and $F_{UZ} = 0$);
$F_{oc} = E_o A_o \left[\alpha_o \Delta T_o + \frac{\Delta x_B}{x_{BB}} \right]$; $x_{BB} \geq 0$.
42
If some slippage occurs in bonded region;
$F_{oc} = E_o A_o \left[\alpha_o \Delta T_o + \frac{\Delta x_{BZ}}{x_{UZ} + x_{BB}} \right]$
57
Compute force in intermediate layer at midslab,
F_{2m}:
overlay
inter-
mediate
layer
60
bond
breaker
F_{2m}
crack
$F_{2m} = E_2 A_2 \left[\frac{F_{cm}}{E_c A_c} + \alpha_2 \Delta T_2 - \alpha_c \Delta T_c \right]$
Q1
Q2
Q

Q1 Q2

Q

58

Compute force in intermediate layer at crack, F_{2c}:

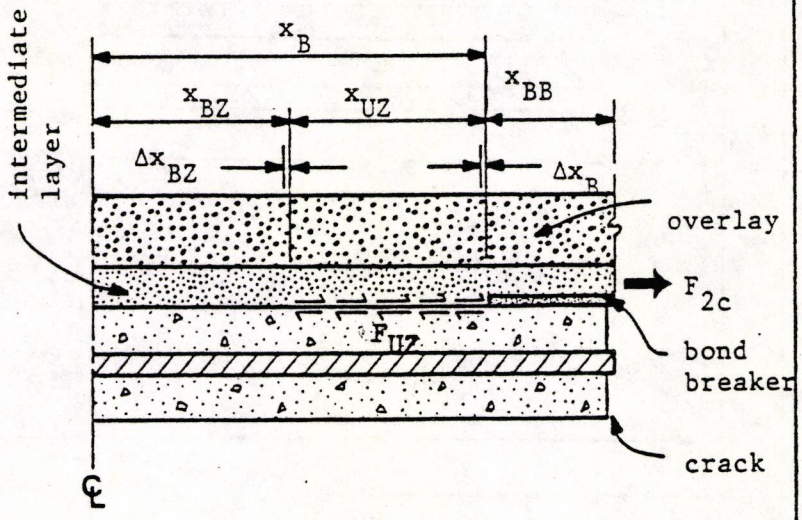

If full friction throughout bonded region (either if user specified or if computed $x_{BZ} = x_B$);

$$F_{2c} = E_2 A_2 \left[\alpha_2 \Delta T_2 + \frac{\Delta x_B}{x_{BB}} \right]; \; x_{BB} \geq 0.$$

If some slippage occurs in bonded region;

$$F_{2c} = E_2 A_2 \left[\alpha_2 \Delta T_2 + \frac{\Delta x_B}{x_{UZ} + x_{BB}} \right]$$

42 60

R

R1 R2

R1 R2

R

59

Compute forces in overlay at midslab, F_{om}, and at crack, F_{oc}:

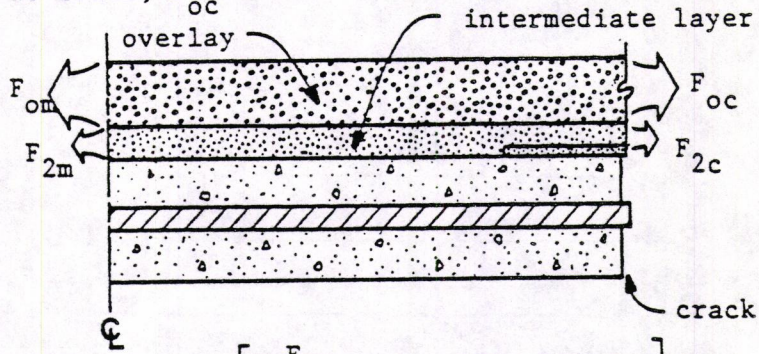

$$F_{om} = E_o A_o \left[\frac{F_{2m}}{E_2 A_2} + \alpha_o \Delta T_o - \alpha_2 \Delta T_2 \right]$$

$$F_{oc} = E_o A_o \left[\frac{F_{2c}}{E_2 A_2} + \alpha_o \Delta T_o - \alpha_2 \Delta T_2 \right]$$

42

60

Compute forces in overlay reinforcement at midslab F_{rm}, and at crack, F_{rc}, if reinforcement exists;

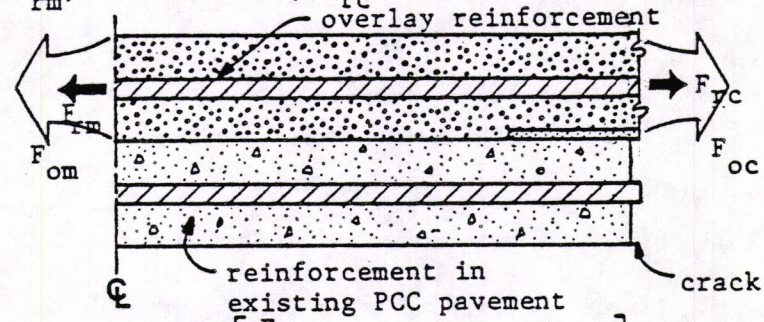

$$F_{rm} = E_r A_r \left[\frac{F_{om}}{E_o A_o} + \alpha_r \Delta T_r - \alpha_o \Delta T_o \right]$$

$$F_{rc} = E_r A_r \left[\frac{F_{oc}}{E_o A_o} + \alpha_r \Delta T_r - \alpha_o \Delta T_o \right]$$

S1

S

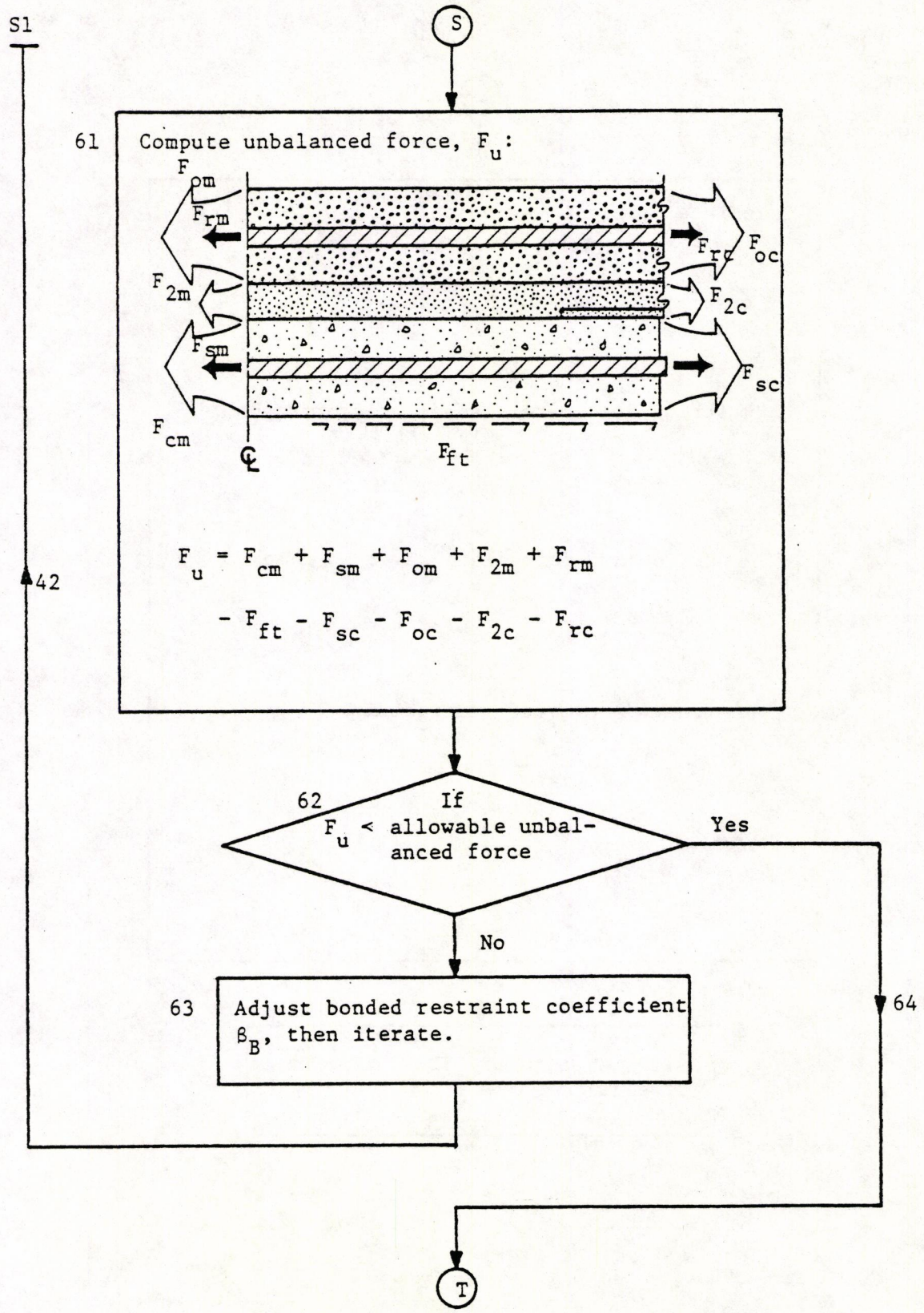
S1
S
61
Compute unbalanced force, F_u:
F_{om}
F_{rm}
F_{2m}
F_{sm}
F_{cm}
F_{rc}
F_{oc}
F_{2c}
F_{sc}
F_{ft}
$F_u = F_{cm} + F_{sm} + F_{om} + F_{2m} + F_{rm} - F_{ft} - F_{sc} - F_{oc} - F_{2c} - F_{rc}$
42
62
If F_u < allowable unbalanced force
Yes
No
63
Adjust bonded restraint coefficient β_B, then iterate.
64
T

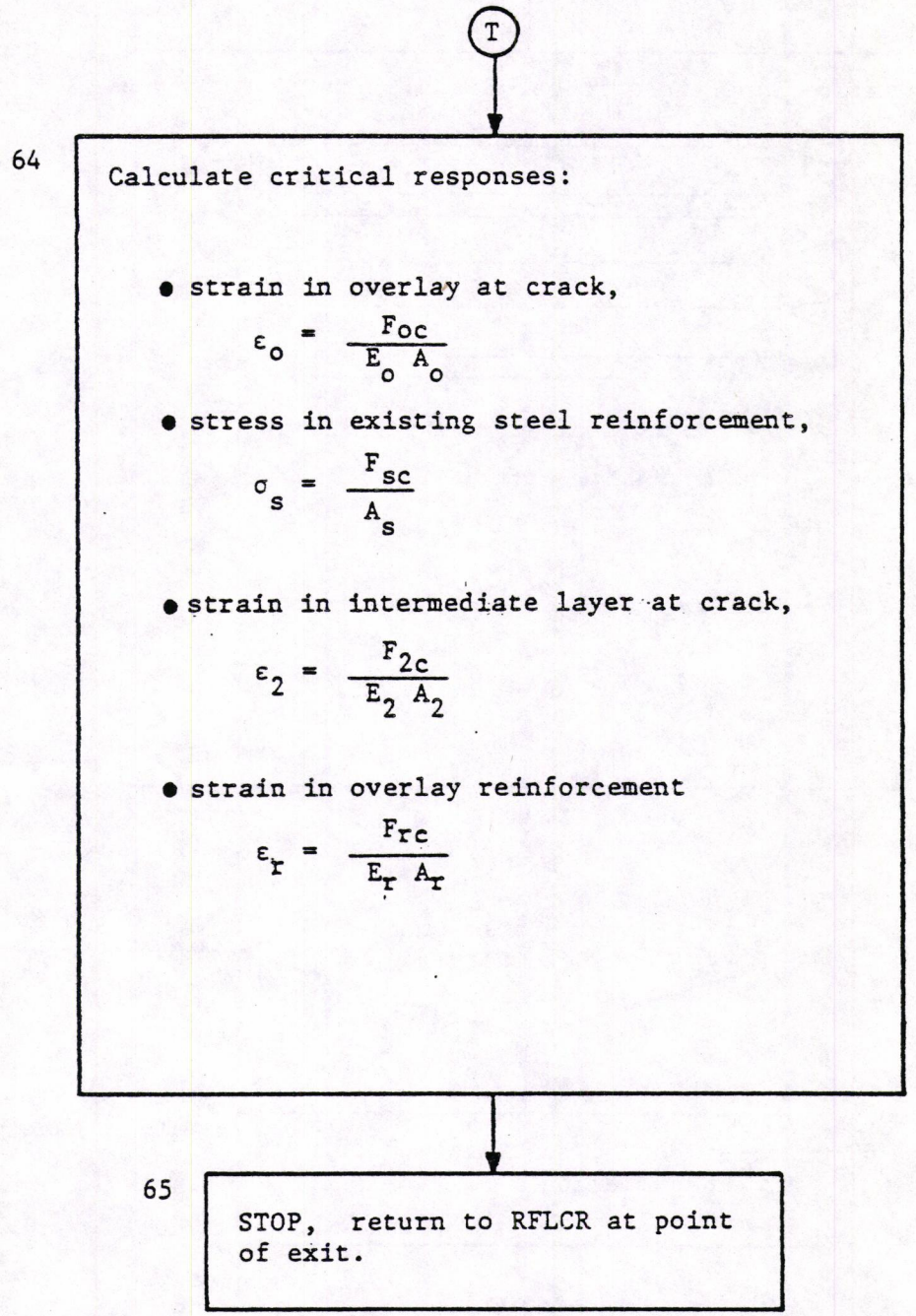
T
64
Calculate critical responses:
• strain in overlay at crack,
$\varepsilon_o = \frac{F_{oc}}{E_o A_o}$
• stress in existing steel reinforcement,
$\sigma_s = \frac{F_{sc}}{A_s}$
• strain in intermediate layer at crack,
$\varepsilon_2 = \frac{F_{2c}}{E_2 A_2}$
• strain in overlay reinforcement
$\varepsilon_r = \frac{F_{rc}}{E_r A_r}$
65
STOP, return to RFLCR at point of exit.

66 VERTM

67 Estimate fraction of load transfer L_T, at the joint (or crack)

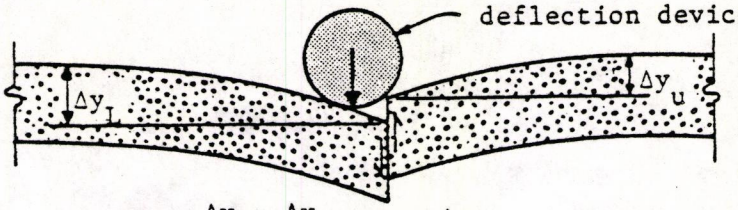

$$L_T = 1 - \frac{\Delta y_L - \Delta y_u}{\Delta y_L} = \frac{\Delta y_u}{\Delta y_L}$$

68 Calculate shear force, P_o, to be carried by overlay: $P_o = L_D (1 - L_T)$

where: L_D = one half the design axle load.

69 Calculate effective thickness, D_e, of overlay, reinforcement and cushion layer:

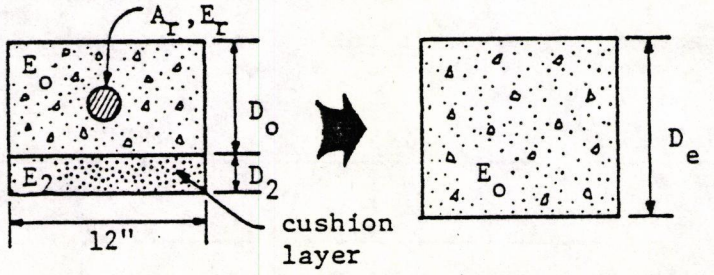

$$D_e = D_o + D_2\left(\frac{E_2}{E_o}\right) + \left(\frac{A_r \cdot E_r}{12 \cdot E_o}\right)$$

U

U

70 Calculate shear stress, τ_o, in overlay:

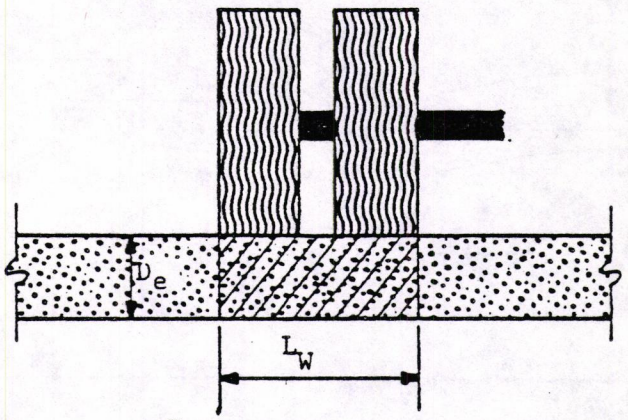

$$\tau_o = \frac{P_o}{D_e \cdot L_W}$$

71 Calculate shear strain, γ_o, in overlay:

$$\gamma_o = \frac{2\,\tau_o\,(1 + \upsilon_o)}{E_o}$$

where: υ_o = poisson's ratio for overlay

72 STOP, return to RFLCR at point of exit.

APPENDIX B

SELECTION OF DATA FOR ARKRC-2 CALIBRATION

Six different overlay sections, two from Arkansas and four from Texas, were selected for developing a new tensile strain fatigue equation and calibrating the new ARKRC-2 computer program. This appendix discusses the selection of the pertinent input data required for each of the sections. These data are discussed in the same general order as that presented in the ARKRC-2 User's Manual (Chapter 6).

EXISTING CONCRETE PAVEMENT CHARACTERISTICS

The input data selected to characterize the existing concrete slab, its reinforcement and its potential for horizontal movement is summarized in Table B.1. The data from the first two categories was obtained from construction plans, records, prior knowledge and from criteria provided in the User's Manual. For the latter category, however, it was not possible to obtain slab horizontal movement data according to the procedure recommended in the User's Manual. In this case, it was necessary to use a computer program called VCARCS (Volume Change Analysis of Reinforced Concrete Slabs) to estimate the amount of movement a slab would undergo during a given temperature change and for a given slab-base friction force versus movement curve (which is dependent on subbase type). This program was run on each Arkansas and Texas calibration section since no pre-overlay movement data were available.

OVERLAY AND INTERMEDIATE LAYER CHARACTERISTICS

A summary of the properties used for both the asphalt concrete overlay and intermediate layer (i.e., open-graded course) for the six calibration sections is presented in Table B.2. Once again, most of these data are based on construction plans and information provided in the User's Manual. It should be pointed out, however, that it was necessary

Table B.1. Summary of existing concrete pavement characteristics for the six calibration sections.

Characteristic	Arkansas Sections		Texas Sections			
	3.	7.	1.	2.	3a.	3b.
Existing Concrete Pavement						
Type	JRCP	JRCP	JCP	JRCP	CRCP	CRCP
Condition	uncracked	uncracked	uncracked	uncracked	cracked	cracked
Joint or crack spacing feet	45.0	45.0	15.0	61.5	2.50	1.85
Slab thickness, inches	9.0	9.0	11.0	10.0	8.0	8.0
Concrete creep modulus, psi	3.8×10^{6}	3.8×10^{6}	4.8×10^{6}	4.8×10^{6}	4.8×10^{6}	4.8×10^{6}
Concrete thermal coefficient, in/in/^{o}F	5.8×10^{-6}	5.8×10^{-6}	6.5×10^{-6}	6.5×10^{-6}	6.5×10^{-6}	6.5×10^{-6}
Concrete unit weight	150	150	150	150	150	150
Movement at sliding	0.05	0.10	0.20	0.20	0.15	0.15
Existing Pavement Reinforcement	(none)	(none)	(none)	(none)		
Bar diameter, inches	-	-	-	-	0.625	0.625
Bar spacing, inches	-	-	-	-	6.5	6.5
Steel elastic modulus, psi	-	-	-	-	30×10^{6}	30×10^{-6}
Steel thermal coefficient, in/in/^{o}F	-	-	-	-	6×10^{-6}	6×10^{-6}
Maximum bond stress, psi	-	-	-	-	550	550
Existing Pavement Movement Characterization						
High temperature, ^{o}F	100	100	80	80	80	80
Joint/crack width at high temperature, in.	.06000	.06000	.02000	.0400	.00800	.00800
Low temperature, ^{o}F	80	80	60	60	60	60
Joint/crack width at low temperature, in.	.09129	.09510	.03170	.08789	.00960	.00922
Minimum temperature observed, ^{o}F	0	0	0	0	0	0

Table B.2. Asphalt concrete overlay and intermediate layer characteristics used for the six calibration sections.

Characteristic	Arkansas Sections		Texas Sections			
	3.	7.	1.	2	3a.	3 b.
Asphalt Concrete Overlay						
Thickness (Binder + Surface), inches	7.0	7.0	3.0	4.0	2.5	6.0
Creep modulus, psi	29,000	29,000	20,000	20,000	20,000	20,000
Dynamic modulus, psi	614,000	614,000	460,000	460,000	460,000	460,000
Thermal coefficient, in/in/^{o}F	1.3×10^{-5}	1.3×10^{-5}	1.3×10^{-5}	1.3×10^{-5}	1.3×10^{-5}	1.3×10^{-5}
Unit weight, pcf	140	140	140	140	140	140
Maximum bond stress, psi	250	250	250	250	250	250
Bond breaker width. ft.	0	0	0	0	0	0
Intermediate Layer			(none)		(none)	(none)
Thickness, inches	3.0	3.0	-	3.5	-	-
Creep modulus, psi	5,000	5,000	-	5,000	-	-
Dynamic modulus, psi	20,000	20,000	-	20,000	-	-
Thermal coefficient, in/in/^{o}F	2.0×10^{-5}	2.0×10^{-5}	-	2.0×10^{-5}	-	-
Unit weight, pcf	120	120	-	120	-	-

to use a "curve-fitting" technique in order to estimate overlay creep moduli for the recommended temperature conditions. This was accomplished by first determining appropriate Penetration Index (PI) values, Ring and Ball Softening Point Temperatures ($T_{R\&B}$) and volume concentration of aggregate (C_v) values which resulted in a "Heukelom and Klomp" creep modulus versus load time curve similar to that shown for AC specimen no. 7 (in Figure 4.5). This sample appeared to be the most representative of the characteristics of an overlay in the field. Thus, it was then possible to estimate the value of the overlay creep modulus at a temperature lower than that used in the laboratory test (as recommended in Table 6.5) and at a longer load rate (6 hours). The PI, $T_{R\&B}$ and C_v values for specimen no. 7 which fit the laboratory curve almost exactly were -1.0, 51.8°C and 0.89, respectively.

It should be noted also, that although dynamic modulus values for the overlay and intermediate layer are shown in Table B.2, they have no effect on overlay tensile strain and are therefore inconsequential to the calibration of the tensile strain component of the ARKRC-2 program.

YEARLY FREQUENCY OF CRITICAL MINIMUM TEMPERATURES

Table B.3 summarizes the yearly frequency of minimum temperature data required by the program. The data for the Arkansas sections was obtained from Table 3.8 while the data for the Texas sections was obtained from a similar table for Texas provided by the National Climatic Center. The reason all the Texas section have the same yearly frequency is because they all lie in the same climatic region.

Table B.3. Yearly frequency(in days) of critical minimum temperatures for six calibration sections.

Range of Minimum Daily Temp. (^{O}F)	Arkansas Sections		Texas Sections (all)
	3.	7.	
49 to 40	56	57	60
39 to 30	72	61	43
29 to 20	36	36	17
19 to 10	12	11	2
9 to 0	1	2	0
-1 to -10	0	0	0
-11 to -20	0	0	0

APPENDIX C

ARKANSAS REFLECTION CRACKING ANALYSIS AND OVERLAY DESIGN PROGRAM
GUIDE FOR DATA INPUT

This appendix provides the necessary input data instructions for operating the ARKRC-2 program. The user should refer to the User's Manual (Chapter 6) for criteria on the selection of appropriate data.

Two data input forms have been provided. The long form is presented first and is the required form of the first problem of every run. A short form is provided to allow the user to change overlay design characteristics (on successive problems) for a given design section without having to repeatedly input the data that remains constant. Figure C.1 provides an illustration of both the long and short data forms.

It should be noted that "real" variables can be placed anywhere in the available field, but must be punched with a decimal point. Interger numbers, on the other hand, should be right justified in their field and punched without the decimal point. Alphanumeric variables allow the use of any combination of numbers and/or letters in available field.

Input Data Long Form

Card No. 1: Problem Description

IPROB = Problem number, integer, Col. 1-4, right justify.
PRODES = Problem description, alphanumeric, Col. 5-80.

Card No. 2: Existing Concrete Pavement

PVTYPE = Pavement type, alphanumeric, Col. 1-4.
" JCP" - plain jointed concrete pavement.
"JRCP" - jointed reinforced concrete pavement.
"CRCP" - continuously reinforced concrete pavement.
UC = Pavement condition, alphanumeric, Col. 5.
"U" - uncracked.
"C" - cracked.
SPACE = Joint (or crack) spacing (feet), real, Col. 11-20.
THC = Concrete slab thickness (inches), real, Col. 21-30.
EC = Creep modulus of concrete (psi), real, Col. 31-40.
ALFC = Concrete thermal coefficient (in/in/^{o}F), real, Col. 41-50.
DENSC = Concrete density or unit weight (pcf), real, Col. 51-60.
DS = Concrete slab movement at sliding (inches), real, Col. 61-70.

Card No. 3: Existing Pavement Reinforcement.

BARD = Longitudinal bar diameter (inches), real, Col. 11-20.
BARS = Longitudinal bar spacing (inches), real, Col. 21-30.
ES = Steel elastic modulus (psi), real, Col. 31-40.
ALFS = Steel thermal coefficient (in/in/^{o}F), real, Col. 41-50.

Figure C.1. Summary input guide for Arkansas Reflection Cracking Analysis and Design Program, ARKRC-2.

Input Data Long Form (required for first problem of every run):

CARD NUMBER \ COLUMN NUMBER	1–5	10	20	30	40	50	60	70	80
1.	IPROB	PRODES (PROBLEM DESCRIPTION)							
2.	PVTYPE		SPACE	THC	EC	ALFC	DENSC	DS	
3.	REINF		BARD	BARS	ES	ALFS	SMU		
4.	MOVMT CHAR		TH	WH	TL	WL	T1		
5.	OVERLAY		THOV	EOV	EOV	ALFV	DENSOV	OVBS	BBW
6.	INTR LAYER		TH2	E2	ED2	ALF2	DENS2		
7.	TRAFFIC		DTN18						
8.	FREQ DAYS		DAY_1	DAY_2	DAY_3	DAY_4	DAY_5	DAY_6	DAY_7
9.	APS								

Input Data Short Form

1.	SHORT IPROB	EOV	THOV	TH2	BBW	DTN18
2.	APS					

SMU = Steel to concrete bonding stress (psi), real, Col. 51-60.

Card No. 4: Existing Pavement Movement Characterization.

TH = High temperature (°F), real, Col. 11-20.
WH = Joint (crack) width at high temperature (inches), real, Col. 21-30.
TL = Low temperature (°F), real, Col. 31-40.
WL = Joint (crack) width at low temperature (inches), real,Col. 41-50.
T1 = Minimum temperature observed (°F), real, Col. 51-60.

Card No. 5: Asphalt Concrete Overlay Characteristics.

THOV = Overlay thickness (inches), real, Col. 11-20.
EOV = Overlay creep modulus (psi), real, Col. 21-30.
EDV = Overlay dynamic modulus (psi), real, Col. 31-40.
ALFV = Overlay thermal coefficient (in/in/°F), real, Col. 41-50.
DENSOV = Overlay density or unit weight (pcf), real, Col. 51-60.
OVBS = Overlay to concrete surface bond-slip stress (psi), real, Col. 61-70.
BBW = Bond breaker width (feet), real, Col. 71-80.

Card No. 6: Intermediate Layer Characteristics.

TH2 = Intermediate layer thickness (inches), real, Col. 11-20.
E2 = Intermediate layer creep modulus (psi), real, Col. 21-30.
ED2 = Intermediate layer dynamic modulus (psi), real, Col. 31-40.
ALF2 = Intermediate layer thermal coefficient (in/in/°F), real, Col. 41-50.
DENS2 = Intermediate layer density or unit weight (pcf), real, Col. 51-60.

Card No. 7: Design Traffic.

DTN18 = Design 18-kip single axle wheel loads, real, Col. 11-20.

Card No. 8: Yearly Frequency of Minimum Temperatures.

DAY_1 = Average number of days during the year in which the minimum temperature is between 40 and 49°F, real, Col. 11-20.
DAY_2 = Average number of days during the year in which the minimum temperature is between 30 and 39°F, real, Col. 21-30.
DAY_3 = Average number of days during the year in which the minimum temperature is between 20 and 29°F, real, Col. 31-40.
DAY_4 = Average number of days during the year in which the minimum temperature is between 10 and 19°F, real, Col. 41-50.
DAY_5 = Average number of days during the year in which the minimum temperature is between 0 and 9°F, real, Col. 51-60.
DAY_6 = Average number of days during the year in which the minimum temperature is between -10 and -1°F, real, Col. 61-70.

DAY_7 = Average number of days during the year in which the minimum temperature is between -20 and -11°F, real, Col. 71-80.

Card No. 9: Instruction Card.

APS = Instruction code for next problem, alphanumeric, Col. 1-4.
= "ALL " - Use input data long form for next problem.
= "PART" - Use input data short form for next problem.
= "STOP" - No more problems, stop execution.

Input Data Short Form

In cases where only the design variables are being changed, it is not necessary for the user to input all the data for each problem (it is still required for the first problem of each run). This short two-card form may be used to change any one or combination of design variables while keeping the rest of the data from the preceding problem constant.

Card No. 1: Short Form for Design Variables.

IPROB = Problem number, integer, Col. 6-10, right justify.
EOV = Overlay creep modulus (psi), real, Col. 11-20.
THOV = Overlay thickness (inches), real, Col. 21-30.
TH2 = Intermediate layer thickness (inches), real, Col. 31-40.
BBW = Bond breaker width (feet), real, Col 41-50.
DTN18 = Design 18-kip single axle wheel loads, real, Col. 51-60.

Card No. 2: Instruction Card (same as card no. 9 in long form).

APPENDIX D
ASPHALT CONCRETE OVERLAY DESIGN PROCEDURE USING DESIGN CHARTS

This appendix describes the use of a simplified design procedure for asphalt concrete overlays on rigid pavements in Arkansas. Because of its importance, the primary emphasis of the design procedure is the control of overlay reflection cracking.

This procedure is different from that presented in Chapter 6, in that the computerized portion of the process is replaced by design charts and nomographs. These design charts were developed based on a statistical analysis of the computer program (ARKRC-2) and are capable of accurately considering several of the factors and conditions associated with asphalt concrete overlays in the State of Arkansas. They do, however, have their limitations and constraints (beyond those of the ARKRC-2 program) which must be recognized before they can be properly applied. Therefore, in order to allow the user to determine if the design chart procedure is applicable to his conditions, the primary constraints of the nomographs will be discussed first.

CONSTRAINTS OF DESIGN CHART PROCEDURE

1. Figure D.1 provides a map of the State of Arkansas and its five composite climatic regions. The nomographs presented herein are limited to Regions B and D. However, recognizing that Region A has the mildest climate and Region E the most severe, it is possible to conservatively design for Region A (using the Region B design nomographs) and for Region C (using interpolation between the results of the Region B and Region D nomographs).

2. The nomographs are based on a portland cement concrete creep modulus of 3.4×10^6 psi and a thermal coefficient 5.0×10^{-6} psi. Although important, the former is representative of most types of concrete

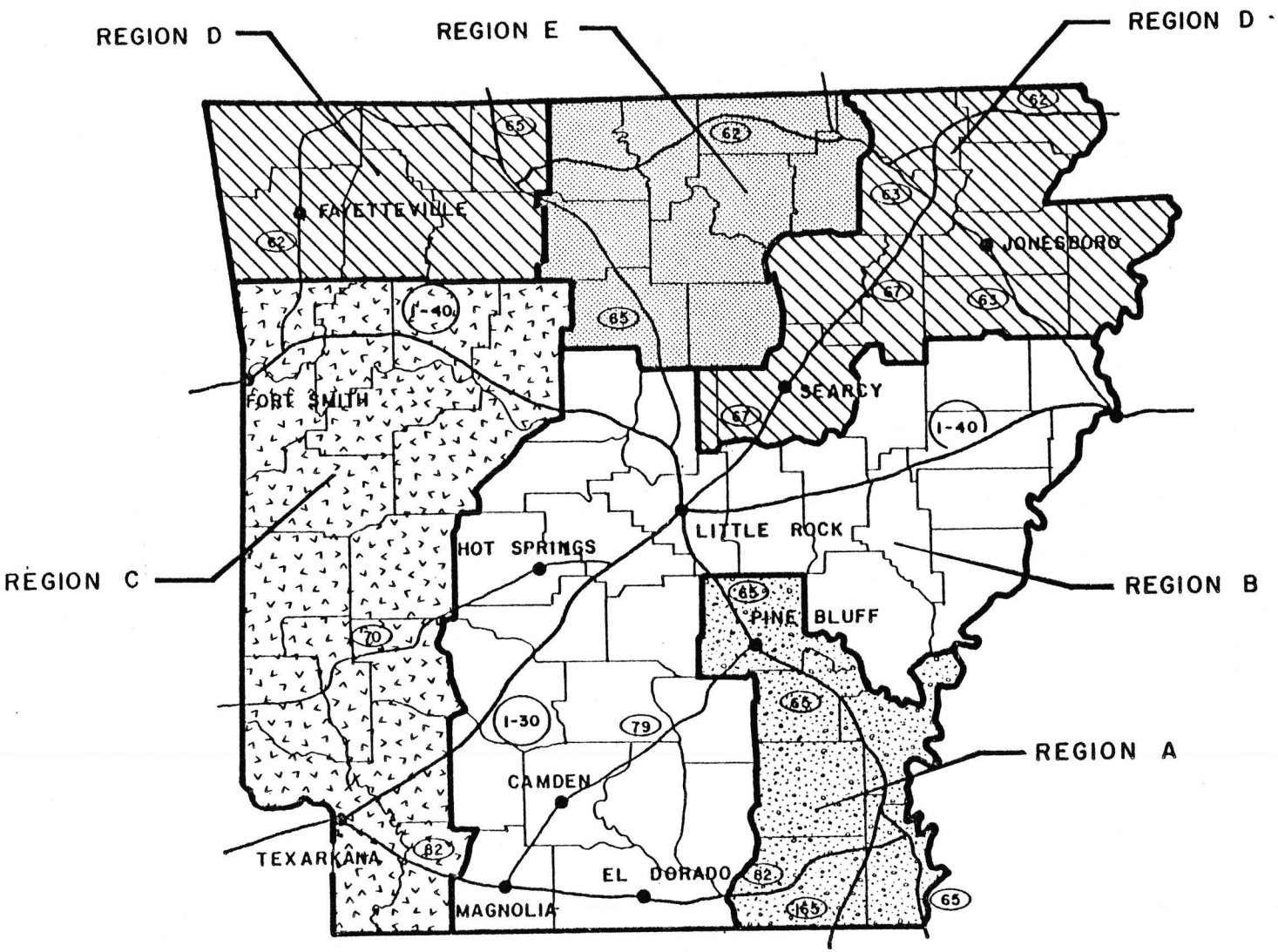

Figure D.1. Five composite Arkans egions.

used in Arkansas and can be assumed for most cases with relatively little error. Thermal coefficient, on the other hand, is more significant and the nomographs can only be accurately applied to concrete which contains a Syenite coarse aggregate. They can, however, be applied conservatively to most Dolomite and limestone coarse aggregates. The nomographs cannot be used for any gravel coarse aggregates or for most sandstones.

3. For CRC pavements, the nomographs apply only to the standard CRCP cross-section used in Arkansas (8-inch slab with No. 5 bars at 6.25-inch centers).

4. For cases where an intermediate layer is used, the nomographs are only applicable to those which have the properties and characteristics of the standard Arkansas Mix open-graded base course (OGBC). It is not conservative to assume that the properties of a denser mix are the same as the standard OGBC.

Although other assumptions were made in order to develop the nomographs and design charts (see Chapter 7), they are less limiting than those presented above.

COLLECTION OF FIELD DATA

In this design procedure, the adequacy of a given overlay strategy to withstand reflection cracking is established based on two types of failure criteria: overlay shear strain and overlay tensile strain. Shear strains are basically the result of the potential for differential vertical movements between adjacent slabs underlying the overlay. Tensile strains, on the other hand, are the result of thermal stresses and horizontal movements of the underlying slab. Because these two types of distress mechanisms are both associated with the existing concrete pavement, it is possible to estimate the amount of influence they will have (on the development of reflection cracking) by making some field measurements of concrete movement prior to overlay placement.

Deflection Measurements

For the case of the vertical shear strain criteria, it is necessary to obtain deflection measurements at several joints (of a JCP or JRCP) or cracks (of a CRCP) in the existing pavement. The required measurements can be obtained easily using the AHTD Dynaflect.

Figure D.2 illustrates the recommended positioning of the Dynaflect and its geophones within the lane and with respect to the joint or crack. Note that the deflection measurements are taken in the outside wheelpath of the outside lane. Note also that the load wheels and geophone no. 1 are located on the upstream side of the joint, while geophone no. 2 must be detached from the mounting bar and placed on the downstream side of the joint, directly across from geophone no. 1. Readings from the other geophones may be recorded, but are not required. Henceforth, the deflections from geophones 1 and 2 (when in this configuration) will be designated as w_ℓ (loaded side) and w_u (unloaded side), respectively.

It is recommended that the deflections be obtained during a period representative of the base support conditions after overlay. In other words, measurements should not be made during spring thaw or after a significant rainfall since the overlay will act as moisture sealant and help improve load transfer conditions during these wet periods. Late spring, summer and autumn are probably the best times to obtain these deflection measurements.

In order to achieve good reliability in the results, it is also important to obtain a good sample of deflection measurements. The number of measurements recommended is dependent upon the spacing between the joints (or cracks) and the possibility of the use of some type of undersealant to improve poor load transfer areas.

For the case of jointed concrete pavements (JCP or JRCP), it is desirable to obtain measurements at every construction joint. This is especially true if an undersealant is being considered, since certain

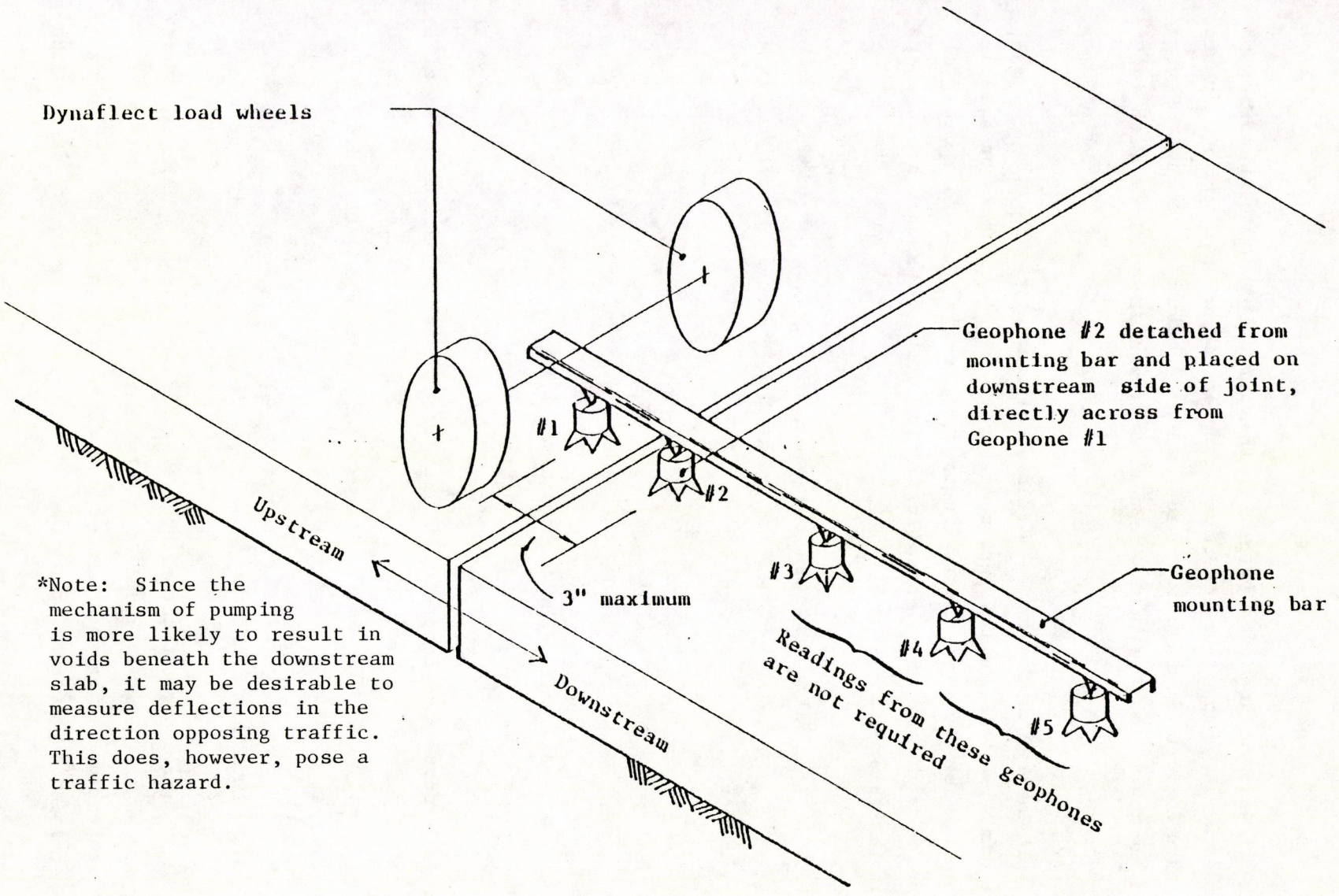

Figure D.2. Required positioning of Dynaflect load wheels and geophones for load transfer deflection measurements.

criteria will be provided later for the selection of which joints to underseal. If an undersealant is not considered and the joint spacing is less than 25 feet, it is probably adequate to obtain measurements at every other joint, so long as there are not any apparent problems with joint pumping.

For the case of continuously reinforced concrete pavements (CRCP), it is recommended that the deflection measurements be obtained for a series of 3 to 5 cracks at approximate 200-foot intervals. 100-foot intervals are recommended if an undersealant is to be considered in areas where pumping is observed.

After the data has been recorded, processing should begin by computing the deflection factor, F_w, for each joint (or crack) using the following equation:

$$F_w = \frac{w_\ell - w_u}{w_\ell + w_u}$$

where:

w_ℓ = deflection on loaded side of joint and

w_u = deflection on unloaded side.

This data reduction is probably best accomplished with the aid of a computer. After the data are reduced, it is then useful to prepare a longitudinal profile plot of F_w versus distance along the roadway for later analysis.

Slab Horizontal Movements

In order to predict the effects of cyclic temperature changes, it is necessary to collect measurements of slab movement as a function of pavement temperature. The recommended procedure for doing this is to install metal reference points on both sides of several joints (or cracks) in the

existing PCC pavement, and then measure the spacing between these points (using a Berry Strain Gauge) over a range of pavement temperature. In order to avoid some of the other external effects, it is recommended that these measurements be obtained at the rate of 5 different temperatures per day (min. 30°F range) for a minimum of 2 consecutive days.

The installation procedure recently used by AHTD to obtain these measurements was to first drill holes on both sides of a joint (crack) and securely glue brass bolts into these holes to act as reference points. The bolts had tiny drilled holes on their heads which functioned as seats for the Berry Strain Gauge. Figure D.3 provides an illustration of the placement of these brass bolts. Note that the bolts should be placed out of the wheelpaths (preferably 12-18 inches from the pavement edge) to minimize wheel load disturbance.

Like the deflection measurements, it is important to obtain a good sample of horizontal movement data from several joints (or cracks) in the existing PCC pavement. Unfortunately, it is not as easy or as safe to obtain horizontal movement data. Consequently, it is up to the user or highway engineer to determine the number of joints (or cracks) which should be measured. It should be recognized, however, that the procedure calls for the joint (crack) movement occurring over a drop in air temperature, and the more locations that are measured, the more likely it is that joints (or cracks) with a high reflection cracking potential will be considered. For continuously reinforced concrete pavements, the measurements must be made in areas which exhibit the average crack spacing for the overlay design section.

Table D.1 provides a sample form for collection of the horizontal movement data from a single joint (crack). The grid at the bottom of the table is provided to allow the user to plot the data after it has been recorded. These plots will be used later as aid in selecting design movement data.

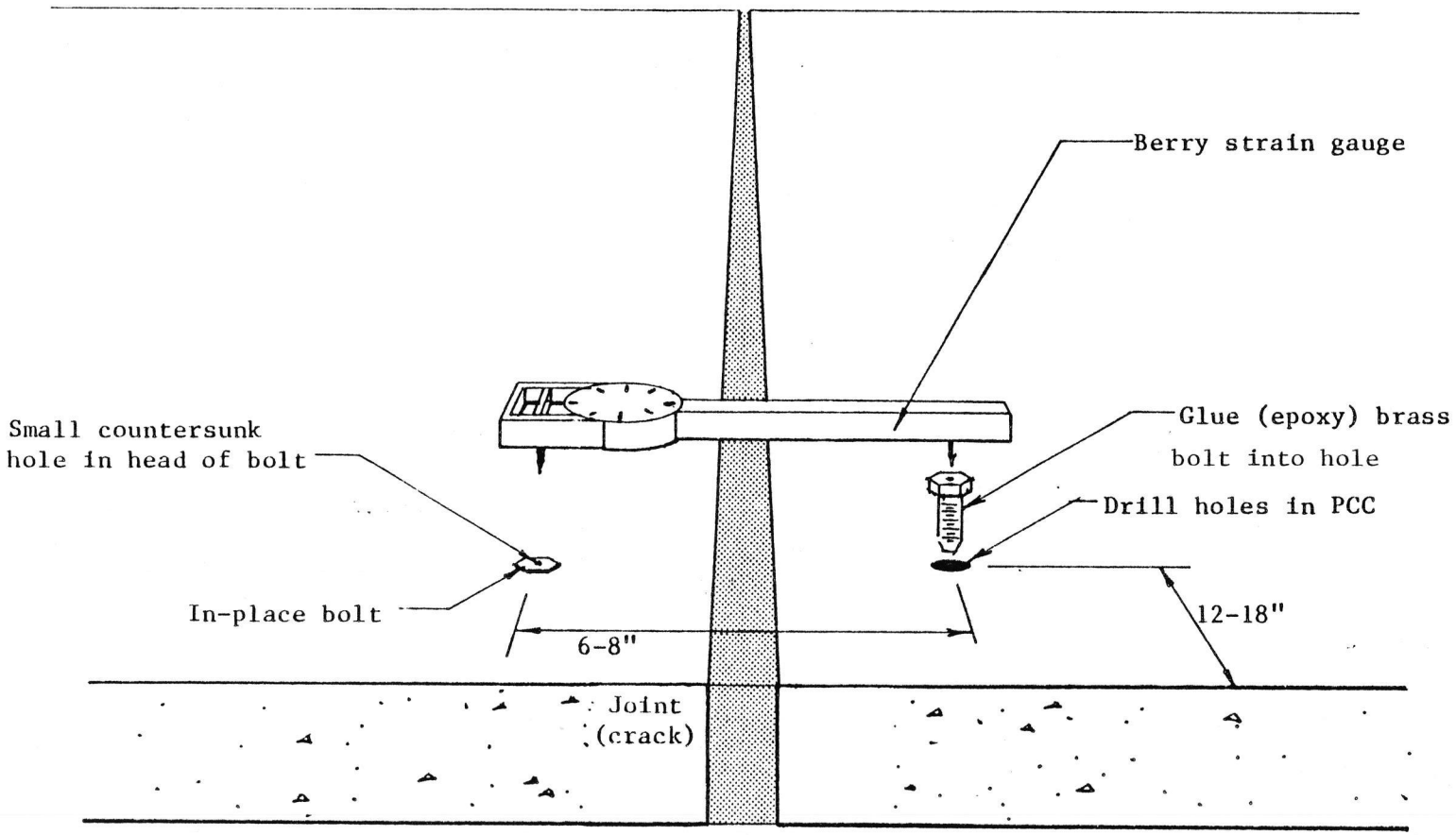

Figure D.3, Placement of brass bolts for measurement of horizontal slab movement.

Table D.1. Sample form for collecting horizontal movement data.

REFLECTION CRACKING ANALYSIS DATA
HORIZONTAL SLAB MOVEMENTS

Project: _____
Location: _____
Joint/crack No. _____ Recorder _____
Slab Lengths: Upstream side _____ Downstream side _____

Measurement Number	Date	Time of Day	Pavement Temperature °F	Joint/Crack Width (inches)
1				
2				
3				
4				
5				
6				
7				
8				
9				
10				
11				
12				
13				
14				
15				

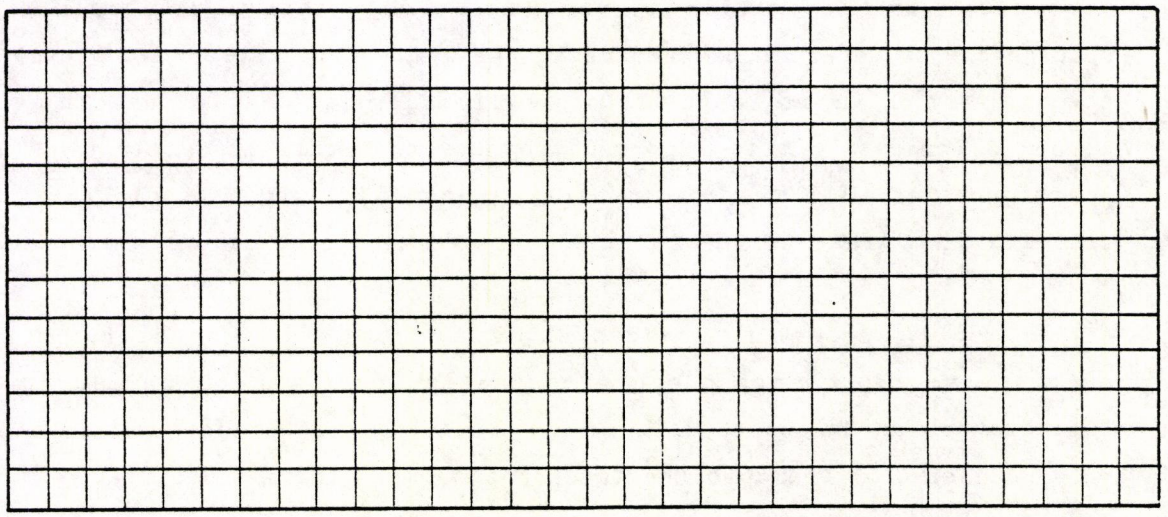

Joint/Crack Width, inches

Pavement Temperature, °F

DATA SELECTION

This section describes, in detail, the selection of appropriate values for the remaining input data required by the design charts. They are named according to their labels used on each nomograph.

1. For each joint (or crack) measured and recorded in the form shown in Table D.1, the user should determine slope, $\Delta C/\Delta T$ of the "best-fit" straight line through the data. Based upon inspection of the slope values for each line, the user should select a data set or series of data sets for use in analyzing the potential for reflection cracking in the section characterized by the data set(s). This means that for some overlay projects, it may be necessary to identify and design different overlay sections. In selecting these sections, the user should recognize that those having the highest slope values will have the greatest potential for reflection cracking (at least from the standpoint of tensile strain). The user should note too, that the slope value is the most important characteristic of the data and that it is not necessary to separate sections which have approximately the same slope but different intercepts. Also, because of the inverse relationship between joint (crack) width and temperature, $\Delta C/\Delta T$ should always have a negative value.

2. SPACE defines the spacing between the joints of a jointed pavement or the average spacing between the cracks of a continuous pavement. If the existing pavement is CRCP, then the average crack spacing can be determined by counting the number of cracks in a section of the highway of known length and then dividing the section length by the number of cracks. It is important to note that this information is used in conjunction with the horizontal movement data which should have been recorded from areas which exhibited the average joint or crack spacing.

3. THOV defines the thickness (in inches) of the asphalt concrete overlay and represents one of the factors that can be varied in the selection of an adequate design for minimizing reflection cracking. THOV should consist of the combined thickness of all binder and surface courses

which are considered to increase the load carrying capacity of the pavement structure. This variable should not include the thickness of any intermediate or strain-absorbing layers (such as an open-graded course).

It is recommended that THOV only be considered a factor in the overlay design if the thermal related tensile strains are predicted to be a probable cause of premature cracking. Although increased overlay thickness is very effective in reducing shear strain, it is recommended that more cost effective methods for improving load transfer, such as undersealing, be considered in reducing excessive overlay shear strains.

4. EDV represents the dynamic modulus of the asphalt concrete overlay to be used in the analysis of overlay shear strain. This value is generally in the range of 400,000 to 800,000 psi for conditions in Arkansas but may be as high as 2,000,000 psi for dense mixes containing stiff asphalts. High values can also be expected for areas which experience sustained cool temperatures.

The recommended procedure for estimating EDV calls for the user to conduct two different laboratory tests on the asphalt bitumen that will be used in the overlay mix. The tests are known as the Ring and Ball Softening Point Test (ASTM D 36) and the Standard Penetration Test (ASTM D 5). The ring and ball softening point temperature, $T_{R\&B}$, the penetration value, PEN, and the penetration test temperature, T, are then used along with Figure D.4 to estimate the asphalt penetration index, PI.

Next, it is necessary to determine the stiffness of the asphalt bitumen at the design temperature, T_{DES}, corresponding to the average year round temperature at the project location. The stiffness modulus of the asphalt bitumen, S_{ac}, can then be determined with the aid of the Heukelom and Klomp nomograph presented in Figure D.5. A loading time of 1 second is recommended in estimating S_{ac}.

The last step of the alternative method is to estimate the overlay dynamic modulus, EDV, as the stiffness modulus of the asphalt mix, S_{mix},

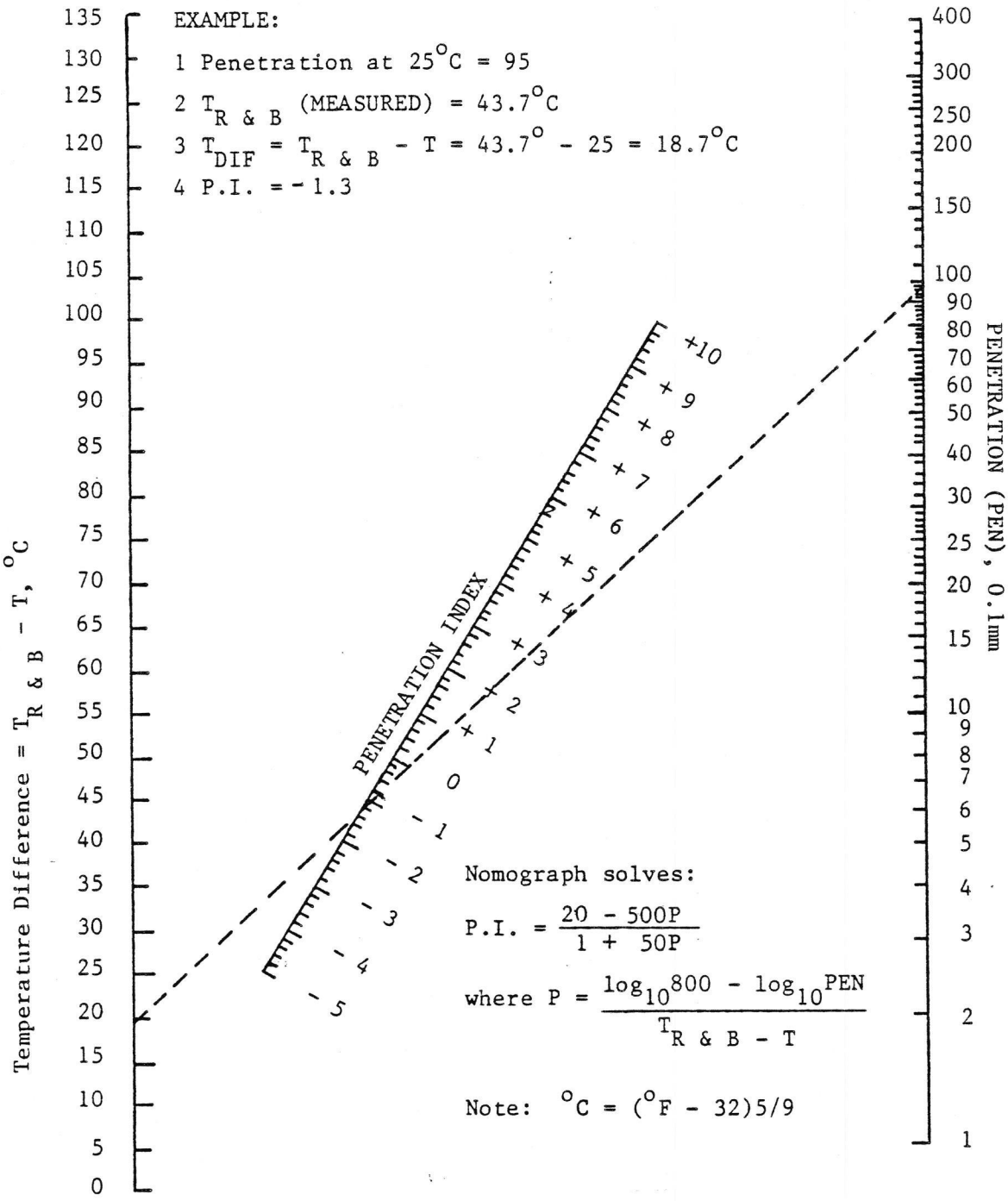

Figure D.4. Nonomgraph for determining Pfeiffer and Van Dorrmaal's Penetration Index (Ref. 70).

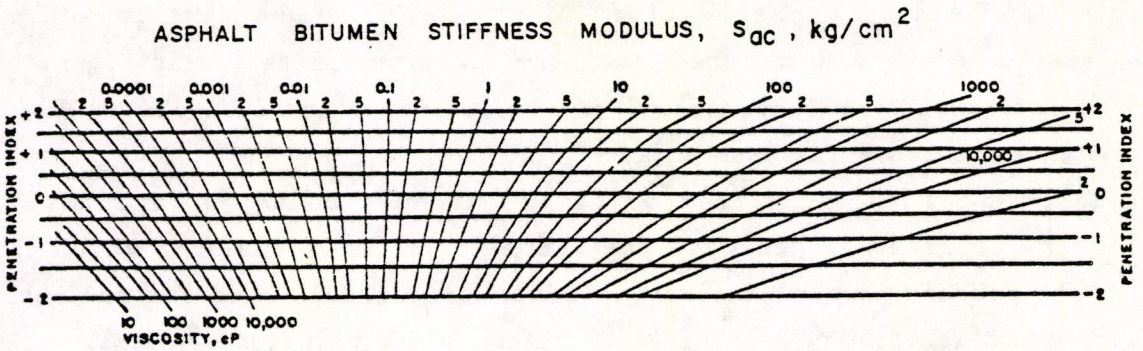

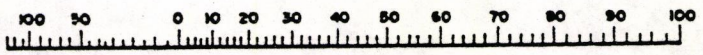

1 psi = 14.223 kg/cm^2

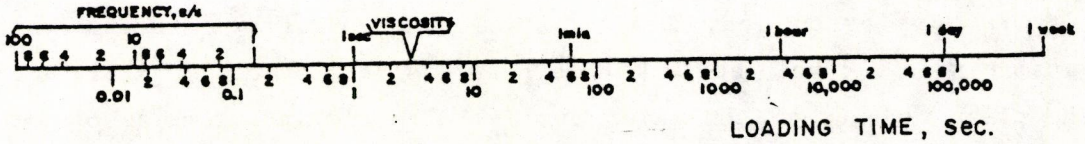

Figure D.5. Nomograph for predicting the stiffness modulus of asphaltic bitumens, after Heukelom and Klomp (Ref. 70).

under the same asphalt bitumen loading time and temperature conditions. This can be done by estimating C_v, the volume concentration of the aggregate in the mix and then using the nomograph presented in Figure D.6. Note that to use this nomograph, the units of S_{ac} (estimated from Figure D.5) must be converted from kg/cm^2 to psi by multiplying by 14.223. Also note that percentage of air voids was assumed to be approximately 3 percent in order to generate the curves. If the actual air voids that will be present in the mix is significantly greater, then the following correction factor may be applied to determine an adjusted C_v value:

$$C_v \text{ (new)} = \frac{C_v}{1 + H}$$

where:

H = actual fraction of air voids in the mix minus 0.03.

The new C_v value can then be used in the same nomograph presented in Figure D.6.

5. TH2 is the variable which defines the thickness (in inches) of the intermediate layer that will be placed prior to overlay (TH2 equals zero if no intermediate layer). An intermediate layer represents a material of certain thickness placed prior to overlay to help minimize reflection cracking brought about by underlying slab movements. The layer is different from a bond breaker layer in that it is designed to internally absorb some of the underlying slab movements before they reach the overlay layers. It is not very effective in reducing reflection cracking brought about by poor load transfer across joints or cracks.

In this procedure, TH2 can have a large effect on the critical tensile strain developed in the asphalt concrete overlay, particularly if the creep modulus of the layer is low. The strain-absorbing open-graded course used in Arkansas is such a material, but it does have its thickness limits. It can not be less than 3 inches since some of the aggregate particles are as large as 2 1/2 inches. Also, because of possible rutting

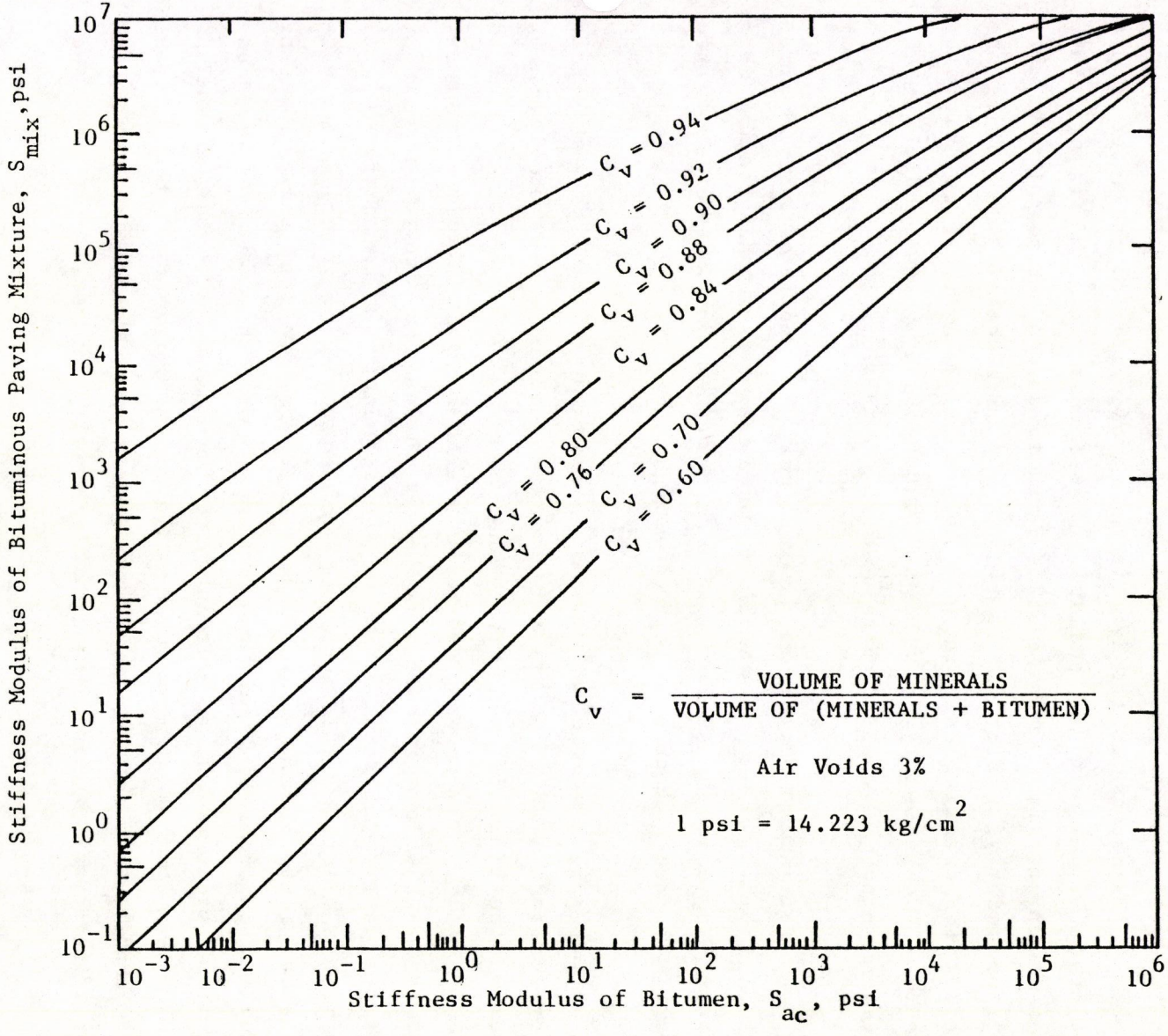

Figure D.6. Relationships between moduli of stiffnes of asphalt cements and paving mixtures containing the same asphalt cements (Based on Hukelom and Klomp) (Ref. 70).

and compaction problems, the open-graded course thickness should not be greater than 5 or 6 inches. Consequently, if the user intends to use some other type of intermediate layer, care should be taken to insure that its possible thickness limits are considered.

6. ED2 represents the dynamic modulus (in psi) of the intermediate layer to be used in the analysis of vertical shear strain criteria. Because an intermediate layer is designed to absorb horizontal movements of the underlying slab, it is relatively ineffective in reducing the reflection cracking associated with poor load transfer at joints or cracks. Consequently, a value of 20,000 psi is recommended for the standard open-graded base course used in Arkansas.

For an intermediate layer material which is capable of carrying shear strains (i.e., materials which have much fewer voids than the Arkansas open-grade course), however, it is recommended that ED2 be determined using the same procedure as that recommended for EDV.

7. DTN18 represents the design 18-kip equivalent single axle load applications (ESAL) before the overlay reaches a certain level of reflection cracking inherent in the vertical shear strain criteria. Consequently, it is recommended that the user estimate DTN18 as the number of 18-kip ESAL that can be expected in the design lane in the overlay direction for the design period. Subsequently, the nomographs will provide a critical deflection factor which can be used in conjunction with the deflection factor plots (discussed in the previous section on the Collection of Field Data) to determine which joints (cracks) have load transfer problems. Based on this, it is recommended that the user design the overlay for the horizontal tensile strain criteria and then improve the condition of the poor performing joints (cracks) by undersealing them or if necessary, by providing increased overlay thickness.

USE OF DESIGN CHARTS

After all the data have been obtained, the following simple design chart procedure may be used to arrive at a suitable overlay design alternative.

1. Select the appropriate nomograph from Figures D.7 through D.10 for the pavement type and Arkansas region considered.

2. Using the chosen nomograph, try different overlay and intermediate layer thickness combinations (THOV and TH2) until an optimum design alternative (for tensile strain criteria) is reached.

3. With the overlay dynamic modulus, EDV, and the design traffic, DTN18, use Figure D.11 to estimate the allowable overlay shear strain.

4. With the trial design (from tensile strain criteria), use the allowable overlay shear strain to determine the allowable deflection factor from Figure D.12.

5. Draw a horizontal line on the longitudinal plot of deflection factor indicating the level of the allowable deflection factor (as illustrated in Figure D.13). If inspection shows that a point or series of points exceeds the allowable deflection factor, then it is necessary to either underseal those joints or use an increased overlay thickness. The design for the latter may be accomplished by re-using Figure D.12 with various increased levels of overlay thickness, THOV.

Design for Different Levels of Reflection Cracking

If the user is interested in estimating when different levels of reflection cracking will be reached (based on tensile strain criteria), the following procedure may be applied:

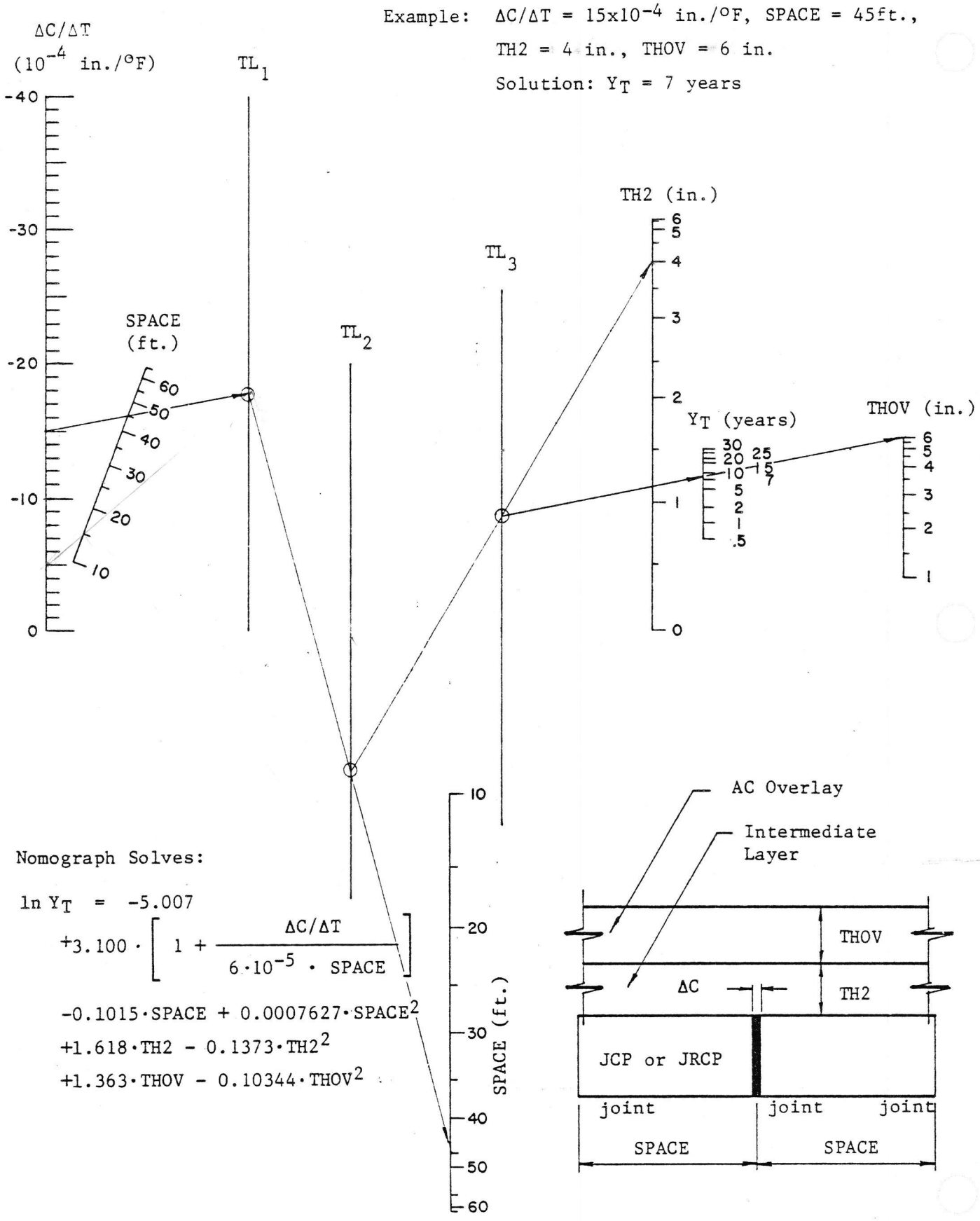

Figure D.7. Asphalt concrete overlay design nomograph for jointed pavements in Arkansas Region B. (Caution: Be aware of restrictions on use of this nomograph.)

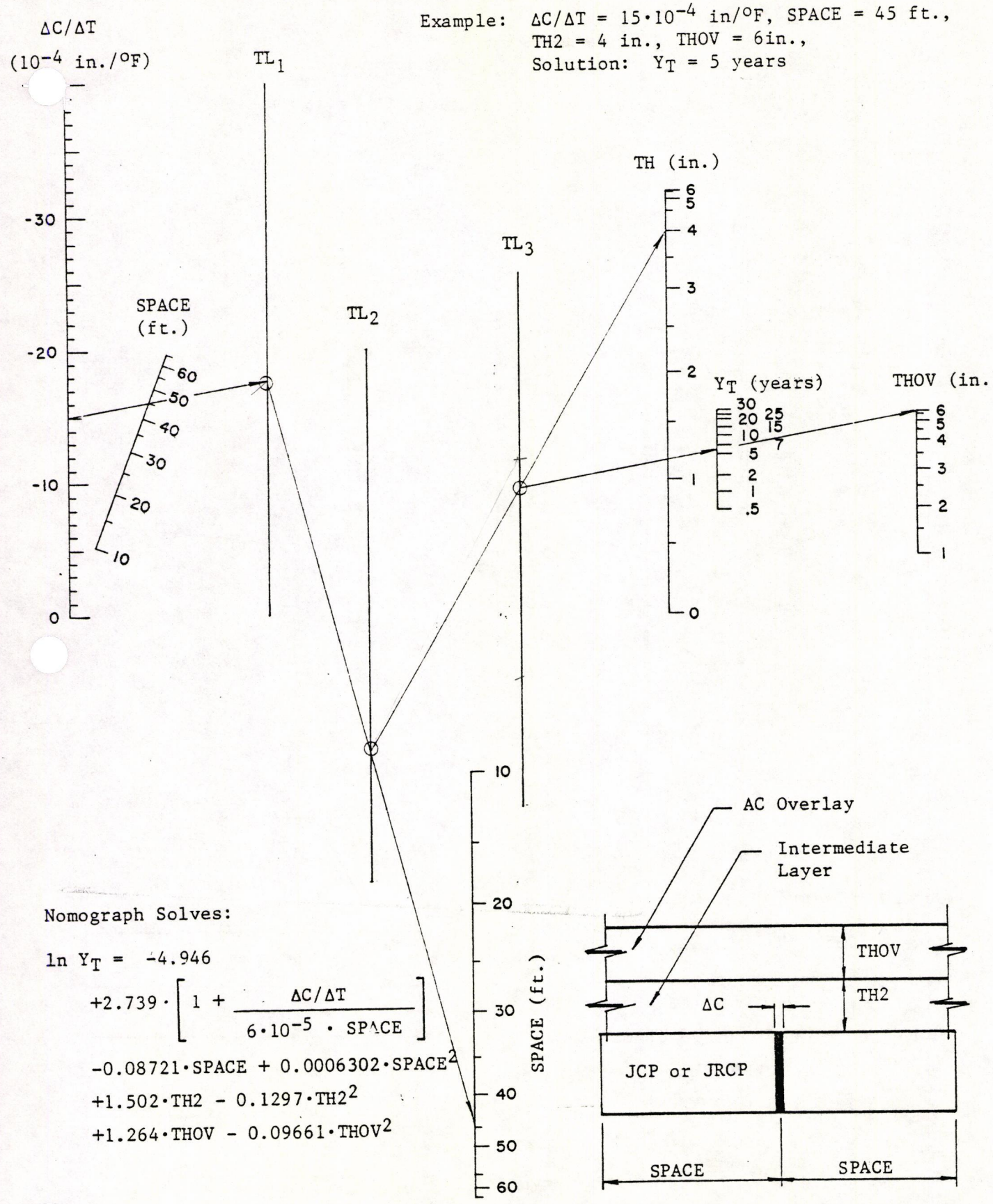

Figure D.8. Asphalt concrete overlay design nomograph for jointed pavements in Arkansas Region D. (Caution: Be aware of restrictions on use of this nomograph.)

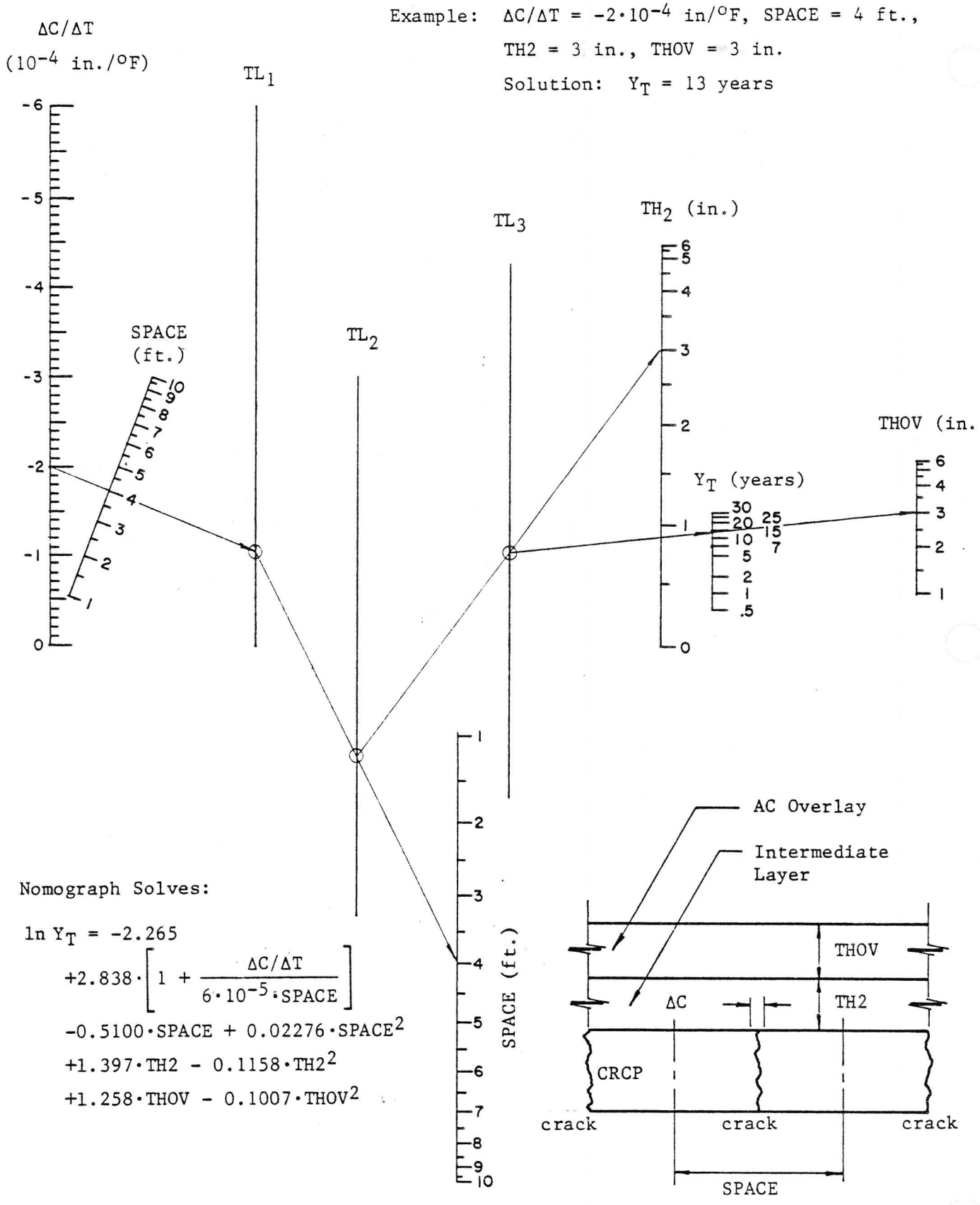

Figure D.9. Asphalt concrete overlay design nomograph for CRC pavements in Arkansas Region B. (Caution: Be aware of restrictions on use of this nomograph.)

Example: $\Delta C/\Delta T = -2 \cdot 10^{-4}$ in./°F, SPACE = 4 ft.,
TH2 = 3 in., THOV = 3 in.
Solution: Y_T = 7 years

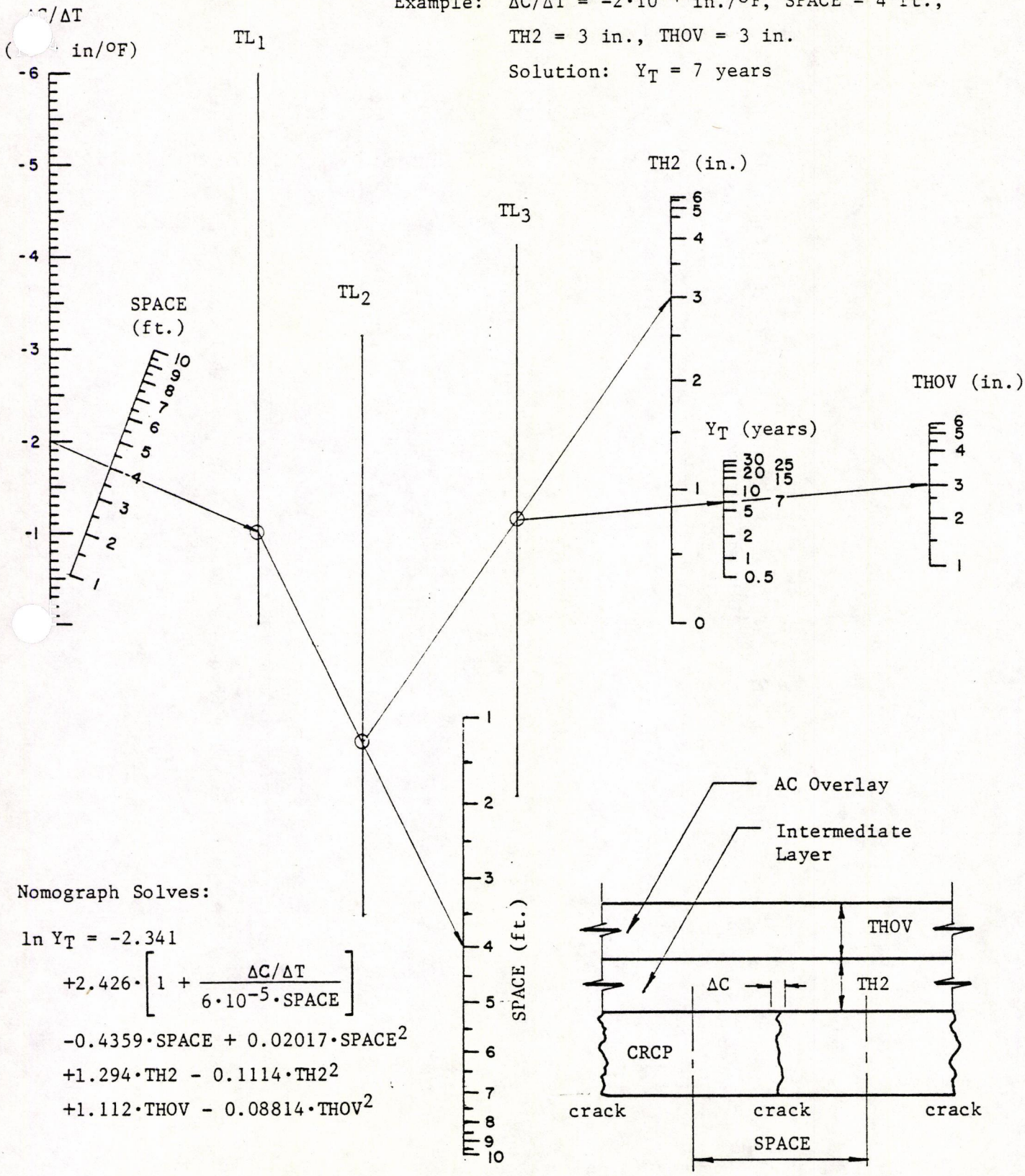

Nomograph Solves:

$$\ln Y_T = -2.341 + 2.426 \cdot \left[1 + \frac{\Delta C/\Delta T}{6 \cdot 10^{-5} \cdot SPACE}\right] - 0.4359 \cdot SPACE + 0.02017 \cdot SPACE^2 + 1.294 \cdot TH2 - 0.1114 \cdot TH2^2 + 1.112 \cdot THOV - 0.08814 \cdot THOV^2$$

Figure D.10. Asphalt concrete overlay design nomograph for CRC pavements in Arkansas Region D. (Caution: Be aware of restrictions on use of this nomograph.)

EXAMPLE: DTN18 = $10 \cdot 10^6$ applications
EDV = 614,000 psi
solution: $\gamma_{OV} = 1.73 \cdot 10^{-4}$ in/in

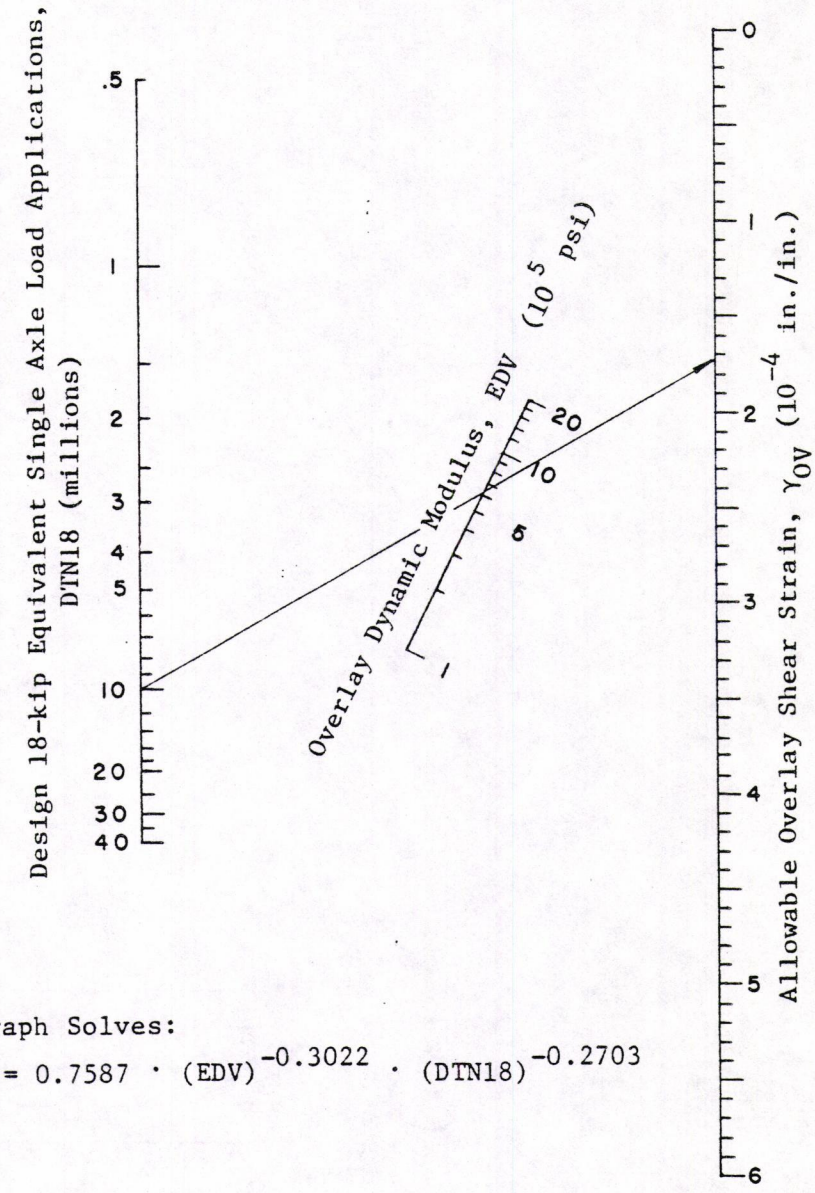

Nomograph Solves:

$$\gamma_{OV} = 0.7587 \cdot (EDV)^{-0.3022} \cdot (DTN18)^{-0.2703}$$

Figure D.11. Nomograph for estimating allowable overlay shear strain.

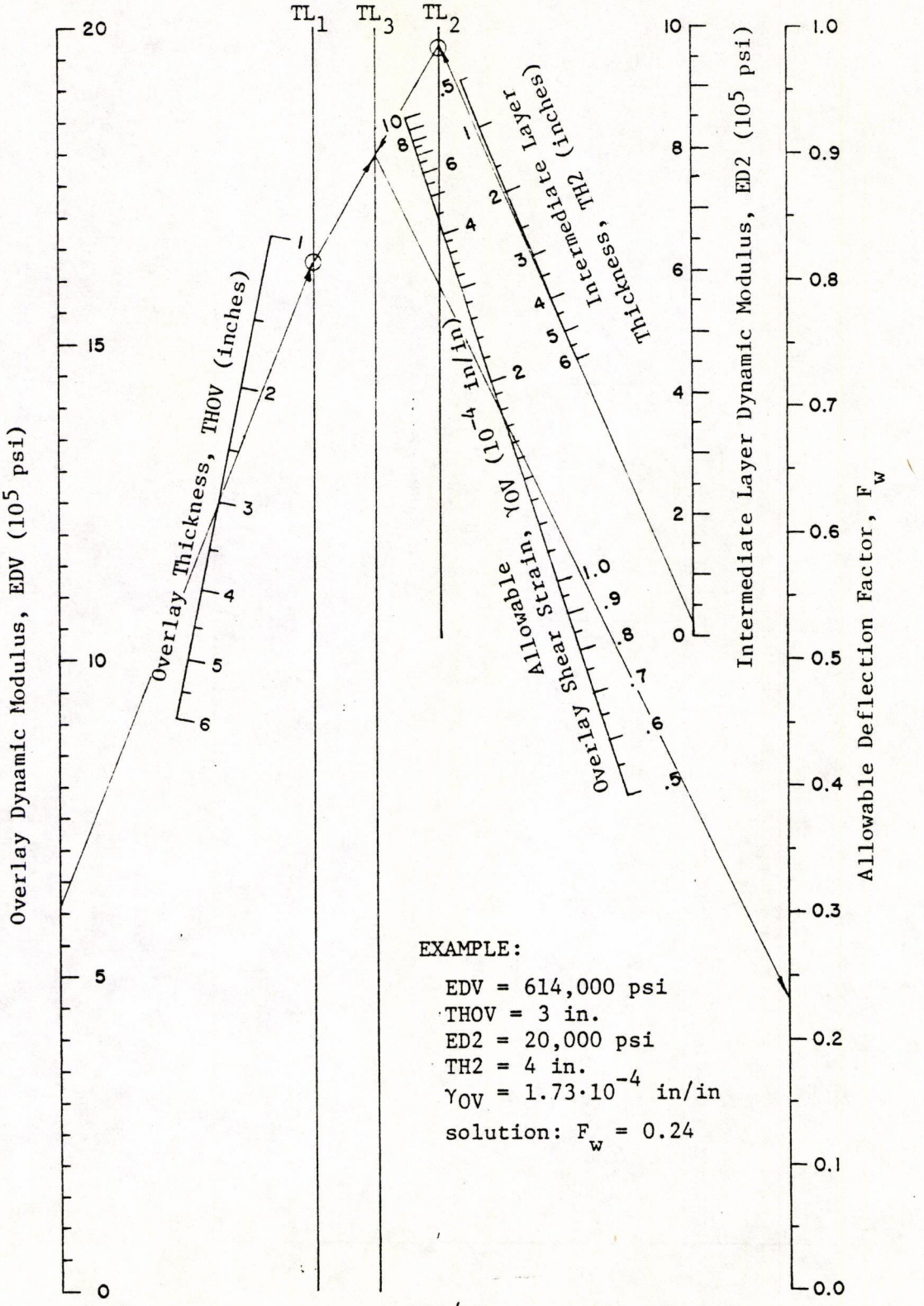

Figure D. 12. Nomograph for determining allowable deflection factor.

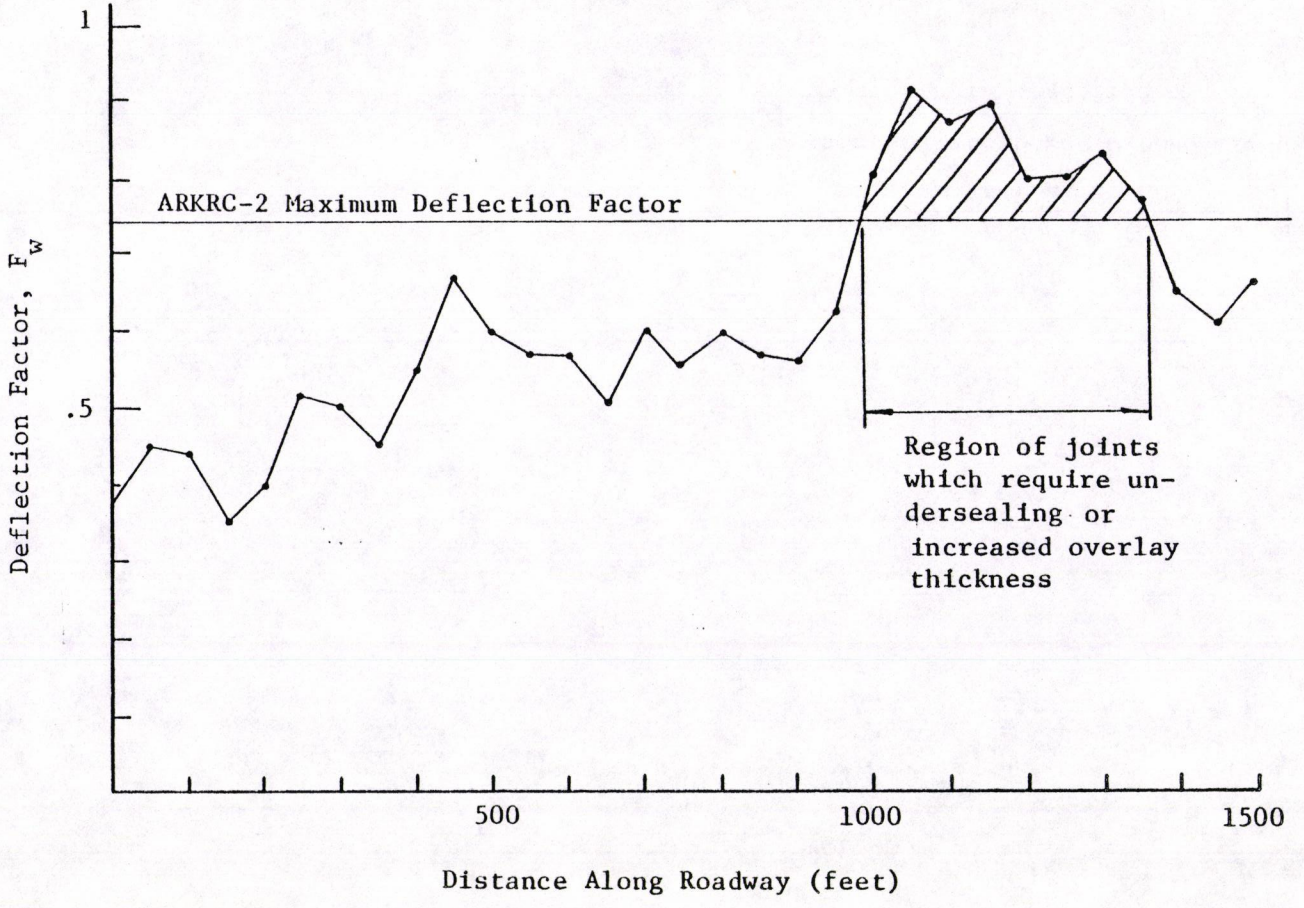

Figure D.13. Graph of field deflection factors for 50-foot JCP illustrating application of ARKRC-2 maximum deflection factor in detecting joints which will cause premature reflection cracking in the overlay design considered.

1. Select the level of reflection cracking considered as a limit. This will range anywhere from 5 to 99 percent.

2. Use Table D.2 to determine the z-value corresponding to the selected reflection cracking level.

3. Solve for the number of years, Y, corresponding to the desired level of reflection cracking, using the following formula:

$$Y = 1.585^{z} \times Y_{50}$$

where:

Y_{50} = number of years before 50 percent reflection cracking is reached (as determined from nomographs).

It should be pointed out that the accuracy of this prediction is decreased for very high or very low levels of reflection cracking.

Table D. 2. z-values corresponding to different levels of reflection cracking.

Percent Reflection Cracking	z-values
1	-2.330
5	-1.645
10	-1.282
15	-1.037
20	-0.841
25	-0.674
30	-0.524
35	-0.385
40	-0.253
45	-0.126
50	0.000
55	0.126
60	0.253
65	0.385
70	0.524
75	0.674
80	0.841
85	1.037
90	1.282
95	1.645
99	2.330

APPENDIX E

ARKRC-2 PROGRAM LISTING

```
      PROGRAM ARKRC2 (INPUT, OUTPUT, TAPE8=INPUT, TAPE2=OUTPUT)
CCC
C     ARKRC - ARKANSAS REFLECTION CRACKING ANALYSIS AND OVERLAY
C             DESIGN PROGRAM - VERSION 2.0 - NOVEMBER 1981
C
C     AUSTIN RESEARCH ENGINEERS, INC.
C     UNIVERSITY OF ARKANSAS
C     ARKANSAS STATE HIGHWAY AND TRANSPORTATION DEPARTMENT
C
      COMMON /ALPHA/ IPROB, PRODES(19), PVTYPE(2), OVTYPE(2), OVRTYP(3)
      COMMON /APS/ APS
      COMMON /CHAR/ EC,THC,DENSC,ALFC,ES,AS,SSIG,SMU,ALFS,BARD,BARS,
     1              E2,TH2,DENS2,ALF2,EOV,THOV,DENSOV,ALFV,OVBS,
     2              ER,AR,ALFR
      COMMON /DESN/ XBB, T1, NTMP, DTC(7), DTV(7), DT2(7), DAY(7)
      COMMON /NUMBER/ EAC,EAS,EA2,EAV,EAR,DTOBS,DTONE,DCOBS,SIGMU,FAC,XL
      COMMON /OBS/ SPACE, ICRAK, WH, WL, TH, TL, DS, IFSLP
      COMMON /OUT1/ BP, AP, XM, XS, STLSB, CSB
      COMMON /OUT2/ BU, AV1, BB, AV2
      COMMON /VERT/ DLOAD,WLOAD,EDV,ED2,EDR,DTN18,OVMU,TWOMU,RFMU
      COMMON / BB / BBW
      COMMON / IO / IN, IOUT
      DATA STOP / 4HSTOP /
    1 CALL RCIN
      CALL PRIVCR
      IF (AS .GT. 0.) GO TO 2
      CALL CHARJ
      GO TO 3
    2 CALL CHARC
    3 CONTINUE
      IFLAG = 0
      CALL BNDOV (IFLAG)
      IF (IFLAG .EQ. 0) GO TO 6
      IF (IFLAG .GT. 0) WRITE(IOUT,60) IFLAG
   60 FORMAT (/5X,35HBNDOV FAILED TO CONVERGE IN SECTION,I3
     1 /5X,27HPROCEEDING TO NEXT PROBLEM.)
      IF (APS .EQ. STOP) GO TO 99
      GO TO 1
    6 CONTINUE
    8 CALL VERTM
      CALL OVLIFE
      CALL RCOUT
      IF (APS .EQ. STOP) GO TO 99
      GO TO 1
   99 STOP
      END
      BLOCK DATA
      COMMON /ALPHA/ IPROB, PRODES(19), PVTYPE(2), OVTYPE(2), OVRTYP(3)
      COMMON /APS/ APS
      COMMON / IO / IN, IOUT
      COMMON /CONST/ CON(10)
      COMMON /OBS/ SPACE, ICRAK, WH, WL, TH, TL, DS, IFSLP
      COMMON /VERT/ DLOAD,WLOAD,EDV,ED2,EDR,DTN18,OVMU,TWOMU,RFMU
      COMMON /DESN/ XBB, T1, NTMP, DTC(7), DTV(7), DT2(7), DAY(7)
```

```
      COMMON /FATCON/ A1, A2, B1, B2
      DATA IPROB / 0 /
      DATA APS / 4HALL  /
      DATA CON / 12., 9*0. /
      DATA DTC /  5., 15., 25., 35., 45., 55., 65. /
      DATA DTV /  5., 15., 25., 35., 45., 55., 65. /
      DATA DT2 /  5., 15., 25., 35., 45., 55., 65. /
      DATA DAY /  7*0. /
      DATA ICRAK, SPACE / 0, 0. /
      DATA DLOAD, WLOAD / 9000., 25. /
      DATA OVMU, TWOMU, RFMU / 0.30, 0.35, 0.25 /
      DATA A1,A2,B1,B2 / 1., -3.70, 1., -0.2703 /
      DATA PRODES /19*1H /, PVTYPE, OVTYPE /4*1H /
      DATA OVRTYP /3*1H /
      DATA IN, IOUT / 8, 2 /
      END
      SUBROUTINE RCIN
CC
C     RCIN - REFLECTION CRACKING INPUT ROUTINE
C
      COMMON /ALPHA/ IPROB, PRODES(19), PVTYPE(2), OVTYPE(2), OVRTYP(3)
      COMMON /APS/ APS
      COMMON /CHAR/ EC,THC,DENSC,ALFC,ES,AS,SSIG,SMU,ALFS,BARD,BARS,
     1              E2,TH2,DENS2,ALF2,EOV,THOV,DENSOV,ALFV,OVBS,
     2              ER,AR,ALFR
      COMMON /CONST/ CON(10)
      COMMON /DESN/ XBB, T1, NTMP, DTC(7), DTV(7), DT2(7), DAY(7)
      COMMON /NUMBER/ EAC,EAS,EA2,EAV,EAR,DTOBS,DTONE,DCOBS,SIGMU,FAC,XL
      COMMON /OBS/ SPACE, ICRAK, WH, WL, TH, TL, DS, IFSLP
      COMMON /VERT/ DLOAD,WLOAD,EDV,ED2,EDR,DTN18,OVMU,TWOMU,RFMU
      COMMON /FATCON/ A1, A2, B1, B2
      COMMON / BB / BBW
      COMMON / IO / IN, IOUT
      DATA PART / 4HPART /
      DATA U / 1HU /
C
C     STATEMENT FUNCTION FOR ESTIMATING FATIGUE EQUATION INTERCEPT
      COEF1( E ) = 8.072E-4 * ( E )**(-1.118)
C ***
C     CHECK  FOR LONG OR SHORT FORM OF DATA, MUST BE LONG FOR
C     FIRST PROBLEM
      IF (APS .EQ. PART) GO TO 80
C
C     LONG FORM
C
C     READ PROBLEM NO. AND DESCRIPTION
      READ (IN,100) IPROB, PRODES
100   FORMAT(I4,19A4)
C
C     READ PAVEMENT TYPE, MODULUS, U/C, JOINT/CRACK SPACING, SLAB
C     THICKNESS, CREEP MODULUS, DENSITY AND MOVEMENT AT SLIDING
      READ(IN,110) PVTYPE(1),UC,SPACE,THC,EC,ALFC,DENSC,DS
110   FORMAT(   A4,A1,5X,6F10.0)
C     ICRAK = 1  CRACKED PAVEMENT
C     ICRAK = 2  JOINTED OR UNCRACKED PAVEMENT
```

```
      ICRAK = 1
      IF (UC .EQ. U)  ICRAK=2
C
C     READ BAR DIAMETER, BAR SPACING, ELASTIC MODULUS, THERMAL COEF.
C     OF STEEL REINF. AND MAX. STEEL TO CONCRETE BONDING STRESS
      READ(IN,120) BARD, BARS, ES, ALFS, SMU
120   FORMAT(   10X,5F10.0)
      IF (ES .LE. 0.) ES=30000000.
C     CALCULATE AREA AND PERIMETER OF STEEL PER FOOT WIDTH
      AS = 0.
      SSIG = 0.
      IF (BARS .LE. 0.) GO TO 30
      AS = 9.425*(BARD**2)/BARS
      SSIG = 37.699*BARD/BARS
   30 CONTINUE
C
C     READ MOVEMENT CHARACTERISTICS OF ORIGINAL PAVEMENT, HI TEMP.,
C     HIGH TEMP. JOINT WIDTH, LO TEMP. AND LOWEST TEMPERATURE OBSERVED
      READ (IN,130) TH,WH,TL,WL,T1
130   FORMAT(   10X,7F10.0)
C
C     READ OVERLAY TYPE, THICKNESS, CREEP MODULUS, DYNAMIC MODULUS,
C     DENSITY, MAX. BONDING STRESS AND BOND BREAKER WIDTH
      READ(IN,150) THOV,EOV,EDV,ALFV,DENSOV,OVBS,BBW
150   FORMAT (   10X,7F10.0)
C
C     OVERLAY REINFORCEMENT NOT USED IN ARKANSAS (DO NOT READ)
C
      ER = 0.0
      ALFR = 0.0
      AR = 0.0
C     READ OVERLAY REINFORCEMENT PROPERTIES (TYPE, ELASTIC MODULUS,
C     THERMAL COEFF., AREA, ALLOWABLE STRAIN)
C     READ(IN,160) OVRTYP,ER,ALFR,AR
C 160 FORMAT(   2A4,A2,4F10.0)
C
C     READ INTERMEDIATE LAYER THICKNESS, CREEP MODULUS, DYNAMIC
C     MODULUS, THERMAL COEF. AND DENSITY
      READ(IN,180) TH2,E2,ED2,ALF2,DENS2,SLPSW
180   FORMAT(   10X,7F10.0)
      IFSLP = 1
      IF (SLPSW .GT. 0.) IFSLP = 0
C
C     READ 18-KIP ESAL DESIGN TRAFFIC
      READ(IN,180) DTN18
C
C     READ YEARLY FREQUENCY OF MINIMUM DAILY TEMPERATURES
      READ (IN,180) DAY
      DO 60 I=2,7
      NTMP = I-1
      IF (DAY(I) .LE. 0.) GO TO 70
   60 CONTINUE
      NTMP = 7
   70 CONTINUE
190   FORMAT(1X,10X,7F10.0)
```

```
C     PROGRAM CALCULATIONS
      XL = 0.5*SPACE*CON(1)
      XBB = BBW*CON(1)*0.5
      IF (XBB .GT. XL) XBB=XL
      DCOBS = 0.5*(WL-WH)
      DTOBS = TH-TL
      SIGMU = SMU*SSIG
      DTONE = TH-T1
      EAC = EC*THC*CON(1)
      EAV = EOV*THOV*CON(1)
      EA2 = E2*TH2*CON(1)
      EAR = ER*AR
      EAS = ES*AS
      EDR = ER
      GO TO 90
C
C     DATA SHORT FORM
C
C     READ  PROBLEM NO., OVERLAY CREEP MODULUS, OVERLAY THICKNESS,
C     INTERMEDIATE LAYER THICKNESS, BOND BREAKER WIDTH AND DESIGN
C     TRAFFIC
   80 READ(IN,200) IPROB,EOV,THOV,TH2,BBW,DTN18
200   FORMAT(   5X,I5,7F10.0)
      XBB = BBW*CON(1)*0.5
      IF (XBB .GT. XL) XBB=XL
      EAV = EOV*THOV*CON(1)
   90 CONTINUE
C     ESTIMATE FATIGUE EQUATION INTERCEPTS
      A1 = COEF1( EOV )
      B1 = 4.*(1.+OVMU) * (COEF1( EDV ))**(-B2)
C     ESTIMATE FACTOR FOR INCREASING FRICTION CURVE SLOPE AFTER OVERLAY
      FAC = 1. + (DENSOV*THOV + DENS2*TH2)/(DENSC*THC)
C
C     READ ALL/PART/STOP FOR NEXT PROBLEM
      READ (IN,300) APS
300   FORMAT(   A4)
      RETURN
      END
      SUBROUTINE PRIVCR
CC
C     PRIVCR - PRINT INPUT VARIABLES FOR REFLECTION CRACKING PROGRAM
C
      DIMENSION CRAK(2),CRJT(2,2)
      COMMON /ALPHA/ IPROB, PRODES(19), PVTYPE(2), OVTYPE(2), OVRTYP(3)
      COMMON /CHAR/ EC,THC,DENSC,ALFC,ES,AS,SSIG,SMU,ALFS,BARD,BARS,
     1              E2,TH2,DENS2,ALF2,EOV,THOV,DENSOV,ALFV,OVBS,
     2              ER,AR,ALFR
      COMMON /DESN/ XBB, T1, NTMP, DTC(7), DTV(7), DT2(7), DAY(7)
      COMMON /OBS/ SPACE, ICRAK, WH, WL, TH, TL, DS, IFSLP
      COMMON /VERT/ DLOAD,WLOAD,EDV,ED2,EDR,DTN18,OVMU,TWOMU,RFMU
      COMMON / BB / BBW
      COMMON / IO / IN, IOUT
      DATA CRAK / 2H  ,2HUN /
      DATA CRJT / 4HCRAC,1HK,
     1            4HJOIN,1HT /
```

```
      DATA ISW / 0 /
C
C     WRITE COVER PAGE ON FIRST CALL TO PRIVCR ONLY
C
      IF (ISW.NE.0) GO TO 10
      IF (IPROB .LT. 0) GO TO 10
      WRITE(IOUT,900)
  900 FORMAT(1H1/////////////////
     0   21X,37HARKANSAS REFLECTION CRACKING ANALYSIS
     1  /21X,31H     AND OVERLAY DESIGN PROGRAM//////
     2  /18X,43H   A     RRRRR    K     K  RRRRR      CCCC
     3  /18X,43H  A A    R    R   K    K   R    R    C    C
     4  /18X,43H A   A   R     R  K  K     R     R  C
     5  /18X,43HA     A  R    R   K K      R    R   C
     6  /18X,43HAAAAAAAA RRRRR    KK K     RRRRR    C
     7  /18X,43HA     A  R   R    K   K    R   R    C
     8  /18X,43HA     A  R    R   K    K   R    R    C    C
     9  /18X,43HA     A  R     R  K     K  R     R    CCCC
     1  ///////34X,11HVERSION 2.0
     2  /33X,13HNOVEMBER 1981
     3  ///24X,31HAUSTIN RESEARCH ENGINEERS, INC.
     4  /28X,22HUNIVERSITY OF ARKANSAS
     5  /14X,52HARKANSAS STATE HIGHWAY AND TRANSPORTATION DEPARTMENT )
      ISW = 1
C
   10 WRITE (IOUT,1000)
 1000 FORMAT (1H1///5X,
     1  57HARKRC - ARKANSAS REFLECTION CRACKING ANALYSIS AND OVERLAY/5X,
     2  52H        DESIGN PROGRAM - VERSION 2.0 - NOVEMBER 1981 )
C
      WRITE (IOUT,1010) IPROB,PRODES
 1010 FORMAT (/5X,8HPROBLEM ,I3,12H DESCRIPTION,39X,6HPAGE 1
     1  /5X,19A4/
     2  /33X,19(1H*)/33X,19H* INPUT VARIABLES */33X,19(1H*) )
C
      WRITE(IOUT,1020) PVTYPE(1), CRAK(ICRAK), (CRJT(J,ICRAK),J=1,2),
     1  SPACE, THC, EC, ALFC, DENSC, DS
 1020 FORMAT(/9X,26HEXISTING CONCRETE PAVEMENT
     1  /15X,4HTYPE,50X,A4
     2  /15X,9HCONDITION,40X,A2,7HCRACKED
     3  /15X,A4,A1,12H SPACING, FT,31X,F10.2
     4  /15X,19HSLAB THICKNESS, IN.,29X,F10.2
     5  /15X,27HCONCRETE CREEP MODULUS, PSI,21X,F10.0
     6  /15X,37HCONCRETE THERMAL COEFFICIENT, IN/IN/F,11X,F10.8
     7  /15X,28HUNIT WEIGHT OF CONCRETE, PCF,20X,F10.1
     8  /15X,23HMOVEMENT AT SLIDING, IN,25X,F10.4)
C
      WRITE (IOUT,1030) BARD, BARS, ES, ALFS, SMU
 1030 FORMAT(/9X,31HEXISTING PAVEMENT REINFORCEMENT
     1  /15X,17HBAR DIAMETER, IN.,31X,F10.3
     2  /15X,16HBAR SPACING, IN.,32X,F10.3
     3  /15X,29HELASTIC MODULUS OF STEEL, PSI,19X,F10.0
     4  /15X,37HTHERMAL COEFFICIENT OF STEEL, IN/IN/F,11X,F10.8
     5  /15X,24HMAXIMUM BOND STRESS, PSI,24X,F10.0)
C
```

```
      WRITE (IOUT,1040) TH,WH,TL,WL,T1
 1040 FORMAT (/9X,43HEXISTING PAVEMENT MOVEMENT CHARACTERIZATION
     2  /15X,27HHIGH TEMPERATURE, DEGREES F,21X,F10.1
     3  /15X,42HJOINT/CRACK WIDTH AT HIGH TEMPERATURE, IN.,6X,F10.7
     4  /15X,26HLOW TEMPERATURE, DEGREES F,22X,F10.1
     5  /15X,41HJOINT/CRACK WIDTH AT LOW TEMPERATURE, IN.,7X,F10.7
     6  /15X,39HMINIMUM TEMPERATURE OBSERVED, DEGREES F,9X,F10.1)
C
      WRITE (IOUT,1060) THOV, EOV, EDV, ALFV, DENSOV, OVBS, BBW
 1060 FORMAT(/9X,40HASPHALT CONCRETE OVERLAY CHARACTERISTICS,
     1  /15X,33HTHICKNESS (BINDER + SURFACE), IN.,15X,F10.2,
     2  /15X,18HCREEP MODULUS, PSI,30X,F10.0
     3  /15X,20HDYNAMIC MODULUS, PSI,28X,F10.0
     4  /15X,28HTHERMAL COEFFICIENT, IN/IN/F,20X,F10.8
     5  /15X,16HUNIT WEIGHT, PCF,32X,F10.1
     6  /15X,24HMAXIMUM BOND STRESS, PSI,24X,F10.0
     7  /15X,23HBOND BREAKER WIDTH, FT.,25X,F10.2)
C
      WRITE (IOUT,1070) TH2, E2, ED2, ALF2, DENS2
 1070 FORMAT (/9X,34HINTERMEDIATE LAYER CHARACTERISTICS,
     1  /15X,14HTHICKNESS, IN.,34X,F10.2
     2  /15X,18HCREEP MODULUS, PSI,30X,F10.0
     3  /15X,20HDYNAMIC MODULUS, PSI,28X,F10.0
     4  /15X,28HTHERMAL COEFFICIENT, IN/IN/F,20X,F10.8
     5  /15X,16HUNIT WEIGHT, PCF,32X,F10.1)
C
      WRITE (IOUT,1075) DTN18
 1075 FORMAT (/9X,28HDESIGN TRAFFIC (18-KIP ESAL),26X,F10.0)
C
      WRITE (IOUT,1000)
C
      WRITE (IOUT,1080) IPROB,PRODES
 1080 FORMAT (/5X,8HPROBLEM ,I3,12H DESCRIPTION,39X,6HPAGE 2
     1  /5X,19A4)
C
      WRITE (IOUT,1090) (DAY(I),I=1,7)
 1090 FORMAT(  /9X,50HYEARLY FREQUENCY OF CRITICAL MINIMUM TEMPERATURES
     1 //15X,30H          MINIMUM      NO. OF
     2  /15X,30HTEMP.   TEMPERATURE   DAYS PER
     3  /15X,30HCLASS  RANGE (DEG F)    YEAR
     4  /15X,30H-----  -------------  --------
     5  /15X,20H  1      +49 TO +40 ,   F8.0,
     7  /15X,20H  2      +39 TO +30 ,   F8.0,
     8  /15X,20H  3      +29 TO +20 ,   F8.0,
     9  /15X,20H  4      +19 TO +10 ,   F8.0,
     0  /15X,20H  5      + 9 TO   0 ,   F8.0,
     1  /15X,20H  6      - 1 TO -10 ,   F8.0,
     2  /15X,20H  7      -11 TO -20 ,   F8.0)
      RETURN
      END
      SUBROUTINE RCOUT
CC
C     RCOUT - OUTPUT ROUTINE FOR REFLECTION CRACKING PROGRAM
C
      COMMON /DESN/ XBB, T1, NTMP, DTC(7), DTV(7), DT2(7), DAY(7)
```

```
      COMMON /SHSTRN/ GAMOV, GAM2, GAMR
      COMMON /TENSTR/ EPSOV(7), EPS2(7), EPSR(7)
      COMMON /OUT1/ BP, AP, XM, XS, STLSB, CSB
      COMMON /OUT2/ BU, AV1, BB, AV2
      COMMON /OUT3/ FATL(7), YRDAM(7), YRDTOT, YRTLIF, FW
      COMMON / IO / IN, IOUT
C
      WRITE(IOUT,1000)
1000  FORMAT(///33X,16(1H*)/33X,16H* ARKRC OUTPUT *,/33X,16(1H*))
C
      WRITE(IOUT,1110) BP, BU, BB
1110  FORMAT(//9X,11HBETA VALUES
     1  /15X,14HBEFORE OVERLAY,34X,F10.5
     2  /15X,31HAFTER OVERLAY (UNBONDED REGION),17X,F10.5
     3  /15X,29HAFTER OVERLAY (BONDED REGION),19X,F10.5)
      WRITE(IOUT,1120) GAMOV, FW
 1120 FORMAT(/9X,28HDESIGN SHEAR STRAIN CRITERIA
     1  /15X,28HMAXIMUM OVERLAY SHEAR STRAIN,20X,F10.6
     2  /15X,25HMAXIMUM DEFLECTION FACTOR,23X,F10.3)
      WRITE(IOUT,1200) (I,DAY(I),EPSOV(I),FATL(I),YRDAM(I),I=1,NTMP)
 1200 FORMAT(/9X,38HFATIGUE LIFE (TENSILE STRAIN CRITERIA)
     1 //15X,42H         NO. OF        OVERLAY     ALLOWABLE
     2  /15X,52HTEMP.  DAYS PER  TENSILE STRAIN   FATIGUE      YEARLY
     3  /15X,52HCLASS    YEAR         (IN/IN)       CYCLES     DAMAGE
     4  /15X,52H-----  --------  --------------  ---------     ------
     57(/15X,I3,F10.0,5X,F10.7,F13.0,F11.4) )
      WRITE(IOUT,1210) YRDTOT,YRTLIF
 1210 FORMAT(61X,6(1H-)/33X,20HTOTAL YEARLY DAMAGE ,F14.4
     1 //15X,47HNO. OF YEARS BEFORE FAILURE CRITERIA IS REACHED,F11.1)
      RETURN
      END
      SUBROUTINE CHARJ
CCCCCCCCC
C  CHARJ - CHARACTERIZES PLAIN JOINTED CONCRETE PAVEMENT
CCCCCCCCC
      COMMON /CHAR/ EC,THC,DENSC,ALFC,ES,AS,SSIG,SMU,ALFS,BARD,BARS,
     1              E2,TH2,DENS2,ALF2,EOV,THOV,DENSOV,ALFV,OVBS,
     2              ER,AR,ALFR
      COMMON /NUMBER/ EAC,EAS,EA2,EAV,EAR,DTOBS,DTONE,DCOBS,SIGMU,FAC,XL
      COMMON /OBS/ SPACE, ICRAK, WH, WL, TH, TL, DS, IFSLP
      COMMON /OUT1/ BP, AP, XM, XS, STLSB, CSB
      COMMON /CONST/ CON(10)
      ETA = ALFC*DTOBS
      XS = 0.0
      BP = BETA(DCOBS,XL,ETA)
      IF (BP .LE. 1.) GO TO 4
      WRITE (IOUT,100)
  100 FORMAT(//5X,46H*** INPUT DATA ERROR RESULTING IN BETA GREATER
     1 9H THAN 1.0/5X,23H*** CHECK MOVEMENT DATA )
      STOP
    4 IF (BP .GT. 0.) GO TO 5
      WRITE (IOUT,200)
  200 FORMAT(//5X,43H*** INPUT DATA ERROR RESULTING IN BETA LESS
     1 9H THAN 1.0/5X,47H*** PCC THERMAL COEFICIENT PROBABLY TOO LOW OR
     2 /5X,27H*** INCORRECT MOVEMENT DATA )
```

```
      STOP
    5 CONTINUE
      FC =EAC*(ETA-DCOBS/XL)
      AP = XL
      IF (DCOBS .GT. DS) AP = ASOLN(ETA,DS,BP,XL)
      CONINT=ETA*(1.-BP)/XL**BP
      TERM = CONINT * AP**(BP+2.)/(BP+2.) + DS*(XL-AP)
      XM = FC/TERM
C     NOW HAVE BETA, A, AND M (SLOPE) FOR CHARACTERIZATION OF PLAIN JCP.
      CSB = FC/(THC*CON(1))
      STLSB = 0.
C     WRITE(2,2) ETA,BP,XL,AP,DS,FC,THC,CONINT,TERM,CSB
 2    FORMAT(10H CHARJ     ,10E12.4)
      RETURN
      END
      SUBROUTINE CHARC
CCCCCCCCCCCC
C   CHARC - CHARACTERIZES REINFORCED CONCRETE PAVEMENT
CCCCCCCCCCCC
      DIMENSION XT(10), DF(10)
      REAL INTERP
      COMMON /CHAR/ EC,THC,DENSC,ALFC,ES,AS,SSIG,SMU,ALFS,BARD,BARS,
     1              E2,TH2,DENS2,ALF2,EOV,THOV,DENSOV,ALFV,OVBS,
     2              ER,AR,ALFR
      COMMON /CONST/ CON(10)
      COMMON /NUMBER/ EAC,EAS,EA2,EAV,EAR,DTOBS,DTONE,DCOBS,SIGMU,FAC,XL
      COMMON /OBS/ SPACE, ICRAK, WH, WL, TH, TL, DS, IFSLP
      COMMON /OUT1/ BP, AP, XM, XS, STLSB, CSB
      COMMON / IO / IN, IOUT
      DATA TEST /50./
      DATA MAX /10/
CCCCCCCCCCC
C     STATEMENT FUNCTIONS FOR OFT-REPEATED CODE.
CCCCCCCCCCC
      AREA(X,B)= X**(B+2.)/(B+2.)
      DELFN (ETA,B,X,XL) = ETA*X*(1.-B)*(X/XL)**B
      ETA = ALFC*DTOBS
      BP = BETA (DCOBS,XL,ETA)
      IF (BP .LE. 1.) GO TO 4
      WRITE (IOUT,100)
  100 FORMAT(//5X,46H*** INPUT DATA ERROR RESULTING IN BETA GREATER
     1 9H THAN 1.0/5X,23H*** CHECK MOVEMENT DATA )
      STOP
    4 IF (BP .GT. 0.) GO TO 5
      WRITE (IOUT,200)
  200 FORMAT(//5X,43H*** INPUT DATA ERROR RESULTING IN BETA LESS
     1 9H THAN 1.0/5X,47H*** PCC THERMAL COEFICIENT PROBABLY TOO LOW OR
     2 /5X,27H*** INCORRECT MOVEMENT DATA )
      STOP
    5 CONTINUE
C     DTONE - MAXIMUM TEMPERATURE CHANGE PVT HAS UNDERGONE BEFORE OVERLAY.
      ETAS1 = ALFS*DTONE
      ETAC1 = ALFC*DTONE
      FACT=(1.-BP)/XL**BP
      I = 0
```

```
      D1XL = DELFN(ETAC1,BP,XL,XL)
      W1 = D1XL + WH*0.5
C     INITIAL ESTIMATE OF XS.
      XS = XL - SQRT(W1*EAS/SIGMU)
C     ITERATE ON XS FOR FORCE BALANCE.
   10 D1XS = DELFN(ETAC1,BP,XS,XL)
      TERM =(D1XS + 0.5*WH)/(XL - XS + 0.5*WH)
      FSC = EAS*(ETAS1 + TERM)
      U = SIGMU*(XL-XS)
      FSXS = FSC - U
      FCXS = EAC*(FSXS/EAS + ETAC1 - ETAS1)
      FIS = FCXS - U
      Q = 0.
      IF (DS .GT. D1XS) GO TO 21
      XM = FIS/(DS*(XL-XS))
      AP = ASOLN(ETAC1, DS, BP, XL)
      GO TO 30
   21 AP = XL
      IF (DS .LT. D1XL) AP = ASOLN(ETAC1, DS, BP, XL)
      Q = ETAC1*FACT*(AREA(AP,BP) - AREA(XS,BP)) + DS*(XL-AP)
      XM = FIS/Q
   30 CONTINUE
      FSCDTZ = .5*WH*EAS/(XL-XS+0.5*WH)
      FCBDTZ = FSCDTZ/(1. + EAS/EAC)
      TERM = FCBDTZ
      FCB = EAC*(ETAC1 - D1XL/XL) + TERM
      FSB = EAS*(FCB/EAC + ETAS1 - ETAC1)
      FI = XM*(ETAC1*FACT*AREA(AP,BP) + DS*(XL-AP))
      DELF = FSB + FCB - FI - FSC
      I = I + 1
      XT(I) = XS
      DF(I) = DELF
      IF (ABS(DELF) .LT. TEST) GO TO 60
      IF  (I .GE. MAX) GO TO 50
      IF (I .GT. 1) GO TO 40
C     SECOND VALUE OF XS.
      DELX = AMIN1(0.1*XS, 0.1*(XL-XS))
      XS = XS - SIGN(DELX,DELF)
      GO TO 10
C     INTERPOLATE IN FUNCTION XS(DELF) FOR DELF = 0. FOR NEXT ESTIMATE OF XS.
   40 XSINT = INTERP(0., DF, XT,I)
      XS = XSINT
C     LIMIT XS IN CASE OF EXTRAPOLATION.
      IF (XS .LE. 0.) XS = .05*XL
      IF (XS .GT. XL) XS = .99*XL
      GO TO 10
C     TOO MANY ITERATIONS.
   50 WRITE (IOUT,1) MAX
    1 FORMAT(35H ITERATIONS IN CHARC EXCEEDED MAX =,I4,6H ABORT)
      CALL EXIT
C     SUCCESS.
   60 CONTINUE
      CSB = FCB/(THC*CON(1))
      STLSB = FSC/AS
C     WRITE(2,2) ETAC1,BP,XS,XL,AP,FACT,D1XL,D1XS,Q,FI
```

```
C     WRITE(2,3) FSC,FSXS,FCXS,FIS,FSCDTZ,FCBDTZ,FCB,FSB,CSB,STLSB
 2    FORMAT(10H CHARC     ,10E12.4)
 3    FORMAT(10H           ,10E12.4)
      RETURN
      END
      SUBROUTINE BNDOV (IFLAG)
CCCCCCCCCCCC
C   BNDOV - BONDED OVERLAY ANALYSIS ROUTINE
CCCCCCCCCCC
C     SAME ROUTINE FOR JCP AND CRCP.  JCP IF AREA(STEEL)=0.
C
      DIMENSION XT(50), DF(50)
      DIMENSION IWRDT(2), IWRDMA(2)
      REAL INTERP
      COMMON /CHAR/ EC,THC,DENSC,ALFC,ES,AS,SSIG,SMU,ALFS,BARD,BARS,
     1              E2,TH2,DENS2,ALF2,EOV,THOV,DENSOV,ALFV,OVBS,
     2              ER,AR,ALFR
      COMMON /CONST/ CON(10)
      COMMON /DESN/ XBB, T1, NTMP, DTC(7), DTV(7), DT2(7), DAY(7)
      COMMON /NUMBER/ EAC,EAS,EA2,EAV,EAR,DTOBS,DTONE,DCOBS,SIGMU,FAC,XL
      COMMON /OBS/ SPACE, ICRAK, WH, WL, TH, TL, DS, IFSLP
      COMMON /OUT1/ BP, AP, XM, XS, STLSB, CSB
      COMMON /OUT2/ BU, AV1, BB, AV2
      COMMON /FATCON/ A1, A2, B1, B2
      COMMON /TENSTR/ EPSOV(7), EPS2(7), EPSR(7)
      COMMON / IO / IN, IOUT
      COMMON /ALPHA/ IPROB, PRODES(19), PVTYPE(2), OVTYPE(2), OVRTYP(3)
      DATA CRCP / 4HCRCP /
      DATA TEST/  20. /, MAX/ 50 /
      DATA MAXT / 50 /
      DATA KLIM / 50 /
      DATA IWRDT / 4HTOTA, 1HL /
      DATA IWRDMA / 4HMAJO,1HR /
CCCCCCCCCC
C   STATEMENT FUNCTIONS
CCCCCCCCCC
      DELFN(ETA,B,X,XL) = ETA*X*(1.-B)*(X/XL)**B
      AREA(X,B) = X**(B+2.)/(B+2.)
CCCCCCCCCCCCCCCCCCCCCCCC
C   FIRST SOLVE PROBLEM UNDER MAX TEMP DROP CONDITIONS
CCCCCCCCCCCCCCCCCCCCCCCC
      ETA = ALFC*DTC(NTMP)
      ETA2 = ALF2*DT2(NTMP)
      ETAV = ALFV*DTV(NTMP)
      ETAR = ALFR*DTV(NTMP)
      ETAS = ALFS*DTC(NTMP)
      DO 15 I=1,10
      XT(I) = 0.
   15 DF(I) = 0.
      FACTOR = FAC
      XMOV = XM*FACTOR
C     FORCE TERMS FOR ZERO TEMP DIFF.
      FSCDTZ = .5*WH*EAS/(XL-XS+0.5*WH)
      FCBDTZ = FSCDTZ/(1. + EAS/EAC)
      TERM = FCBDTZ
```

```
C    IF SLOPE OF FRICTION CURVE NOT ADJUSTED FOR INCREASED OVERBURDEN
C     THEN
       BU = BP
       IF (FACTOR .LE. 1.) GO TO 90
       I = 0
C      ASSUME BETA FOR UNBONDED PORTION.
       BU = AMIN1( 1.15*BP, 0.96 )
C      ITERATE ON BETA (BU) FOR FORCE BALANCE.
   10  DC = DELFN(ETA,BU,XL,XL)
       DCXS = DELFN(ETA,BU,XS,XL)
       FCB = EAC*(ETA-DC/XL)
       FCB = FCB + TERM
       AV1 = XL
       IF (DS .LT. DC) AV1 = ASOLN(ETA, DS, BU, XL)
       FACTU=(1.-BU)/XL**BU
       FI = XMOV*(ETA*FACTU*AREA(AV1,BU) + DS*(XL-AV1))
       FSB = EAS*(FCB/EAC + DTC(NTMP)*(ALFS - ALFC))
       FSC = EAS*(ETAS + (DCXS + 0.5*WH)/(XL + 0.5*WH - XS))
       FLHS = FCB + FSB
       FRHS = FI + FSC
       DELF = FLHS - FRHS
       I = I + 1
       DF(I) = DELF
       XT(I) = BU
       IF (ABS(DELF) .LT. TEST) GO TO 90
       IF (I .GE. MAX) GO TO 60
       IF (I .GT. 1) GO TO 20
C      SECOND ESTIMATE FOR BU.
       IF (DELF .GT. 0.) BU=0.95*BU
       IF (DELF .LT. 0.) BU=1.05*BU
       IF (BU .GT. 1.0) BU=0.99
       GO TO 10
C      INTERPOLATE IN BU(DELF) FOR DELF=0. FOR NEXT ESTIMATE.
   20  BU = INTERP (0., DF, XT, I)
C      LIMIT BU IN CASE OF EXTRAPOLATION.
       IF (BU .GE. 1.) BU = 1. - (0.1)**I
       IF (BU .LE. 0.) BU = 0.1**I
       GO TO 10
C      TOO MANY ITERATIONS.
   60  WRITE(IOUT,1) IWRDMA,MAX,DELF,DELF
    1  FORMAT(1X,A4,A1,35H ITERATIONS IN BNDOV EXCEEDED MAX =I4,6H ABORT
      *    / 7H DELF= ,E12.4,5H XZ= ,E12.4)
C      SET IFLAG=1 TO INDICATE FAILURE HERE.
       IFLAG = 1
       RETURN
C      SUCCESS
   90  CONTINUE
C      WRITE(2,2) ETA,ETA2,ETAV,ETAS,EAS,EAC,BU,TERM,AV1
 2     FORMAT(10H BNDOV     ,10E12.4)
C      WRITE(2,3) FSCDTZ,FCBDTZ,DC,DCXS,FCB,FI,FSB,FSC,FLHS,FRHS
 3     FORMAT(10H UNBOUND   ,10E12.4)
       DO 95 I=1,10
       XT(I) = 0.
   95  DF(I) = 0.
  100  CONTINUE
```

```
C     ASSUME BETA (BONDED)
      BB = BU
      KNT = 0
      XB = XL - XBB
      IT = 0
        I=0
        IBB=-1
        DELF=-1.
  110 IF (DELF.GT.0. .AND. IBB.EQ.-1) IBB=1
      DCXB = DELFN(ETA, BB, XB, XL)
      IT = IT+1
      IF (IT .GT. MAXT) GO TO 999
      DCXS = DELFN(ETA, BB, XS, XL)
      CALL CLCXLE(DCXB,ETA,BU,XBB,XL,XLE)
      XSE = 0.
      AV2E = 0.
      AREAB = 0.
      FACTUE = 0.
      XBE = 0.
      AREAU = 0.
      IF (XS.LE.XB) GO TO 115
      XSE = XS-XL+XLE
      DCXS=DELFN(ETA,BU,XSE,XLE)
  115 CONTINUE
      FCB = EAC*(ETA - DCXB/XB) + TERM
      FSB = EAS*(FCB/EAC + ETAS - ETA)
      FSC = EAS*(ETAS + (DCXS + 0.5*WH)/(XL + 0.5*WH - XS))
      AV2 = ASOLN (ETA, DS, BB, XL)
      IF (AV2.GT.XL) AV2=XL
      FACTB = (1.-BB)/XL**BB
      IF (AV2 .GT. XB) GO TO 120
      FI = XMOV*(ETA*FACTB*AREA(AV2,BB) + DS*(XL-AV2))
      GO TO 124
  120 CONTINUE
      AV2E = ASOLN(ETA, DS ,BU, XLE)
      IF (AV2E .GT. XLE) AV2E=XLE
      AV2 = AV2E + XL - XLE
      IF (AV2 .GT. XL) AV2 = XL
      AREAB = FACTB * AREA(XB,BB)
      FACTUE = (1. - BU) / XLE**BU
      XBE = XB - XL + XLE
      AREAU = FACTUE * (AREA(AV2E,BU) - AREA(XBE,BU))
      FI = XMOV * (ETA *(AREAB+AREAU) + DS*(XL-AV2))
  124 CONTINUE
      IF (OVBS .EQ. 0.) GO TO 126
      UZ = FCB + FSB - FI - FSC
      XZ = UZ/(OVBS*CON(1))
C     WRITE(2,4) BB,DCXB,XLE,XSE,DCXS,FCB,FSB,FSC,FACTB,FI,AV2,AV2E,
C    *    AREAB,AREAU,XBE,UZ,XZ
      D = XL - XBB
      IF ( XZ .GT. 0.) GO TO 125
      ZJQ=.003
      IF (PVTYPE(1).NE.CRCP) ZJQ=.012
      BB=BB+ZJQ
      KNT = KNT+1
```

```
      IF (KNT .LT. KLIM) GO TO 110
      WRITE (IOUT,5) KLIM
    5 FORMAT(/21H KNT EXCEEDS LIMIT OF,I4)
C     SET IFLAG=2 TO INDICATE FAILURE IN THIS SECTION.
      IFLAG = 2
      RETURN
  125 XZP = D - XZ
      DCXZP = DELFN(ETA,BB,XZP,XL)
  126 CONTINUE
      STRATO = 0.0001
      IF (THOV .GE. 9.) GO TO 123
      STRATO = 0.3021*ALOG(9.-THOV) + 0.3362
  123 CONTINUE
      ARO = (STRATO-1.)/ALOG(STRATO)
      IF (TH2 .GT. 0.) GO TO 127
      F2B = 0.
      F2C = 0.
      FOB = EAV*(ETAV + ARO*(FCB/EAC-ETA) )
C     IF (OVBS .LE. 0. .AND. XBB .LE. 0.), THEN ASSUME .25-IN SLIP ZONE
      STRNM = DCXB/0.25
      STRN2M = 0.0
C
      IF (OVBS .LE. 0. .AND. XBB.GT.0.) STRNM = DCXB/XBB
      IF (OVBS .GT. 0.) STRNM = DCXZP/(XZ+XBB)
      FOC = EAV*(ETAV + ARO*STRNM)
      GO TO 128
  127 CONTINUE
      ETERM = ALOG(EOV)/ALOG(E2)
      XSTRT2 = 5.9223 -0.50742*ALOG(TH2) -5.5061*ETERM
     +         -0.52215*ALOG(THOV)*ETERM
      STRAT2 = EXP( XSTRT2 )
      AR2 = (STRAT2-1.)/ALOG(STRAT2)
      F2B = EA2*(ETA2 + AR2*(FCB/EAC-ETA))
      STRN2M = DCXB/0.25
      IF (OVBS .LE. 0. .AND. XBB.GT.0.) STRN2M = DCXB/XBB
      IF (OVBS .GT. 0.) STRN2M = DCXZP/(XZ+XBB)
      F2C = EA2*(ETA2 + AR2*STRN2M)
      STRNM = STRAT2*STRN2M
      FOC = EAV*(ETAV + ARO*STRNM)
      STRNMB = STRAT2*(FCB/EAC-ETA)
      FOB = EAV*(ETAV + ARO*STRNMB)
  128 CONTINUE
      FRB = EAR*(FOB/EAV + ETAR - ETAV)
      FRC = EAR*(FOC/EAV + ETAR - ETAV)
      FLHS = FCB + F2B + FOB + FRB + FSB
      FRHS = FI  + F2C + FOC + FRC + FSC
      DELF = FLHS - FRHS
C     WRITE(2,4) XZP,DCXZP,F2B,F2C,FOB,FOC,FRB,FRC,FLHS,FRHS,DELF
 4    FORMAT(10H BOUND     ,10E12.4)
      I = I + 1
      DF(I) = DELF
      XT(I) = BB
      IF (ABS(DELF) .LT. TEST .AND. XZ.LE.D) GO TO 170
      IF (I .GE. MAX) GO TO 160
      ZJQ=.003
```

```
      IF (PVTYPE(1).NE.CRCP) ZJQ=.012
      IF (IBB.EQ.-1) BB=BB+ZJQ
      IF (IBB.EQ.1)  BB= INTERP(0.,DF(I-1), XT(I-1), 2)
      GO TO 110
C     TOO MANY ITERATIONS
  160 WRITE (IOUT,1) IWRDMA,MAX,DELF,XZ
C     SET IFLAG=2 TO INDICATE FAILURE IN THIS SECTION.
      IFLAG = 2
      RETURN
C     SUCCESS.
  170 CONTINUE
      EPSOV(NTMP) = STRNM + ETAV
      EPS2(NTMP) = STRN2M + ETA2
      EPSR(NTMP) = 0.
      IF (EAR .GT. 1.) EPSR(NTMP) = FRC/EAR
CCCCCCCCCCCCCCCCCC
C  NOW SOLVE FOR STRAINS DURING OTHER DESIGN TEMP DROP CONDITIONS
CCCCCCCCCCCCCCCCCC
      IF (NTMP .LE. 1) GO TO 300
      NT1 = NTMP-1
      DO 250 ITMP=1,NT1
      ETA = ALFC*DTC(ITMP)
      ETAS = ALFS*DTC(ITMP)
      ETA2 = ALF2*DT2(ITMP)
      ETAV = ALFV*DTV(ITMP)
      ETAR = ALFR*DTV(ITMP)
      DCXB = DELFN( ETA, BB, XB, XL )
      IF (XZP .LT. 0.) XZP=0.
      DCXZP = DELFN( ETA, BB, XZP, XL )
      IF (TH2 .GT. 0.) GO TO 200
      STRN2M = 0.0
      STRNM = DCXB/0.25
      IF (OVBS .LE. 0. .AND. XBB .GT. 0.) STRNM = DCXB/XBB
      IF (OVBS .GT. 0.) STRNM = DCXZP/(XZ+XBB)
      GO TO 210
  200 CONTINUE
      STRN2M = DCXB/0.25
      IF (OVBS .LE. 0. .AND. XBB .GT. 0.) STRN2M = DCXB/XBB
      IF (OVBS .GT. 0.) STRN2M = DCXZP/(XZ+XBB)
      STRNM = STRAT2*STRN2M
  210 CONTINUE
      FRC = EAR*(FOC/EAV + ETAR - ETAV)
C
      EPSOV(ITMP) = STRNM + ETAV
      EPS2(ITMP) = STRN2M + ETA2
      EPSR(ITMP) = 0.
      IF (EAR .GT. 1.) EPSR(ITMP)=FRC/EAR
  250 CONTINUE
C     WRITE (2,4) EPSOV
C     WRITE (2,4) EPS2
C     WRITE (2,4) EPSR
C
  300 CONTINUE
      RETURN
  999 WRITE (IOUT,1) IWRDT,MAXT,DELF,XZ
```

```
C     SET IFLAG=2 TO INDICATE FAILURE IN THIS SECTION.
      IFLAG = 2
      RETURN
      END
      SUBROUTINE VERTM
      COMMON /CHAR/ EC,THC,DENSC,ALFC,ES,AS,SSIG,SMU,ALFS,BARD,BARS,
     1              E2,TH2,DENS2,ALF2,EOV,THOV,DENSOV,ALFV,OVBS,
     2              ER,AR,ALFR
      COMMON /VERT/ DLOAD,WLOAD,EDV,ED2,EDR,DTN18,OVMU,TWOMU,RFMU
      COMMON /SHSTRN/ GAMOV, GAM2, GAMR
      COMMON /FATCON/ A1, A2, B1, B2
      COMMON /OUT3/ FATL(7), YRDAM(7), YRDTOT, YRTLIF, FW
      COMMON /CONST/ CON(10)
C
      IF (EDV .GT. 0. .AND. DTN18 .GT. 0.) GO TO 10
      GAMOV = 0.
      FW = 0.
      GAMR = 0.
      GAM2 = 0.
      RETURN
   10 CONTINUE
C     MAXIMUM ALLOWABLE OVERLAY SHEAR STRAIN
      GAMOV = B1*(DTN18)**B2
C     SHEAR MODULI
      GOV = EDV/(2.*(1.+OVMU))
      G2 = ED2/(2.*(1.+TWOMU))
      GR = ER/(2.*(1.+RFMU))
C     EFFECTIVE OVERLAY THICKNESS
      THEF = THOV + TH2*G2/GOV + (AR/CON(1))*GR/GOV
C     MAXIMUM OVERLAY SHEAR STRESS
      TAUOV = GAMOV*GOV
C     MAXIMUM OVERLAY SHEAR FORCE
      VO = 0.6667*TAUOV*THEF*WLOAD
C     MAXIMUM ALLOWABLE DEFLECTION FACTOR
      FW = VO/DLOAD
      RETURN
      END
      SUBROUTINE OVLIFE
CC
C     OVLIFE - ESTIMATE LIFE OF OVERLAY
C
      COMMON /FATCON/ A1, A2, B1, B2
      COMMON /SHSTRN/ GAMOV, GAM2, GAMR
      COMMON /TENSTR/ EPSOV(7), EPS2(7), EPSR(7)
      COMMON /DESN/ XBB, T1, NTMP, DTC(7), DTV(7), DT2(7), DAY(7)
      COMMON /OUT3/ FATL(7), YRDAM(7), YRDTOT, YRTLIF, FW
C
      FATIG(C1,C2,STRN) = C1*( STRN )**C2
C     WRITE(2,99) A1,A2
C
C     LIFE OF OVERLAY - TENSILE STRAIN CRITERIA
      YRDTOT = 0.
      DO 20 I=1,NTMP
      FATL(I) = FATIG( A1, A2, EPSOV(I) )
      YRDAM(I) = DAY(I)/FATL(I)
```

```
      YRDTOT = YRDTOT + YRDAM(I)
C     WRITE(2,99) FATL(I), YRDAM(I), YRDTOT
   20 CONTINUE
      YRTLIF = 1./YRDTOT
   99 FORMAT(10H OVLIFE   ,10E12.4)
      RETURN
      END
      FUNCTION BETA (DEL, XL, ETA)
CCCCCCCCCCCCC
C  BETA - SOLVE FOR RESTRAINT COEFFICIENT (BETA)
C         DEL = SLAB END MOVEMENT
C          XL = HALF-SLAB LENGTH
C         ETA = CONCRETE THERMAL COEFFICIENT
C                * OBSERVED TEMPERATURE DROP
CCCCCCCCCCCCCC
      BETA = 1. - DEL/(ETA*XL)
      RETURN
      END
      FUNCTION ASOLN(ETA, DEL, BETA, XL )
CCCCCCCCCCCCCC
C   ASOLN - SOLVE FOR LOCATION OF A GIVEN MOVEMENT ALONG SLAB
C            ETA = THERMAL COEF. * TEMP. DROP
C             DEL = MOVEMENT AT DESIRED LOCATION
C             XL = HALF SLAB LENGTH
C           BETA = RESTRAINT COEFFICIENT
CCCCCCCCCCCCCC
      IF (BETA.GE.1.) GO TO 10
      TOP = DEL * XL**BETA
      BOT = ETA * (1. - BETA)
      EX = 1. / (BETA+1.)
      ASOLN = (TOP/BOT)**EX
      RETURN
 10   CONTINUE
C    FULL RESTRAINT, NO SLIDING
      ASOLN=XL
      RETURN
      END
      REAL FUNCTION INTERP (XR, X, F, N)
      DIMENSION X(N), F(N)
      IF (N .GT. 2) GO TO 10
      FI = F(1) + (XR-X(1))*(F(2)-F(1))/(X(2)-X(1))
      GO TO 99
   10 CALL ORDER (X, F, N)
C     ORDER PLACES X AND F IN ORDER OF INCREASING X.
      IB = 1
      IF (N .EQ. 3) GO TO 30
      DO 15 I=2,N
      IX = I
      IF (X(I) .GT. XR) GO TO 20
   15 CONTINUE
   20 IF ((XR-X(IX-1)) .LT. (X(IX)-XR)) IX = IX - 1
      IB = IX - 1
      IF (IB .LT. 1) IB = 1
      IF (IB .GT. (N-2)) IB = N-2
   30 FI = PARAB (XR, X(IB), F(IB))
```

```
   99 INTERP = FI
      RETURN
      END
      SUBROUTINE ORDER (X, F, N)
      DIMENSION X(N), F(N)
      DO 20 J=2,N
      I = J-1
      XS = X(J)
      FS=F(J)
   10 IF (XS .GE. X(I)) GO TO 15
      X(I+1) = X(I)
      F(I+1) = F(I)
      I = I-1
      IF (I .GT. 0) GO TO 10
   15 X(I+1) = XS
      F(I+1) = FS
   20 CONTINUE
      RETURN
      END
      FUNCTION PARAB (XR, X, F)
      DIMENSION X(3), F(3)
      XL = X(2) - X(1)
      XU = X(3) - X(2)
      D = XL*XU*(X(3) - X(1))
      P1 = XL*(F(3)-F(2))
      P2 = XU*(F(2)-F(1))
      S1 = P1*XL+P2*XU
      S2 = P1 - P2
      T = XR - X(2)
      PARAB =F(2)+ (S1 +S2*T)*T/D
      RETURN
      END
      SUBROUTINE CLCXLE (DCXB,ETA,BU,XBB,XL,XLE)
      REAL X(2),Y(2),YI(6),INTERP
      DATA YI / 0., .2, .4, .6, .8, .9999 /
CCCCCCCCCCCC
C STATEMENT FUNCTIONS
CCCCCCCCCCCC
      F(Z)=-DCXB+ETA*(1.-BU)*Z*(1.-XBB/Z)**(BU+1.)
C     WRITE(2,2) DCXB,ETA,BU,XBB,XL
 2    FORMAT(10H CLCXLE    ,6E12.4)
      Y(1)=XBB
      X(1)=-DCXB
      DO 10 I=2,6
      Y(2)=XBB+YI(I)*(XL-XBB)
      S=Y(2)
      X(2)=F(S)
      IF ( X(1).LT.0. .AND. X(2).GT.0. ) GO TO 14
      X(1)=X(2)
      Y(1)=Y(2)
 10   CONTINUE
      XLE = XBB + .99995*(XL-XBB)
C     WRITE(2,3) XLE
 3    FORMAT(48H SUBROUTINE CLCXLE ALL FUNCTION VALUES ARE ZERO ,
     *       / 10H XLE=      ,E12.4)
```

```
      RETURN
 14   II=0
 15   CONTINUE
      II=II+1
      ZY = INTERP(0.,X,Y,2)
      ZX = F(ZY)
      IF (II.LT.100) GO TO 25
C     WRITE(1,400) X(1),Y(1),X(2),Y(2),ZY
      GO TO 50
 400  FORMAT(16H 100 ITERATIONS     /25H SEE SUBROUTINE CLCXLE    /9X,
     * 60HX(1)          Y(1)          X(2)          Y(2)          ZY /,
     * 5E14.6)
 25   IF (ZX .GE. 0.) GO TO 30
         X(1)=ZX
         Y(1)=ZY
         GO TO 35
 30   IF(ZX.EQ.0.) GO TO 50
         X(2)=ZX
         Y(2)=ZY
 35   YY=ABS(Y(1)-Y(2))
      IF (YY.GT.0.01) GO TO 15
      XLE=(Y(1)+Y(2))/2.
      RETURN
 50   XLE=ZY
      RETURN
      END
```